Pharmacological modulation of pancreatic beta-to-alpha cell transdifferentiation in diabetes

Neil Tanday, MSc

School of Biomedical Sciences

Faculty of Life and Health Sciences

Ulster University

Thesis submitted for the degree of

Doctor of Philosophy

February 2019

I confirm that the word count of this thesis is less than 100,000 words excluding the title page, contents, acknowledgments, abstract, tables, figures and references.

CONTENTS

Acknowledgments

My sincerest gratitude to my supervisor Professor Peter Flatt who provided me this opportunity to join the Diabetes Research Group at Ulster. His continuous support and guidance of my PhD research has helped develop me into a better researcher.

I would like to thank my other supervisors: Dr Charlotte Moffett and Professor Neville McClenaghan. Their advice and support has helped to keep me motivated throughout my research.

I would like to express my appreciation to my friends and colleagues that have supported me throughout these past three years: Shruti Mohan, Ryan Lafferty Chris McClaughlin, Andrew McCloskey, Sarah Craig, Rachele Perry, Natalie Klempel, Prawej Ansari, Vishal Musale, Michael Miskelly, Dawood Khan, Annie Hasib and Corrina Simpson. Their friendship and support have helped to create a friendly, positive environment that have made coming to work each day a joy.

Finally I would like to thank my parents and brothers for their unconditional love and support throughout my life and during this PhD.

The presented studies were supported by the PhD studentship award from DoE and project grant from Diabetes UK.

Summary

Loss of mature pancreatic beta cell identity and reversion to a progenitor endocrine state has been defined as beta cell dedifferentiation. Research has shown this to occur in beta cell lines to rodent and non-human primate models of diabetes and pancreatic islets of humans with diabetes. A concurrent increase in alpha cell mass alongside this beta cell dedifferentiation suggests that beta-to-alpha cell transdifferentiation also occurs in diabetes. This thesis examines beta-to-alpha cell transdifferentiation using beta cell lines and mouse models of diabetes. In INS-1 and MIN6 cells cultured under lipotoxic and cytokine conditions displayed reductions in insulin expression in conjunction with increased glucagon expression and a rise of cells co-expressing both hormones. INS-1 cells in particular also exhibited changes in gene expression with reduced beta cell markers and increased alpha cell and progenitor markers consistent with the beta-to-alpha cell transdifferentiation. Histological analysis of islets from mice treated with streptozotocin, hydrocortisone or high fat fed diet revealed morphological changes consistent with impaired beta cell identity. To truly ascertain beta cell transdifferentiation in animal models, lineage tracing studies were carried out using *Ins1*$^{cre/+}$;Rosa26-eYFP C57Bl/6 mice with specifically labelled beta cells. Studies in these mice confirmed previously suspected beta-to-alpha cell transdifferentiation in multiple low-dose streptozotocin, high fat fed and hydrocortisone models of diabetes. Taking this further, the incretin therapies, liraglutide and sitagliptin, and novel peptide agents, apelin and xenin, were able to prevent this transdifferentiation in these mice. SGLT2 inhibition had no effect on beta cell transdifferentiation. These results suggest the potential benefit of beta cell restoration therapy of transdifferentiated beta cells for the treatment of diabetes.

Abbreviations

ALDH1A3	Aldehyde dehydrogenase 1 A3
ARX	Aristaless related homeobox
ATP	Adenosine triphosphate
AUC	Area under curve
BRN4	Brain-4
BSA	Bovine serum albumin
$C_6H_5Na_3O_7.2H_2O$	Trisodium citrate
Ca^{2+}	Calcium
$CaCl_2.6H_2O$	Calcium chloride
CH_2Cl_2	Dichloromethane
CNS	Central nervous system
DAPI	4',6'—diamidino-2-phenylindole
DMEM	Dulbecco's modified Eagle's medium
DMSO	Dimethyl sulfoxide
DPPIV	Dipeptidyl peptidase 4
EDTA	Ethylene diaminetetraacetic acid
ELISA	Enzyme-linked immunosorbent assay
ER	Endoplasmic reticulum
FBS	Foetal bovine serum
FGF2	Fibroblast growth factor 2
FITC	Fluorescein isothiocyante
FOXO1	Forkhead box protein O1

GCK	Glucokinase
GIP	Gastric inhibitory polypeptide
GFP	Green fluorescent protein
GLP-1	Glucagon-like peptide 1
GLUT2	Glucose transporter 2
GLUT4	Glucose transporter 4
GTT	Glucose tolerance test
HBSS	Hank's buffered saline solution
HCl	Hydrochloric acid
HES1	Hairy and enhancer of split-1
HFF	High fat fed
IFNγ	Interferon γ
IL-1β	Interleukin 1β
INS	Insulin
K_{ATP}	Potassium ATP
KCl	Potassium chloride
KH_2PO_4	Potassium dihydrogen orthophosphate
KRBB	Krebs ringer bicarbonate buffer
MAFA	Musculoaponeurotic fibrosarcoma oncogene family A
MAFB	Musculoaponeurotic fibrosarcoma oncogene family B
$MgSO_4.7H_2O$	Magnesium sulphate
MIN	Mouse insulinoma
MiR-7	MicroRNA-7

MTT	3-(4,5-dimethylthiazol-2-yl)-2,5-diphenyltetrazolium bromide
MYC	Myelocytomatosis
NaCl	Sodium chloride
$NaHCO_3$	Sodium bicarbonate
NaH_2PO_4	Sodium dihydrogen orthophosphate
NEDH	New England Deaconess Hospital
NEUROD1	Neurogenic differentiation 1
NIH	National Institute of Health
Ngn3	Neurogenin-3
NKX2.2	Homeobox protein Nkx-2.2
NKX6.1	Homeobox protein Nkx-6.1
NSB	Non-specific binding
OCT4	Octamer-binding transcription factor 4
PAX4	Paired box gene 4
PBS	Phosphate buffered saline
PC1	Prohormone convertase 1
PC2	Prohormone convertase 2
PDX1	Pancreatic and duodenal homeobox 1
PFA	Paraformaldehyde
PP	Pancreatic polypeptide
PPAR	Peroxisome proliferator activation receptor
PYY	Peptide YY
RAS	Renin-angiotensin system

RIA	Radioimmunoassay
RIN	Rat insulinoma
RLU	Relative light units
RPMI	Roswell Park Memorial Institute Medium
RFU	Relative fluorescence units
RYGB	Roux-en-Y gastric bypass
SGLT2	Sodium/glucose cotransporter 2
SOX9	SRY-related HMG-box 9
STZ	Streptozotocin
SV40	Simian vacuoating virus 40
TNFα	Tumour necrosis factor α
TRITC	Tetramethylrhodamine isothiocyanate
TRIS	Trisaminomethane
TUNEL	Terminal deoxynucleotidyl transferase dUTP nick end labelling
TZD	Thiazolidinediones
Ucn3	Urocortin-3
YFP	Yellow fluorescent protein

Declaration

"I hereby declare that for 2 years following the date on which the thesis is deposited in the Research Office of Ulster University, the thesis shall remain confidential with access or copying prohibited. Following expiry of this period I permit:

1. The Librarian of the University to allow the thesis to be copied in whole or in part without reference to me on the understanding that such authority applies to the provision of single copies made for study purposes or for inclusion within the stock of another library
2. The thesis to be made available through the Ulster Institutional Repository and/or EThOSunder the terms of the Ulster eTheses Deposit Agreement which I have signed.

IT IS A CONDITION OF USE OF THIS THESIS THAT ANYONE WHO CONSULTS IT MUST RECOGNISE THAT THE COPYRIGHT RESTS WITH THE UNIVERSITY AND THEN SUBSEQUENTLY TO THE AUTHOR ON THE EXPIRY OF THIS PERIOD AND THAT NO QUOTATION FROM THE THESIS AND NO INFORMATION DERIVED FROM IT MAY BE PUBLISHED UNLESS THE SOURCE IS PROPERLY ACKNOWLEDGED."

Publications arising from thesis

Tanday N, Moffett RC, McClean S and Flatt PR 2016 Evaluation of beta to alpha cell transdifferentiation in the INS-1 cell line *Irish Journal of Medical Science* **185** 373 (Irish Endocrine Society 40th Annual Conference, oral presentation.

Tanday N, Flatt PR and Moffett RC 2018 Liraglutide prevents beta-to-alpha cell transdifferentiation in a multiple low-dose streptozotocin model of diabetes *Diabetic Medicine* **35:** 23 (Diabetes UK Annual Professional Conference, oral presentation).

Tanday N, Flatt PR McClenaghan NH, and Moffett CR 2019 Effect of dapagliflozin on alpha cells and beta-to-alpha cell transdifferentiation in multiple low-dose streptozotocin *Diabetic Medicine* (Diabetes UK Annual Professional Conference, poster presentation).

Moffett RC, **Tanday N**, McClenaghan NH and Flatt PR 2019 Prevention of beta-to-alpha cell transdifferentiation using sitagliptin in multiple low-dose streptozotocin and high fat fed models of diabetes *Diabetic Medicine* (Diabetes UK Annual Professional Conference, poster presentation)

Chapter 1

General Introduction

1.1 Endocrine Pancreas

The exocrine portion of the pancreas constitutes 98% of its mass and is accountable for the production of digestive enzymes delivered to the small intestine via the pancreatic duct. However the pancreas has come to be known as the essential organ involved in regulation of blood glucose despite only 2% of its mass being involved in this function. This endocrine portion of the pancreas consists of spherical islets of Langerhans, on average 100µm in size, scattered throughout the organ. Each islet consists of several thousand cells which are categorised depending on the polypeptide hormone they secrete surrounded by a capsule of connective tissue (Bosco et al, 2010). Islets have a rich blood supply and are innervated by the autonomic nervous system enabling them to finely regulate hormone secretion in response to nutrients, hormones and regulatory peptides. In both humans and mice insulin secreting beta cells comprise the bulk of each islet making up 50-70% and 60-80% of the islet mass respectively. Glucagon producing alpha cells are the next major cell type making up 20-40% and 10-20% of human and mouse islets respectively. Somatostatin secreting delta cells and pancreatic polypeptide secreting PP cells make up a further 10% and 5% of human and mouse islets respectively. Finally less than 1% of islet cells are ghrelin containing epsilon cells (Saito et al, 1979; Kim et al, 2009; Steiner et al, 2010; Cabrera et al, 2006; Brissova et al, 2005). Although islet size distribution is similar between humans and mice, the spatial distributions of the cell types comprising the islets differ. Mouse islet architecture consists of a central core of beta cells surrounded by a mantle of predominantly alpha cells with some delta cells (Cabrera et al, 2006). Humans however, display a disorganised cellular composition with alpha cells dispersed throughout the islet (Wieczorek et al, 1998).

Paracrine interactions between these endocrine cell types can influence secretory activity of constituent cell types (Bosco et al, 1989).

1.2 Diabetes prevalence

Diabetes mellitus is a chronic metabolic disorder of impaired blood glucose control and is characterised by hyperglycaemia. The worldwide prevalence of diabetes has increased rapidly over recent decades. This is largely attributed to increased urbanisation and adoption of sedentary lifestyles. In 1980 there was an estimated 108 million people living with diabetes (NCD Risk Factor Collaboration, 2016). 20 years later, at the turn of the millennium, this estimated prevalence increased to 151 million people (IDF, 2014). The most recent report based on 2017 data estimates that there are 451 million people living with diabetes, with this number expected to increase to 693 million by 2045 (Cho et al, 2018). To put these numbers into perspective, based on the 2017 global population of 7.6 billion people (UN, 2017), diabetes affects 6% of the world's population. The impact of treating diabetes comes at a high economic burden. In the UK, the NHS spends 10% of its budget (£10 billion a year) on treating diabetes and associated complications with this cost expected to increase over the next 20 years (Hex et al, 2012). Similarly, in the US the cost of treating diabetes, based on 2017 figures, was $327 billion, with medical bills for diabetics being on average 2.3 times higher than for individuals without diabetes (Diabetes Care, 2018).

1.3 Diabetes: type-1 & type-2

Diabetes is classified into two main types. Type-1 diabetes is due to autoimmune destruction of insulin secreting beta cells and accounts for ~10% of diabetic cases. What triggers this predominantly T cell mediated autoimmune attack, whether environmental or genetic, is poorly understood (Lehuen et al, 2010). Typically, this type of diabetes is diagnosed in children and young adults (<30 years) which usually present to clinicians with severe hyperglycaemia. At this point of symptomatic diagnosis, 60-80% of pancreatic beta cells have already been lost (Nokines and Lernmark, 2001). Given that type-1 diabetes can be partly inheritable, many genes have now been implicated to giving a predisposition towards developing type-1 diabetes such as alleles of major histocompatibility locus (HLA). Although thought of as disease of insulin-deficiency, insulin resistance is becoming recognised as increasingly common in type-1 patients, likely a result of the high doses of exogenous insulin administered (Fourlanos et al, 2004).

The remaining 90% of cases are made up of type-2 diabetes which is characterised by impaired insulin secretion, initially elevated before declining due to worsening insulin resistance in peripheral tissues (muscle, liver and adipose), culminating in poor glycaemic control and hyperglycaemia (Lin and Sun, 2010). Endoplasmic reticulum (ER) stress, hypoxic stress, oxidative stress, cytotoxicity, glucotoxicity, lipotoxicity and beta cell dedifferentiation are thought to be the major causes of this beta cell dysfunction (Accili et al, 2010; Kitamura, 2013). This form of diabetes is largely attributed to hedonistic and physically inactive Western lifestyles (Leahy, 2005). Obesity is the biggest risk factor for type-2 diabetes with an estimated 80% of

type-2 diabetes being overweight or obese (Bloomgarden, 2000). Coincident with global rates of obesity rising, there has been a large increase in the number of people diagnosed with diabetes. Children are not spared from this fate with increases in childhood obesity resulting in more and more young people presenting with type-2 diabetes. As developing countries follow the trend of urbanisation and adoption of Western diets the prevalence of type-2 diabetes is set to dramatically increase. That said the risk is not entirely environmental with genetic factors and ageing also influencing the risk.

1.4 Diabetic Complications

Acute, life-threatening complications of diabetes can occur if left entirely untreated as a result of severe fluctuations in blood glucose such as ketoacidosis from excessive hyperglycaemia and hypoglycaemic comas (Forbes and Cooper, 2013). Long-term vascular complications of diabetes are equally devastating and fall under two groups, microvascular and macrovascular, both partly due to damage caused by chronic hyperglycaemia. Microvascular complications refer to those affecting small blood vessels including retinopathy, nephropathy and neuropathy. Macrovascular complications however relate to large artery damage such as accelerated cardiovascular and cerebrovascular disease resulting in myocardial infarction and strokes respectively. Dementia (Cukierman et al, 2005), depression (Nouwen et al, 2011), and sexual dysfunction (Adeniyi et al, 2011; Thorve et al, 2011) are other less well recognised chronic complications of diabetes.

1.4.1 Diabetic Nephropathy

Diabetic nephropathy is characterised by proteinuria and progressive decline in glomerular filtration rate. Left untreated, nephropathy is a major cause of end-stage renal failure and can be fatal (Gilbertson et al, 2005; Mogensen et al, 1983). Development of nephropathy is complicated, and the diabetic kidney presents with hyperplasia and hypertrophy of glomeruli (Seyer-Hansen et al, 1980). As kidney tubules grow, the kidney filters increasing amounts of glucose, fatty acids, amino acids, growth factors and cytokines which set off pathological pathways such as energy imbalances, redox complications, inflammation and fibrosis (Mauer et al, 1984; Vallon et al, 2003). Furthermore, kidney disease presents as a risk factor for macrovascular complications (Lancet, 2010), hypertension and impaired glycaemic control (UKPDS, 1998).

1.4.2 Diabetic Retinopathy

Diabetic retinopathy is the major cause of blindness in adults characterised by retinal lesions and changes in vascular permeability, capillary degeneration and excessive neovascularisation (Frank, 2004; Hirai et al, 2011). Retinopathy is defined by non-proliferative and proliferative disease stages. The non-proliferative stage involves hyperglycaemia induced intramural pericyte death and thickening of the basement membrane altering the blood-retinal barrier and vascular permeability but produces no visual impairment (Frank et al, 2004). Ischaemia and release of angiogenic factors can lead to degeneration and occlusion of retinal capillaries and progression into the

proliferative stage where neovascularisation and macular oedema impair vision (Bresnick et al, 1976).

1.4.3 Diabetic Neuropathy

Diabetic neuropathy is estimated to affect more than half of diabetic individuals and brings with it a 15% risk of lower limb amputation (Abbott et al, 2011). Neuropathy is characterised by nerve fiber deterioration leading to loss of sensory perception due to alterations in sensitivity to vibrations and thermal thresholds. Up to 50% of patients with neuropathy experience pain along with hyperalgesia, paraesthesia and allodynia, which collectively impede quality of life (Obrosova et al, 2009). Longer neurons are first to lose conduction velocity hence why loss of sensation is first observed in the feet and later the hands, termed “glove and stocking” distribution. This loss of sensation can allow for injury and infection to go unnoticed leading to the need for amputations (Forbes and Cooper, 2013). There are currently no approved therapies for neuropathy which makes optimised glycaemic control ever more important.

1.4.4 Macrovascular complications

Diabetes increases the risk of cardiovascular disease, raising the risk of myocardial infarction threefold, and accounts for more than half the mortality in diabetes (Haffner et al, 1998; Laing et al, 2003; Domanski et al, 2002). Diabetic individuals exhibit premature atherosclerosis and diastolic dysfunction. The former can give rise

to atherosclerotic plaques that occlude vessels giving rise to cardiovascular events (Okon et al 2005), whilst the latter cardiomyopathy can lead to exertional dyspnoea and heart failure (Boudina et al, 2007). Glycaemic control, assessed using HbA1c, is used to predict cardiovascular risk in diabetes (Borg et al, 2010; Cederberg et al, 2010). Control of glycaemia can limit oxidative stress and chronic inflammation, both of which influence the development of pathogenic thrombogenic plaques (Feng et al, 2005).

1.5 Diabetes therapies

1.5.1 Insulin replacement therapy

For type-1 diabetes insulin replacement therapy is the safest and most widely used treatment. However insulin replacement therapy is increasingly used in type-2 diabetes when oral and peptide derived drugs fail to provide adequate blood glucose control. Correct timing/dosing of insulin to prevent hypoglycaemia is however a risk of this therapy. Advances in chemical modifications to produce insulin formulations with varied half-lives enable patients to achieve both long and short term glycaemic control. Technological advancement has allowed for the development of closed-loop insulin pump systems that act dynamically to release insulin in response to sensing a rise in blood glucose levels (Tasuchmann and Hovorka, 2014). Beta cell replacement therapy either by whole pancreas or islet transplantation has the potential to cure type-1 diabetes (Shapiro et al, 2000) but is limited due to the scarcity of donor islets and adverse effects of long term immunosuppressant drug use. Furthermore, this expensive surgery is not long lasting, with patients showing a decline in islet graft

function over time warranting further transplants. Currently, this therapy is limited to diabetics with intractable hypoglycaemia and brittle diabetes.

For most cases of type-2 diabetes there are a number of different agents available to regulate blood glucose when healthy lifestyle changes fail to keep hyperglycaemia in check. Current anti-diabetic pharmacotherapies improve insulin sensitivity, stimulate glucose-induced insulin secretion and increase excretion / decrease absorption of glucose and carbohydrates respectively.

1.5.2 Biguanides

Metformin is a biguanide drug and is a first line treatment prescribed for type-2 diabetes for almost 4 decades (Pappachan et al, 2018). The anti-diabetic effect of metformin stems from its ability to inhibit hepatic gluconeogenesis and improve insulin sensitivity in peripheral tissues. The mechanism of action is poorly understood, however it is suggested to involve inhibition of mitochondrial respiratory chain. Metformin is generally well tolerated with gastrointestinal side effects (nausea, vomiting and diarrhoea) only being transient. However, a firm contra-indication for metformin use is kidney failure due to increased risk of lactic acidosis (Bailey, 1993). Some studies have found metformin to also reduce body weight and reduce HbA1c particularly when coupled with healthy lifestyle changes (Meneghini et al, 2011; Domecq et al, 2015). Metformin has also been found beneficial for gestational diabetes (Jiang et al, 2015), polycystic ovary syndrome

(Naderpoor et al, 2015) and non-alcoholic fatty liver disease (Chalasani et al, 2012), all of which are conditions that feature insulin resistance.

1.5.3 Sulfonylureas

When metformin is unable to manage type-2 diabetes, clinicians regularly move on to second-line agents such as sulfonylureas (tolbutamide, glicazide) as an additional therapy. These drugs stimulate beta cell insulin release by binding to the ATP-dependant K^+ (K_{ATP}) channel, thus closing the channel leading to cell membrane depolarisation causing voltage gated calcium channels to open and Ca^{2+} influx to the beta cell culminating in exocytosis of insulin containing vesicles (Lebovitz et al 1978; Burke et al, 2008). Given that this mechanism works irrespective of the prevailing glucose level, improper use of sulfonylureas can cause hypoglycaemia. The increase in insulin secretion can also lead to weight gain, with average weight gain reported as 1.8-2.6kg (Domecq et al, 2015), making this anti-diabetic agent less favourable for patients given that obesity is a common co-morbidity.

1.5.4 Meglitinides

Meglitinides, such as regagliinide and nateglinide, have a similar mechanism of action as sulfonylureas albeit with a weaker affinity to the K_{ATP} channel (Malaisse, 2003). These drugs show similar risk of hypoglycaemia however weight gain was found to be lower than treatment with sulfonylureas (Stein et al, 2013).

1.5.5 Thiazolidinediones

Thiazolidinediones, such as pioglitazone, act as insulin sensitizers. They bind to and activate the peroxisome-proliferator-activated receptor gamma (PPARγ), expressed on liver, muscle and adipose tissues (Yki-Jarvinen, 2004), to stimulate glucose and fat metabolism, ultimately reducing glucose levels without affecting insulin release (Grossman et al, 1997). These drugs are used with caution, as rosiglitazone was withdrawn due to cardiovascular concerns, whilst pioglitazone use has been associated with heart failure (Liao et al, 2017), secondary osteoporosis (Billington et al, 2015), fractures (Liao et al, 2017) and urinary bladder cancer (Yan et al, 2018). Furthermore patients can be reluctant to opt for this agent given the mean weight gain of 2.6kg associated with its use (Domecq et al, 2015).

1.5.6 Alpha-glucosidase inhibitors

As the name suggests alpha-glucosidase inhibitors (e.g. acarbose and voglibose) inhibit this brush border enzyme found in the small intestine responsible for cleaving monosaccharides from complex carbohydrates. These drugs act to retard carbohydrate absorption in the intestine which in turn slows glucose release (Lebovitz, 1997). Meta-analysis of α-glucosidase inhibitor use, revealed favourable anti-diabetic outcomes such as a 0.55% reduction in HbA1c, a 3mmol/L reduction in 2 hour postprandial glucose and average 0.63kg body weight reduction (Gao et al, 2018). Many patients discontinue use due to unfavourable side effects of flatulence and diarrhoea.

1.5.7 Dipeptidyl peptidase-4 inhibitors

Dipeptidyl peptidase-4 (DPPIV) inhibitors, such as sitagliptin and vidagliptin, act as incretin enhancers by inhibiting enzymatic breakdown of GLP-1 and GIP. Maintaining active levels of GLP-1 and GIP helps stimulate glucose-dependent insulin release with these two hormones accounting for 50-70% of total insulin secreted in response to oral glucose (Baggio and Drucker, 2007). Furthermore, their actions suppress glucagon release, delay gastric emptying and promote both satiety and weight loss (Mest et al, 2005; Arthen and Schmidtz, 2004; Song et al, 2017; Nauck et al, 1997; Flint et al, 1998). Studies using DPPIV inhibitors in Zucker rats (Pospisilik et al, 2002) showed improved beta cell function, whilst type-2 diabetic patients (Herman et al, 2006) displayed improved glycaemic control and insulin secretion. Additionally, a meta-analysis of DPPIV inhibitor use confirmed reduced postprandial glucose elevation, fasting plasma glucose and HbA1c levels (average 0.5-1% reduction) with little risk of hypoglycaemia or effect on body weight (Lyu et al, 2017; Pappachan et al, 2015). Some murine studies have observed an increase in pancreatic ductal metaplasia, although no such effects have been found in humans (Engel et al, 2013).

1.5.8 GLP-1 receptor agonists

Injectable GLP-1 receptor agonists such as exenatide and liraglutide are DPPIV resistant forms of GLP-1 given to overcome the short half-life of endogenous GLP-1 (Drucker and Nauck, 2006). By exogenous administration they produce the anti-diabetic effects of GLP-1 previously outlined. GLP-1 receptor agonists have been found to benefit other systems, having cardiovascular protective effects (Marso et al,

2016), reducing dyslipidaemia, non-alcoholic fatty liver disease, diabetic kidney disease, blood pressure and affording neuronal protection (Pappachan et al, 2015; Tuduri et al, 2016; Nauck et al, 2017). Given that diabetes and obesity increases the risk of many of these disorders, GLP-1 receptor agonists may provide a useful tool in the arsenal against them. In particular, liraglutide has also been shown to be effective against obesity. When given at a 1.2mg daily dose a 1.7kg body weight loss was reported (Domecq et al, 2015) whilst a supramaximal 3mg daily dose reported a mean weight loss of 8.4kg (Pi-Sunyer et al, 2015). FDA (US Food and Drug Administration) concerns regarding pancreatitis and pancreatic cancer associated with GLP-1 receptor agonist use have been refuted by long-term studies in non-human primates and randomised controlled trials. However, a risk of cholelithiasis was noted (Nybord et al, 2012; Monami et al, 2017).

1.5.9 Sodium glucose cotransporter-2 inhibitors

Sodium glucose cotransporters (SGLT) expressed on kidney tubules are responsible for glucose reabsorption. 90% of glucose filtered through renal glomeruli is reabsorbed by SGLT2 whilst the remaining 10% is reabsorbed by SGLT1 (Gallo et al, 2015). Evidence that SGLT can be pharmacologically inhibited to increase renal glucose excretion has been in the literature since the 1930s (Chasis et al, 1933). Despite this, SGLT2 inhibitor drugs have only been trialled in the past decade. Inhibitors such as dapagliflozin and empagliflozin prevent glucose reabsorption within the proximal renal tubules to increase urinary glucose excretion, ultimately lowering blood glucose in an insulin independent mechanism. SGLT2 inhibitor use

has been shown to reduce HbA1c by 0.66%, body weight by 1.8kg, reduce systolic blood pressure by 4.45 mm of Hg and improve cardiovascular and kidney disease (Vasilakou et al, 2013; Zinman et al, 2015; Wanner et al, 2016). Common side effects and causes for discontinuation are urinary tract infections and genital fungal infections due to high urinary glucose levels (Abdelgadir et al, 2018). The EMPA-REG trial noted prolonged use of empagliflozin resulted in gradual loss of hypoglycaemic effect (Zinman et al, 2015). Reasons for this are not fully understood but many suspect an increase in pancreatic alpha cell mass and increased glucagon release resulting in hepatic gluconeogenesis (Bonner et al, 2015; Hattersley and Thorens, 2015).

1.5.10 Amylin

Amylin is a polypeptide co-secreted with insulin from beta cells and is involved in regulation of insulin and glucagon secretion (Mieticki-Baase, 2016). Pramlinitide is a synthetic analogue prescribed in the USA for both type-1 and 2 diabetes to suppress glucagon secretion and improve metabolic control (Qiao et al, 2017). Major side effects include nausea, vomiting and risk of hypoglycaemia especially when used in conjunction with insulin (Fineman et al, 2002; Qiao et al, 2017).

1.5.11 Bariatric surgery

Bariatric surgery, such as Roux-en-Y gastric bypass (RYGB), gastric banding and vertical sleeve gastrectomy, are currently used for the treatment of gross obesity.

These procedures also induce improvements of blood glucose control and, in some cases, remission of type-2 diabetes (Maleckas et al, 2015). Indeed weight loss by pharmacotherapies has been shown to improve type-2 diabetes by restoring insulin sensitivity, however eventual weight regain leads to worsening diabetes (Johansson et al, 2014; Franz et al, 2007). A meta-analysis concluded that bariatric surgery achieved notably greater weight loss and reductions in HbA1c and fasting plasma glucose compared to medical treatment (Ribaric et al, 2014). Improvements in diabetes are usually observed before substantial weight loss occurs following surgery with the exact reasons for this still not fully understood. The incretin theory suggests that following RYGB there is rapid nutrient delivery to the distal small intestine where L cells are located resulting in increased GLP-1 and peptide YY (PYY) secretion (Strader et al, 2005). Alternative theories to explain the anti-diabetic effect of bariatric surgery include suppression of hepatic glucose production (Mithieux, 2009), increased bile acid production reducing insulin resistance and altering gut microbiota (Watanabe et al 2006; Pournaras et al, 2012; Liou et al, 2013).

These current anti-diabetic agents have undoubtedly improved quality of life for diabetic patients, however they are not without their own adverse effects. Despite their use, secondary diabetic complications still develop and persist. Only through strict blood glucose control have these complications been shown to be slowed (UKPDS 1998; Heller, 2009). As a result, new anti-diabetic therapies that impact development of complications are much sought after. New peptides and hybrid formulations are currently being explored. Novel approaches to restore functional

beta cell mass are being researched including transdifferentiation from other islet cell types to insulin secreting cells, stimulating beta cell proliferation and promoting islet neogenesis from pancreatic progenitor cells (Márquez-Aguirre et al, 2015).

1.6 Islet endocrine plasticity – transdifferentiation

The pathogenesis of beta cell dysfunction in type-2 diabetes has not been fully elucidated. Advancement in lineage tracing technology has brought to light evidence of mature pancreatic beta cells changing from their differentiated state to become dedifferentiated or transdifferentiated into another cell type in models of type-2 diabetes. Beta cell dedifferentiation is classed as a loss of mature beta cell components, usually associated with an increase in the expression of progenitor markers, resulting in reduced insulin secretion (Weir et al, 2013). Transdifferentiation is classified as a differentiated islet cell losing its mature phenotype to produce a different hormone entirely. This process can be direct, in which an islet cell starts to express a second hormone before losing expression of its initial hormone or indirect whereby an intermediate dedifferentiation stage occurs prior to reactivation of transcription factors that lead to differentiation into a different islet cell type (van der Meulen and Huising, 2015).

Murine beta cells have been shown to be capable of dedifferentiating and transdifferentiating into both alpha cells and delta cells. So far extreme experimental conditions have been utilised to cause transdifferentiation of islet endocrine cells, including but not limited to extreme beta cell ablation (Thorel et al, 2010), genetically altering expression of specific transcription factors such as Arx (Courtney et al, 2013),

Pax4 (Collombat et al, 2007), PDX-1 and FOXO1 (Talchai et al, 2012). These transcription factors are clearly vital for both inducing islet endocrine cell differentiation and maintaining this differentiated phenotype. When expression of these transcription factors are lost so too is the mature islet endocrine cell phenotype. This has been shown by Talchai et al, (2012) where natural loss in FOXO1 expression caused by aging results in susceptibility to developing diabetes due to dedifferentiation of beta cells. This process is not restricted to mice with human beta cells both *in vitro* (Weinberg et al, 2007), *ex vivo* (Spikjer et al, 2013; Gershengorn, et al, 2014; Diedisheim et al, 2018) and from type-2 diabetic donors (Cinti et al, 2015) displaying dedifferentiation. This implicates dedifferentiation as a mechanism in the development of type-2 diabetes. Table 1.1 highlights the breadth of studies that have observed changes in beta cell differentiation.

Further studies in both animal models and type-2 diabetic patients (Butler et al, 2007) show low levels of beta cell apoptosis suggesting that these beta cells could be dedifferentiating or transdifferentiating. The latter beta to alpha cell transdifferentiation would also help to explain the increase in alpha cell number and alpha cell infiltration into the core of the islets. However, examination of islets from type-2 diabetics has also suggested that the relative expansion in alpha cell number is partly due to the reduction in beta cell number (Henquin and Rahier, 2011).

A number of specific transcription factors vital for promoting and maintaining mature beta and alpha cells (Figure 1.1) have been outlined by Huising et al, (2015). Beta cell maturity and dedifferentiation and transdifferentiation processes can be monitored using these transcription factors. For beta cells, these transcription factors include

Pdx-1, Foxo1, Nkx6.1 and the secretory hormone insulin. For alpha cells the secretory product glucagon as well as transcription factors Arx and Brn4 can be assessed. Arx is essential for alpha cell development and maturity (Bramswig and Kaestner, 2011) whilst Brn4 is considered to be an alpha cell specific transcription factor (Heller et al, 2004). The progenitor marker Ngn3 can be monitored for identifying dedifferentiated endocrine cells (Talchai et al, 2012).

1.7 Animal models of diabetes

Animal models have played an essential role in the understanding of disease pathology and in identifying novel therapeutic targets (Al-awar et al, 2016). Given the complexity of diabetes and with variations in pathogenesis between type-1 (insulin deficiency) and type-2 (beta cell dysfunction/insulin resistance) a number of different animal models can be employed. For type-1 models, insulin deficiency is commonly attained by chemical ablation of pancreatic beta cells (streptozotocin and alloxan) or through inbreeding of mice strains that spontaneously develop autoimmune diabetes (BB rats, NOD mice and Akita mice) (King, 2012). For type-2 models, recreating insulin resistance and beta cell failure is key. Given that human diabetes is closely related to obesity it is no surprise that diet-induced (high fat fed) and genetic obesity ($Lep^{ob/ob}$ and $Lep^{db/db}$ mice) animal models display type-2 diabetes development.

Streptozotocin is a nitrosurea analogue which shares a similar structure to glucose and is taken up by the pancreatic bet cells via the GLUT2 transporter (Lenzen, 2008; Wang and Gleichmann, 1998). Within the beta cell, streptozotocin alkylates DNA

leading to DNA fragmentation and cell death. A single high dose of streptozotocin (100-200mg/kg in mice) induces rapid destruction of beta cells ensuring hyperglycaemia (Srinivasan and Ramaro, 2007; Dekel et al, 2009). Alternatively multiple low-doses (20-50mg/kg in mice) of streptozotocin administered over 5 days induces insulitis leading to a reduction in islet number and insulin secretory capacity (Gleichman, 1998; Bonnevie-Nielsen et al, 1981; Like and Rossini, 1976). These mice exhibit severe hyperglycaemia with reduced levels of plasma and pancreatic insulin. Reciprocal increases in plasma and pancreatic glucagon are also noted with plasma GLP-1 also raised (Vasu et al, 2015). Islet morphology is markedly altered with severe loss of beta cell mass, largely due to beta cell apoptosis, and expansion of alpha cell mass (Vasu et al, 2015; O'Brien et al, 1996).

Diet induced high fat feeding of C57Bl/6 mice was first used in 1988 to induce type-2 diabetes (Surwit et al, 1988). Several weeks of high fat feeding (approximately 50% fat content) results in obesity and impaired glucose homeostasis attributed to inadequate compensation by islet beta cells. (Winzell and Ahren, 2004). Strain specific variations have been noted with NIH Swiss mice exhibiting hyperglycaemia whilst this isn't present in high fat fed C57Bl/6 mice (Gault et al, 2007; Moffett et al, 2015). C57Bl/6 mice kept on high fat diet for 45 weeks show increased pancreatic insulin content, reduced pancreatic glucagon content with no significant changes in pancreatic GLP-1 and GIP contents (Moffett et al, 2015). Histologically, high fat fed mice exhibit larger islets due to increases in both beta and alpha cell mass, apoptosis and proliferation with altered size distribution favouring larger islets ($<25{,}000\mu m^2$) over smaller islets ($<10{,}000\mu m^2$) (Moffett et al, 2015).

The corticosteroid hydrocortisone can be administered to mice to induce insulin resistance (Bailey and Flatt, 1982; Swali et al, 2008). Despite having no impact on non-fasting glycaemia, hydrocortisone, induces peripheral insulin resistance and causes an increase in plasma and pancreatic insulin levels (Vasu et al, 2015). Histologically, hydrocortisone dosed mice display larger islets associated with increased beta and alpha cell areas with size distribution favouring larger islets. Beta cell proliferation was found markedly increased in these mice with beta cell apoptosis raised but to a much lesser extent (Vasu et al, 2015; Khan et al, 2016; Khan et al, 2017).

1.8 Aims of thesis

The studies presented in this thesis explore beta cell transdifferentiation using *in vitro* and *in vivo* models of diabetes. This is further expanded on to investigate the impact of current antidiabetic therapies on beta-to-alpha transdifferentiation. The aim of each chapter is outlined below:

1. To identify beta-to-alpha cell transdifferentiation by protein and gene expression using established pancreatic beta cell lines. Preliminary investigations into beta cell transdifferentiation in streptozotocin, hydrocortisone, high-fat fed and db/db models of diabetes.
2. To investigate the role of incretin therapies (liraglutide and sitagliptin) on beta-to-alpha cell transdifferentiation in a multiple low-dose streptozotocin, high-fat fed and hydrocortisone models of diabetes.
3. To explore the effect SGLT2 inhibition and insulin on beta cell transdifferentiation in multiple low-dose streptozotocin, high-fat fed and hydrocortisone models of diabetes.
4. To investigate the role of emerging peptide therapies (apelin and xenin) on beta-to-alpha cell transdifferentiation in a multiple low-dose streptozotocin, high-fat fed and hydrocortisone of diabetes.

These studies will attempt to elucidate if beta cell transdifferentiation plays a role in islet adaptation and glucose regulation during diabetes and high fat feeding. Furthermore these studies hope to identify a possible mechanism in which both current and future therapies can treat type-2 diabetes.

Table 1.1: Transdifferentiation of pancreatic endocrine cells

Beta cell dedifferentiation	Reference
Human diabetic donor islets	Cinti et al, 2015
Human islets	Gershengorn et al, 2014
Human islets / EndoC-βH1 cell line, FGF2 exposure	Diedisheim et al, 2018
Non-human primate, diet induced diabetes/obesity	Fiori et al, 2013
Neonatal diabetes	Wang et al, 2014
Db/db mice	Sheng et al, 2015; Ishida et al, 2017
K_{ATP}-GOF mice	Wang et al, 2014
miR-7 overexpressing mice	Latreille et al, 2014
Nkx2.2 knock out	Sussel et al, 1998
Ex vivo mouse islets	Weinberg et al, 2007
Rat 85-95% pancreatectomy	Jonas et al, 1999
β-to-α cell transdifferentiation	**Reference**
Human islets	Spijker et al, 2013
Beta cell specific FOXO1 knock out	Talchai et al, 2012
Misexpression of Arx in beta cells	Collombat et al, 2007
Beta cell specific Pdx-1 knock out	Gao et al, 2014
Nkx2.2 knock out	Papizan et al, 2011
Beta cell specific DNA methyltransferase knock out	Dhawan, 2011
α-to-β cell transdifferentiation	**Reference**
Diphtheria toxin-induced beta cell ablation	Chera et al, 2014
Diphtheria toxin-induced beta cell ablation	Thorel et al, 2010
Metronidazole-induced beta cell ablation	Ye et al, 2015
Alpha cell specific Arx knock out	Courtney et al, 2010
Forced expression of Pax4	Collombat et al, 2010

Figure 1.1: Transcription factors involved in the development and maintenance of alpha, beta and delta cells

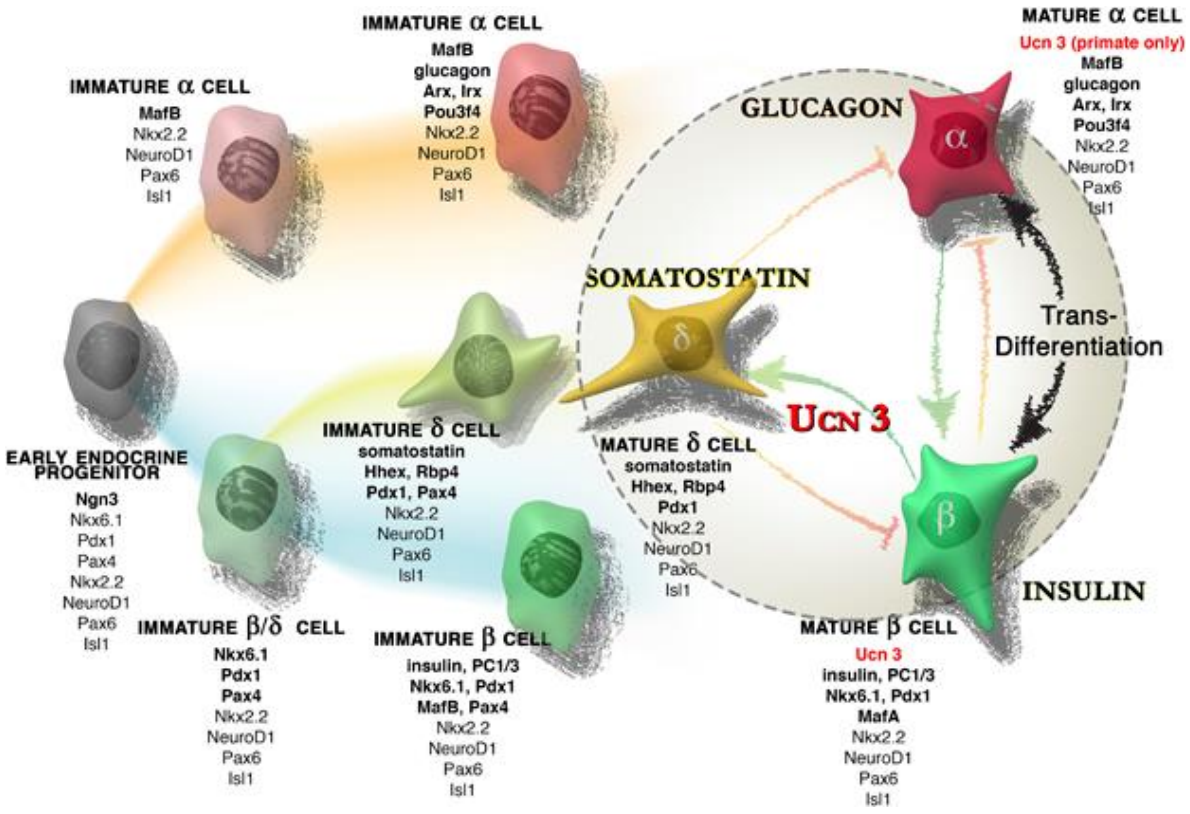

Development of pancreatic endocrine alpha, beta and delta cells derive from a common precursor. The expression and maintenance of specific transcription factors drives maturation into the insulin secreting beta cell or glucagon secreting alpha cell (Huising et al, 2015)

Chapter 2

Materials and Methods

2.1 Materials

Distilled water was produced by a Milli-Q water purification system (Millipore, Millford, MA, USA). Chemicals and reagents were sourced as follows:

Abcam (Cambridge, UK): mouse monoclonal antibody to insulin, goat polyclonal antibody to GFP, rabbit polyclonal antibody to ki-67, rabbit polyclonal antibody to Pdx-1, rabbit polyclonal antibody to GLUT2, rabbit polyclonal antibody to Foxo-1, rabbit polyclonal antibody to Ngn-3 and rabbit polyclonal antibody to Arx.

BDH Chemicals Ltd. (Poole, UK): Acetic acid (glacial), calcium chloride ($CaCl_2.6H_2O$), dichloromethane (CH_2Cl_2), di-sodium hydrogen orthophosphate ($Na_2HPO_{4)}$, ethanol, D-glucose, hydrochloric acid (HCl), magnesium sulphate ($MgSO_4.7H_2O$), paraformaldehyde (PFA), potassium dihydrogen orthophosphate (KH_2PO_4), sodium bicarbonate ($NaHCO_3$), sodium chloride (NaCl), tri-sodium citrate ($C_6H_5Na_3O_7.2H_2O$) and sodium dihydrogen orthophosphate (NaH_2PO_4).

Gibco Life Technologies Ltd. (Paisley, UK): Antibiotics (100U/ml penicillin and 0.1g/L streptomycin), Dulbecco's Modified Eagle Medium (DMEM) (25mM glucose) supplemented with 4500mg/L glucose, L-glutamine and without pyruvate, DMEM (11.1mM glucose) supplemented with L-glutamine and 15mM HEPES, foetal bovine serum (FBS), Hanks buffered saline solution (HBSS 10x stock) and trypsin/EDTA (10x stock).

Invitrogen (Paisley, UK): Alexa Fluor 594 goat anti-mouse IgG (H+L), Alexa Fluor 488 goat anti-mouse IgG (H+L), Alexa Fluor 350 goat anti-mouse IgG (H+L), Alexa Fluor 594 goat anti-guinea-pig IgG (H+L), Alexa Fluor 488 goat anti-guinea-pig IgG (H+L),

Alexa Fluor 594 goat ant-rabbit IgG (H+L), Alexa Fluor 488 goat anti-rabbit IgG (H+L), Alexa Fluor 488 donkey anti-goat IgG (H+L), 100bp DNA ladder, SYBR® Safe DNA gel stain and xylene.

Oxoid (Basingstoke, UK): Phosphate buffered saline (PBS) tablets

Perkin Elmer (Cambridge, UK): Sodium iodide – ^{125}I (74Mbq/20µl stock)

Sigma-Aldrich Chemical Company Ltd. (Poole, UK): Acetonitrile, bovine insulin (crystalline), bovine serum albumin (essentially fatty acid free, endotoxin free), charcoal (activated/untreated), dextran T-70, 4',6-diamidino-2-phenylindole (DAPI), diethyl pyrocarbonate (DEPC), dimethyl sulphoxide (DMSO), C,N-diphenyl-N'-4,5-dimethyl thiazol 2 yl tetrazolium bromide (MTT), ethylene diaminetetraacetic acid (EDTA), glycerol, hydrogen peroxide (H_2O_2; 30% w/w), N-2-hydroxyethylpeprazine-N'-2-ethane=sulphonic acid (HEPES), isopropanol, 2-mercaptoethanol, palmitic acid sodium salt, potassium chloride (KCl), sodium hydroxide (NaOH), standard agarose, streptozotocin, 1,3,4,6-tetrachloro-3α,6α-diphenylglycouril (iodogen), thimerosol, Triton X-100, trizma base, trizma hydrochloride, trypan blue solution (0.4%), tunel reaction mixture and tween-20.

VWR International (Lutterworth, UK): Polysine™ coated slides

2.2 Tissue Culture

All cell lines used were cryopreserved at Ulster University, Coleraine in liquid nitrogen. Cells were cultured in aseptic conditions as described. Thawed cells were suspended in 10ml of warmed tissue culture media and centrifuged at 900rpm for 5

minutes. The resulting pellet was resuspended in a tissue culture flask and stored in an LEEC incubator (Laboratory Technical Engineering, Nottingham, UK) at 37°C supplied with 5% CO_2 and 95% air.

All cell lines were sourced from the Ulster University's cell technology unit. The rat-derived INS-1 clonal cell line was cultured in RPMI-1640 (11.1mM glucose) supplemented with 10% FBS, 1% penicillin-streptomycin (5000IU/l), 200µM 2-mercaptoethanol and 1mM sodium pyruvate (Shi et al, 2011). INS-1 cells contain a high insulin content, are glucose responsive and maintain these beta cell characteristics over 116 passages (Asfari et al, 1992; Merglen et al, 2004). The mouse insulinoma, MIN6 cell line was cultured in high glucose DMEM (22.2mM glucose), 10% FBS, 1% penicillin-streptomycin (5000IU/L) and 200µM 2-mercaptoethanol (Vasu et al, 2015). These cells respond appropriately to glucose within the physiological range however this response has been noted to decline through successive passages (Miyazaki et al, 1990). The rat insulinoma, RINm5F cell line was cultured in RPMI-1640 (11.1mM glucose), 10% FBS and 1% penicillin-streptomycin (5000IU/L) (Flatt et al, 1988; Gazdar et al, 1980). These cell consist of and mainly secrete insulin but have been shown to also produce glucagon and somatostatin (Skelin et al, 2009). Additionally, these cells differ from primary beta cells by their abnormal glucose transport and sensitivity to glucose (Halban et al, 1983).

Cells were routinely passaged in the following manner. Confluent flasks of cells were aspirated of media and washed with hanks buffered saline solution (HBSS) to remove the FBS coating. 5ml of warmed trypsin (50ml 10X trypsin-EDTA with 450ml HBSS) was added to culture flasks and kept at 37°C for 5 minutes to allow cellular

detachment from the flask surface. After confirmation of detachment under the microscope, trypsin action was neutralised by the addition of 7ml trypsin and transferred to a sterlin tube (Sterlin Ltd, Hounslow, UK) and cells were pelleted by centrifugation at 900rpm for 5 minutes. The supernatant was discarded and a single cell suspension was created by addition of fresh media. 100µl of this suspension was counted using a Neubauer haemocytometer (Scientific Supplies Co., UK). Once counted cells were seeded at a specified density for experiments or returned to the culture flasks.

2.3 Determination of cell viability by MTT

The MTT is a colorimetric assay to indirectly assess mitochondrial oxidative processes to determine cell viability. This assay was conducted on cell monolayers (INS-1, MIN6 & RINm5F) cultured in 24 well plates for 24 or 48 hours in the following test conditions: normal media, glucotoxic (25mM glucose), lipotoxic (0.25mM palmitate), cytokine cocktail (300U/ml IL-1β, IFN-γ and 40U/ml TNF-α) and hydrogen peroxide (1mM). 5mg/ml stock MTT was made by dissolving MTT (C,N-diphenyl-N'-4, 5-dimethyl thiazol-2-yl tetrazolium bromide) (Sigma-Aldrich,) powder in KRB buffer which was then wrapped in foil to protect from light. Working MTT was prepared by a 1:10 dilution of this stock with KRB buffer with 5.6mM glucose. 1ml of this working solution was pipetted to each well and allowed to incubate at 37°C for 60 minutes. This incubation time allows metabolically active and thus viable cells to reduce this tetrazole to form a precipitate. Following aspiration of the MTT solution 250µl of DMSO was added to each well to solubilise the precipitate. 100µl aliquot of each

sample was transferred to a 96 well plate and read using a Flexstation spectrophotometer measuring absorbance at 570nm.

2.4 Immunocytochemistry

Fluorescent immunocytochemistry was carried out on cell monolayers to assess protein expression. Cell lines were cultured on sterilised 16mm circular glass cover slips in the previously stated test conditions for 24 and 48 hours. Following culture, media was aspirated from the wells and cells were washed with PBS before fixation by immersion in 4% paraformaldehyde for 30 minutes. Heat mediated antigen retrieval was carried by addition of 1ml sodium citrate buffer and incubation for 20 minutes at 95°C followed by a further 20 minutes at room temperature to cool. BSA blocking was then carried out by addition of 1ml 3% BSA solution and incubation at room temperature for 45 minutes. Primary antibodies were then made up to the manufacturer's guidelines (Table 2.1) and 200µl added per well and allowed to incubate overnight at 4°C. The next day, cells were washed twice with PBS to remove excess antibody. Fluorescently labelled secondary antibody (Table 2.1) was diluted 1/300 and added, 200µl/well, and allowed to incubate at 37°C for 45 minutes. After this period cells were washed twice with PBS before addition and incubation with DAPI for a further 15 minutes at 37°C. A final two washes with PBS was then carried out before careful removal of the cover slips onto polysine coated slides. Cells could then be imaged and photographed using a fluorescent microscope (Olympus system microscope, model BX51) fitted with FITC (488nm) and TRITC (594nm) filters with Cell^F software. Immunocytochemistry was quantified by counting expression of

proteins of interest within the cells from >5 frames, with each frame containing >150 cells using ImageJ software.

2.5 mRNA extraction and conversion to cDNA

mRNA was extracted from cultured cells using the trizol method as follows. Cultured cells were first washed in HBSS before 10 minutes incubation with 1ml TRI reagent (Sigma-Aldrich,). After mixing, the lysed cell solution was transferred to a 1.5ml Eppendorf and centrifuged at 12,000G for 10 minutes at 4°C. The resulting supernatant was transferred to a fresh Eppendorf, leaving behind the insoluble material. 200µl of chloroform was then added to the cell lysate and mixed thoroughly before centrifuging at 12,000G for 15 minutes at 4°C. Of the three distinct layers produced, the upper aqueous layer of RNA was extracted and mixed with 500µl isopropanol and centrifuged at 14,000G for 20 minutes at 4°C in order to precipitate the RNA. The RNA precipitate was washed thrice in 75% ethanol before finally being solubilised in 20µl RNA-free water. To determine the concentration and purity of RNA a 1µl sample was tested on a NanoDrop ND-1000 UV/Vis spectrophotometer. All mRNA samples were stored at -70°C, however only samples showing an OD260/OD280 ratio >1.8 were considered pure and used for cDNA conversion.

1-3µg of cDNA was generated by reverse transcription of mRNA as follows. OligoDT was added to RNA samples and heated to 70°C within a thermocycler to denature the secondary structure of RNA and allow annealing. A mastermix of first strand buffer, dNTPs, DTT and superscript reverse transcriptase was then added and left to incubate in the thermocycler at 42°C for 1 hour. Following this time the mixture was

then heated to 70°C to inactivate the transcriptase enzyme. The concentration of cDNA was confirmed using a NanoDrop ND-1000 UV/Vis spectrophotometer. cDNA samples were stored at -20°C until required.

2.6 Real time reverse transcription polymerase chain reaction (Real time RT-PCR)

An 18µl PCR reaction mix was established comprised of 9µl SYBR green, 6µl RNA-free water, 1µl primers (forward and reverse) and 1µl previously generated cDNA. A negative template control for each primer and a housekeeping β-actin positive control was run with each PCR. Reactions were conducted in 8-well low tube strips with clear low flat caps (BioRad). Amplification was carried out using a Miniopticon two-colour real time PCR detection system under the following conditions: 1. Initial denaturation 95°C, 5 minutes, 2. Final denaturation 95°C, 30 seconds, 3. Annealing 58°C, 30 seconds, 4. Extension 72°C, 30 seconds. The results were analysed using crossing points (Cp) from genes of interest normalised in respect the housekeeping β-actin control.

2.7 Animals

8 week old male C57Bl/6 mice were purchased from [Envigo, UK]. Breeding pairs of *Ins1*$^{cre/+}$ and Rosa26-eYFP mice were purchased from the Jackson Laboratory, New York, USA (Thorens et al, 2015). In brief *Ins1*$^{cre+/-}$ mice were generated by homologous recombination of *Cre* within the second exon of the *Ins1* gene. These *Ins1*$^{Cre+/-}$ mice were then crossed with established *Rosa26-eYFP* mice to generate *Ins1*$^{cre/+}$;Rosa26-

eYFP mice (Figure 2.1; Srinivas et al, 2001). Selective Cre recombination of floxed *eYFP* gene within beta cells tags them with a fluorescent marker from birth allowing for lineage tracing experiments (Figure 2.2). Identification of tagged cells is carried out by immunohistochemical staining for GFP which binds to the YFP expressed only within tagged cells (Thorens et al, 2015). Generation of this double-transgenic colony was carried out in-house by crossbreeding both strains of mice and subsequent inbreeding of double knock-in transgenic mice. Genotyping was carried out, once 3-4 weeks old, to confirm the genotype of the offspring. For streptozotocin/hydrocortisone studies, mice were used aged 12 weeks. For diet-induced diabetic studies, mice were kept on a high fat diet for 11 weeks until obese. Animals were housed within the University Behavioural and Biomedical Research Unit kept in temperature-controlled rooms (22°C) under 12 hour light-dark cycle (0800-2000hr) with access to standard chow diet (60% carbohydrate, 30% protein and 10% fat) (Trouw Nutrition, Cheshire, UK) and drinking water *ad libitum*. To ensure welfare, the unit was maintained by fully trained staff. When conducting studies animals were single-housed with access to food and drinking water *ad libitum*, unless stated. All procedures were carried out with ethical approval and strict adherence to the UK Animals (Scientific Procedures) Act 1986.

2.8 Genotyping

To confirm genotype of transgenic mice genotyping was carried out. Mice were lightly anaesthetised under isoflurane before excision of 1mm section of ear tissue which was then kept in RNA-free water (39µl). To digest the tissue and extract DNA,

10µl 5X Bioline PCR buffer and 1.3µl Proteinase K (20mg/ml) were added to make a 50µl reaction mix. Samples were run in the thermocycler to induce heat-activated proteinase K enzyme action first for 40 minutes at 60°C, followed by 10 minutes at 95°C to terminate enzyme activity. PCR was then used to amplify the inserted genes of interest (*Ins1*^{Cre} and eYFP). A 25µl reaction mix was concocted using 18µl RNA-free water, 2.5µl 5X Bioline PCR buffer, 0.2µl primer pair mix (50µM), 1.25µl DMSO, 0.1µl Bioline Taq Polymerase and 3µl of Proteinase K reaction mix. PCR amplification was carried out on the thermocycler under the following settings: 1. Initial denaturation 94°C, 3 minutes, 2. Final denaturation 94°C 1 minute, 3. Annealing 58°C, 4. Extension 72°C, 1 minutes, 5. Repeat steps for 35 cycles. The PCR product was then run on a 1% agarose gel to visualise expression of transgenes to determine mice genotype. 250ml 50X Tris Acetate-EDTA (TAE) buffer for electrophoresis was made up consisting of 60.5g TRIS base, 14.275ml glacial acetic acid, 4.65g disodium EDTA and 250ml water. Ultrapure agarose (Invitrogen, UK) was dissolved in 1X TAE buffer (1% w/v) by heating. Upon cooling SYBR Safe DNA dye (Invitrogen, UK) was added (1µl/10ml) before casting into moulds and combs added to create wells. Once solidified gel was placed in an electrophoresis tank and immersed in 1X TAE buffer. To identify loaded wells PCR reaction products were mixed with orange G dye (2mg/ml, dissolved in 30% glycerol) (Sigma-Aldritch, UK) before loading into wells. To identify bands 5µl of 100bp ladder (Invitrogen, UK) was all loaded into one well. The current was set to 100V and the electrophoresis allowed to run for 25 minutes whereby DNA had separated by size and traversed the gel. Gels were then read on the G-box imaging machine where visualisation of *Ins1*$^{Cre/+}$ (675bp) and eYFP (422bp) bands were a

positive confirmation of genotype (Figure 2.1). Amplification and visualisation of housekeeping β-catenin (220bp) was used as a positive control.

2.9 Glucose tolerance test

Intraperitoneal glucose tolerance tests were conducted on overnight fasted mice. A tail vein bleed from conscious mice was used to withdraw blood which was collected into heparin-coated microcentrifuge tubes (Sarstedt, Numbrecht, Germany) and kept on ice. Blood was collected by this method at time point 0 minute prior to dosing the glucose load (18mmol/kg body weight) and at 15 minute, 30 minute and 60 minute time points. Determination of blood glucose was also conducted at these time points using an Accu-Check® Aviva meter with their associated Aviva® sensor test strips. To separate plasma from blood cells, blood samples were centrifuged for 5 minutes at 13000g at 4°C using a Beckman microcentrifuge (Beckman Instruments, Galway, Ireland). Separated plasma, needed for determining plasma insulin, was stored in 1.5ml Eppendorf tubes at -20°C.

2.10 Pancreatic insulin and protein content

Upon completion of an *in vivo* study, the pancreas was harvested from each mouse and sectioned longitudinally, with half kept for histological analysis and half snap frozen in liquid nitrogen and kept for protein extraction. This latter half was weighed and homogenised in ice cold acid ethanol (75% (v/v) ethanol, 23.5% (v/v) distilled water and 1.5% (v/v) 12N HCl) within 8ml bijou tubes. Protein extract samples were

centrifuged at 3000RPM for 20 minutes at 4°C and the resulting supernatant transferred to a 15ml centrifuge tube. pH neutral TRIS buffer was added and samples dried out to a fine powder within the speedvac. Finally, protein samples were resuspended in 2ml TRIS buffer and stored at -20°C until needed. Insulin content was assessed using an insulin radioimmunoassay, whilst total protein content in extracts was assessed using a Bradford assay as described. BSA standards were prepared in triplicate ranging from 0 – 2 mg/ml (0, 0.13, 0.17, 0.23, 0.3, 0.4, 0.55, 0.75, 0.96, 1.31, 1.75 & 2mg/ml) concentrations in distilled water whilst 5µl of diluted samples were added in duplicate to a 96 well plate. 250µl of 1:8 distilled water diluted Bradford reagent was then added to all wells and left to incubate at room temperature for thirty minutes. Following this incubation the plate was read using a V_{max} plate reader to measure absorbance at 595nm wavelength. Sample protein content was then determined using the linear range of the generated standard curve (Figure 2.3).

2.11 Plasma and pancreatic glucagon content

Glucagon levels were assessed by glucagon ELISA (EZGLU-30K, Millipore, Millford, MA, USA) conducted under manufacturer's guidelines. Plasma and pancreatic extract samples were first processed to extract protein. 50µl plasma or 150µl pancreatic extract was mixed with 75µl or 225µl acetonitrile respectively before centrifugation at 17,000G for 5 minutes. The resulting supernatant was transferred to a fresh Eppendorf and dried down to a fine powder using the speedvac. Samples were reconstituted in 30µl of assay buffer for ELISA. Glucagon standards were established in duplicate ranging from 0-2ng/ml (0, 0.02, 0.05, 0.1, 0.2, 0.5, 1 & 2ng/ml, Figure 2.4)

in assay buffer. The ELISA plate was rinsed in wash buffer prior to use and addition of 20µl assay buffer, 10µl standards/samples and 20µl antibody capture/detection mixture. The plate was sealed and left on a rocker at 4°C for 44 hours. Following this incubation period, the plate was rinsed three times in wash buffer before the addition of 100µl of enzyme solution and a further incubation at room temperature for 30 minutes. A further six washes were carried out after this incubation and 100µl working substrate solution added. The plate was left on a plate shaker for 1 minute and then relative light units were recorded on a luminometer plate reader at 425nm.

2.12 Iodination of insulin

To quantify insulin levels in cell and plasma samples an in-house radioimmunoassay was carried out using iodinated insulin. Our in-house protocol for iodinating insulin involves: overnight evaporation of 100µl iodogen (1,3,4,6-tetrachloro-3α, 6α-diphenylcoluril) dichloromethane solution (100µl/ml) within a flow hood. The next day, bovine insulin was made up by dissolving 1mg in 10mM HCl before being diluted in sodium phosphate buffer to 125µg/ml. 20µl of this bovine insulin solution was transferred to the coated iodogen tubes before addition of 5µl $Na^{125}I$ (74MBq/20µl). This solution was allowed to mix on ice for 15 minutes. After this time, the solution was transferred to a fresh Eppendorf tube containing 500µl sodium phosphate buffer (50mM). Reverse phase high performance liquid chromatography (LKB, Bromma, Sweden) was carried out to separate the reaction mixture. Solvent A (0.12% (v/v) trifluoroacetic acid (TFA) in water) and solvent B (0.1% (v/v) TFA in 70% acetonitrile dissolved in 30% (v/v) water) made up the mobile phase of the reaction. The 4.6

x250mm Vydar C-8 analytical reverse HPLC column (Hesperia, Ca, USA) was first washed with solvent A. The reaction mixture was then added and the concentration of solvent B raised in the following stages: 0% - 40% duration 10 minutes, 40% - 80% duration 40 minutes, 80% - 100% duration 10 minutes. 1ml of eluent was collected each minute over the 60 minute period. From these 60 fractions, 5µl from each was analysed for radioactivity on the gamma counter (1261 Multigamma counter LKB Wallac, Finland) and those with a suitable binding affinity were kept at 4°C (Figure 2.5).

2.13 Insulin Radioimmunoassay (RIA)

Insulin release was determined by dextran-coated charcoal radioimmunoassay characterised by Flatt and Bailey (1981). Stock RIA buffer was prepared consisting of 40mM sodium phosphate buffer, 0.3% (w/v) sodium chloride, 0.02% (w/v) thimerosal. 40mM sodium dihydrogen orthophosphate base was then added to adjust the pH of the final stock to pH7. A working RIA buffer was then used by dissolving bovine serum albumin (BSA) (0.5g/100ml) in stock RIA buffer. Rat insulin standards were serial diluted in working RIA buffer from 20ng/ml to 0.039ng/ml in triplicate LP3 tubes. Unknown samples were used in duplicates and contained 200µl of sample, 100µl guinea pig anti-porcine insulin antiserum (IAS PID, 1:30,000-1:45,0000 dilution) and 100µl of labelled I^{125} insulin (~10,000 counts per minute (CPM) per 100µl in working RIA buffer). To allow equilibrium, between labelled and unlabelled insulin, samples were kept at 4˚C for 48 hours. To prepare stock dextran coated charcoal (DCC) solution, 5g dextran T70 and 50g charcoal was dissolved in 1

litre stock RIA buffer and kept at 4°C until required. A 1:4 dilution of this stock DCC with stock RIA buffer was used to generate working DCC with 1ml added to every standard and sample tube except for total counts and allowed to incubate at 4°C for 20 minutes. The tubes were then centrifuged for 20 minutes at 4°C at 2500rpm (Model J-6B centrifuge, Beckmann instruments Inc, UK). Following decantation of the resulting supernatant, the remaining charcoal pellet was assessed for radioactivity in the gamma counter (1261 Multigamma counter, LKB Wallac, Finland). The spline curve-fitting algorithm was used to determine the concentration of insulin in unknown samples.

2.14 Tissue processing for Immunohistochemistry

Excised pancreatic tissues from mice were fixed in paraformaldehyde solution (4% w/v in phosphate buffered saline) for ~48 hours to cross-link proteins, thereby preserving cellular architecture. Tissue processing was then carried out using an automated tissue processor (Leica Biosystems, Nussloch, Germany). In brief, this involved dehydrating tissues in increasing concentrations of ethanol (70-100%) before immersion in xylene to clear the alcohol and allow for embedding in warm paraffin wax. Once embedded and cooled the tissues were then sectioned into 5µl slices using a microtome (Leica Biosystems, Nussloch, Germany) and placed onto Polysine coated slides (VWR,).

2.15 Immunohistochemistry (fluorescence immunoreactivity)

Immunoreactive staining for insulin, glucagon, GFP, Pdx-1, GLUT2 and ki-67 was assessed, first by dewaxing slides by immersion in xylene for 20 minutes. Following this, sections were rehydrated in decreasing concentrations of ethanol (100-50%) before carrying out heat-mediated antigen retrieval, to break down PFA cross-links so antibody can later bind, in sodium citrate buffer (10mM sodium citrate, pH6.0) for 20 minutes at 95°C. Slides were then given 20 minutes to cool before addition of 3% bovine serum albumin (BSA) blocking solution (3% w/v in phosphate buffered saline), to block non-specific antibody binding, for 45 minutes at room temperature. Sections were then incubated overnight at 4°C with primary antibodies listed in Table 2.1. The next day, excess antibody was removed by rinsing slides three times in PBS for 5 minutes each. Slides were then incubated with the relevant fluorophore conjugated secondary antibodies (table 2.1) for 45 minutes at 37°C. Excess antibody was then removed by washing slides thrice in PBS for 5 minutes each. Slides were then incubated with nuclear stain DAPI dihydrochloride (300nM in PBS) for 15 minutes at 37°C. A final set of rinsing in PBS was done to remove excess DAPI before mounting the slides using aqueous mounting medium (glycerol:PBS – 1:1) and cover slips. Resulting slides were viewed using a fluorescent microscope (Olympus system microscope, model BX51) fitted with the FITC, TRITC and DAPI filters. Islets were photographed under TRITC and FITC filters using the linked camera adapter system (DP70 digital camera system) on Cell^F software. To assess beta cell apoptosis a TUNEL assay was carried out following manufacturer's guidelines (In situ cell death kit, Fluorescein, Roche Diagnostics, UK). In brief, following immunostaining for

insulin/glucagon, slides were incubated in TUNEL solution for 1 hour at 37°C before subsequent rinsing in PBS.

2.16 Image Analysis

Images were analysed using Cell^F imaging software to assess: islet area, beta cell area, alpha cell area (expressed at μm^2), percentage beta cells and percentage alpha cells. For islet size distribution islets were defined as small, medium or large if they were <10,000μm^2, 10,000-25,000μm^2 or 25,000μm^2 respectively. Islet architecture was defined by the proportion of islets displaying central alpha cells. To define beta cell transdifferentiation, insulin, GFP staining was assessed by quantifying the number of insulin negative, GFP positive staining cells, whilst glucagon, GFP staining was assessed by quantifying glucagon positive, GFP positive staining cells. Beta cell and alpha cell apoptosis was quantified by counting the number of insulin positive or glucagon positive, TUNEL positive cells respectively. Similarly this was done to analyse proliferation in beta and alpha cells using ki-67 co-stained with insulin or glucagon respectively. ImageJ software was used to quantify beta cell Pdx1 expression, expressed as a percentage of the number of insulin positive cells expressing Pdx1. All counts were determined in a blinded manner with >60 islets analysed per treatment group.

2.17 Statistics

Graphpad PRISM (version 5) software was used to analyse results with data presented as mean plus or minus standard error of the mean (SEM). Groups of data

were compared and statistical analysis carried out using two-tailed unpaired Student's *t*-tests or one-way ANOVA, two-way ANOVA, with Bonferroni post-hoc test as specified. Results were deemed significant if $p<0.05$.

Table *2*.1: Antibodies used for immunohistochemistry and immunocytochemistry

Primary Antibodies				
Target	**Host**	**Clonality**	**Dilution**	**Source**
Insulin	Mouse	Monoclonal	1:400	Abcam (ab6995)
Glucagon	Guinea-pig	Polyclonal	1:400	Raised in-house (PCA2/4)
GFP	Goat	Polyclonal	1:1000	Abcam (ab5450)
Ki-67	Rabbit	Polyclonal	1:500	Abcam (ab15580)
Pdx-1	Rabbit	Polyclonal	1:200	Abcam (ab47267)
GLUT2	Rabbit	Polyclonal	1:200	Abcam (ab54460)
Foxo-1	Rabbit	Polyclonal	1:200	Abcam (ab52857)
Ngn-3	Rabbit	Polyclonal	1:200	Abcam (ab38548)
Secondary Antibodies				
Target	**Host**	**Reactivity**	**Dilution**	**Source**
IgG	Goat	Mouse	1:400	Alexa Fluor 594, Invitrogen
IgG	Goat	Mouse	1:400	Alexa Fluor 488, Invitrogen
IgG	Goat	Mouse	1:400	Alexa Fluor 350, Invitrogen
IgG	Goat	Guinea-pig	1:400	Alexa Fluor 594, Invitrogen
IgG	Goat	Guinea-pig	1:400	Alexa Fluor 488, Invitrogen
IgG	Goat	Rabbit	1:400	Alexa Fluor 594, Invitrogen
IgG	Goat	Rabbit	1:400	Alexa Fluor 488, Invitrogen
IgG	Donkey	Goat	1:400	Alexa Fluor, 488, Invitrogen

Figure 2.1: *Ins1*$^{cre+/-}$*;Rosa26-eYFP* mice

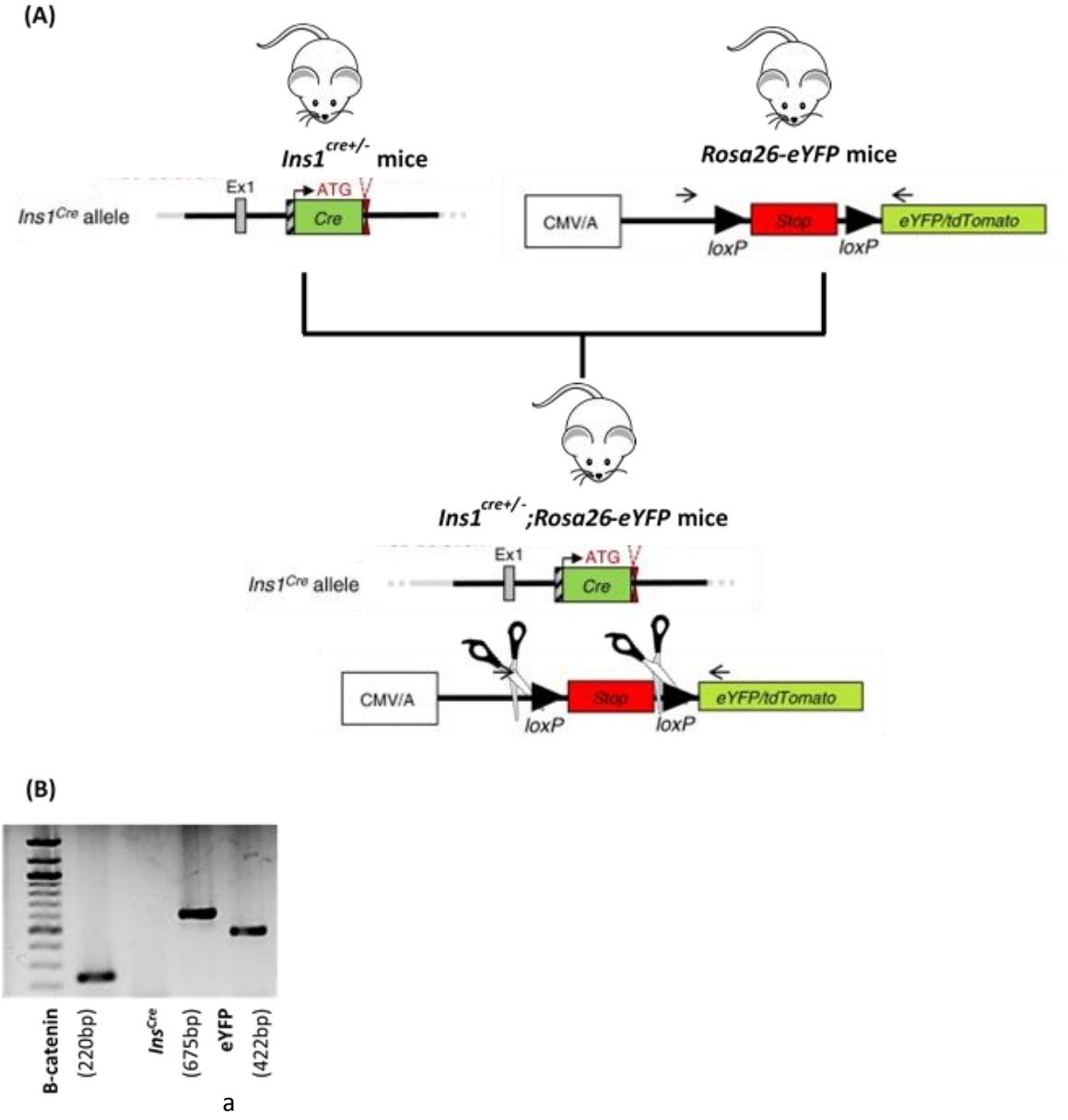

Generation of double knock-in *Ins1*$^{cre+/-}$*;Rosa26-eYFP* mice (Thorens et al, 2015). (A) Tissue specific cre-lox mediated expression of eYFP within beta cells due to selective knock in of Cre recombinase within *Ins1* gene. (B) PCR analysis confirming expression of *Ins1*^{cre}and *eYFP* transgenes.

Figure 2.2: Beta cell specific GFP expression in *Ins1*$^{cre+/-}$*;Rosa26-eYFP* mice

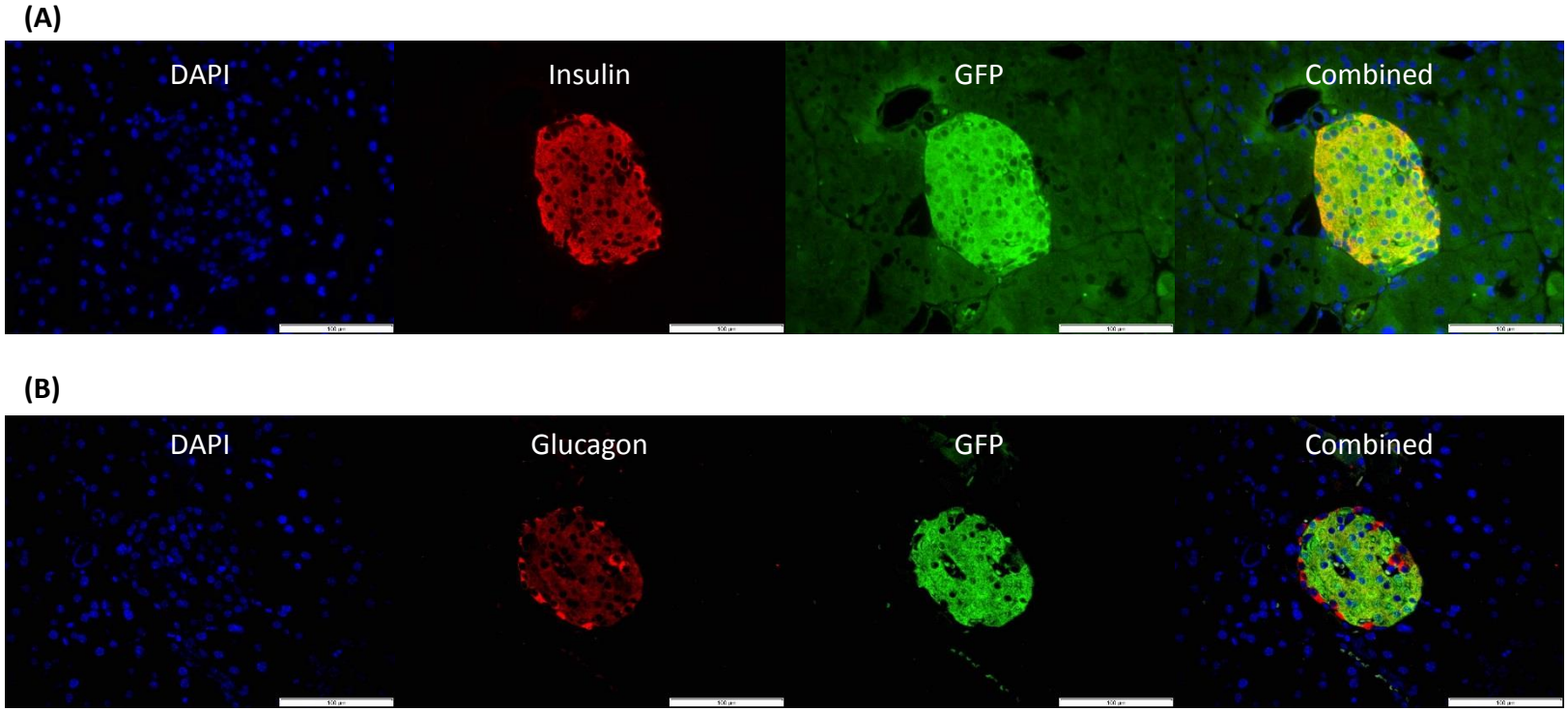

Representative images from *Ins1*$^{cre+/-}$*;Rosa26-eYFP* mice showcasing expression of GFP exclusively within pancreatic beta cells. Confirmed by immunohistochemistry for (A) insulin (red) and GFP (green) and (B) glucagon (red) and GFP (green).

Figure 2.3: Quantification of total proteins by Bradford assay using BSA standards

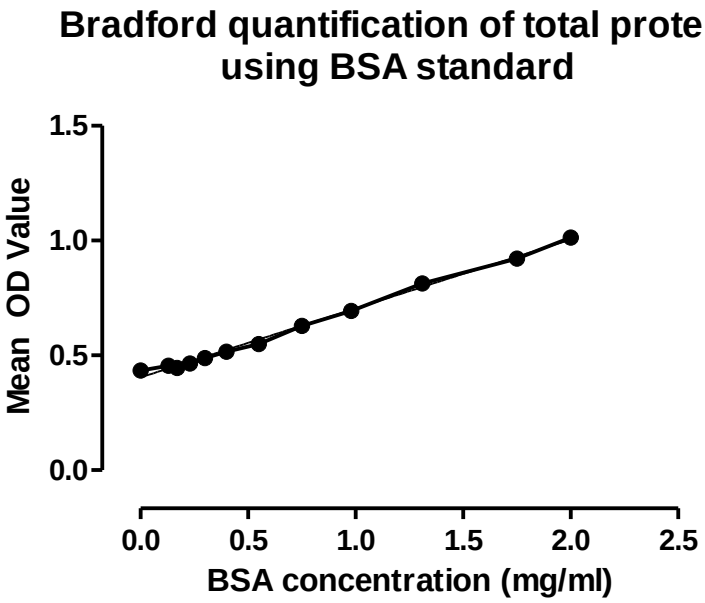

Figure 2.1: Total protein quantification determined by Bradford assay using bovine serum albumin as standards from concentrations ranging from 0-2mg/ml. Values are mean±SEM, n=3

Figure 2.4: Glucagon ELISA standard curve

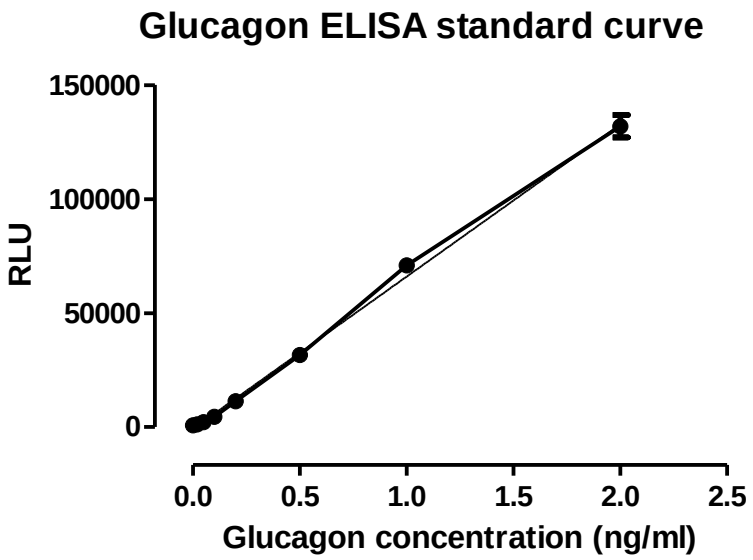

Figure 2.2: Glucagon quantification determined by ELISA using standards from concentrations ranging from 0-2ng/ml. Values are mean±SEM, n=3.

Figure 2.5 Iodination of insulin

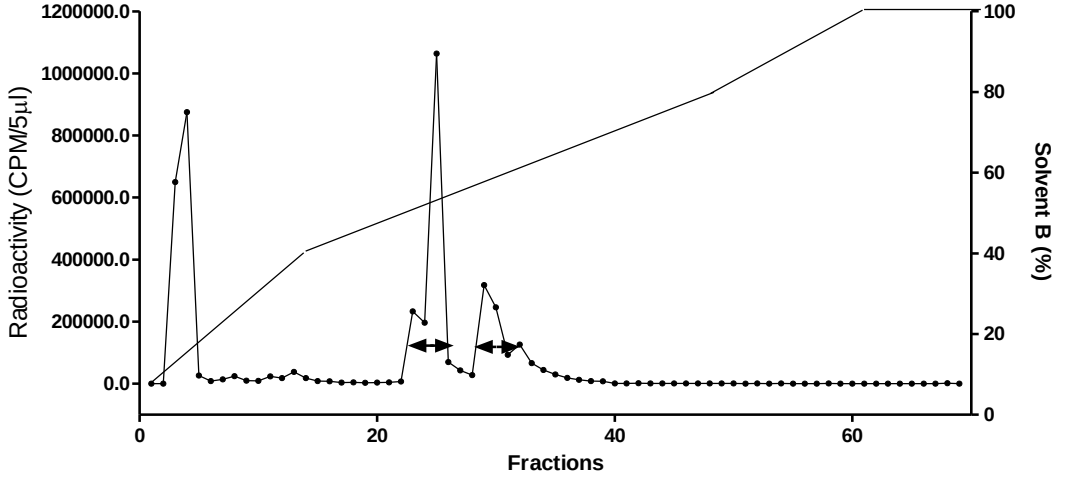

Figure 2.3: Purification of iodinated insulin by RP-HPLC. I^{125} labelled insulin was prepared by solid-phase iodogen method and purified by HLPC. The peak fraction, eluting at 23-35 minutes (see arrows), was used for insulin RIA.

Chapter 3

Signs of beta cell transdifferentiation *in vitro* and *in vivo*

3.1 Summary

Beta-to-alpha cell transdifferentiation was assessed using beta cell lines (INS-1, MIN6 and RINm5F cells) following long-term exposure to known beta cell stressors (high glucose, lipid toxicity and cytokine toxicity). INS-1 cells proved to be most susceptible to changes in plasticity with lipotoxic and cytokine exposure resulting in an increase in cells co-expressing insulin and glucagon or purely expressing glucagon. Changes suggestive of beta cell transdifferentiation were observed at a gene expression level with downregulation of beta cell markers (insulin, GLUT2 and FOXO1), upregulation of alpha cell (glucagon and Arx) and progenitor markers (Ngn-3). Streptozotocin treated C57Bl/6 mice exhibited hyperglycaemia linked to a loss of beta cell mass. Alpha cell mass was greatly expanded and distributed within the core of the islet. Beta cell markers Pdx1 and GLUT2 were reduced which, considered in the context of alpha cell expansion, could suggest beta-to-alpha cell transdifferentiation. Hydrocortisone produced beta cell mass expansion to overcome steroid induced insulin resistance. Hydrocortisone did not impact alpha cell mass greatly so the potential for beta-to-alpha cell transdifferentiation was limited. However reductions in Pdx1 and GLUT2 observed suggest beta cell dedifferentiation. Similarly, there was little suggestion of beta cell transdifferentiation in db/db mouse islets as beta and alpha cell masses expanded proportionally to one another. High fat fed mouse islets displayed a disproportional increase in alpha cell mass compared to beta cell mass expansion suggestive of beta-to-alpha cell transdifferentiation. Exendin-4 limited this alpha cell expansion implicating the role of incretins in maintaining beta cell maturity. These studies emphasize the need for lineage tracing to reliable identify and quantify beta-to-alpha cell transdifferentiation.

3.2 Introduction

Beta cell lines have been generated to mimic primary beta cell physiology in order to investigate beta cell function and dysfunction. Understanding this physiology may aid the development of novel therapies for diabetes. Given that primary beta cells poorly proliferate, much effort has been taken to generate immortalised beta cell lines that retain regulated insulin secretory activity. Ideally these cells lines should contain a high insulin content, express beta cell specific proteins (glucokinase and GLUT2) and exhibit glucose responsive insulin secretion (Skelin et al, 2010).

The insulinoma cell line INS-1 is a rat derived X-ray radiation induced cell line (Asfari et al, 1992; Merglen et al, 2004). Despite only producing 20% of the total insulin content of primary beta cells the INS-1 cell line is glucose responsive due to expression of GLUT2 and glucokinase. MIN6 cells are derived from a transgenic mouse expressing the SV40 T-antigen within the insulin promoter leading to an insulinoma (Miyazaki et al, 1990; Vasu et al, 2015). The rat insulinoma cell line (RINm5F) were one of the first beta cell lines generated from the X-ray radiation induced insulinoma in NEDH rats (Gazdar et al, 1980; Skelin et al, 2009). These cells contain small amounts of insulin however they also contain glucagon and somatatosatin. Other abnormalities in glucose responsiveness and transport have also been noted. (Gazdar et al, 1980; Praz et al, 1983; Halban et al, 1983).

A number of stressors have been found to impact on the viability and function of pancreatic beta cell lines. These effects translate to both rodent and human islets, emphasising the benefits of cell models in understanding diabetes aetiology (Vasu et al, 2014). Pancreatic beta cell lines show reduced insulin content and gene expression

when exposed to a cytokine cocktail of IFNγ, IL-1β and TNFα or lipotoxic conditions (Vasu et al, 2013; Vasu et al, 2014). Similarly, INS-1 and MIN6 cells have been found to be susceptible to lipotoxic palmitate which induces ER stress leading to beta cell apoptosis (Sargysan et al, 2011; Lee et al, 2011; Karaskov et al, 2006). Long term culture in these stress conditions may have the potential to cause beta cell transdifferentiation within cell lines.

The leptin receptor deficient db/db mice are widely used as a monogenic model of obesity and type-2 diabetes. This spontaneous mutation originated within the Jackson Laboratory and was found to be caused by an autosomal recessive mutation in the leptin receptor (Hummel et al, 1966; Chen et al, 1996; Lee et al, 1996). Leptin, an adipokine, is involved in satiety with its loss of function resulting in hyperphagia, obesity, hyperinsulinaemia and hyperglycaemia (Srinivasan and Ramarao, 2007; Pathak et al 2015). Islets from these mice show irregular morphology displaying islet hypertrophy with the ordered architecture of beta and alpha cells becoming mixed (Kawasaki et al, 2005). These mice can also be used as a model of beta cell dedifferentiation given their reduction in several beta cell markers (insulin, Foxo1, MafA and NeuroD1) and upregulation of progenitor marker Aldh1a3 (Ishida et al, 2017; Kjørholt et al, 2005).

The present studies will utilise the three described cell lines (INS-1, MIN6 and RINm5F) hoping to identify beta cell transdifferentiation in response to known beta cell stressors. Preliminary *in vivo* studies involving C57Bl/6 mice will look to identify signs of beta cell transdifferentiation in multiple low dose streptozotocin and hydrocortisone models of diabetes. Finally analysis of islet morphology using samples

from high fat fed mice (Vasu et al, 2017) and leptin receptor deficient mice (Pathak et al, 2015) will be examined for signs of beta cell transdifferentiation.

3.3 Methods

Materials and methods have been briefly summarised below. Full explanations of each method can be found within Chapter 2.

3.3.1 Cell Culture and stressor conditions

All cell lines were cultured under aseptic conditions as described. INS-1 cells were cultured within RPMI-1640 (11.1mM glucose) supplemented with 10% FBS, 1% penicillin-streptomycin antibiotics, 200μM 2-mercaptoethanol and 1mM sodium pyruvate. MIN6 cells were maintained in DMEM (4.5g/L glucose), 10% FBS, 1% penicillin-streptomycin antibiotics and 2-mercaptoethanol. RINm5F cells were cultured in RPMI-1640 (11.1mM glucose), 10% FBS and penicillin-streptomycin. For high glucose culture media RPMI-1640 was supplemented with glucose to generate a 25mM solution (INS-1 and RINm5F) and sterile filtered before use. For MIN6 high glucose DMEM (22mM) was used. For lipotoxic media RPMI-1640 (INS-1 and RINm5F) and low glucose DMEM (2mM) was supplemented with sodium palmitate, dissolved in 50% ethanol. An intermediate stock was made up in fatty acid free BSA before being diluted in media to 0.25mM. For glucolipotoxic media sodium palmitate was similarly diluted in high glucose media counterparts. For cytokine treatments a cocktail was made up consisting of IL-1β (150U/ml and 300U/ml), IFN-γ (150U/ml and 300U/ml) and TNF-α (20U/ml and 40U/ml) at low and high concentrations respectively. All cell lines were cultured in these stress conditions (high glucose,

lipotoxic, glucolipotoxic, low and high cytokines) for 24 and 48 hours. Following this culture, cells underwent MTT assay to assess viability and immunocytochemistry for insulin/glucagon. Cells were only used for RNA extraction and qPCR following 48 hour culture within stressor conditions.

3.3.2 MTT

MTT powder was dissolved into a stock solution of 5mg/ml in working KRBB without glucose. Working MTT was made up by a 1/10 dilution of stock MTT with 5.6mM glucose KRBB. Cultured cells were incubated with working MTT for one hour at 37°C. After this period a precipitate had formed which was solubilised by addition of DMSO. The plate was then read on a Flexstation at wavelength 570nm.

3.3.3 Immunocytochemistry

For immunocytochemistry, cells were cultured on sterilised 16mm round glass cover slips within 12 well plates. Following 24 or 48 hour incubation, the cells were rinsed in PBS before being fixed in 4% PFA. After this time antigen retrieval was carried out by incubation in citrate buffer heated to 90°C. Cells were then blocked in BSA before incubation with primary antibodies (mouse anti-insulin and guinea pig anti-glucagon) for 2 hours at 37°C. Unbound antibody was then removed by two washes in PBS before incubation with secondary antibodies (goat anti-mouse 594 and goat anti-guinea pig 488) for 45 minutes at 37°C. Excess antibody was removed by PBS washes and cells were incubated for a final time with DAPI to stain nuclei. After a final wash in PBS, the cover slips were carefully removed from each well and mounted onto

polysine histology slides ready for imaging. Images were taken using an Olympus fluorescent microscope fitted with DAPI (350nm) FITC (488nm) and TRITC (594nm) filters and a DP70 camera adapter system

3.3.4 RNA extraction, cDNA conversion and qPCR

For RNA isolation cells were seeded in 6 well plates at a density of 500,000 cells and cultured for 48 hours in different stress conditions. Following the culture period cells were washed in HBSS before addition of ice cold Trizol to lyse the cells. The homogenous lysate was transferred to an Eppendorf and centrifuged at 12,000G for 10 minutes at 4°C and the supernatant removed to a fresh Eppendorf. Phase separation was then carried out using chloroform and centrifugation at 12,000G for 15 minutes at 4°C. Of the resulting 3 layers, the upper transparent aqueous layer of RNA was extracted into a fresh Eppendorf. RNA precipitation was then carried out using isopropanol and centrifuged at 14,000G for 20 minutes at 4°C. The resulting RNA pellet was then washed three times in 75% ethanol before being air-dried. The RNA pellet was then solubilised by the addition of RNA-free water. A NanoDrop ND-1000 UV/Vis spectrophotometer was used to determine RNA quantity and quality. Quality was assessed by 260/280 OD ratios >1.8. RNA was stored at -70°C.

cDNA (1µg) was produced by reverse transcription of isolated RNA. In short, oligoDT was mixed with RNA samples and heated to 70°C using a thermocycler. A mastermix of dNTPs, DTT, first strand buffer and superscript reverse transcriptase was added to

the samples and heated to 42°C for 1 hour. To terminate the reaction after this time the mixture was heated to 70°C.

qPCR was carried out using a Miniopticon two-colour real time PCR detection system. Using an 18µl reaction mix consisting of SYBR green, RNA-free water, primers and cDNA. A negative template control was added for each primer and β-actin used as a housekeeping control. qPCR was run under the following conditions: 1. Initial denaturation 95°C, 5 minutes, 2. Final denaturation 95°C, 30 seconds, 3. Annealing 58°C, 30 seconds, 4. Extension 72°C, 30 seconds. Results were analysed using Cp values normalised in respect to β-actin.

3.3.5 Animals

8 week old male C57Bl/6 mice were purchased and single housed within the BBRU. Mice had free access to standard chow diet and drinking water and kept in temperature controlled rooms on a 12 hour light-dark cycle. Mice were divided into three treatment groups: 1. Saline control, 2. Streptozotocin-treated and 3. Hydrocortisone-treated. The first group received daily ip injections of saline (0.9% NaCl) for the ten day duration of the study. The second group received five consecutive daily injections of streptozotocin (50mg/kg) freshly dissolved in 0.5M citrate buffer, pH4.5. The third group received ten daily doses of hydrocortisone (70mg/kg). Mice were allocated 8 per treatment group with body weight, blood glucose, calorie and fluid consumption monitored regularly.

Pancreas blocks were obtained from previously carried out study using high fat fed NIH Swiss mice treated with saline or exendin-4 (Vasu et al, 2017). In this study 8 week old male mice (8 mice/group) were kept on high fat diet (45% fat, 20% protein and 35% carbohydrate) for 20 weeks, with exendin-4 (25nmol/kg, ip) dosed twice daily for 28 days. Additional pancreas samples were obtained from a db/db leptin receptor deficient mice study treated with saline, GIP(6-30)Cex-K40[Pal], a GIP antagonist, or liraglutide (Pathak et al, 2015). In this study 13 week old male db/db mice were allocated 8 per treatment group and dosed twice daily with liraglutide (0.25nmol/kg, ip) or GIP(6-30)Cex-K40[Pal] (2.5nmol/kg, ip) for 28 days.

3.3.6 Immunohistochemistry

Pancreatic tissue was excised from C57Bl/6 mice at the end of the study and fixed in 4% PFA for 48 hours. Tissues were then put through a Leica automated tissue processor to dehydrate the tissue ready for embedding into wax blocks. 5µm sections were cut and collected on to polysine coated slides. Immunohistochemistry was carried out starting with immersion in xylene to clear wax followed by rehydration in an ethanol gradient (100-50%). Heat mediated antigen retrieval was carried out using citrate buffer heated to 90°C, followed by blocking in 4% BSA solution. Primary antibody was then added to the slides and allowed to incubate overnight at 4°C. The following antibodies were used: mouse monoclonal anti-insulin antibody (ab6995, 1:1000; Abcam), guinea-pig anti-glucagon antibody (PCA2/4, 1:200; raised in-house), guinea pig anti-Pdx1 antibody (ab47267, 1:200; Abcam) and rabbit anti-GLUT2 (1:200; Abcam). Unbound antibody was cleared the next day by washing in PBS before incubation with secondary antibodies. The following secondary antibodies

were used as appropriate: Alexa Fluor488 goat anti-guinea pig IgG — 1:400, Alexa Fluor 594 goat anti-mouse IgG — 1:400, Alexa Fluor 488, goat anti-rabbit IgG — 1:400, Alexa Fluor 594 goat anti-rabbit IgG — 1:400. Excess secondary antibody was washed away by two rinses with PBS. Slides were then incubated with DAPI to stain nuclei. Upon completing a final PBS wash slides were mounted with glass cover slips, ready for imaging on an Olympus fluorescent microscope fitted with DAPI (350nm) FITC (488nm) and TRITC (594nm) filters and a DP70 camera adapter system.

3.3.7 Image Analysis

Cell^F imaging software was used to assess islet area, beta cell area, alpha cell area (expressed as μm^2. Islets were quantified at small (<10,000 μm^2), medium (10,000-25,000 μm^2) or large (>25,000 μm^2) to assess islet size distribution. Islet architecture was deemed irregular by the abnormal presence of centrally located alpha cells. GLUT2 expression was assessed by fluorescence intensity. Beta cell Pdx1 expression was assessed using Image J software and expressed as a percentage of the number of insulin positive cells co-expressing Pdx1. >60 islets were analysed per treatment group. Additionally Image J was used to assess insulin and glucagon expression from stained cell lines. 6 frames were analysed per treatment group, with each frame consisting of ~150 cells.

3.3.8 Statistics

All graphs and Figures were produced using GraphPad PRISM v.5 software with data presented as mean ± SEM. For comparisons between two groups the Student's t-test was implemented. For comparisons between more than two groups, one-way

ANOVA tests utilising Bonferroni post-hoc tests were carried out. For animal data where multiple groups were compared with each other over various time points two-way RM ANOVA tests were conducted using Bonferroni post-hoc tests. A p-value <0.05 was deemed a significant result.

3.4 Results

3.4.1 Viability of INS-1 cells exposed to beta cell stressors

After 24 hours in culture with beta cell stressors INS-1 cells exposed to lipotoxic (58.0 ± 1.5 vs 92.2 ± 4.1%, p<0.001, Figure 3.1A) and both low (54.4 ± 8.3%, p<0.001) and high cytokine (44.3 ± 1.2%, p<0.001) conditions displayed a significant reduction in cell viability. Cell viability remained reduced even after 48 hours culture in lipotoxic (66.8 ± 09 vs 96.9 ± 1.2%, p<0.001, Figure 3.1B) or low cytokine (53.5 ± 0.9%, p<0.001) conditions. Culture in a higher dose of cytokines exacerbated the reduction in cell viability after 48 hours (34.4 ± 0.5%, p<0.001). Hydrogen peroxide was used as a positive control to determine maximal cell death.

3.4.2 Insulin and glucagon expression from INS-1 cells exposed to beta cell stressors

Expression of insulin and glucagon from INS-1 cells was determined by immunocytochemistry. After 24 hours culture in high glucose media INS-1 cells displayed an increase in cells solely expressing insulin (68.8 ± 2.3 vs 61.3 ± 0.4%, p<0.05, Figure 3.2A) whilst lipotoxic culture showed an reduction (54.6 ± 2.4%, p<0.05). The number of INS-1 cells solely expressing glucagon was unchanged during

24 hours culture in these conditions (Figure 3.2B). Of interest INS-1 cells began to show dual expression of insulin and glucagon following 24 hours culture in lipotoxic (13.2 ± 0.5 vs 7.6 ± 0.6%, $p<0.001$, Figure 3.2C), high cytokine (12.6 ± 1.1%, $p<0.01$) and glucolipotoxic (12.6 ± 1.4%, $p<0.05$) conditions. Following 48 hours culture there was a notable reduction in INS-1 cells exclusively expressing insulin from lipotoxic (46.6 ± 3.9 vs 65.3 ± 2.9%, $p<0.01$, Figure 3.2D), high cytokine (57.2 ± 0.6%, $p<0.01$) and glucolipotoxic (52.2 ± 4.2%, $p<0.05$) conditions. The proportion of INS-1 cells solely expressing glucagon was markedly increased after 48 hours culture in high glucose 23.8 ± 1.1 vs 13.1 ± 1.0%, $p<0.001$, Figure 3.2E), lipotoxic (23.6 ± 2.0%, $p<0.01$), high cytokine (20.3 ± 1.7%, $p<0.05$) and glucolipotoxic (19.1 ± 0.5%, $p<0.01$) conditions. All tested conditions caused an increase in INS-1 cells dual expressing insulin and glucagon after 48 hours culture: high glucose (7.0 ± 0.5 vs 3.7 ± 0.4%, $p<0.01$, Figure 3.2F), lipotoxic (14.5 ± 1.4%, $p<0.001$), low cytokine (11.6 ± 0.7%, $p<0.001$), high cytokine (13.5 ± 0.7%, $p<0.001$) and glucolipotoxic (8.3 ± 1.8%, $p<0.05$).

3.4.3 INS-1 cells gene expression of beta, alpha and progenitor markers

Gene expression was assessed from INS-1 cells cultured for 48 hours in high glucose, low cytokine and high cytokine conditions. Quality RNA from lipotoxic conditions could not be obtained. High glucose culture resulted in increased expression of insulin (1.7 ± 0.06 vs 1.0 ± 0.2AU, $p<0.05$, Figure 3.3A), urocortin-3 (2.1 ± 0.06 vs 10 ± 0.3AU, $p<0.05$, Figure 3.3D), Pdx-1, (3.2 ± 0.1 vs 1.0 ± 0.1 AU, $p<0.001$, Figure 3.3E), neurogenin-3 (1.9 ± 0.2 vs 1.0 ± 0.2 AU, $p<0.05$, Figure 3.3F), glucagon (2.6 ± 0.1 vs

1.0 ± 0.2 AU, p<0.01, Figure 3.3G), Arx (7.8 ± 0.08 vs 1.0 ± 0.2 AU, p<0.001, Figure 3.3H) and PC1 (21.2 ± 0.08 vs 1.0 ± 0.2 AU, p<0.001) whilst reducing PC2 expression (0.6 ± 0.1 vs 1.0 ± 0.02 AU, p<0.05, Figure 3.3J). Low cytokine culture notably reduced Foxo1 (0.2 ± 0.1 AU, p<0.05) and PC2 (18.4 ± 0.4 AU, p<0.001) gene expression whilst upregulating expression of urocortin-3 (15.1 ± 1.2 AU, p<0.001), neurogenin-3 (7.0 ± 1.0 AU, p<0.01), Arx (3.0 ± 0.3 vs 1.0 ± 0.2 AU, p<0.01) and PC1 (18.4 ± 0.4 vs 1.0 ± 0.2 AU, p<0.001). Culturing INS-1 with high cytokine supplemented media caused similar changes in gene expression with the addition of reducing insulin (0.2 ± 0.2 AU, p<0.05) and GLUT2 (0.03 ± 0.2 AU, p<0.05) gene expression.

3.4.4 Viability of MIN6 cells exposed to beta cell stressors

MIN6 cells incubated for 24 hours displayed reduced cell viability when cultured in high glucose (88.4 ± 2.5 vs 97.4 ± 1.7%, p0.01, Figure 3.4A) , lipotoxic (40.4 ± 0.9%, p<0.001), low and high cytokine (92.2 ± 1.1%, p<0.05 and 88.8 ± 1.5%, p<0.01 respectively) and glucolipotoxic (45.3 ± 1.0%, p<0.001) conditions. A similar reduction in cell viability was found when incubation time was extended to 48 hours. In particular lipotoxic (15.8 ± 0.4 vs 97.6 ± 1.0%, p<0.001, Figure 3.4B) and glucolipotoxic (25.4 ± 0.8%, p<0.001) conditions showed worsening cell viability.

3.4.5 Insulin and glucagon expression from MIN6 cells exposed to beta cell stressors

Following 24 hours culture immunocytochemistry for insulin and glucagon displayed a reduction in MIN6 cells solely expressing insulin in lipotoxic (74.3 ± 0.6 vs 89.6 ±

1.6%, p<0.001, Figure 3.5A) and low cytokine conditions (78.8 ± 1.1%, p<0.001). Lipotoxic culture increased the number of MIN6 cells solely expressing glucagon (9.8 ± 0.6 vs 4.1 ± 0.7%, p<0.001, Figure 3.5B) and cells dual expressing insulin and glucagon (16.0 ± 0.7 vs 3.7 ± 0.4%, p<0.001, Figure 3.5C). Similarly low cytokine (8.9 ± 0.7%, p<0.001) and glucolipotoxic (7.7 ± 0.8%, p<0.01) conditions increased the number of MIN6 cells co-expressing insulin and glucagon. After 48 hours culture further reductions in MIN6 insulin expression were found in lipotoxic (59.4 ± 4.1 vs 81.2 ± 0.6%, p<0.01, Figure 3.5D) and cytokine conditions with the former still exhibiting an increase in cells co-expressing insulin and glucagon (16.6 ± 1.8 vs 3.9 ± 0.2%, p<0.01, Figure 3.5F).

3.4.6 MIN6 cells gene expression of beta and alpha cell markers

Gene expression was assessed from MIN6 cells cultured for 48 hours in high glucose, low cytokine and high cytokine conditions. Lipotoxic conditions failed to produce quality RNA. In MIN6 cells high glucose culture resulted in a reduction in insulin (0.4 ± 0.03 vs 1.0 ± 0.1 AU, p<0.01, Figure 3.6A) and Pdx-1 (0.4 ± 0.08 vs 1.0 ± 0.08 AU, p<0.01, Figure 3.6B) expression whilst glucagon gene expression was elevated (2.1 ± 0.2 vs 1.0 ± 0.2 AU, p<0.05, Figure 3.6C). Low cytokine treatment elicited an increase in insulin (1.6 ± 0.1 AU, p<0.05) gene expression despite Pdx-1 expression diminishing (0.4 ± 0.8 AU, p<0.01), whist glucagon expression increased (1.9 ± 0.07 AU, p<0.01). High cytokine treatment displayed similar changes in gene expression albeit without the increase in insulin expression observed by low cytokines.

3.4.7 Viability of RINm5F cells exposed to beta cell stressors

Rat derived RINm5F showed reduced viability when cultured with high glucose (71.6 ± 0.7 vs 98.8 ± 0.6%, $p<0.001$, Figure 3.7A), lipotoxic (24.3 ± 0.6%, $p<0.001$), high cytokine (80.7 ± 1.6%, $p<0.001$) and glucolipotoxic (28.3 ± 2.9%, $p<0.001$) conditions for 24 hours. Extending culture time to 48 hours exacerbated the reduction in viability observed in high glucose (37.2 ± 0.7 vs 96.4 ± 1.3%, $p<0.001$, Figure 3.7B), lipotoxic (13.1 ± 0.4%, $p<0.001$) and glucolipotoxic (8.9 ± 0.2%, $p<0.001$) conditions.

3.4.8 Insulin and glucagon expression from RINm5F cells exposed to beta cell stressors

Immunocytochemistry was used to assess protein expression of insulin and glucagon. After 24 hours culture all tested conditions exhibited a reduction in RINm5F cells solely expressing insulin: high glucose (83.0 ± 1.1 vs 91.6 ± 1.3%, $p<0.001$, Figure 3.8A), lipotoxic (77.0 ± 0.5%, $p<0.001$), low cytokine (84.9 ± 1.4%, $p<0.01$), high cytokine (83.2 ± 2.1%, $p<0.05$) and glucolipotoxic (67.8 ± 2.3%, $p<0.001$). During this time cells starting to exclusively express glucagon appeared in high glucose (12.0 ± 0.7 vs 7.0 ± 1.0%, $p<0.01$, Figure 3.8B), lipotoxic (13.6 ± 0.7%, $p<0.01$) and glucolipotoxic (16.6 ± 2.3%, $p<0.05$) conditions. The number of cells co-expressing insulin and glucagon was increased by all culture conditions after 24 hours: high glucose (5.0 ± 0.6 vs 1.4 ± 0.2, $p<0.05$, Figure 3.8C), lipotoxic (9.4 ± 0.6%, $p<0.001$), low cytokine (7.9 ± 0.7%, $p<0.001$), high cytokine (7.9 ± 1.1%, $p<0.01$) and glucolipotoxic (15.5 ± 2.4%, $p<0.01$). After 48 hours cells cultured in normal RPMI media started to reduce insulin (Figure 3.8D) and increase glucagon (Figure 3.8E)

expression and as a result many of the stressor conditions failed to significantly affect expression. Cells dual expressing insulin and glucagon continued to be raised after 48 hour culture. Of note 48 hours with lipotoxic culture elicited the greatest reduction in insulin (51.5 ± 2.7 vs 81.3 ± 3.3%, $p<0.001$, Figure 3.8D) expression alongside the greatest increase in glucagon (18.7 ± 1.7 vs 11.9 ± 1.2%, $p<0.05$, Figure 3.8E) and dual expressing cells (31.7 ± 1.8 vs 5.2 ± 0.9%, $p<<0.001$, Figure 3.8F).

3.4.9 Effects of streptozotocin or hydrocortisone on body weight, cumulative energy intake, cumulative fluid intake and blood glucose in C57Bl/6 mice

C57Bl/6 mice showed a decline in body weight (Figure 3.9A) and percentage body weight change when treated with streptozotocin (-6.0 ± 0.4 vs 1.2 ± 0.8% $p<0.001$, Figure 3.9B) or hydrocortisone (-3.1 ± 1.4%, $p<0.05$). Cumulative energy intake was only reduced by streptozotocin (496.7 ± 10.3 vs 550.1 ± 14.1kJ, $p<0.05$, Figure 3.9C) whilst no effect on fluid intake (Figure 3.9D) was found. Non-fasting blood glucose was progressively elevated by streptozotocin (19.5 ± 1.8 vs 8.1 ± 0.6mM, $p<0.001$, Figure 3.9E-F) whereas hydrocortisone had no sustained effect on blood glucose despite being lower at the final day (5.8 ± 0.3mM, $p<0.01$).

3.4.10 Effects of streptozotocin or hydrocortisone on pancreatic islet area, beta cell area, alpha cell area, islet size distribution, percentage beta cells and percentage alpha cells and islet architecture

Representative images of islets stained for insulin (red) and glucagon (green) are presented in Figure 3.10A. Streptotozocin resulted in a massive reduction in islet area (2748 ± 165.3 vs 10140 ± 1016μm^2, p<0.001, Figure 3.10B) due to a loss of beta cell area (3112 ± 249.2 vs 7446 ± 542.9μm^2, p<0.001, Figure 3.10C) despite alpha cell area increasing (2341 ± 246.2 vs 1547 ± 207.6μm^2, p<0.05, Figure 3.10D). Hydrocortisone elicited an increase in islet area (16400 ± 1262μm^2, p<0.001) due to an increase in beta cell area (10370 ± 1019μm^2, p0.05). Islet size distribution was markedly altered by streptozotocin with complete ablation of large and medium sized islets (Figure 3.10E) whilst hydrocortisone reduced the proportion of small sized islets (38.0 ± 1.3 vs 65.3 ± 5.0%, p<0.001, Figure 3.10E) and increased medium sized islets (49.0 ± 1.0% vs 23.6 ± 5.7%, p<0.001, Figure 3.10E). Percentage beta cells was reduced (59.7 ± 1.6 vs 85.7 ± 1.0%, p<0.001, Figure 3.10F) by streptozotocin with reciprocal increase in percentage alpha cells (38.3 ± 1.6 vs 13.6 ± 0.9%, p<0.001, Figure 3.10G). Hydrocortisone elicited the opposite change with increased percentage beta cells (89.9 ± 0.6%, p<0.001) and reduced percentage alpha cells (10.0 ± 0.6%, p<0.01). The number of islets with irregularly located central alpha cells was increased by streptozotocin (59.4 ± 2.6 vs 21.3 ± 3.5%, p<0.001, Figure 3.10H) and to a lesser extent by hydrocortisone (31.4 ± 2.6%, p<0.05).

3.4.11 Effects of streptozotocin or hydrocortisone on pancreatic beta cell markers

Representative images of islets stained for insulin (red) alongside either Pdx-1 (green) or GLUT2 (green) are displayed in Figure 3.11A and B respectively. The percentage of beta cells expressing Pdx-1 was equally reduced by streptozotocin (59.6 ± 1.8 vs 72.0 ± 1.9%, $p<0.001$, Figure 3.11C) and hydrocortisone (60.7 ± 2.1%, $p<0.001$). GLUT2 expression, determined by fluorescence intensity (MFI), was similarly reduced by streptozotocin (60.4 ± 4.1 vs 93.3 ± 3.4MFI, $p<0.001$, Figure 3.11D) and hydrocortisone (62.6 ± 5.0MFI, $p<0.001$).

3.4.12 Effects of high fat feeding alone or in combination with exendin-4 on pancreatic islet area, beta cell area, alpha cell area, islet size distribution, percentage beta cells, percentage alpha cells and islet architecture

Characteristic images of islets from exendin-4 treated high fat fed mice are presented in Figure 3.12A showing insulin (red) and glucagon (green). High fat feeding resulted in an increase in islet area (27130 ± 3552 vs 10240 ± 1027μm^2, $p<0.001$, Figure 3.12B) with similar elevations in beta cell area (21450 ± 3081 vs 7401 ± 992.2μm^2, $p<0.01$, Figure 3.12C) and alpha cell area (3239 ± 347.8 vs 1755 ± 241.4μm^2, $p<0.01$, Figure 3.12D). Exendin-4 treatment exacerbated these elevations in islet area (48320 ± 7072μm^2, $p<0.05$) and beta cell area (43120 ± 6625μm^2, $p<0.01$) whilst having no discernible effect on alpha cell area. High fat feeding altered islet size distribution with increases in the number of large sized islets (41.7 ± 3.1% vs 27.5 ± 4.8%, $p<0.05$, Figure 3.12E) at the expense of medium sized islets (18.3 ± 1.7 vs 30.0 ± 4.1%, $p<0.05$, Figure 3.12E). Treatment with exendin-4 had no additional effect on islet size

distribution. Percentage beta cells was reduced (82.8 ± 1.1 vs 89.0 ± 0.9%, p<0.001, Figure 3.12F) by high fat feeding with a mutual increase in percentage alpha cells (17.5 ± 1.1 vs 12.9 ± 1.1%, p<0.01, Figure 3.12G). Exendin-4 therapy was able to reduce percentage alpha cells (12.6 ± 1.0% p<0.001) back to levels similar to lean mice. The number of islets showcasing central alpha cells was increased in high fat fed mice (78.8 ± 8.3 vs 32.1 ± 6.0%, p<0.01, Figure 3.12H) with exendin-4 treatment having no significant effect on this.

3.4.13 Effects of GIP antagonist or liraglutide treatment on pancreatic islet area, beta cell area, alpha cell area, islet size distribution, percentage beta cells, percentage alpha cells and islet architecture in leptin receptor deficient (db/db) mice

Representative images of db/db mice treated twice daily with GIP(6-30)Cex-K40[Pal] (2.5nmol/kg) or liraglutide (0.25nmol/kg) for 28 days are presented in Figure 3.13A showing insulin (red) and glucagon (green). Compared to WT C57Bl/6 mice, leptin receptor deficient db/db mice exhibit larger islets (16920 ± 1245 vs 9776 ± 827.2µm^2, p<0.001, Figure 3.13B), with increased beta cell area (13910 ± 1045 vs 8725 ± 730.9µm^2, p<0.001, Figure 3.13C) and alpha cell area (2984 ± 245.6 vs 1501 ± 111.7µm^2, p<0.001, Figure 3.13D). Islet size distribution is similarly altered with an increase in medium (35.8 ± 4.4 vs 20.0 ± 4.4%, p<0.05, Figure 3.13E) and large (21.8 ± 4.0 vs 8.3 ± 1.9%, p<0.05, Figure 3.13E) sized islets at the expense of smaller ones (43.1 ± 5.4 vs 70.6 ± 5.5%, p<0.01, Figure 3.13E). Islet architecture was found dysregulated with a significant number of islets found with central alpha cells (69.2 ±

4.3 vs 21.3 ± 3.5%, $p<0.001$, Figure 3.13H). Treatment with GIP antagonist had no additional change on islet morphology or size distribution in these mice. Liraglutide however impacted islet morphology reducing islet area (12620 ± 964.4μm^2, $p<0.05$), beta cell area (10430 ± 802.9μm^2, $p<0.05$) and alpha cell area (2207 ± 208.2μm^2, $p<0.05$) but had no impact on islet size distribution.

3.5 Discussion

Beta cell lines offer great insight into the pathophysiology of diabetes and the identification of novel therapeutics. The present work utilises three widely used beta cell lines (INS-1, MIN6 and RINm5F) to try and identify beta cell plasticity.

INS-1 cells offered the best opportunity to investigate beta cell transdifferentiation with these cells showing substantial responses to beta cell stressors. In particular lipotoxic and cytokine culture resulted in a consistent increase in cells co-expressing insulin and glucagon and cells purely expressing glucagon, suggestive of a beta-to-alpha transdifferentiation. The latter cytokine cocktail in particular altered INS-1 gene expression with reduction in mature beta cell proteins insulin, GLUT2 and FOXO1 linked with increases in progenitor marker Ngn3 and alpha cell marker Arx. Loss of FOXO1 has been shown to lead to beta cell dedifferentiation (Talchai et al, 2012) with the increase in Arx indicative of beta-to-alpha cell transdifferentiation (Collombat et al, 2007).

MIN6 cells proved more robust against cytokine-induced changes in viability however they showed similar increases in cells co-expressing insulin and glucagon. Preliminary gene expression studies revealed reductions in beta cell marker Pdx1 and increases

in glucagon. Loss of Pdx1 (Gao et al, 2014) and activation of Arx (Collombat et al, 2007) expression has been shown to trigger beta-to-alpha cell transdifferentiation making it plausible that MIN6 exposed to cytokines undergo this process. RINm5F cells were highly susceptible to glucotoxic and lipotoxic stress but cells that tolerated these insults showed co-expression of insulin and glucagon. However given how toxic these conditions were on the cells gene expression analysis could not be reliably conducted.

Most beta cell lines are not purely insulin producing with many of them producing additional islet hormones such as glucagon and somatostatin to some degree (Skelin et al, 2009). This is quite unlike primary beta cells that are defined by the hormone they secrete thus making the use of these cell lines a limitation when investigating beta cell transdifferentiation. With two of these cell lines being derived from a radiation induced NEDH rat insulinoma it is questionable whether they resemble true beta cells. As a result beta cell plasticity is best studied using *in vivo* models of diabetes.

C57Bl/6 mice became characteristically hyperglycaemic following 5 doses of streptozotocin (Vasu et al, 2015). Islet area was markedly reduced due to loss of beta cell mass despite substantial increases in alpha cell mass. Islet morphology was altered with alpha cells now making up 40% of the islet following streptozotocin treatment. Mature beta cell proteins GLUT2 and Pdx1 were also reduced by streptozotocin supporting the notion that beta-to-alpha cell transdifferentiation could account for these changes (Talchai et al, 2012). This is of particular interest in

light of human data in type-2 diabetics showing similar expansions in alpha cell mass and loss of beta cell mass and insulin content (Yoon et al, 2003).

Hydrocortisone had little impact on metabolic parameters of C57Bl/6 mice despite substantially increasing islet area and beta cell mass (Vasu et al, 2015). This strongly implies that these mice were insulin resistant given how much beta cell mass expanded in order to maintain normoglycaemia. These mice showed reductions in Pdx1 and GLUT2 a sign that these beta cells may be dedifferentiating (Talchai et al, 2012).

Pancreatic tissues from past high fat fed NIH Swiss mouse studies were examined by immunohistochemistry (Vasu et al, 2017). Metabolically these mice displayed severe obesity and hyperglycaemia, associated with hyperinsulinemia, hyperglucagonemia and impaired insulin sensitivity (Vasu et al, 2017). Histological analysis of high fat fed mice islets revealed increases in beta cell and alpha cells masses resulting in overall islet mass expansion. Alpha cell mass increased disproportionately to beta cell mass, which didn't increase to the same extent. This could suggest that some beta cells may be transdifferentiating towards alpha cells, especially given the rise of cells co-expressing insulin and glucagon. Diet induced diabetes has already been shown to cause beta cell dedifferentiation in non-human primates therefore may have the potential to lead towards alpha cell transdifferentiation (Fiori et al, 2013). Treatment with exendin-4 appeared to exacerbate islet hypertrophy however it limited this alpha cell mass expansion. This could implicate GLP-1 has an effect on maintaining beta cell maturity in addition to its known metabolic benefits of reduced calorie consumption, blood glucose and HbA1c (Vasu et al, 2017).

Histology samples were obtained from previous C57Bl/KsJ db/db mice study and examined for signs of beta cell transdifferentiation (Pathak et al, 2015). Metabolically, these mice displayed hyperglycaemia and hyperinsulinemia associated with impaired glucose tolerance. Leptin receptor deficient mice showed characteristic changes in islet morphology becoming hypertrophied with disordered distribution of beta and alpha cells (Kawasaki et al, 2005). Given that beta cell mass and alpha cell mass expand to similar extents it may be unlikely that a transdifferentiation is occurring in these mice. However this may be a reflection on the severity of diabetes in these mice. Severely diabetic db/db mice have been shown to have reduced proportion of insulin expressing cells with increases in glucagon and somatostatin expressing cells. The inverse change was found in db/db mice with only mild diabetes including: islet hypertrophy with an increase in insulin expressing cells and reduction in glucagon and somatostatin expressing cells (Baetens et al, 1978). Nonetheless, treatment of these mice with the GLP-1 receptor agonist liraglutide was sufficient to limit islet hypertrophy. GIP antagonism had no discernible impact on islet morphology despite similar studies showing prevention of islet hypertrophy in leptin deficient ob/ob mice (Gault et al, 2005). In terms of glucose homeostasis however, both GLP-1 activation and GIP antagonism reduced plasma insulin and glucose levels (Pathak et al, 2015). Although not presently examined, others have identified beta cell dedifferentiation in db/db mice shown through loss of beta cell markers (insulin, Foxo1, MafA and NeuroD1) and upregulation of progenitor marker, Aldh1a3 (Ishida et al, 2017). This dedifferentiation can be potentiated by treatment with angiotensin-2 quantified by further reductions in Pdx1 and Foxo1 and elevations in Ngn3 (Chen et al, 2018). These authors speculate that

activation of the renin-angiotensin system (RAS) increases oxidative stress and contributes to beta cell dedifferentiation.

The major limitation of these *in vivo* studies is that beta cells cannot be tracked in order to reliably conclude that beta-to-alpha cell transdifferentiation is occurring. Alternative causes of these changes in islet morphology could be apoptosis of beta cells or proliferation or reduced apoptosis of alpha cells. Lineage tracing studies whereby pancreatic beta cells are tagged with a protein marker enable them to be identified when they lose insulin expression and potentially start to express glucagon.

Figure 3.1: Viability of INS-1 cells exposed to beta cell stressors

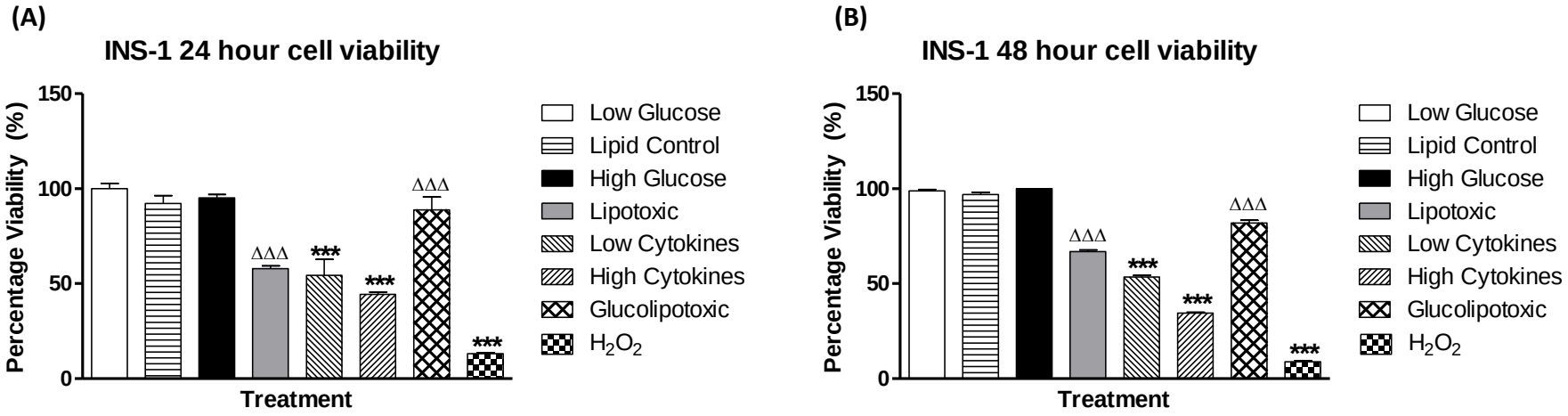

Viability of INS-1 cells exposed to beta cell stressors for (A) 24 and (B) 48 hours determined by MTT. INS-1 cells were cultured in the following conditions: low glucose (11.1mM), lipid control (50µl 50% ethanol), high glucose (25mM), lipotoxic (0.25mM palmitate), low cytotoxic (100U IFNy, IL-1B, 20U TNFa), high cytotoxic (300U IFNy, IL-1B, 40U TNFa) and glucolipotoxic (25mM glucose, 0.25mM palmitate). Values are mean ± SEM, n=8/treatment. Comparisons are versus low glucose (*) or versus lipid control (Δ), significant when ***/ΔΔΔ $p<0.001$.

Figure 3.2: Insulin and glucagon expression from INS-1 cells exposed to beta cell stressors

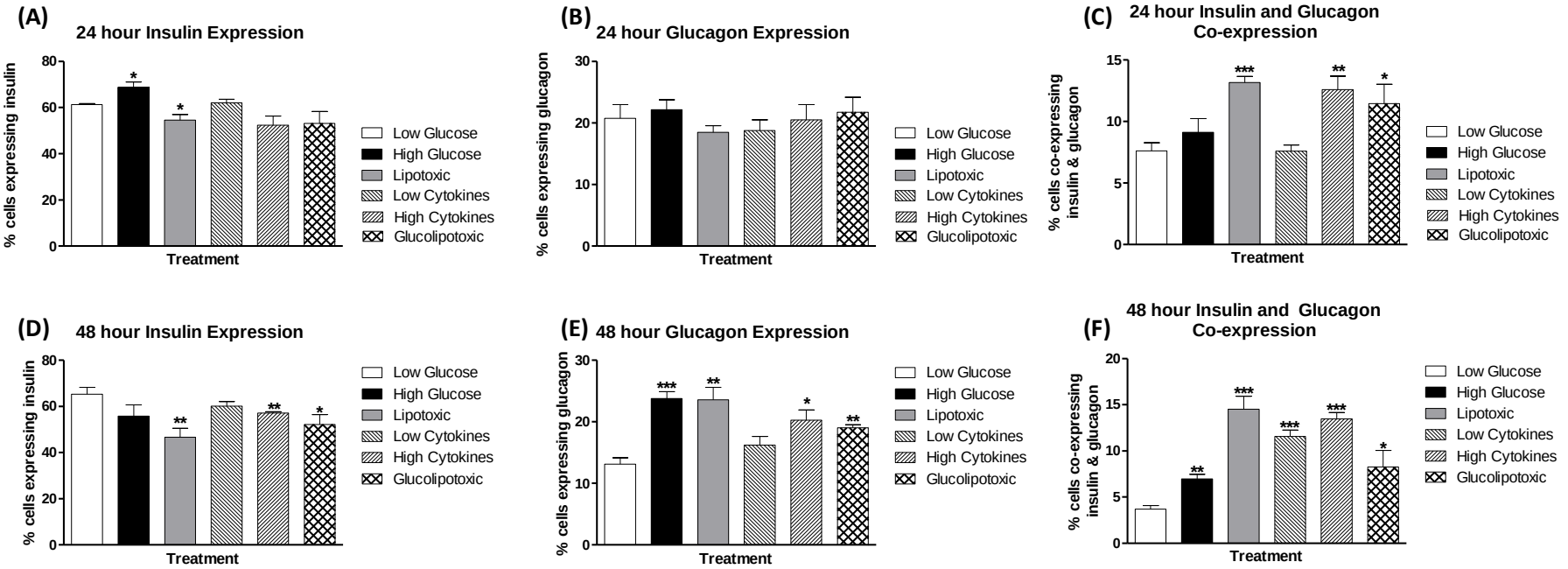

Percentage of INS-1 cells expressing insulin, glucagon or dual expression of both proteins following (A-C) 24 hour and (D-F) 48 hour culture with beta cell stressors: low glucose (11.1mM), high glucose (25mM), lipotoxic (0.25mM palmitate), low cytotoxic (IFNy, IL-1B, TNFa), high cytotoxic (IFNy, IL-1B, TNFa) and glucolipotoxic (25mM glucose, 0.25mM palmitate) prior to immunocytochemical staining for insulin and glucagon. Values are mean ± SEM, n=6 frames/treatment, each frame comprising >100 cells. Comparisons are versus low glucose (*) significant when * $p<0.05$, ** $p<0.01$ and *** $p<0.001$.

Figure 3.3 INS-1 cells gene expression of beta, alpha and progenitor markers

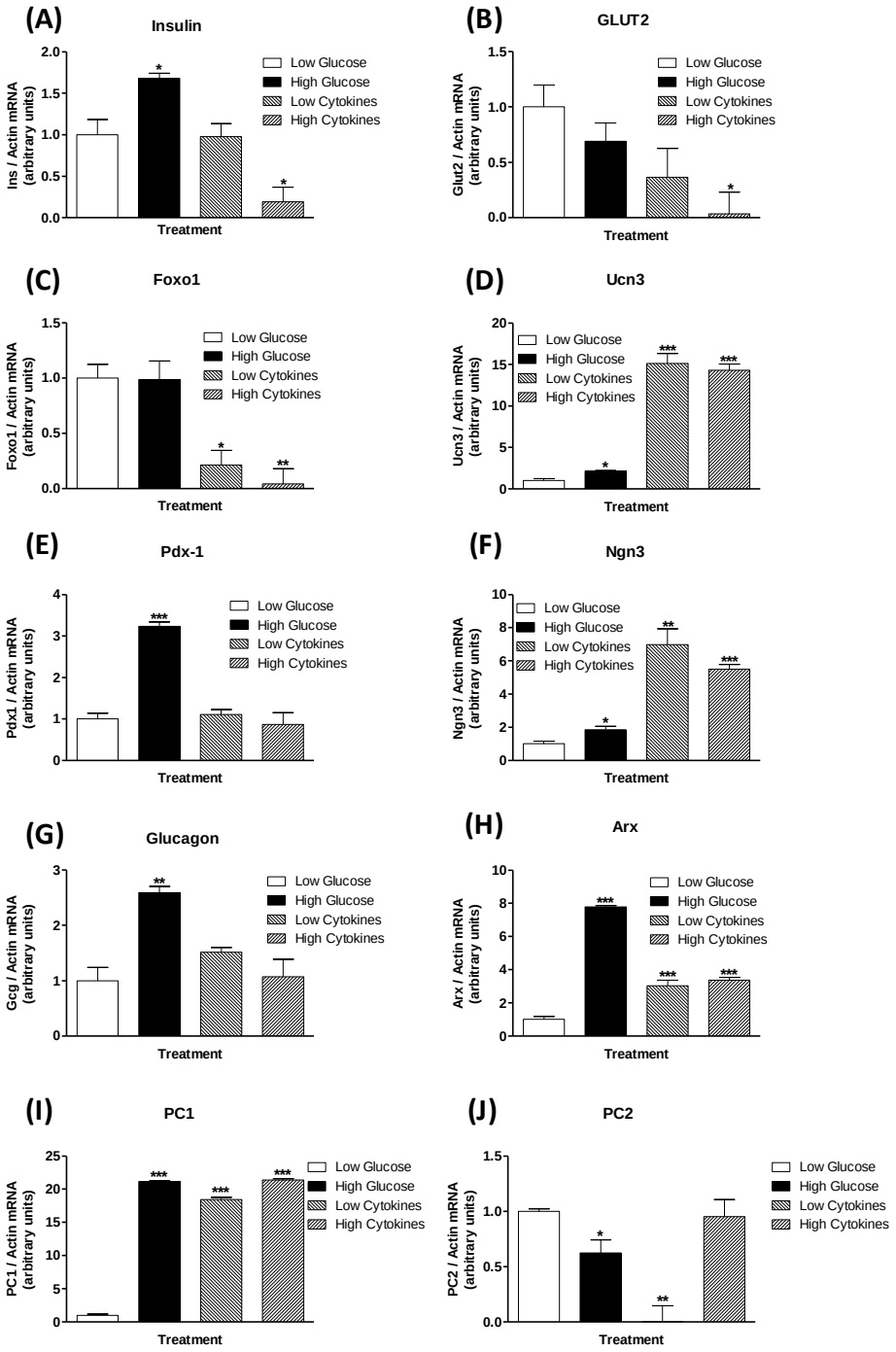

INS-1 gene expression of (A) insulin, (B) GLUT2, (C) Foxo1 (D) Ucn3, (E) Pdx1, (F) Ngn3, (G) Glucagon, (H) Arx (I) PC1 and (J) PC2 following 48 hour culture with low glucose, high glucose, low cytokine and high cytokine conditions. Gene expression was normalised to Actin gene expression. Values shown are mean ± SEM (n=3). *p<0.05, **p<0.01, ***p<0.001 compared to low glucose control.

Figure 3.4 Viability of MIN6 cells exposed to beta cell stressors

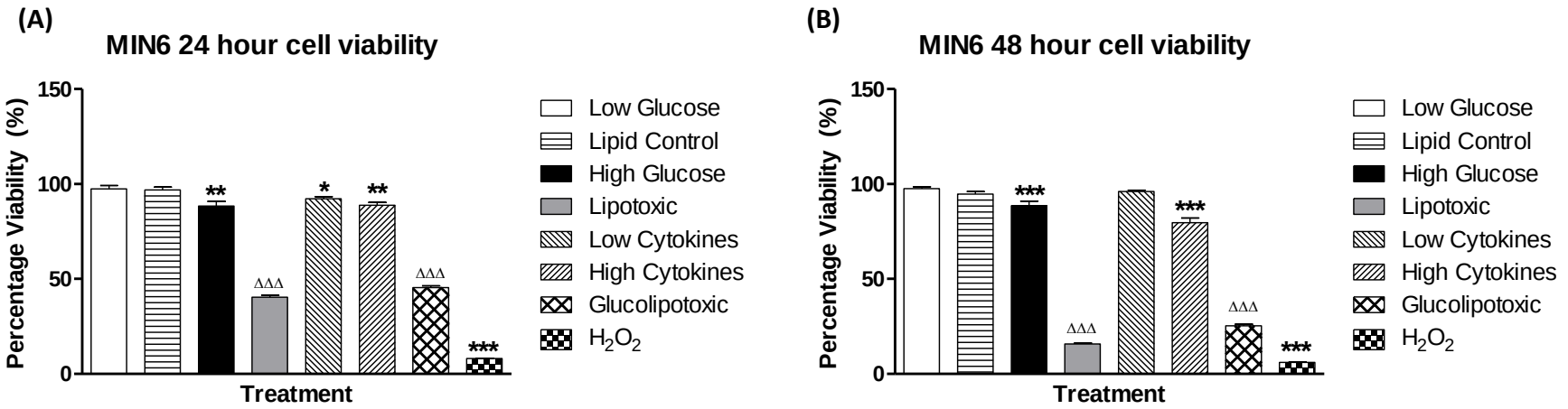

Viability of MIN6 cells exposed to beta cell stressors for (A) 24 and (B) 48 hours determined by MTT. MIN6 cells were cultured in the following conditions: low glucose (2mM), lipid control (50% ethanol), high glucose (22mM), lipotoxic (0.25mM palmitate), low cytotoxic (100U IFNy, IL-1B, 20U TNFa), high cytotoxic (300U IFNy, IL-1B, 40U TNFa) and glucolipotoxic (25mM glucose, 0.25mM palmitate). Values are mean ± SEM, n=8/treatment. Comparisons are versus low glucose (*) or versus lipid control (Δ), significant when ***/ΔΔΔ $p<0.001$.

Figure 3.5: Insulin and glucagon expression from MIN6 cells exposed to beta cell stressors

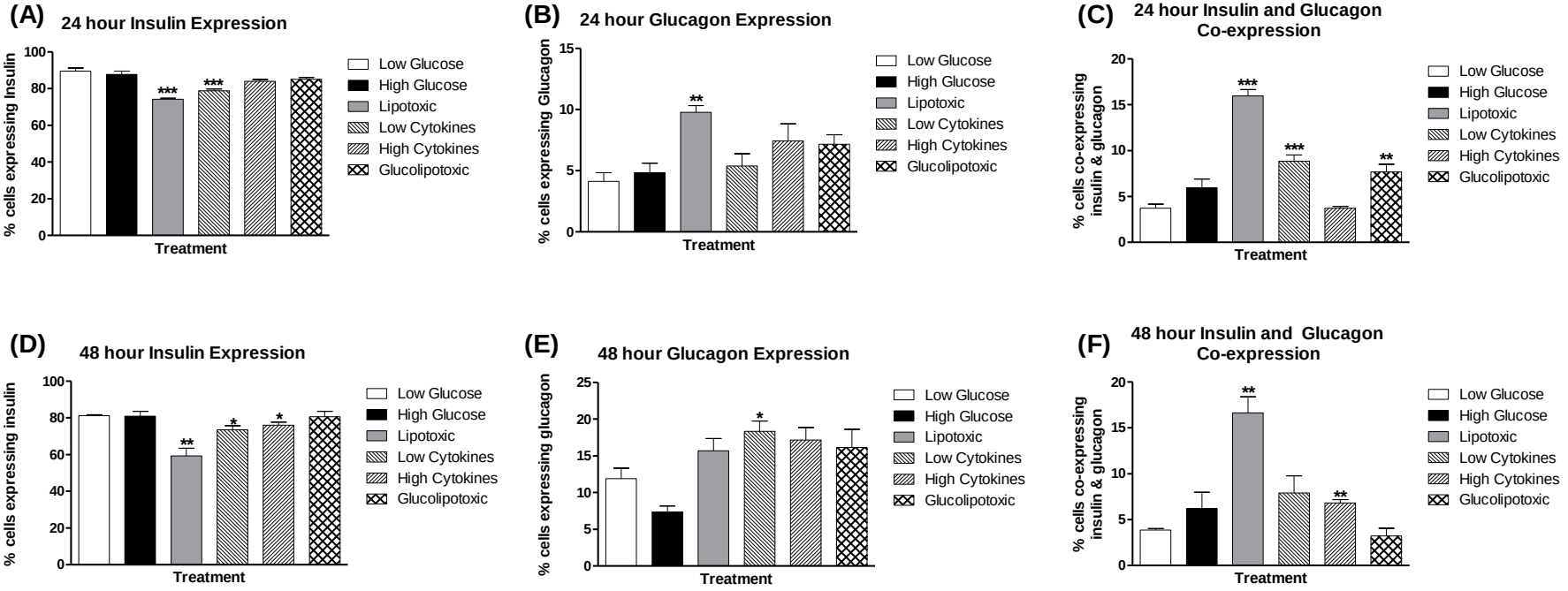

Percentage of MIN6 cells expressing insulin, glucagon or dual expression of both proteins following (A-C) 24 hour and (D-F) 48 hour culture with beta cell stressors: low glucose (2mM), high glucose (22mM), lipotoxic (0.25mM palmitate), low cytotoxic (IFNy, IL-1B, TNFa), high cytotoxic (IFNy, IL-1B, TNFa) and glucolipotoxic (22mM glucose, 0.25mM palmitate) prior to immunocytochemical staining for insulin and glucagon. Values are mean ± SEM, n=6 frames/treatment, each frame comprising >100 cells. Comparisons are versus low glucose (*) significant when * $p<0.05$, ** $p<0.01$ and *** $p<0.001$.

Figure 3.6 MIN6 cells gene expression of beta and alpha cell markers

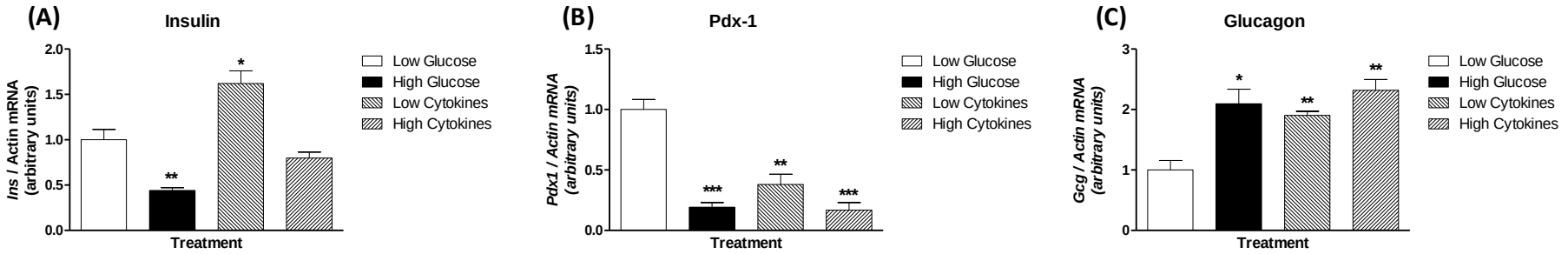

MIN6 gene expression of (A) insulin, (B) GLUT2 and (C) Pdx-1 following 48 hour culture with low glucose, high glucose, low cytokine and high cytokine conditions. Gene expression was normalised to Actin gene expression. Values shown are mean ± SEM (n=3). *p<0.05, **p<0.01, ***p<0.001 compared to low glucose control.

Figure 3.7: Viability of RINm5F cells exposed to beta cell stressors

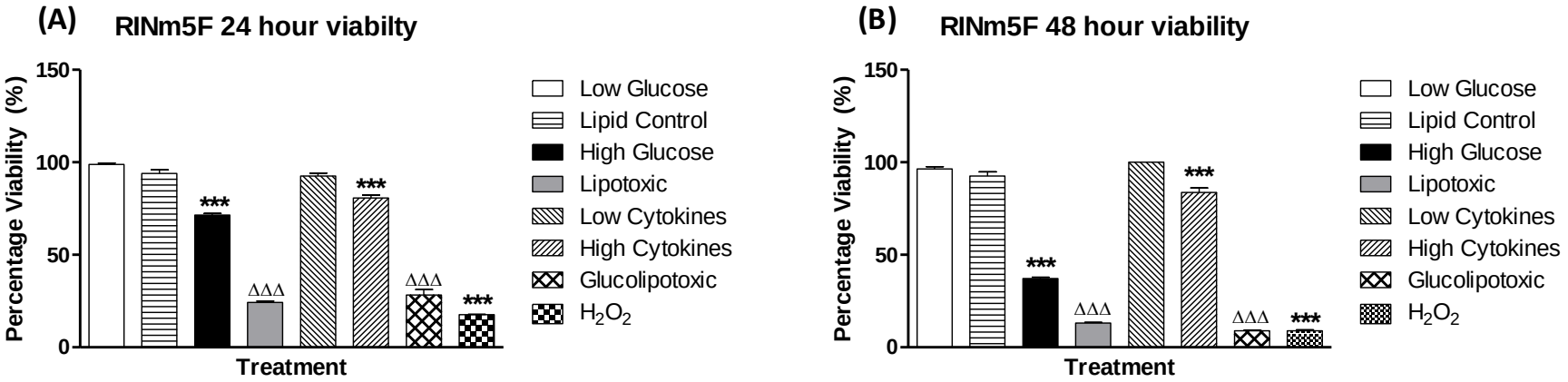

Viability of RINm5F cells exposed to beta cell stressors for (A) 24 and (B) 48 hours determined by MTT. RINm5F cells were cultured in the following conditions: low glucose (11.1mM), lipid control (50µl 50% ethanol), high glucose (25mM), lipotoxic (0.25mM palmitate), low cytotoxic (100U IFNy, IL-1B, 20U TNFa), high cytotoxic (300U IFNy, IL-1B, 40U TNFa) and glucolipotoxic (25mM glucose, 0.25mM palmitate). Values are mean ± SEM, n=8/treatment. Comparisons are versus low glucose (*) or versus lipid control (Δ), significant when ***/ΔΔΔ $p<0.001$.

Figure 3.8: Insulin and glucagon expression from RINm5F cells exposed to beta cell stressors

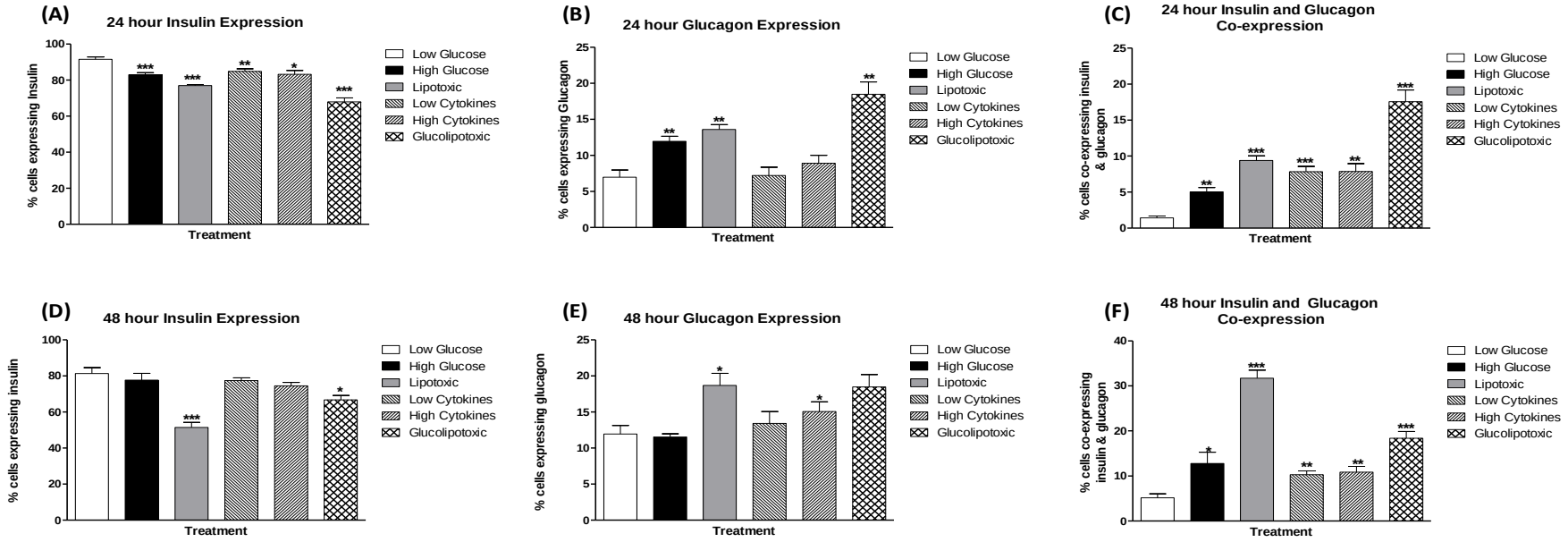

Percentage of RINm5f expressing insulin, glucagon or co-expression of both following (A-C) 24 hour and (D-F) 48 hour culture with beta cell stressors: low glucose (11.1mM), high glucose (25mM), lipotoxic (0.25mM palmitate), low cytotoxic (IFNy, IL-1B, TNFa), high cytotoxic (IFNy, IL-1B, TNFa) and glucolipotoxic (25mM glucose, 0.25mM palmitate) prior to immunocytochemical staining. Values are mean ± SEM, n=6 frames/treatment, each frame comprising >100 cells. Comparisons are versus low glucose (*) significant when * $p<0.05$, ** $p<0.01$ and ***$p<0.001$.

Figure 3.9: Effect of streptozotocin or hydrocortisone on body weight, cumulative energy intake, cumulative fluid intake and blood glucose in C57Bl/6 mice

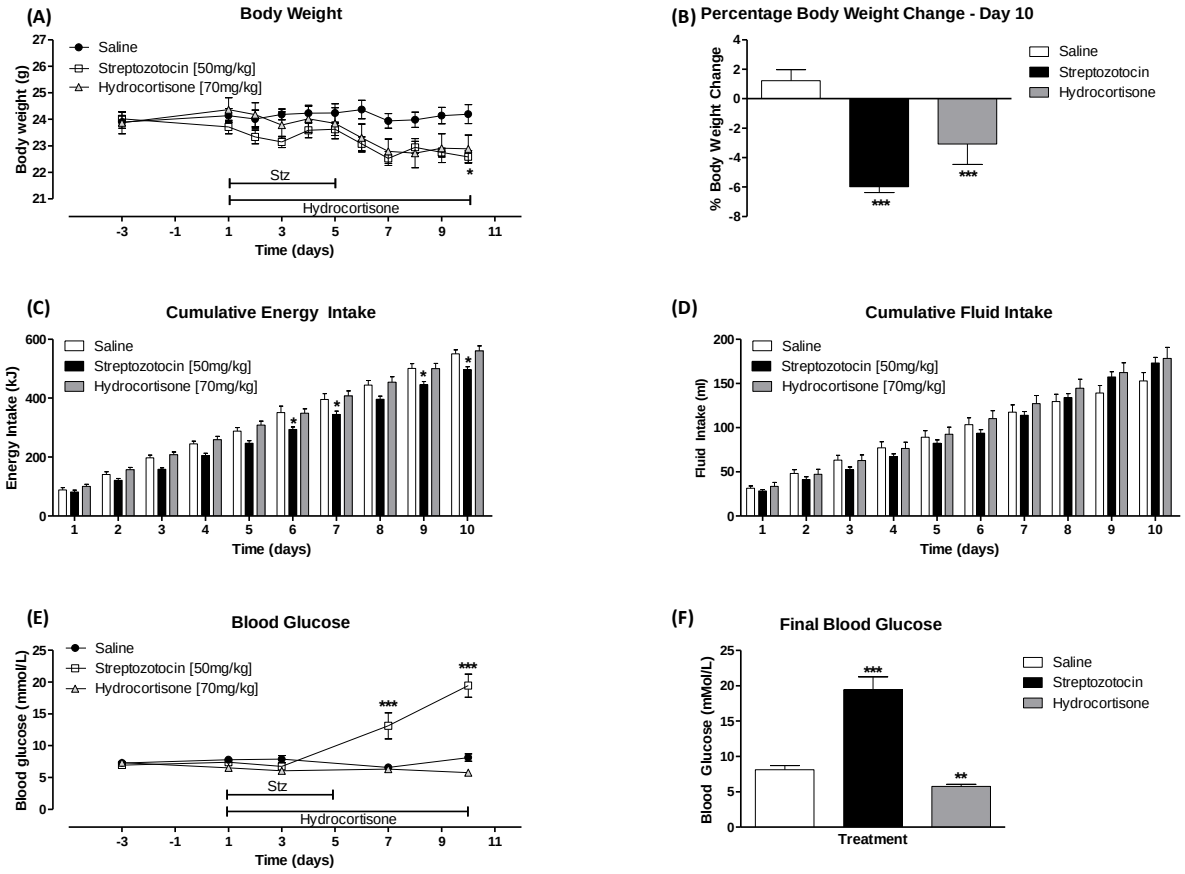

12 week old C57Bl/6 mice were treated with administered with streptozotocin (50mg/kg, ip, once daily, 5 days) or hydrocortisone (70mg/kg, ip, once daily, 10 days) n=8 mice/group. (A) Body weight, (B) percentage body weight change, (C) cumulative energy intake, (D) cumulative fluid intake, (E) blood glucose and (F) final blood glucose.

Comparisons were made against saline treated mice (*). Values were significant when $p<0.05$ *, $p<0.01$ ** and $p<0.001$ ***.

Figure 3.10: Effects of streptozotocin or hydrocortisone on pancreatic islet area, beta cell area, alpha cell area, islet size distribution, percentage beta cells and percentage alpha cells

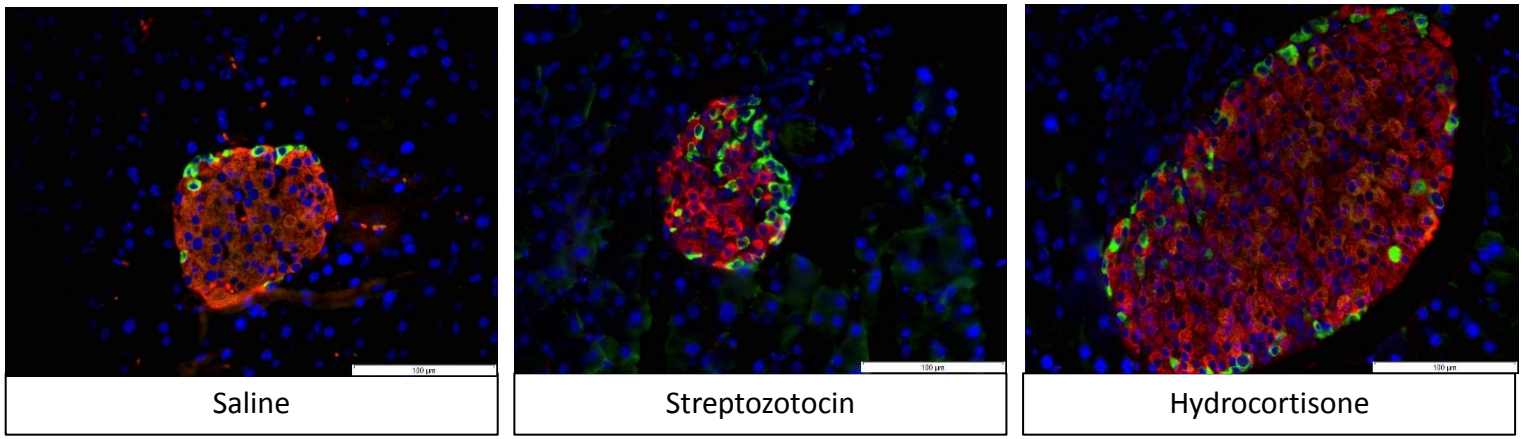

* Legend overleaf

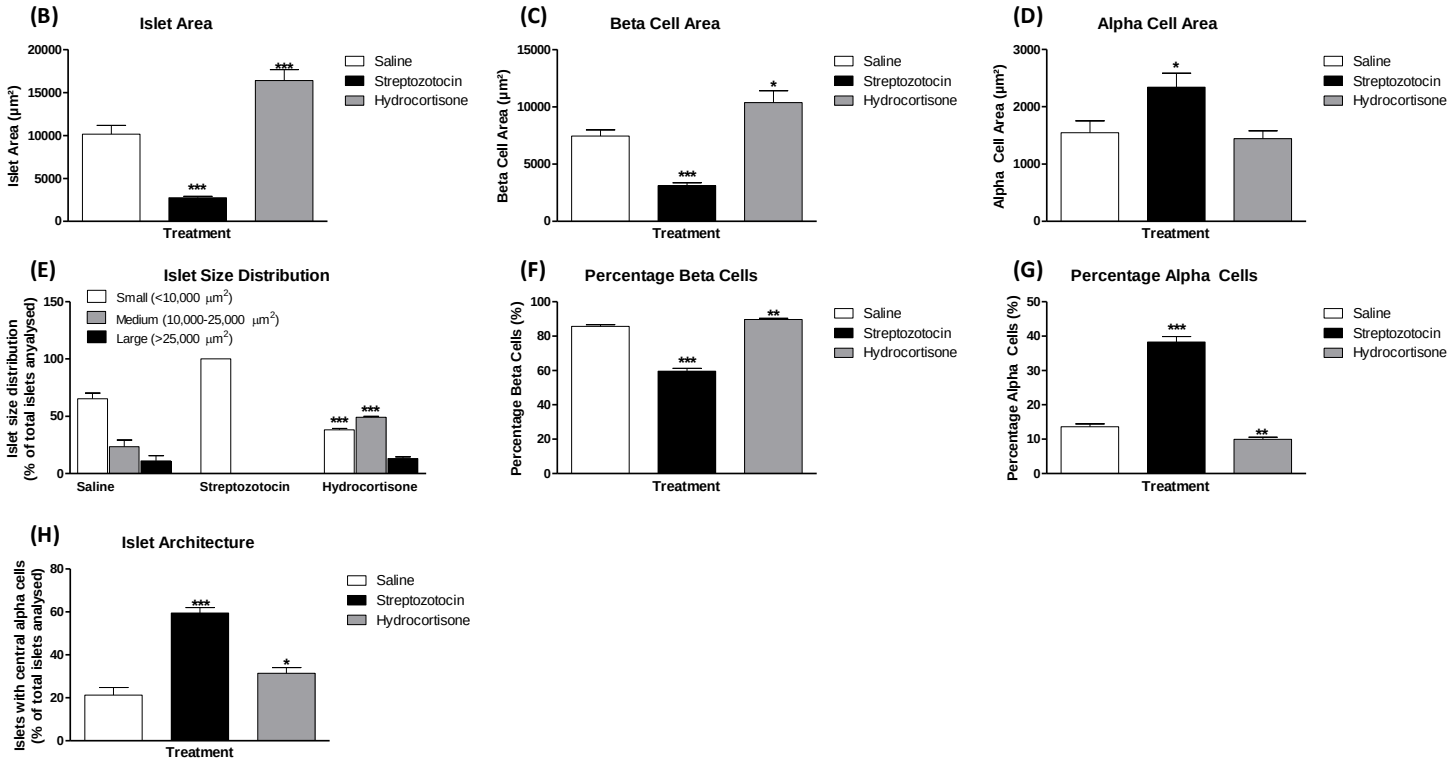

(A) Representative images of islets from saline, streptozotocin and hydrocortisone treated mice showing insulin (red), glucagon (green) and DAPI (blue). (B) Islet area, (C) beta cell area, (D) alpha cell area, (E) islet size distribution, (F) percentage beta cells, (G) percentage alpha cells and (H) islet architecture. Values are mean ± SEM(n=8 mice/group). Comparisons are versus saline, significant when *p<0.05, **p<0.01 and ***p<0.001.

Figure 3.11: Effects of streptozotocin or hydrocortisone on pancreatic beta cell markers

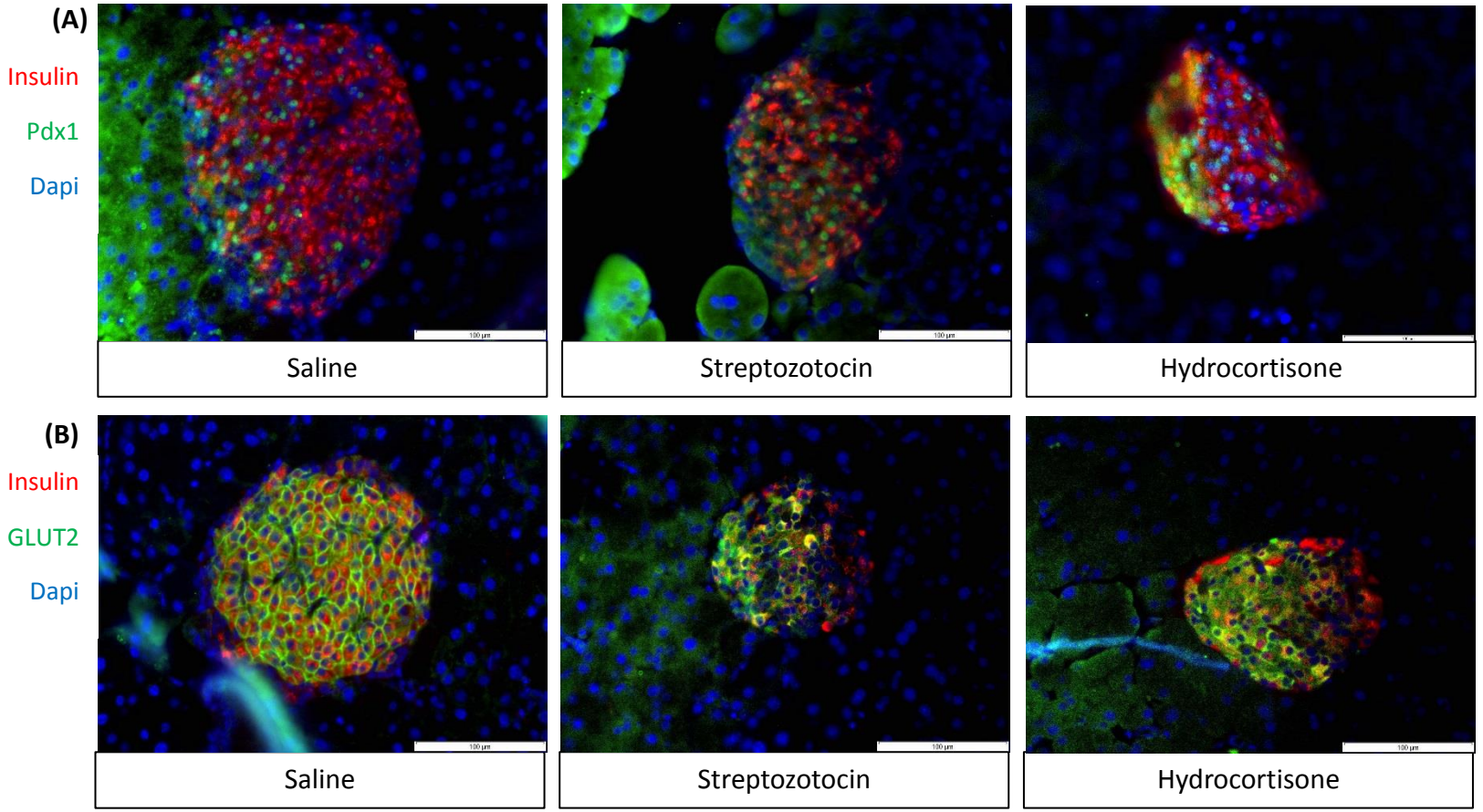

* Legend overleaf

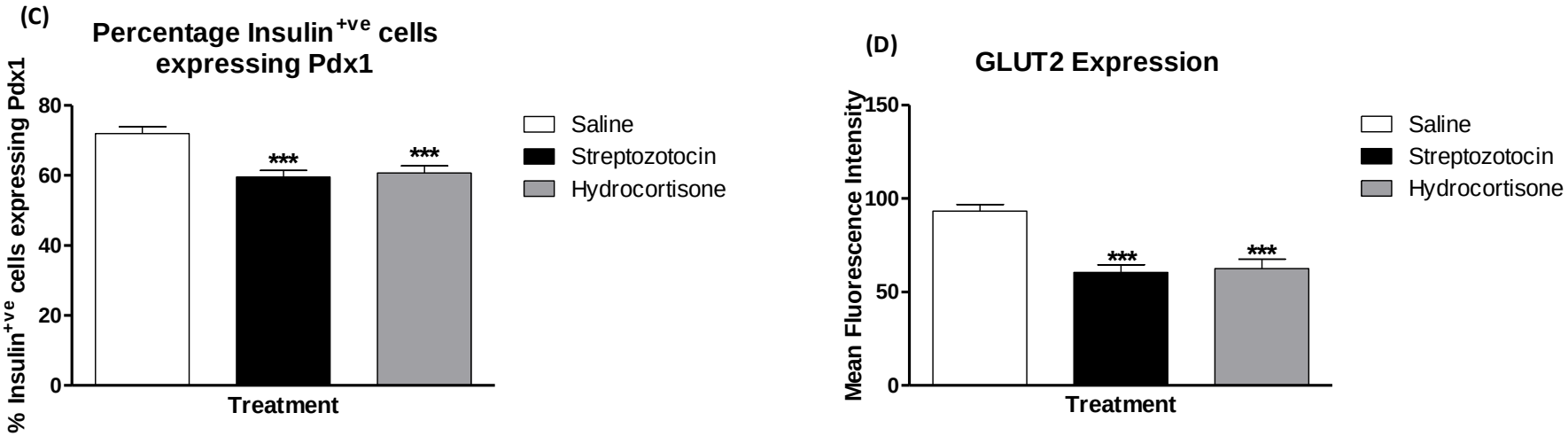

Beta Cell Markers

Representative images of islets from saline, streptozotocin and hydrocortisone treated mice stained for (A) insulin (red) and Pdx1 (green) or (B) insulin (red) and GLUT2 (green). (C) Percentage insulin positive cells expressing Pdx1 and (D) GLUT2 fluorescence intensity. Determined by histological analysis of insulin/Pdx1 and insulin/GLUT2 double immunofluorescence staining.

Values are mean ± SEM(n=8 mice/group). Comparisons are versus saline, significant when *p<0.05, **p<0.01 and ***p<0.001.

Figure 3.12: Effects of high fat feeding alone or in combination with exendin-4 on pancreatic islet area, beta cell area, alpha cell area, islet size distribution, percentage beta cells, percentage alpha cells and islet architecture

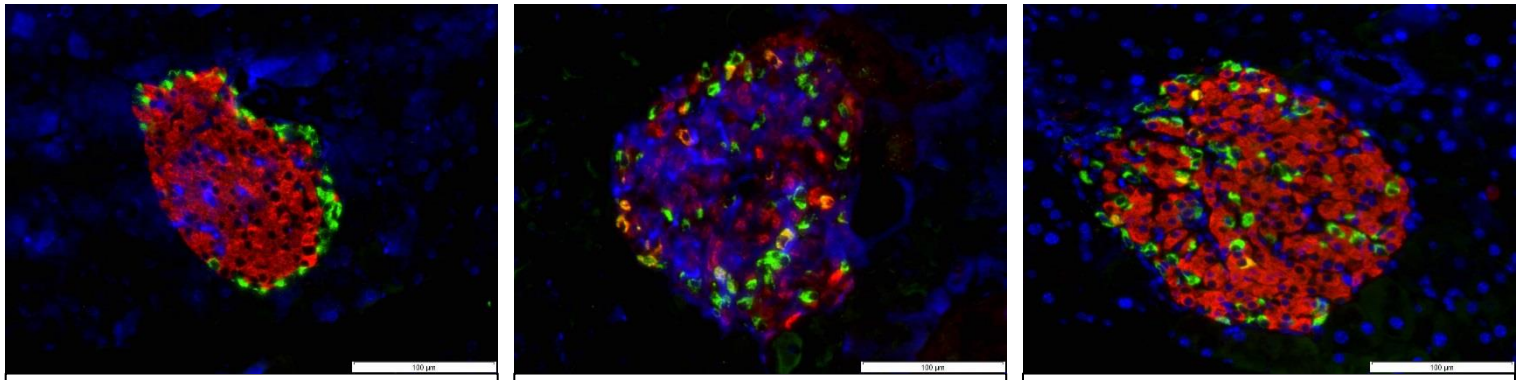

Lean Saline	High Fat	High Fat + Exendin-4

Insulin / Glucagon / DAPI

* Legend overleaf

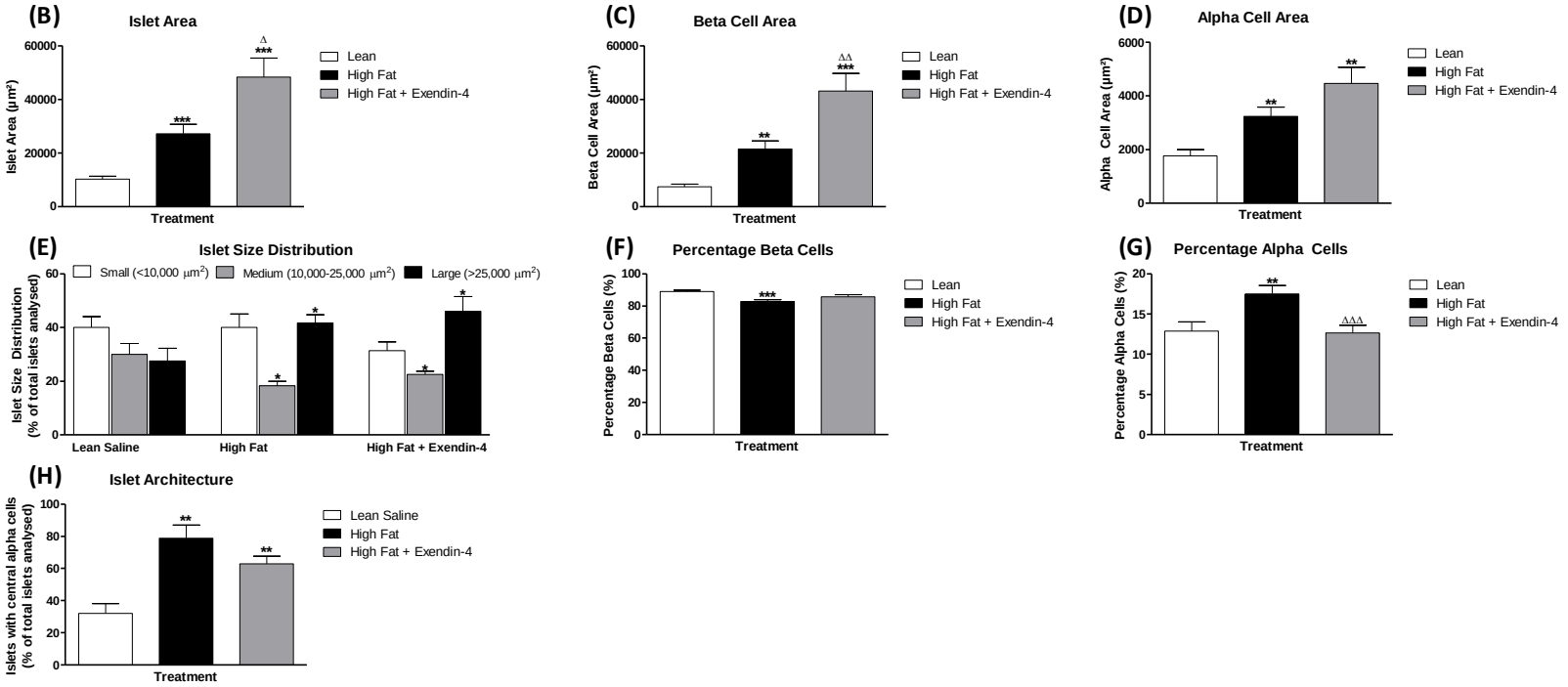

(A) Representative images of islets from lean saline, high fat fed and high fat fed + exendin-4 treated mice showing insulin (red), glucagon (green) and DAPI (blue). (B) Islet area, (C) beta cell area, (D) alpha cell area, (E) islet size distribution, (F) percentage beta cells, (G) percentage alpha cells and (H) islet architecture. Values are mean ± SEM. Comparisons are versus saline, significant when *p<0.05, **p<0.01 and ***p<0.001.

Figure 3.13: Effects of GIP or liraglutide treatment on pancreatic islet area, beta cell area, alpha cell area, islet size distribution, percentage beta cells, percentage alpha cells and islet architecture in leptin receptor deficient (db/db) mice

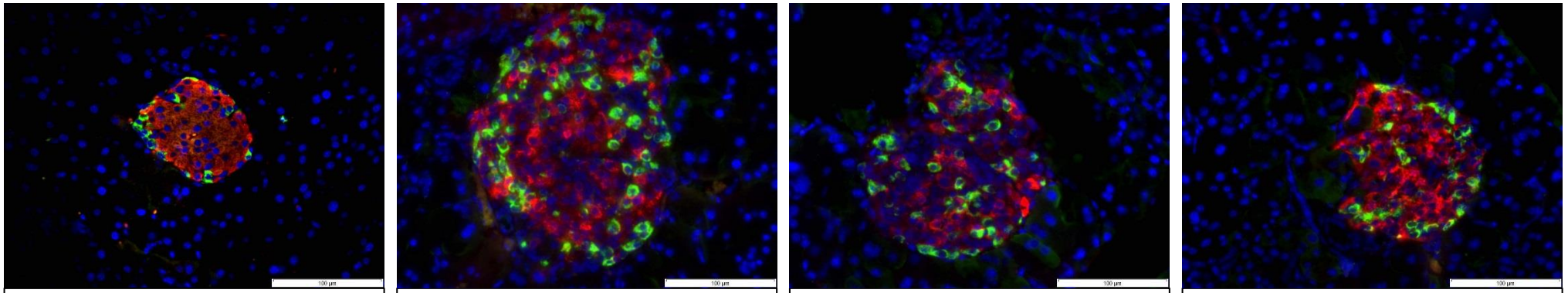

WT Saline	db/db Saline	db/db + GIP Antagonist	db/db + Liraglutide

Insulin / Glucagon / DAPI

* Legend overleaf

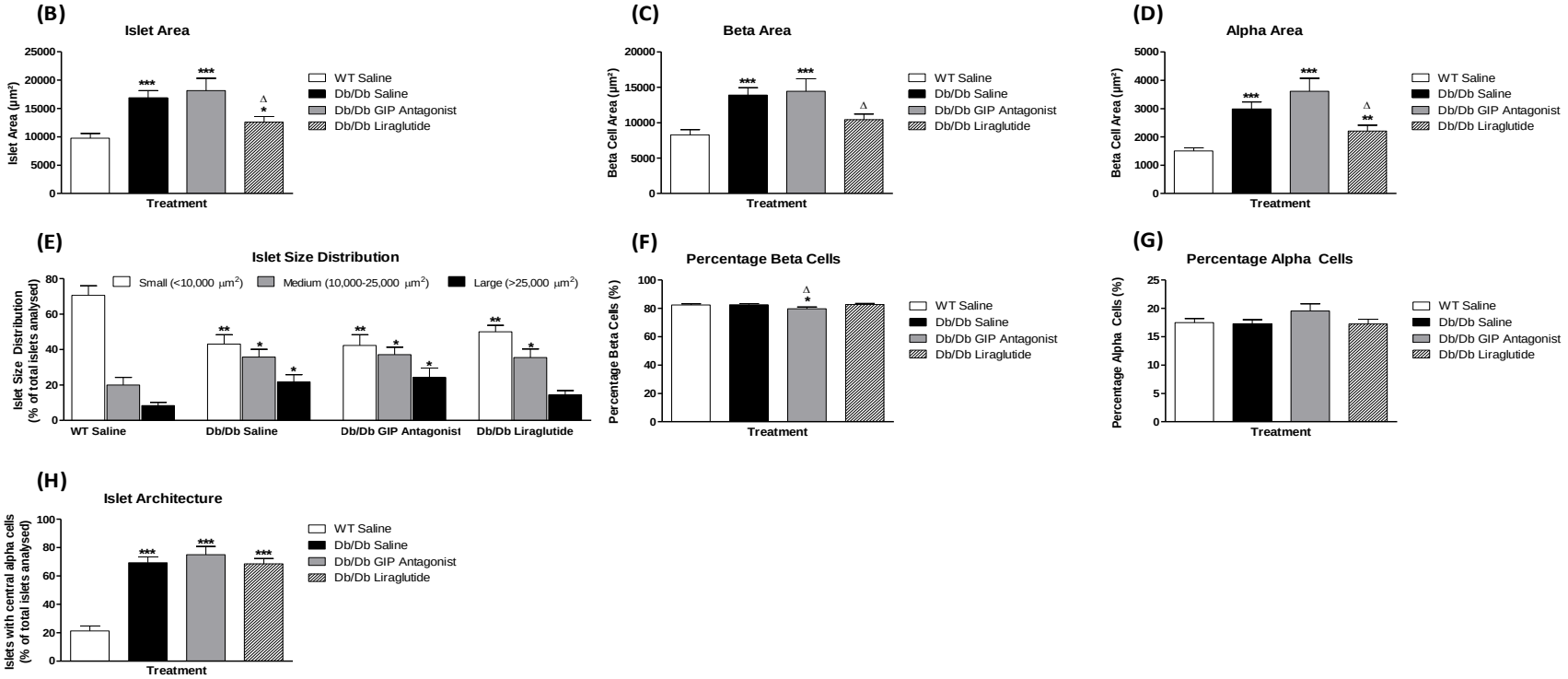

(A) Representative images of islets from C57Bl/6 wild-type saline, Db/db C57Bl/6 saline, Db/db + GIP and Db/db + liraglutide treated mice showing insulin (red), glucagon (green) and DAPI (blue). (B) Islet area, (C) beta cell area, (D) alpha cell area, (E) islet size distribution, (F) percentage beta cells, (G) percentage alpha cells and (H) islet architecture. Values are mean ± SEM. Comparisons are versus saline, significant when *p<0.05, **p<0.01 and ***p<0.001.

Chapter 4

Effect of GLP-1 mimetic (liraglutide) and DPPIV inhibitor (sitagliptin) on islet morphology and beta-to-alpha cell transdifferentiation

4.1 Summary

The effects of GLP-1 mimetic, liraglutide, and DPPIV inhibitor, sitagliptin, on beta cell transdifferentiation were explored in streptozotocin, hydrocortisone and high fat fed *Ins1*$^{cre/+}$;Rosa26-eYFP C57Bl/6 mice**.** All diabetic models exhibited disturbances in glucose homeostasis and islet stress with induced beta-to-alpha cell transdifferentiation with streptozotocin eliciting this to a greatest extent. Beta cell transdifferentiation was reduced by 12 days treatment with twice daily 25nmol/kg liraglutide or once daily 50mg/kg sitagliptin in streptozotocin induced diabetes. Both agents suppressed hyperglycaemia, restored circulating and pancreatic insulin levels whilst keeping plasma and pancreatic glucagon levels suppressed. Within the pancreas liraglutide was proficient in stimulating beta cell proliferation. In high fat fed mice these treatments were unable to affect beta cell transdifferentiation. However, both incretin therapies increased pancreatic insulin content, suppressed plasma glucagon and beta cell apoptosis. In hydrocortisone treated mice these agents were able to prevent transdifferentiation to alpha cells but were unable to maintain beta cell maturity, with the number of insulin deficient beta cells still raised. In these mice only liraglutide was able to restore pancreatic insulin and glucagon contents whist suppressing both beta cell apoptosis and alpha cell proliferation. These data suggests that *Ins1*$^{cre/+}$;Rosa26-eYFP C57Bl/6 mice display beta cell transdifferentiation in multiple animal models of diabetes. Treatment with the GLP-1 receptor agonist, liraglutide, and the DPPIV inhibitor, sitagliptin, was sufficient to limit beta cell transdifferentiation. This shows that incretin therapies are capable of preventing beta-to-alpha transdifferentiation offering a potential new mechanism of anti-diabetic therapy through restoration of lost transdifferentiated beta cells.

4.2 Introduction

4.2.1 Liraglutide

GLP-1 receptor agonists, such as liraglutide, are a widely used drug class for the treatment of type-2 diabetes. GLP-1 is endogenously produced and secreted from the intestinal enteroendocrine L cells in response to feeding. GLP-1 receptors are expressed throughout the body with their activation resulting in a wide variety of responses, many of which beneficial for the treatment of type-2 diabetes and obesity. Within the endocrine pancreas GLP-1 acts on beta cells to potentiate glucose-dependant insulin secretion, increase insulin biosynthesis, promote beta cell proliferation and reduce beta cell apoptosis, whilst on alpha cells it acts to inhibit glucagon secretion. The latter process is thought to be mediated through indirect paracrine stimulation of somatostatin secretion (Gromada et al, 1998; Nauck et al, 1992). Within the gut GLP-1 acts to delay gastric emptying and through this and actions within the CNS inhibits feeding (Mest et al, 2005; Arthen and Schmidtz, 2004; Song et al, 2017; Nauck et al, 1997; Flint et al, 1998). Other central actions of GLP-1 receptor activation include improved memory and cognition which may be useful for elucidating new treatments for cognitive disorders such as Alzheimer's and dementia (Porter et al, 2013; Porter et al, 2010). Liraglutide in particular is GLP-1 mimetic stabilised due to the fatty acid incorporated into its structure prolonging its half-life against DPPIV degradation and delaying renal excretion.

In streptozotocin induced diabetic mice and rats, liraglutide has been shown to reduce streptozotocin induced changes in blood glucose, plasma insulin and oxidative stress (Hendarto et al, 2012; Wen et al, 2018). Within the pancreas, liraglutide and

other GLP-1 based therapeutics have been shown to preserve beta cell mass in streptozotocin diabetes by reducing beta cell apoptosis and stimulating beta cell proliferation (Brubaker and Drucker, 2004; Vilsboll, 2009). In high fat fed mice liraglutide has been shown to cause a number of metabolic changes that aid to alleviate their diabetic condition. These range from reducing body weight without affecting food intake, reducing blood glucose and plasma insulin whilst increasing pancreatic insulin content and reducing pancreatic glucagon content, ultimately improving insulin resistance (Wang et al, 2015; Millar et al, 2017; O'Harte et al, 2018). This was associated with reduction of beta cell mass in both high fat fed and standard chow fed mice, whilst not discernibly impacting alpha cell mass (Mondragon et al, 2014; Millar et al, 2017). The effect of GLP-1 receptor agonists have yet to be published in hydrocortisone treated mice.

4.2.2 Sitagliptin

DPPIV is a serine threonine protease enzyme responsible for the cleavage and inactivation of many gut derived hormones. Its actions on GLP-1 and GIP cause cessation of the incretin effect. As a result pharmacological inhibitors of this enzyme, such as sitagliptin, increase the half-life of circulating GLP-1 and GIP to enhance glucose-stimulated insulin secretion and reduce postprandial elevations in glucagon to treat type-2 diabetes (Mest et al, 2005). Whether this is all attributable to elevated GLP-1 and GIP levels remains uncertain given that DPPIV inhibitors also prolong the half-life of other circulating gut hormones such as PYY.

Current literature states sitagliptin in streptozotocin induced diabetic mice protects against hyperglycaemia, improves glucose stimulated insulin secretion, and increases plasma insulin whilst lowering plasma glucagon (Ansarullah et al, 2013; Takeda et al, 2012). Additionally, sitagliptin therapy has been shown to alleviate the reduction in insulin content whilst suppressing the elevation of glucagon content found in streptozotocin treated mice (Takeda et al, 2012). On an islet level, sitagliptin therapy increased beta cell mass and limited streptozotocin induced increase in alpha cell mass. DPP4 inhibition was also demonstrated to increase beta cell proliferation (Ansaraullah et al, 2013), reduce alpha cell proliferation and reduce apoptosis of beta and alpha cells in streptozotocin treated mice (Cho et al, 2011; Takeda et al, 2012). Quite elegantly these authors have shown that sitagliptin's actions are more profound when the drug is administered in conjunction with streptozotocin compared with started treatment post streptozotocin insult. In high fat fed mice sitagliptin treatment has been shown to reduce body weight, non-fasting blood glucose, whilst elevating plasma insulin and GLP-1 levels (Cox et al, 2017; Gault et al, 2015). Similar to GLP-1 mimetics, sitagliptin has also been shown to improve cognitive function in high fat fed mice (Gault et al, 2015). Interesting Cox et al, (2017) have noted that depending on the duration of treatment sitagliptin has varied effects on beta cell proliferation, with short term (2 weeks) treatment increasing beta cell proliferation whilst long term (10 weeks treatment) reduced proliferation of beta cells. Similar to liraglutide, no data has yet been published on sitagliptin therapy in hydrocortisone treated mice.

The present studies utilised transgenic *Ins1*$^{cre/+}$;Rosa26-eYFP C57Bl/6 mice that constitutively express a fluorescent marker (eYFP) within their beta cells allowing for lineage tracing studies (Thorens et al, 2015). This permitted investigation of beta cell dedifferentiation and transdifferentiation within animal models of diabetes. Three models of diabetes were explored each of which recreate a particular hallmark of diabetes. These were: multiple low-dose streptotozocin (insulin deficiency), high fat fed (insulin resistance with declining beta cell function) and multiple dose hydrocortisone (insulin resistance). Following identification of beta cell transdifferentiation in these models the actions of liraglutide and sitagliptin have on beta cell maturity or transdifferentiation were explored.

4.3 Materials and Methods

Materials and methods have been briefly summarised below. Full explanations of each method can be found within chapter 2.

4.3.1 Animals

Ins1$^{cre/+}$;Rosa26-eYFP C57Bl/6 mice were bred in house at the Biomedical and Behavioural Research Unit (BBRU) at Ulster University, Coleraine. The original background of these mice have been characterised by Thorens et al, 2015. Mice were kept individually housed in a temperature controlled room (22±2°C) on a regular 12 hour light/dark cycle. Mice had access to standard chow (Trou Nutrition, Norwich, UK) and drinking water *ad libitum*. All *in vivo* experiments were approved by Ulster

University Animal Ethics Review Committee and conducted in accordance to the UK Animals (Scientific Procedures) Act 1986.

Diabetes was induced in 12 week old male mice through administration of different chemicals as specified. For streptozotocin studies, mice were given 5 days consecutive intraperitoneal injections of 50mg/kg streptozotocin, freshly dissolved in citrate buffer, with diabetic symptoms presenting within the following 5 days. For hydrocortisone studies, mice were given 10 days consecutive intraperitoneal injections of 70mg/kg hydrocortisone, dissolved in saline (0.9% NaCl). In both of these models twice daily intraperitoneal administration of 25nmol/kg liraglutide and once daily oral administration of 50mg/kg sitagliptin was started two days prior to administration of streptozotocin/hydrocortisone and this dosing was continued until the end of the study at day 10.

For high-fat feeding studies mice were kept on a high fat diet (45% fat) from weaning (4 weeks old) with experiments conducted at 15 weeks old when the now obese mice were similarly dosed with twice daily 25nmol/kg liraglutide or once daily 50mg/kg sitagliptin for 12 days. For all conducted studies mice were 8 per treatment group with body weight, blood glucose, calorie and fluid consumption monitored regularly. Dosing regimen was selected based on previously established literature (Moffet et al, 2014; Gault et al, 2015). Prior to the end of the study, a glucose tolerance test was conducted whereby overnight fasted mice were subjected to an 18.8mMol/kg glucose load with blood glucose assessed regularly for the following hour. Timelines of each animal study are presented in Figure 4.0. For all *in vivo* studies measurements

of body weight, non-fasting blood glucose, calorie and fluid consumption were assessed regularly.

4.3.2 Biochemical Analysis

Snap frozen pancreatic tissues, taken at the end of each study, were homogenised in acid ethanol (ethanol (75% (v/v) ethanol, 5% (v/v) distilled water and 1.5% (v/v) 12N HCl) and protein extracted in a pH neutral TRIS buffer. Protein content was determined using Bradford reagent (Sigma-Aldrich, Dorset, UK). Plasma and pancreatic insulin content was determined by an in-house insulin radioimmunoassay. Plasma and pancreatic glucagon content were determined by ELISA (glucagon chemiluminescent assay, EZGLU-30K, Millipore) following the manufacturers guidelines.

4.3.3 Immunohistochemistry

Upon termination of studies, pancreatic tissue was extracted and fixed in 4% PFA for 48 hours at 4°C. Tissues were processed and embedded in paraffin wax blocks using an automated tissue processor (Leica TP1020, Leica Microsystems, Nussloch, Germany) and 5µm sections were cut on a microtome (Shandon finesse 325, Thermo scientific, UK). For immunohistochemistry, slides were dewaxed by immersion in xylene and rehydrated through a series of ethanol solutions (100-50%). Heat mediated antigen retrieval was then carried out at 95°C in citrate buffer (pH6) for 20 minutes. Sections were then blocked in 4% BSA solution before 4°C overnight incubation with the

following primary antibodies as appropriate: mouse monoclonal anti-insulin antibody (ab6995, 1:1000; Abcam), guinea-pig anti-glucagon antibody (PCA2/4, 1:200; raised in-house), rabbit anti-Ki67 antibody (ab15580, 1:200; Abcam) and rabbit anti-Pdx1 antibody (ab47267, 1:200; Abcam). Following this, slides were incubated for 45 minutes at 37°C with secondary antibodies: Alexa Fluor488 goat anti-guinea pig IgG — 1:400, Alexa Fluor 594 goat anti-mouse IgG — 1:400, Alexa Fluor 488 goat anti-rabbit IgG — 1:400, Alexa Fluor 594 goat anti-rabbit IgG — 1:400 or Alexa Fluor 488 donkey anti-goat IgG — 1:400. Sections were then incubated a final time with DAPI for 15 minutes at 37°C. Slides were then mounted and ready for imaging using a fluorescent microscope (Olympus system microscope, model BX51) fitted with DAPI (350nm) FITC (488nm) and TRITC (594nm) filters and a DP70 camera adapter system. To assess apoptosis a TUNEL assay was carried out following manufacturer's guidelines (In situ cell death kit, Fluorescein, Roche Diagnostics, UK).

4.3.4 Image Analysis

Cell^F imaging software (Olympus Soft Imaging Solutions, GmbH) was used to analyse the following islet parameters: islet area, beta cell area, alpha cell area (expressed at μm^2), percentage beta cells and percentage alpha cells. Islets were deemed small (<10,000 μm^2), medium (10,000-25,000 μm^2) or large (>25,000 μm^2) to determine islet size distribution. The number of islets per mm^2 pancreas and proportion of islets with central alpha cells were judged in a blinded fashion. For transdifferentiation analysis beta cells expressing GFP with no insulin were termed "$insulin^{-ve}$, GFP^{+ve} cells", an indication of dedifferentiated beta cells, whilst those expressing GFP with

glucagon were termed "glucagon^{+ve}, GFP^{+ve} cells", an indication of beta-to-alpha cell transdifferentiated cells. To quantify apoptosis beta and alpha cells co-expressing TUNEL alongside insulin and glucagon respectively were counted. Similarly for proliferation Ki-67 and insulin/glucagon positive cells were totalled. Beta cell Pdx1 expression was quantified using ImageJ software, counting the total number of insulin positive beta cells within an islet and expressing the number of those expressing Pdx1 as a percentage of that total. All cell counts were determined in a blinded manner with >60 islets analysed per treatment group.

4.3.5 Statistics

All results were generated and analysed using GraphPad PRISM (version 5), with data presented as mean ± SEM. Comparative analyses between groups were carried out using Student's unpaired t-test, one-way ANOVA with a Bonferroni post-hoc test or a two-way repeated measures ANOVA with a Bonferroni post-hoc test where appropriate. Results were deemed significant once $p<0.05$.

4.4 Results

4.4.1 Effects of streptozotocin alone or in combination with liraglutide or sitagliptin treatment on body weight, energy intake and fluid intake

All mice displayed a decline in body weight which was not significant between groups (Figure 4.1A). Compared to the non-diabetic animals all mice treated with

streptozotocin showed a significant decline in percentage body weight change (-7.6 ± 0.3 vs -0.7 ± 0.8%; $p<0.001$, Figure 4.1B) with mice treated with sitagliptin showing a further reduction (-9.0 ± 0.6%; $p<0.05$, Figure 4.1B) relative to the diabetic animals. Streptozotocin treated mice displayed reduced cumulative calorie consumption from day 4 of the study onwards compared to saline-treated animals. Diabetic mice treated with liraglutide or sitagliptin showed a further reduction ($p<0.05$ and $p<0.05$, Figure 4.1C) in calorie consumption which was significantly lower than mice given solely streptozotocin from days 8 and 6 onwards respectively. Cumulative fluid intake was only raised ($p<0.01$) in streptozotocin treated animals after day 9 of the study. A stark contrast to mice that also received liraglutide and sitagliptin that showed raised fluid consumption ($p<0.001$ and $p<0.001$) from days 2 and 4 respectively (Figure 4.1D).

4.4.2 Effects of streptozotocin alone or in combination with liraglutide or sitagliptin treatment on blood glucose, plasma insulin/glucagon and pancreatic insulin/glucagon content

Following 5 daily doses mice treated with streptozotocin alone showed an increase ($p<0.001$) in non-fasting glucose concentrations from day 7 onwards peaking to 26.3 ± 1.4 vs 7.7mM by day 10 (Figure 4.2A). Treatment with liraglutide and sitagliptin resulted in a delayed, subdued increase in non-fasted glucose levels peaking only to 14.8 ± 1.8mM and 21.0 ± 0.5mM respectively; significantly lower ($p<0.001$) than the non-treated diabetic animals yet still higher ($p<0.001$) than normoglycaemic saline treated mice (Figure 4.1B). Plasma and pancreatic insulin were both reduced (5.2 ±

0.4 vs 9.2 ± 1.1ng/ml; p<0.001 and 29.1 ± 1.9 vs 42.6 ± 2.1ng/mg protein; p<0.001, Figure 4.2C-D) within streptozotocin treated diabetic animals respectively. Mice receiving liraglutide or sitagliptin were able to preserve circulating (10.5 ± 1.5ng/ml; p<0.001 and 8.4 ± 0.8ng/ml; p<0.01 respectively, Figure 4.2C) and pancreatic (43.3 ± 3.1ng/mg protein; p<0.001 and 39.3 ± 4.3ng/mg protein; P<0.05, Figure 4.2D) insulin levels compared to the diabetic animals, to levels equivalent to the non-diabetic mice. Circulating glucagon levels were substantially higher in streptozotocin treated mice (0.08 ± 0.009 vs 0.02 ± 0.001ng/ml; p<0.001, Figure 4.2E). Plasma glucagon from liraglutide and sitagliptin treated mice were still raised compared to the non-diabetic animals however liraglutide treatment showed a reduction compared to the diabetic animals (0.04 ± 0.003ng/ml, p<0.01, Figure 4.2E). Likewise pancreatic glucagon content was raised in streptozotocin treated animals (18.7 ± 1.2 vs 7.8 ± 1.2ng/mg protein, p<0.01, Figure 4.2F) whist both the GLP-1 mimetic and DPPIV inhibitor capable of reducing these levels (8.5 ± 0.6ng/mg protein, p<0.001 and 11.8 ± 0.9ng/mg protein, p<0.01, respectively, Figure 4.2F). Liraglutide in particular was able to restore pancreatic glucagon content to levels comparable to non-diabetic mice.

4.4.3 Effects of streptozotocin alone or in combination with liraglutide or sitagliptin treatment on islet parameters

Representative images of islets from saline, streptozotocin, liraglutide plus streptozotocin an sitagliptin plus streptozotocin treated mice display insulin (red), glucagon (green) and nuclei (blue) (Figure 4.3A). Streptozotocin treated mice displayed reduced islet area (4407 ± 393.3 vs 8893 ± 942.6μm^2; p<0.01, Figure 4.3B),

beta cell area (3309 ± 287.5 vs 7546 ± 814.0μm^2; p<0.01, Figure 4.3C) and increased alpha cell area (2635 ± 271.8 vs 1589 ± 156.2μm^2; p<0.001, Figure 4.3D). Treatment with liraglutide or sitagliptin showed similar, albeit subdued, changes in islet morphology. Islet area in liraglutide and sitagliptin treated groups was improved comparative to streptozotocin treated mice (7279 ± 625.8; p<0.001 and 6934 ± 815.3μm^2; p<0.05 respectively) due to conservation of beta cell area and elevations in alpha cell area (Figure 4.3B-D). Streptozotocin treated mice showed an ablation of large islets with medium sized islets predominating (31.7 ± 1.7 vs 19.3 ± 1.5%; p<0.01, Figure 4.3E). Percentage beta cells was significantly reduced (58.9 ± 1.8 vs 79.4 ± 0.9%; p<0.001, Figure 4.3F) in all groups that received streptozotocin with the sitagliptin treated mice showing a further reduction (51.8 ± 1.7%; p<0.01, Figure 4.3F) comparative to the streptozotocin only animals. Reciprocal changes were also observed in percentage alpha cells which increased (43.1 ± 2.1 vs 20.4 ± 0.9%; p<0.001, Figure 4.3G) in all streptozotocin treated groups (49.1 ± 1.8%; p<0.01, Figure 4.3G). Streptozotocin treatment severely disrupted islet architecture, quantified by the percentage of islets showing centrally located alpha cells (70.0 ± 4.4 vs 20.0 ± 4.0%, p<0.001, Figure 4.3H). Liraglutide and sitagliptin therapies were able to substantially protect normal murine islet architecture, with the former able to do this to a much greater extent (liraglutide 33.0 ± 4.0%, p<0.001 and sitagliptin 56.0 ± 2.7%, p<0.05, Figure 4.3H).

4.4.4 Effects of streptozotocin alone or in combination with liraglutide or sitagliptin treatment on beta-to-alpha cell transdifferentiation

Beta-to-alpha cell transdifferentiation was determined by populations of insulin negative, GFP positive cells and glucagon positive, GFP positive cells with representative images shown in Figure 4.4A and Figure 4.4B respectively. Streptozotocin treated mice display a greater number of islets showing insulin negative, GFP positive cells (5.6 ± 0.7 vs 0.4 ± 0.1%, $p<0.001$, Figure 4.4C) and glucagon positive, GFP positive cells (5.7 ± 0.6 vs 1.4 ± 0.3%, $p<0.001$, Figure 4.4D). Mice given liraglutide in conjunction with streptozotocin had a reduced number of insulin negative, GFP positive cells (5.6 ± 0.7%; $p<0.001$, Figure 4.4C) and glucagon positive, GFP positive cells (3.6 ± 0.7%, $p<0.05$, Figure 4.4D) in comparison to the streptozotocin only treated animals. Similarly mice treated with sitagliptin exhibited islets with reduced insulin negative, GFP positive cells (3.3 ± 0.4%, $p<0.01$, Figure 4.4C) and glucagon positive, GFP positive (3.6 ± 0.6%, $p<0.05$, Figure 4.4D) compared to the streptozotocin treated mice.

4.4.5 Effects of streptozotocin alone or in combination with liraglutide or sitagliptin treatment on beta cell and alpha cell apoptosis

Beta cell and alpha cell apoptosis was assessed by populations of islets expressing TUNEL positive cells and insulin positive (Figure 4.5A) or glucagon positive cells (Figure 4.5B) respectively. Non-diabetic animals displayed low levels of beta cell apoptosis (2.7 ± 0.5%) compared to mice treated with streptozotocin (11.0 ± 1.8%,

p<0.001). Liraglutide (6.7 ± 1.1%, p<0.05) and sitagliptin (6.4 ± 0.9%, p<0.001, Figure 4.5C) limited this death of beta cells. Similarly the number of alpha cells undergoing apoptosis was also increased by streptozotocin (4.6 ± 0.9 vs 1.7 ± 0.3%, p<0.001, Figure 4.5D). Treatment with sitagliptin had no effect on this raised apoptotic level however liraglutide treatment was able to elicit a reduction in alpha cell apoptosis (2.5 ± 0.6%, p<0.05, Figure 4.5D).

4.4.6 Effects of streptozotocin alone or in combination with liraglutide or sitagliptin treatment on beta cell and alpha cell proliferation

Immunohistochemistry of insulin and ki-67 was used to assess beta cell proliferation (Figure 4.6A). Streptozotocin alone and in combination with sitagliptin had no impact on beta cell proliferation. Treatment with the GLP-1 receptor agonist, liraglutide, however produced a substantial elevation in beta cell proliferation (9.0 ± 1.2 vs 3.9 ± 0.8%, p<0.001, Figure 4.6C). Alpha cell proliferation was evaluated by quantifying glucagon positive, ki-67 positive cells (Figure 4.6B). Non-diabetic animals exhibited low levels of glucagon proliferation (3.3 ± 0.6%) in contrast with the increase found in diabetic streptozotocin treated mice (8.2 ± 1.1%, p<0.001, Figure 4.6D). Mice treated with liraglutide showed no profound change in alpha cell proliferation, whilst sitagliptin treatment reduced alpha cell proliferation (4.5 ± 0.9%, p<0.05, Figure 4.6D).

4.4.7 Effects of streptozotocin alone or in combination with liraglutide or sitagliptin treatment on beta cell Pdx1 expression

Expression of the mature beta cell marker Pdx1 was quantified by the number of Pdx1 positive, insulin positive cells as represented in Figure 4.7A. Non-diabetic mice showed substantial expression of Pdx1 within beta cells (65.7 ± 1.3%) differing greatly from streptozotocin treated mice that depleted beta cell Pdx1 expression (53.3 ± 1.0%, $p<0.0001$). Treatment with either liraglutide or sitagliptin was sufficient to restore Pdx1 expression (62.2 ± 1.1%, $p<0.0001$ and 60.2 ± 1.7%, $p<0.0001$ respectively, Figure 4.7B).

4.4.8 Effects of high fat feeding alone or in combination with liraglutide or sitagliptin treatment on body weight, energy intake and fluid intake

All mice kept on a high fat diet showed a significant increase in body weight (39.8 ± 1.3 vs 25.7 ± 0.2g, $p<0.001$, Figure 4.8A) compared to lean mice at all time points. Between the first and last time points high fat fed mice treated with liraglutide had lost significant percentage of body weight (-13.3 ± 0.7%vs 0.7 ± 1.3%, $p<0.001$ Figure 4.8B). High fat fed mice treated with sitagliptin maintained their percentage body weight comparative to the lean fed mice. As expected cumulative energy intake was increased in high fat fed mice throughout the study (887.2 ± 78.0 vs 538.8 ± 13.3kJ, $p<0.001$, Figure 4.8C). Mice treated with liraglutide exhibited less energy intake than high fat fed mice however this did not meet significance (Figure 4.8C). Similarly cumulative fluid consumption was significantly raised in high fat fed mice (216.0 ± 7.0

vs 92.4 ± 4.2ml, p<0.001, Figure 4.8D). However unlike energy intake, fluid consumption was significantly reduced in high fat fed mice given liraglutide and sitagliptin (154.5 ± 2.0ml, p<0.001 and 154.7 ± 12.4ml, <0.001 respectively, Figure 4.8D).

4.4.9 Effects of high fat feeding alone or in combination with liraglutide or sitagliptin treatment on blood glucose, plasma insulin/glucagon, pancreatic insulin/glucagon and glucose tolerance test

Over the study period mice between all treatment groups exhibited no substantial change in non-fasting blood glucose levels (Figure 4.9A). However final blood glucose reading was notably reduced in liraglutide and sitagliptin treated mice compared to high fat fed alone (7.5 ± 0.2mM, P<0.01 and 7.6 ± 0.2mM, p<0.01 respectively vs 8.7 ± 0.3mM, Figure 4.9B). Plasma insulin was increased in all mice kept on high fat diet (13.7 ± 2.6 vs 6.9 ± 0.3ng/ml, p<0.05, Figure 4.9C) with no discernible difference between liraglutide and sitagliptin groups. Despite this increase, pancreatic insulin content was raised in liraglutide and sitagliptin treated groups (54.6 ± 3.0ng/mg protein, p<0.001 and 51.5 ± 2.6ng/mg protein, p<0.001 vs high fat fed alone 35.1 ± 1.7ng/mg protein, Figure 4.9D). Similar to plasma insulin, circulating glucagon levels were only raised in high fat fed saline treated mice (0.05 ± 0.003 vs 0.02 ± 0.002ng/ml, p<0.001, Figure 4.9E). This was reduced in mice treated with liraglutide (0.03 ± 0.002ng/ml, p<0.01) and sitagliptin (0.02 ± 0.003ng/ml, p<0.01) with the latter being equivalent to the lean mice. Contrasting findings were found with only high fat fed saline treated mice exhibiting lower pancreatic glucagon content (3.9 ± 0.6 vs 7.8 ±

1.2ng/mg protein, P<0.05, Figure 4.9F). An intraperitoneal glucose tolerance test was conducted at the end of the study. All high fat fed mice displayed raised blood glucose levels at 30 minute and 60 minute time points. Only sitagliptin treated mice were able to significantly lower blood glucose at 60 minutes compared to the high fat fed saline mice (20.8 ± 0.6 vs 23.8 ± 1.2mM, p<0.05, Figure 4.9G). Despite this, when analysed by area under the curve only liraglutide treatment was able to reduce AUC compared to the high fat saline animals (1110 ± 42.0 vs 1266 ± 38.2, p<0.05, Figure 4.9H).

4.4.10 Effects of high fat feeding alone or in combination with liraglutide or sitagliptin treatment on islet parameters

Representative images of islets from lean saline, high fat fed saline, high fat fed plus liraglutide and high fat fed plus sitagliptin treated mice displaying insulin (red), glucagon (green) and nuclei (blue) (Figure 4.10A). High fat fed mice pancreatic tissue contained much larger islets showing increases in islet area (19360 ± 1567 vs 7617 ± 721.1µm^2, P<0.001, Figure 4.10B), beta cell area (16590 ± 1347 vs 5926 ± 567.8µm^2, p<0.001, Figure 4.10C) and alpha cell area (2778 ± 258.0 vs 1690 ± 185.2µm^2, p<0.001, Figure 4.10D). Most prominently sitagliptin was able to elicit significant reductions in islet area (13400 ± 1274µm^2, p<0.05, Figure 4.10B), beta cell area (11230 ± 1108µm^2, p<0.01, Figure 4.10C) and alpha cell area (1950 ± 177.5, p<0.05, Figure 4.10D). Liraglutide however was only able to notably reduce beta cell area (11600 ± 1332µm^2, p<0.05, Figure 4.10C). Islet size distribution was markedly altered with all high fat fed groups displaying reductions in small islets (33.8 ± 2.1 vs 70.5 ± 2.4%, p<0.001, Figure 4.10E) with reciprocal increases in the number of medium and

large sized islets (40.1 ± 2.5 vs 19.1 ± 1.2%, p<0.001 and 27.9 ± 2.7 vs 10.8 ± 1.4%, p<0.01 respectively, Figure 4.10E). Of note sitagliptin therapy was able to restore normal size distribution by increasing the proportion of smaller islets (51.2 ± 3.0%, p<0.001, Figure 4.10E) whilst reducing larger islets (11.3 ± 1.5%, p<0.001, Figure 4.10E) to proportions comparable to lean mice. Twice daily liraglutide therapy was only able to raise the proportion of smaller islets (48.6 ± 1.6% p<0.001, Figure 4.10E) found within the pancreas compared to high fat fed mice. In line with these changes percentage beta cells was also increased in high fat fed mice (85.3 ± 0.6 vs 80.5 ± 08%, p<0.001. Figure 4.10F). Both treated groups produced a significant reduction in percentage beta cells (liraglutide 80.9 ± 1.0%, p<0.001 and sitagliptin 83.3 ± 0.8%, p<0.05, Figure 4.10F) however only liraglutide was able to reduce this to levels comparable to lean mice. Conversely percentage alpha cells was significantly reduced in high fat fed mice (14.7 ± 0.6 vs 19.9 ± 0.8%, p<0.001, Figure 4.10G) with liraglutide only able to return this to levels equivalent to lean mice (19.6 ± 1.1%, Figure 4.10G). Islet architecture became severely dysregulated with high fat feeding resulting in islets containing centrally located alpha cells (41.3 ± 3.9 vs 20.0 ± 4.0%, p<0.01, Figure 4.10H). Liraglutide and sitagliptin treatments were able to preserve normal islet architecture however only the former was statistically significant (24.2 ± 2.3%, p<0.01, Figure 4.10H).

4.4.11 Effects of high fat feeding alone or in combination with liraglutide or sitagliptin treatment on beta-to-alpha cell transdifferentiation

Representative images of beta cell transdifferentiation, assessed by immunohistochemical staining of insulin with GFP and glucagon with GFP are presented in Figure 4.11 A and B respectively. There was a moderate increase in the percentage of islets displaying insulin negative, GFP positive cells in high fat fed mice (6.9 ± 0.7 vs 0.4 ± -0.1%, $p<0.001$, Figure 4.11C) which was reduced by both liraglutide (3.2 ± 0.4%, $p<0.001$, Figure 4.11C) sitagliptin treatments (4.2 ± 0.6%, $p<0.01$, Figure 4.11C). Likewise, glucagon positive, GFP positive cells increased in high fat fed mice (6.7 ± 0.6 vs 1.4 ± 0.3%, $p<0.001$, Figure 4.11D) although in this case only liraglutide elicited a reduction in this parameter (3.7 ± 0.4%, $p<0.001$, Figure 4.11D).

4.4.12 Effects of high fat feeding alone or in combination with liraglutide or sitagliptin treatment on beta and alpha cell apoptosis

Representative histology images of beta cell apoptosis and alpha cell apoptosis are displayed in Figure 4.12A and B respectively. High fat feeding resulted in an increase in both beta cell (4.9 ± 0.7 vs 2.7 ± 0.6%, $p<0.05$, Figure 4.12C) and alpha cell apoptosis (4.8 ± 1.1 vs 1.7 ± 0.3%, $p<0.01$, Figure 4.12D). Both liraglutide and sitagliptin were able to elicit reductions in beta cell apoptosis (liraglutide 2.9 ± 0.6%, $p<0.05$ and sitagliptin 1.5 ± 0.4%, $p<0.001$, Figure 4.12C) whilst not affecting alpha cell apoptosis.

4.4.13 Effects of high fat feeding alone or in combination with liraglutide or sitagliptin treatment on beta and alpha cell proliferation

Representative images displaying the effect of high fat feeding with liraglutide and sitagliptin on beta cell proliferation and alpha cell proliferation are displayed in Figure 4.13A and 4.13B respectively. High fat feeding caused a significant increase in the number of beta cells and alpha cells undergoing proliferation (beta cells 5.9 ± 1.1 vs 2.2 ± 0.5%, $p<0.01$, Figure 4.13C and alpha cells 5.7 ± 0.9 vs 3.3 ± 0.6%, $p<0.01$, Figure 4.13D). Liraglutide had no further impact on beta cell or alpha proliferation, both with levels equivalent to the high fat fed saline group. Sitagliptin however was able to bring about a reduction in alpha cell proliferation (2.6 ± 0.6%, $p<0.05$, Figure 4.13D).

4.4.14 Effects of high fat feeding alone or in combination with liraglutide or sitagliptin treatment on beta cell Pdx1 expression

Typical images of islets stained for insulin and Pdx1 from high fat fed mice treated with liraglutide or sitagliptin are presented in Figure 4.14A. High fat feeding caused a notable reduction in insulin positive cells expressing Pdx1 (49.6 ± 1.3 vs 65.7 ± 1.3%, $p<0.001$, Figure 4.14B). Although not able to restore Pdx1 expression to levels similar to lean mice, high fat fed mice treated with liraglutide showed a higher number of insulin positive cells expressing Pdx1 (54.2 ± 1.4%, $p<0.05$, Figure 4.14B), whilst sitagliptin had no additional impact on Pdx1 expression.

4.4.15 Effects of hydrocortisone alone or in combination with liraglutide or sitagliptin treatment on body weight, energy intake and fluid intake

Ins1$^{cre/+}$;Rosa26-eYFP C57Bl/6 mice were giving daily doses of hydrocortisone alone or with liraglutide or sitagliptin over the course of 10 days. Body weight was not significantly altered however percentage body weight change was notably reduced by treatment with hydrocortisone (-6.5 ± 1.0 vs -0.4 ± 0.8%, $p<0.001$, Figure 4.15B), with liraglutide and sitagliptin treated groups showing similar reductions. Cumulative energy intake was only raised in the hydrocortisone treated mice during the final two days of the study (day 10, 512.3 ± 16.0 vs 473.2 ± 17.8kJ, $p<0.05$, Figure 4.15C). Mice given liraglutide or sitagliptin showed an initial reduction in energy consumption at day 4, whilst consistent reductions became apparent from day 7 until the end of the study (day 10 liraglutide 431.3 ± 12.0kJ, $p<0.001$ and day 10 sitagliptin 436.3 ± 10.0, $p<0.001$, Figure 3.15C). Fluid intake was notable raised in hydrocortisone alone, liraglutide and sitagliptin treated mice from days 7, 3 and 6 respectively. Both hydrocortisone alone and with liraglutide increased fluid consumption to similar levels, in great contrast to mice given sitagliptin that showed a dramatic increase in fluid consumption (day 10 sitagliptin 149.8 ± 12.5 vs day 10 hydrocortisone alone 110.4 ± 5.6ml, $p<0.001$, Figure 415D).

4.4.16 Effects of hydrocortisone alone or in combination with liraglutide or sitagliptin treatment on blood glucose, plasma insulin/glucagon and pancreatic insulin/glucagon

Mice dosed solely with hydrocortisone were able to maintain non-fasting plasma glucose levels equivalent to saline treated mice, however mice treated with liraglutide or sitagliptin showed a reduction in blood glucose levels within 3 days of starting treatment until the end of the study (day 10 liraglutide 5.6 ± 0.5, $p<0.001$ and day 10 sitagliptin 6.6 ± 0.3mM, Figure 4.16A/B). Plasma insulin was raised by hydrocortisone treatment (9.9 ± 1.1 vs 6.4 ± 0.3ng/ml, $p<0.01$, Figure 4.16C) and rose further with sitagliptin treatment (15.0 ± 0.6ng/ml, $p<0.05$, Figure 4.16C). Similarly pancreatic insulin content increased in hydrocortisone treated mice (77.6 ± 7.7 vs 42.6 ± 2.1ng/mg protein, $P<0.01$, Figure 4.16D) with sitagliptin treated mice displaying equivalent increases. Liraglutide treatment however produced a reduction in pancreatic insulin content (50.7 ± 2.5ng/mg protein, $p<0.01$, Figure 4.16D). Circulating glucagon levels were elevated in hydrocortisone mice (0.03 ± 0.002 vs 0.02 ± 0.001ng/ml, $p<0.05$, Figure 4.16E). Liraglutide and sitagliptin therapies were able to lower plasma glucagon levels however only the latter treatment was significant (0.02 ± 0.001ng/ml, $p<0.05$, Figure 4.16E). Liraglutide treatment was able to elicit a reduction in pancreatic glucagon content relative to the hydrocortisone alone treated animals (4.0 ± 0.4 vs 6.2 ± 0.06, $p<0.05$, Figure 4.16F).

4.4.17 Effects of hydrocortisone alone or in combination with liraglutide or sitagliptin treatment on islet parameters

Typical images of islets from mice treated with hydrocortisone alone or with liraglutide or sitagliptin are presented in Figure 4.17A. Islet area was increased by treatment with hydrocortisone (10790 ± 907.4 vs 7617 ± 721.1μm^2, $p<0.01$, Figure 4.17B) with notable increases in beta cell area accounting for this expansion (9499 ± 805.2 vs 5926 ± 567.8μm^2, $p<0.001$, Figure 4.17C). Hydrocortisone treated mice given liraglutide exhibited similar morphological changes. Sitagliptin treated mice however were found to have an expansion in alpha cell area (1838 ± 154.1 vs 1430 ± 141.2μm^2, $p<0.05$, Figure 4.17D) in addition to increased beta cell area. Islet size distribution was largely unchanged by hydrocortisone or these treatments with the only remarkable change being an increase in medium sized islets (31.5 ± 4.5 vs 17.1 ± 2.6%, $p<0.05$, Figure 4.17E) found in sitagliptin treated mice comparative to those just dosed with hydrocortisone. Percentage beta cells, a guide to whether islets have increased in size proportionally, was raised by hydrocortisone treatment (89.2 ± 0.4 vs 79.4 ± 0.9%, $p<0.001$, Figure 4.17F). Liraglutide and sitagliptin however was able to reduce percentage beta cells (liraglutide 86.0 ± 1.7%, $p<0.01$ and sitagliptin 84.2 ± 0.8%, $p<0.001$, Figure 4.17F) compared to hydrocortisone alone treated mice. Percentage alpha cells (Figure 4.17G) and islet architecture (Figure 4.17H) was unremarkable between these groups.

4.4.18 Effects of hydrocortisone alone or in combination with liraglutide or sitagliptin treatment on beta-to-alpha cell transdifferentiation

Beta to alpha cell transdifferentiation was determined by immunohistochemistry staining for insulin with GFP and glucagon with GFP, with representative images displayed in Figure 4.18A and 4.18B respectively. Islets expressing insulin scarce, GFP positive cells were raised by hydrocortisone treatment (5.8 ± 0.8 vs 0.4 ± 0.1%, $p<0.001$, Figure 4.18C) with liraglutide and sitagliptin treated mice showing similar increases. In parallel with this, glucagon rich, GFP positive cells were also raised by hydrocortisone (6.1 ± 0.9 vs 1.4 ± 0.3%, $p<0.001$, Figure 4.18D). Liraglutide reduced the number of glucagon positive, GFP positive cells (4.0 ± 0.4%, $p<0.05$, Figure 4.18D).

4.4.19 Effects of hydrocortisone alone or in combination with liraglutide or sitagliptin treatment on beta and alpha cell apoptosis

Immunohistochemistry for TUNEL in combination with insulin or glucagon was conducted to determine beta and alpha cell apoptosis respectively, with representative images presented in Figure 4.19A and 4.19B respectively. Hydrocortisone treatment produced an increase in both beta cell (8.9 ± 1.0 vs 2.7 ± 0.6%, $p<0.001$, Figure 4.19C) and alpha cell (11.5 ± 1.4 vs 1.7 ± 0.4%, $p<0.001$, Figure 4.19D) apoptosis. Liraglutide was able to prevent this beta cell (1.1 ± 0.4%, $p<0.001$, Figure 4.19C) and alpha cell (4.1 ± 0.7%, $p<0.001$, Figure 4.1D) death. Sitagliptin however was only able to elicit reductions in beta cell apoptosis (5.4 ± 1.1%, $p<0.05$, Figure 4.19C).

4.4.20 Effects of hydrocortisone alone or in combination with liraglutide or sitagliptin treatment on beta and alpha cell proliferation

Immunohistochemical staining for Ki-67 in conjunction with insulin or glucagon was carried out to quantify beta cell (Figure 4.20A) and alpha cell (Figure 4.20B) proliferation respectively. Beta cell proliferation was substantially elevated by hydrocortisone treatment (13.2 ± 1.6 vs 2.2 ± 0.5%, $p<0.001$, Figure 4.20C). Alpha cell proliferation was largely unremarkable between treatment groups with hydrocortisone.

4.4.21 Effects of hydrocortisone alone or in combination with liraglutide or sitagliptin treatment on beta cell Pdx1 expression

Representative images of islets stained for insulin (red) and Pdx1 (green) are displayed in Figure 4.21A and used to assess Pdx1 expression, an indication of beta cell maturity. Hydrocortisone treatment resulted in a reduction in the percentage of insulin positive cells also expression Pdx1 (57.3 ± 1.0 vs 65.7 ± 1.3%, $p<0.001$, Figure 4.21B). Likewise, therapy with sitagliptin showed a similar reduction in beta cells expressing Pdx1. Liraglutide however was able to significantly preserve Pdx1 expression within beta cells (63.6 ± 1.1%, $p<0.001$, Figure 4.21B) to levels equivalent to non-diabetic saline treated mice.

4.5 Discussion

These studies have utilised genetically modified *Ins1*$^{cre/+}$;Rosa26-eYFP mice to identify beta cell transdifferentiation within three well defined animal models of diabetes. Multiple-low dose streptozotocin instilled significant beta cell plasticity and beta-to-alpha cell transdifferentiation. Up to 6% of beta cells from these mice were no longer producing insulin, with 6% of now co-expressing glucagon. Corresponding increases in both beta cell apoptosis and alpha cell proliferation were also observed in streptozotocin treated mice. Collectively, these three mechanisms account for the reduction in beta cell mass and elevation in alpha cell mass seen in streptozotocin-induced diabetes.

High fat fed diabetic mice showed significant beta-to-alpha cell transdifferentiation. In this insulin resistant diabetes model, beta cell mass is expanded by hyperplasia and increased beta cell proliferation. Persistent insulin resistance induced beta cell stress still induces notable beta cell apoptosis and contributed to beta cell dedifferentiation and transdifferentiation. This beta-to-alpha transdifferentiation combined with increased alpha cell proliferation outweighed alpha cell apoptosis to bring about an increase in alpha cell mass.

Similarly hydrocortisone induced insulin resistant mice exhibited beta-to-alpha cell transdifferentiation. Beta cell proliferation occurred to overcome this steroid induced insulin resistance however the increased functional demand on beta cells led to their apoptosis. Loss of beta cell identity and subsequent beta-to-alpha cell transdifferentiation occurred in an attempt to spare these stressed beta cells from death.

Previously beta cell transdifferentiation has been demonstrated in genetic animal models by insertion or knocking out specific alpha and beta cell transcription factors respectively (Collombat et al, 2009; Hu et al, 2011; Talchai et al, 2012). The present studies however confirm that a similar level of beta cell plasticity can be induced by pharmacological treatment of streptozotocin or hydrocortisone and by high fat feeding. This opens further speculation whether this transdifferentiation process is common to diabetes pathogenesis regardless of the stressor used to induce disease and whether this is preserved up the phylogenetic tree within humans. Observations in type-2 diabetic patients have noticed low levels of beta cell apoptosis (Butler et al, 2007). Given that hyperglucagonemia is present in these patients, it is plausible that beta-to-alpha cell transdifferentiation could be occurring. It also raises the question if current anti-diabetic agents can limit this transdifferentiation and if this alleviates diabetic symptoms and pathologies in these animals.

GLP-1 receptor agonists, liraglutide, and DPPIV inhibitors, sitagliptin, are two widely used drug classes prescribed for the treatment of type-2 diabetes. In streptozotocin treated mice both of these agents were able to limit the number of islets displaying transdifferentiated beta cells and maintain beta cell maturity by upholding Pdx1 expression (Gao et al, 2014). Collectively this shows that in streptozotocin-induced diabetes, liraglutide and sitagliptin maintain beta cell maturity which helped to limit beta-to-alpha cell transdifferentiation. This suggests that in this model increasing GIP alongside GLP-1 provides no additive protection against beta cell transdifferentiation

and further supports that increasing circulating GLP-1 levels is sufficient to protect against transdifferentiation.

In high fat fed mice only liraglutide was capable of reducing the number of beta cell transdifferentiating towards alpha cells. Interestingly liraglutide also maintained Pdx1 expression further implying that maintaining beta cell maturity is key to preventing transdifferentiation (Gao et al, 2014). Sitagliptin treatment here maintained the number of beta cells expressing insulin, without reducing beta cell glucagon expression, suggesting there is a degree of double hormone expression whilst beta cells transdifferentiate. In hydrocortisone treated mice, an insulin resistance model of diabetes, liraglutide notably reduced the number islets showing glucagon expressing beta cells. Given that islets showing insulin null beta cells were raised within this group, this suggests that liraglutide was able to prevent beta-to-alpha cell transdifferentiation however beta cell maturity was lost despite retaining Pdx1 expression. Similarly sitagliptin treatment in these mice only appeared to exacerbate beta-to-alpha transdifferentiation.

In addition to this change these models display other well characterised traits of diabetes. As is widely documented administration of streptozotocin leads to development of a diabetic phenotype displaying hyperglycaemia, polydipsia and immune infiltration within islets. When conducted in genetically modified *Ins1*$^{cre/+}$;Rosa26-eYFP C57Bl/6 mice the result is no different with mice consistently displaying diabetic changes. In terms of metabolic parameters blood glucose is significantly elevated showing impaired glycaemic control (Vasu et al, 2015). This is accounted for by losses in both plasma and pancreatic insulin content and increases

in circulating plasma and pancreatic glucagon content. High fat fed *Ins1*$^{cre/+}$;Rosa26-eYFP mice display insulin resistance, confirmed by glucose tolerance test, hyperinsulinemia and hyperglucagonemia and reduced pancreatic glucagon. This fits in line with other studies utilising this model and in type-2 diabetics showcasing hyperinsulinemia and hyperglucagonemia as insulin resistance develops. Hydrocortisone treated *Ins1*$^{cre/+}$;Rosa26-eYFP mice displayed evidence of insulin resistance shown by hyperinsulinemia and hyperglucagonemia, in line with similar studies conducted in WT C57Bl/6 mice (Vasu et al, 2015; Khan et al, 2016).

Within these transgenic mice liraglutide and sitagliptin improved metabolism as expected in line with the current literature. Liraglutide treatment in particular was able to exert consistent reductions in percentage body weight change in all three diabetic mice models. This is consistent with clinical and preclinical data. In humans this has been shown to be effective in healthy individuals (Bays et al, 2017; Manigault and Thurston, 2016), type-2 diabetic patients and obese individuals (Santilli et al, 2017). Similarly GLP-1 and analogues such as liraglutide has been shown to act centrally to reduce appetite and calorie consumption (Flint et al, 1998). Although the central actions of liraglutide have not been directly examined in these present studies it can be confirmed here that liraglutide consistently reduced calorie consumption in both lean and high-fat fed mice. In this streptozotocin model liraglutide and sitagliptin were able to restore plasma and pancreatic insulin content but could not however do this with glucagon to levels comparable with non-diabetic mice. As a result of this, non-fasting blood glucose was lowered by treatment with liraglutide and sitagliptin but this failed to keep mice glycaemia to levels equivalent to non-

diabetic mice. In diet-induced diabetes, incretin therapies improved insulin resistance by increased pancreatic insulin content, reduced circulating glucagon levels and improved glucose tolerance. In hydrocortisone mice incretin based therapies produced elevations in both circulating insulin and glucagon levels and pancreatic insulin content were present. In these mice, liraglutide was able to reduce pancreatic insulin content implying these mice required less insulin to meet metabolic demand, thus improving insulin resistance.

In light of these results a number of questions can be raised. Firstly, what triggers this transdifferentiation in these models? Given that streptozotocin induced diabetes elicited more beta cells transdifferentiating than the other tested models it could be plausible that prolonged hyperglycaemia can trigger this transfer. This opens up new lines of thought in which are these anti-diabetic agents acting directly to prevent transdifferentiation or whether this occurs due to a secondary effect from suppressing hyperglycaemia. Further studies in streptozotocin mice using insulin or SGLT2 inhibitors to maintain normoglycaemia may shed light on this and are explored in later chapters. Additionally *ex vivo* studies utilising isolated islets from *Ins1*$^{cre/+}$;Rosa26-eYFP C57Bl/6 mice can be conducted. By controlling the glucose environment the islets are in the direct or indirect effect of the anti-diabetic agents on transdifferentiation can be elucidated. Finally, why does a fixed dose of liraglutide and sitagliptin produce differing effects in these models of diabetes? Differences in hyperglycaemic vs insulin resistant beta cell stress within these models may shed light on this matter.

The presented studies highlight the beneficial actions of incretin therapies, liraglutide and sitagliptin, on improving diabetic symptoms in streptozotocin, diet-induced and hydrocortisone mouse models of diabetes. Taking this further, lineage tracing studies utilising *Ins1*$^{cre/+}$;Rosa26-eYFP C57Bl/6 mice have shown these treatments to prevent beta-to-alpha cell transdifferentiation, highlighting their potential as beta cell restoration therapies.

Figure 4.0: Timeline of presented *in vivo Ins1*$^{cre/+}$;Rosa26-eYFP C57Bl/6 studies

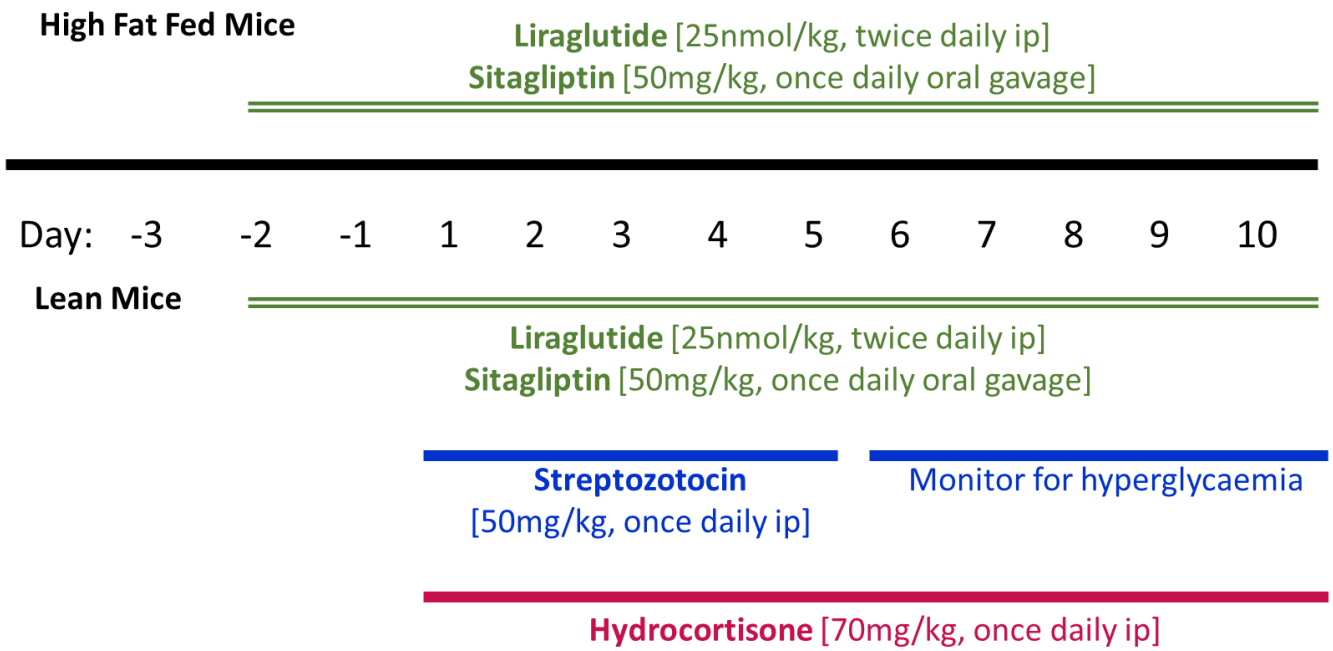

Figure 4.1: Effect of streptozotocin alone or in combination with liraglutide or sitagliptin on body weight, cumulative energy intake and cumulative fluid intake

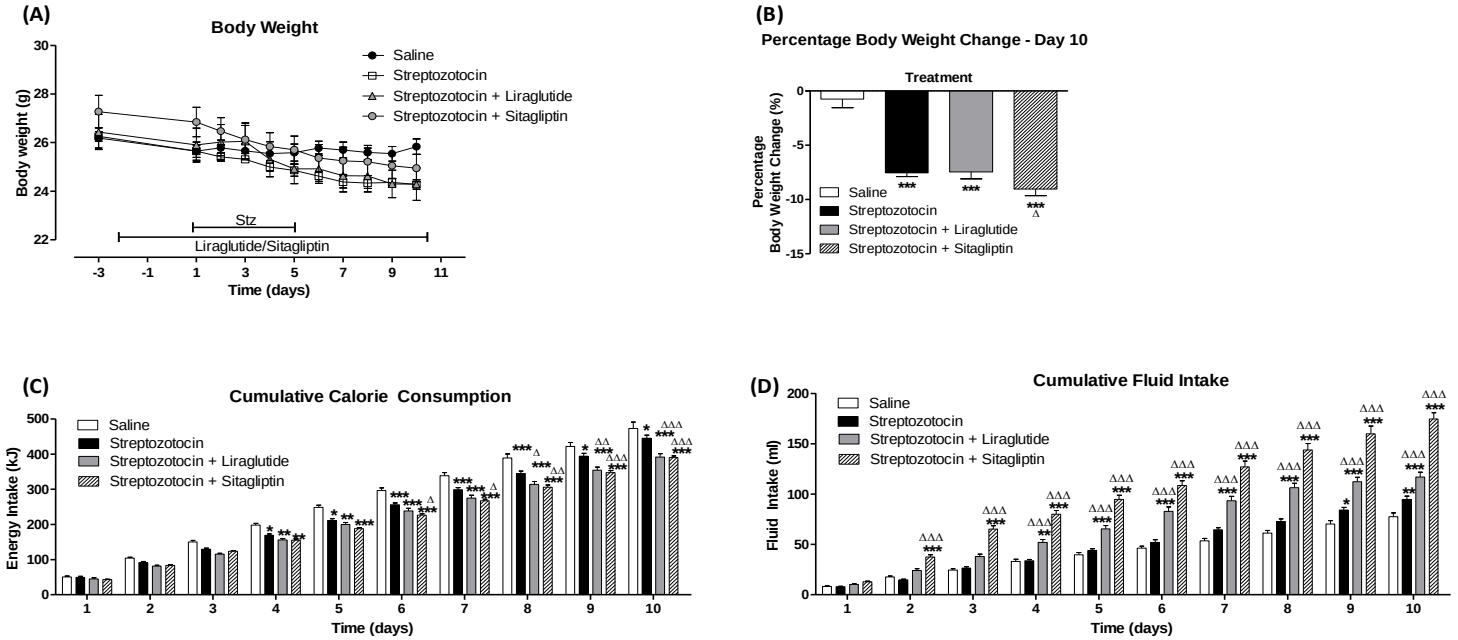

12 week old InsCre;Rosa26-eYFP C57Bl/6 mice were treated with liraglutide or sitagliptin for two days prior to and in conjunction with administration of streptozotocin (50mg/kg, ip, once daily), n=8 mice/group. (A) Body weight, (B) percentage body weight change, (C) cumulative energy intake and (D) cumulative fluid intake. Comparisons were made against saline (*) or against streptozotocin treated (Δ). Values were significant when $p<0.05$ */Δ, $p<0.01$ **/ΔΔ and $p<0.001$ ***/ΔΔΔ.

Figure 4.2: Effect of streptozotocin alone or in combination with liraglutide or sitagliptin on blood glucose, plasma insulin, pancreatic insulin content, plasma glucagon and pancreatic glucagon content

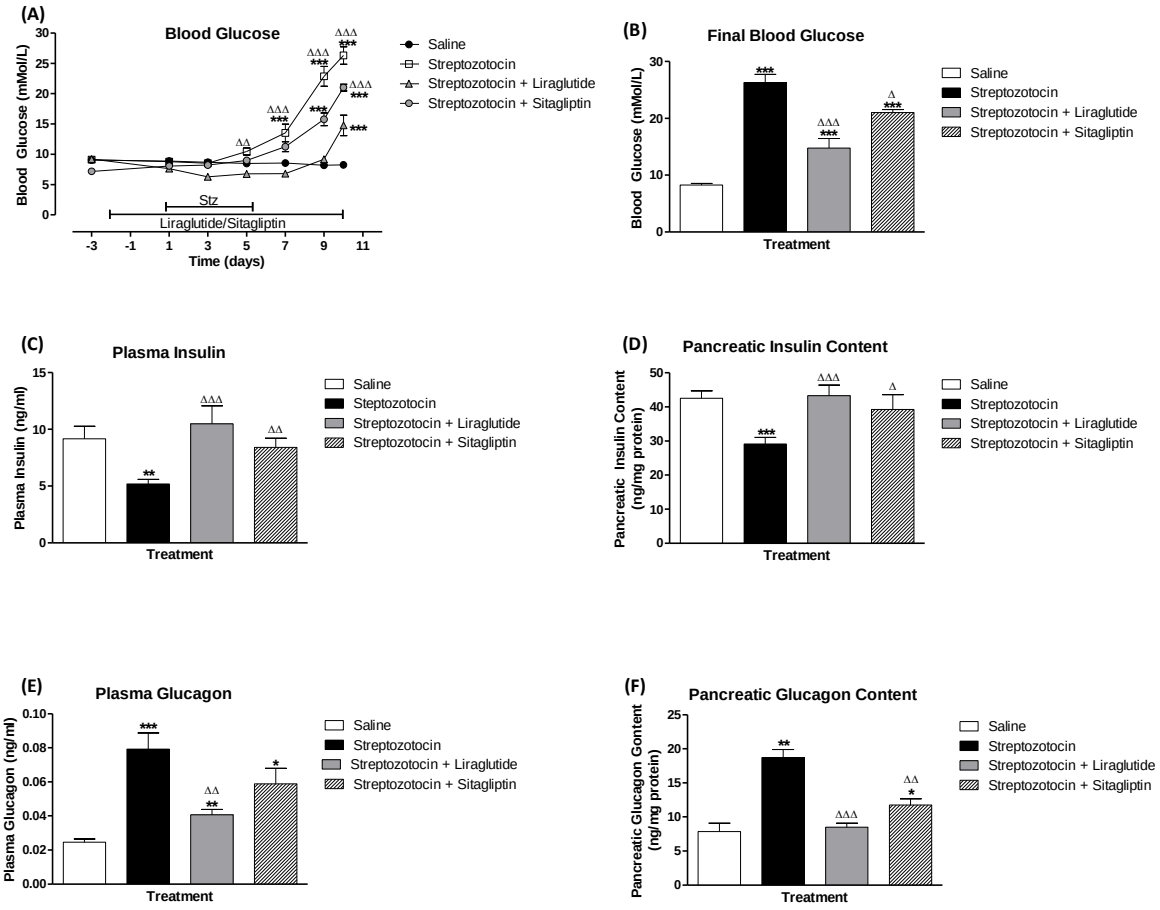

12 week old InsCre;Rosa26-eYFP C57Bl/6 mice were treated with liraglutide or sitagliptin for two days prior to and in conjunction with administration of streptozotocin (50mg/kg, ip, once daily), n=8 mice/group. Terminal blood was taken to assess plasma insulin and glucagon. (A) Blood glucose, (B) final blood glucose, (C) plasma insulin, (D) pancreatic insulin content, (E) plasma glucagon and (F) pancreatic glucagon content. Comparisons were made against saline (*) or against streptozotocin treated (Δ). Values were significant when $p<0.05$ */Δ, $p<0.01$ **/ΔΔ and $p<0.001$ ***/ΔΔΔ.

Figure 4.3: Effects of streptozotocin alone or in combination with liraglutide or sitagliptin on pancreatic islet area, beta cell area, alpha cell area, islet size distribution, percentage beta cells and percentage alpha cells

(A)

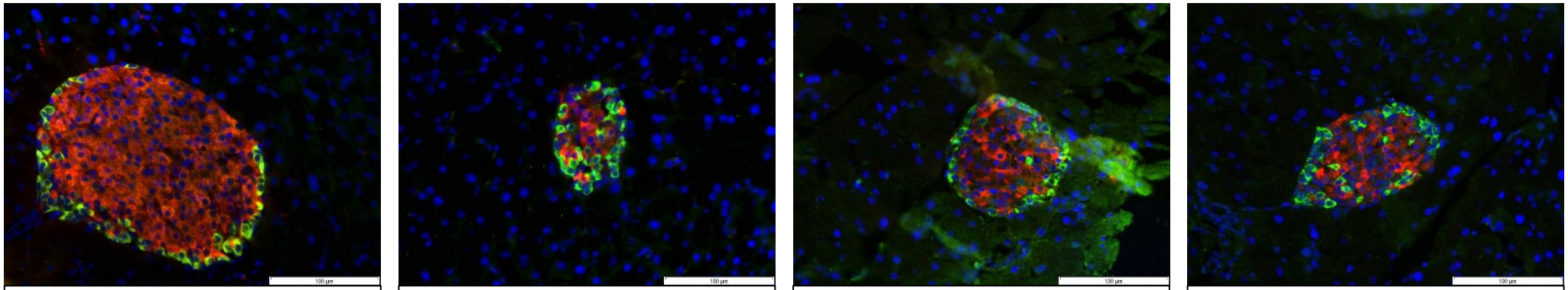

Saline	Streptozotocin	Streptozotocin + Liraglutide	Streptozotocin + Sitagliptin

Insulin / Glucagon / DAPI

* Legend overleaf

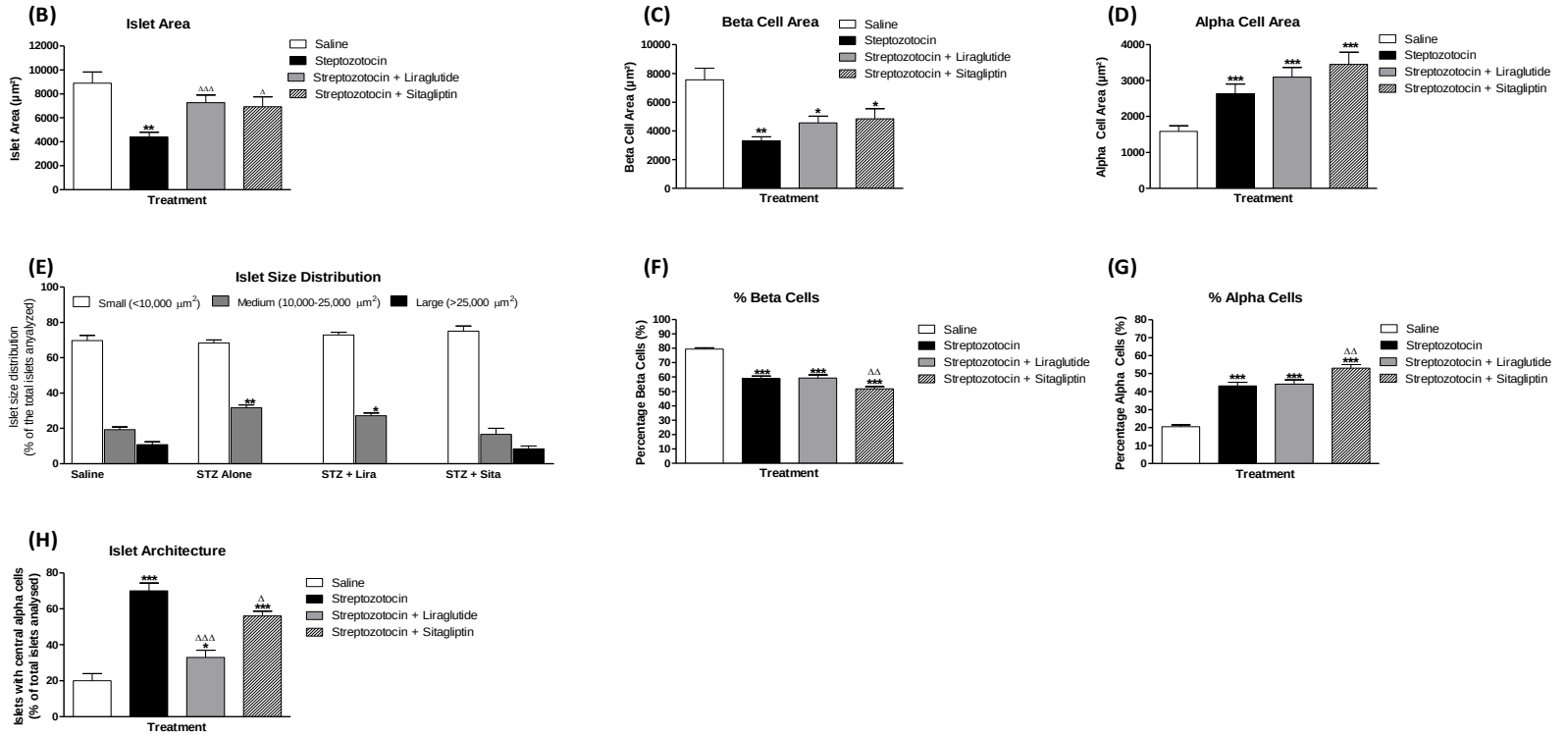

(A) Representative images of islets from saline, STZ, STZ plus liraglutide and STZ plus sitagliptin treated mice showing insulin (red), glucagon (green) and DAPI (blue). (B) Islet area (µm^2), (C) beta cell area (µm^2), (D) alpha cell area (µm^2), (E) islet size distribution, (F) percentage beta cells (%), (G) percentage alpha cells (%) and (H) islet architecture. Values are mean ± SEM (n=8 mice/group). Comparisons versus saline control (*) or versus streptozotocin (Δ), significant when */Δp<0.05, **/ΔΔp<0.01 and ***/ΔΔΔp<0.001.

Figure 4.4 Effects of streptozotocin alone or in combination with liraglutide or sitagliptin on pancreatic islet beta-to-alpha cell transdifferentiation

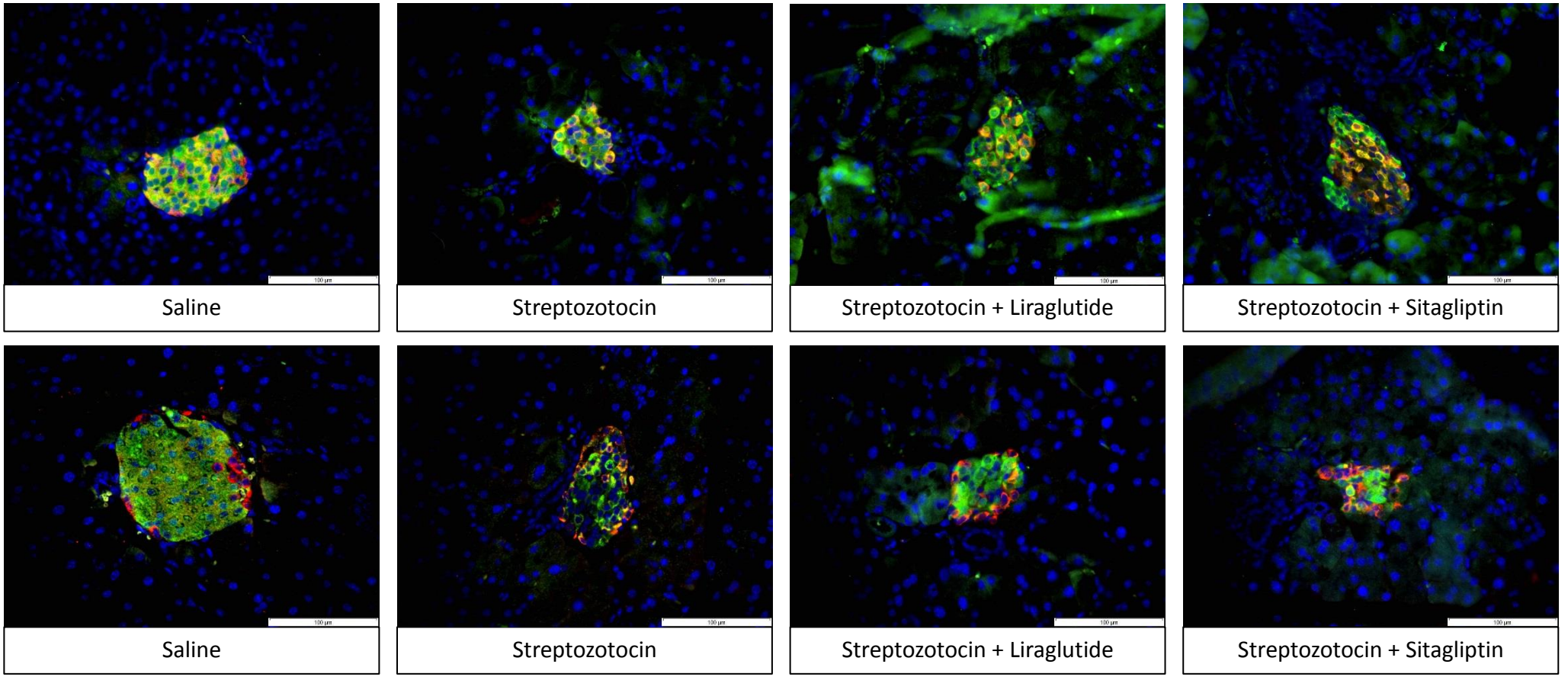

* Legend overleaf

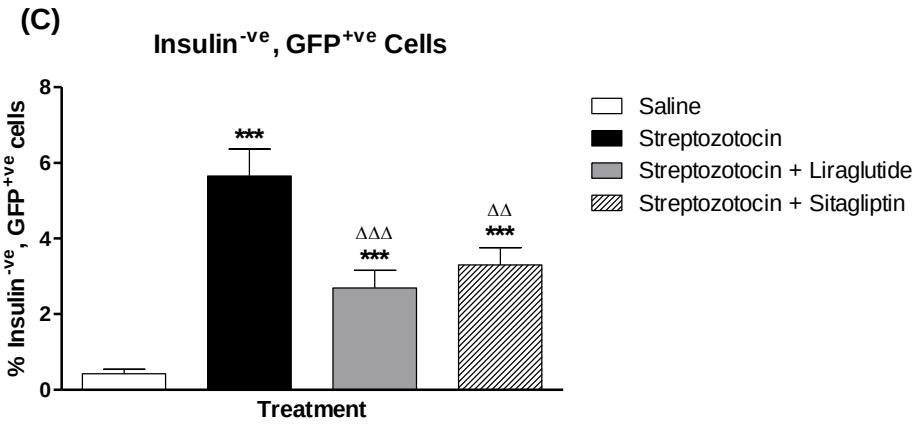

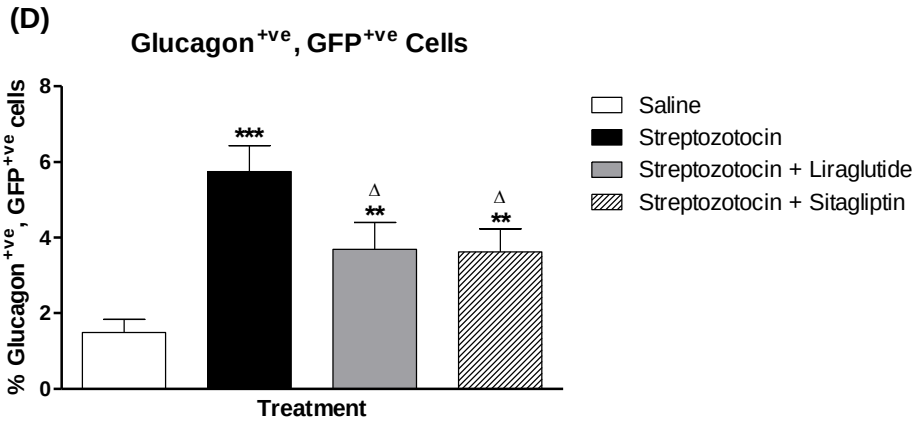

Transdifferentiation Analysis

Representative images of islets from mice treated with saline, streptozotocin, streptozotocin plus liraglutide and streptozotocin plus sitagliptin stained for (A) insulin and GFP or (B) glucagon and GFP. Beta cell transdifferentiation determined by populations of insulin negative, GFP positive cells (C) and glucagon positive, GFP positive cells (D) using double immunofluorescence staining showing insulin/glucagon (red) and GFP (green). Values are mean ± SEM (n=8 mice/group). Comparisons versus saline control (*) or versus streptozotocin (Δ), significant when */Δp<0.05, **/ΔΔp<0.01 and ***/ΔΔΔp<0.001.

Figure 4.5: Effects of streptozotocin alone or in combination with liraglutide or sitagliptin on beta cell and alpha cell apoptosis

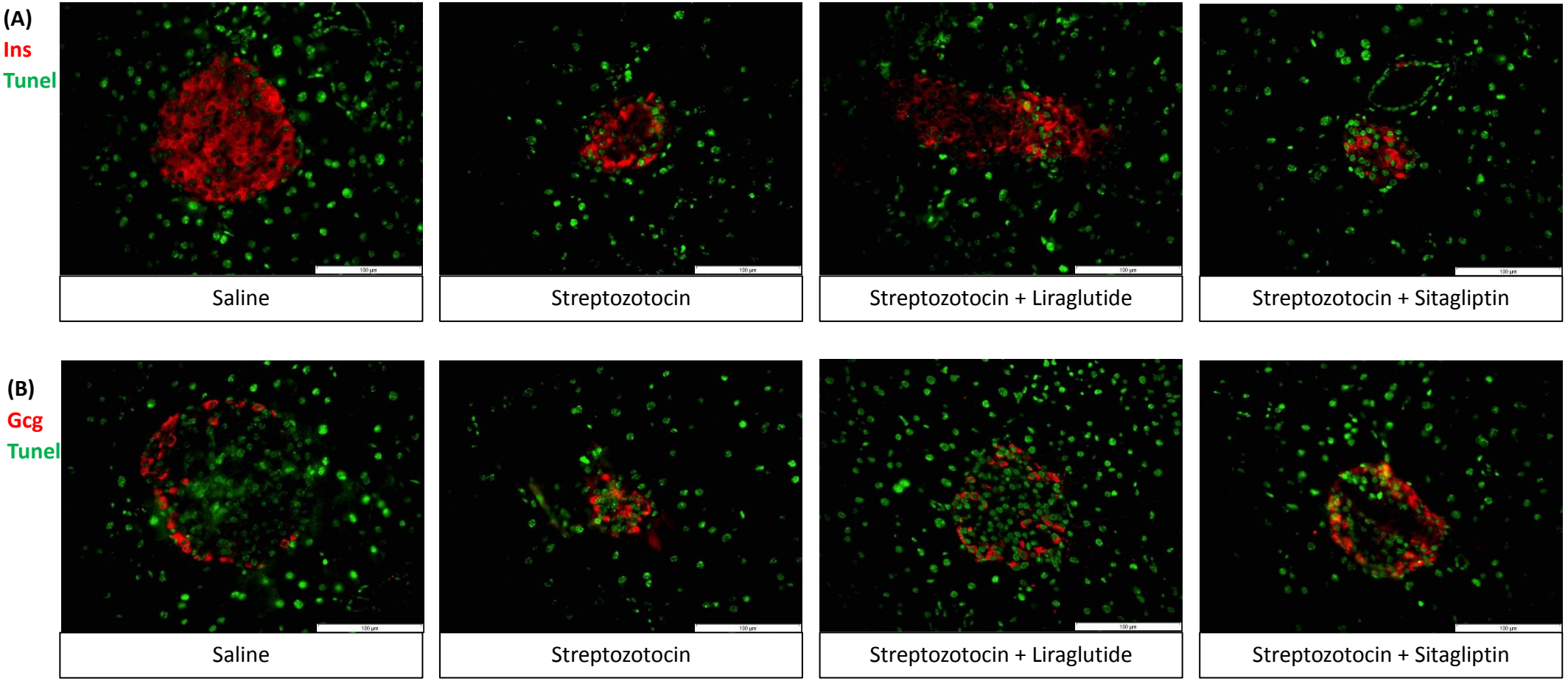

* Legend overleaf

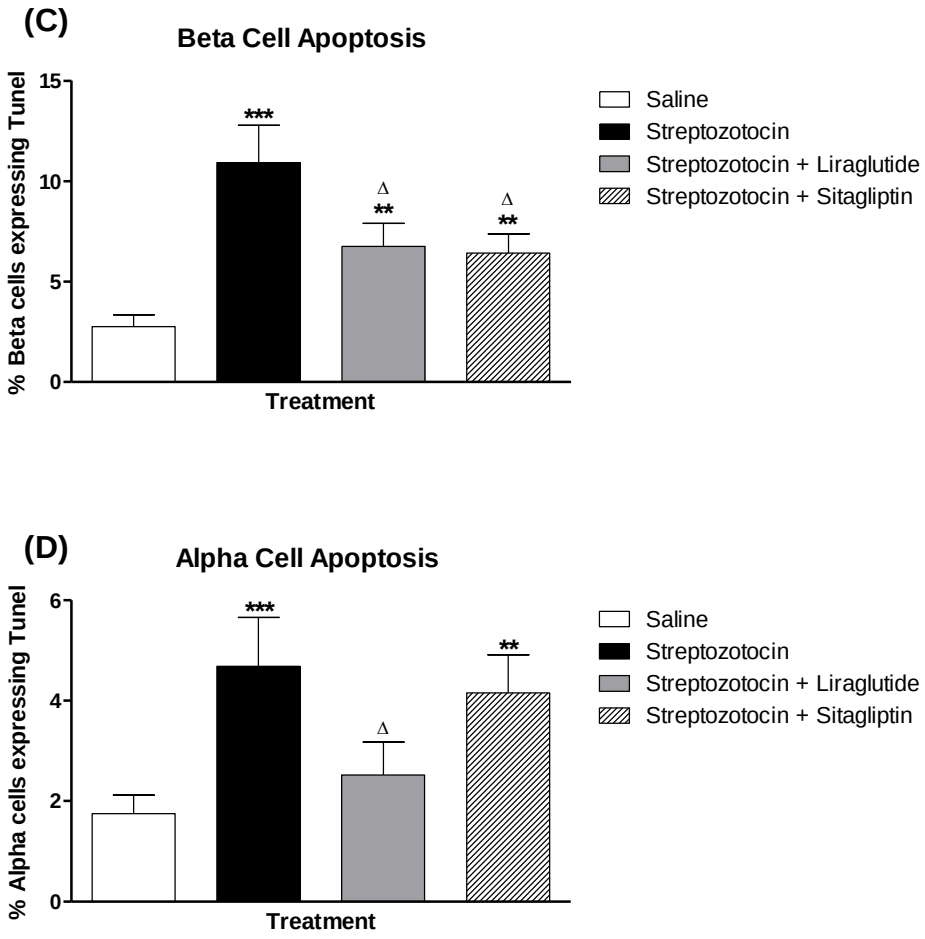

Apoptosis Analysis

Representative images of islets from mice treated with saline, streptozotocin, streptozotocin plus liraglutide and streptozotocin plus sitagliptin stained for (A) insulin and TUNEL or (B) glucagon and TUNEL. Beta cell apoptosis and alpha cell apoptosis determined by populations of insulin positive, TUNEL positive (C) and glucagon positive, TUNEL positive (D) cells respectively by double immunofluorescence staining. Values are mean ± SEM (n=8 mice/group). Comparisons versus saline control (*) or versus streptozotocin (Δ), significant when */Δp<0.05, **/ΔΔp<0.01 and ***p<0.001.

Figure 4.6: Effects of streptozotocin alone or in combination with liraglutide or sitagliptin on beta cell and alpha cell proliferation

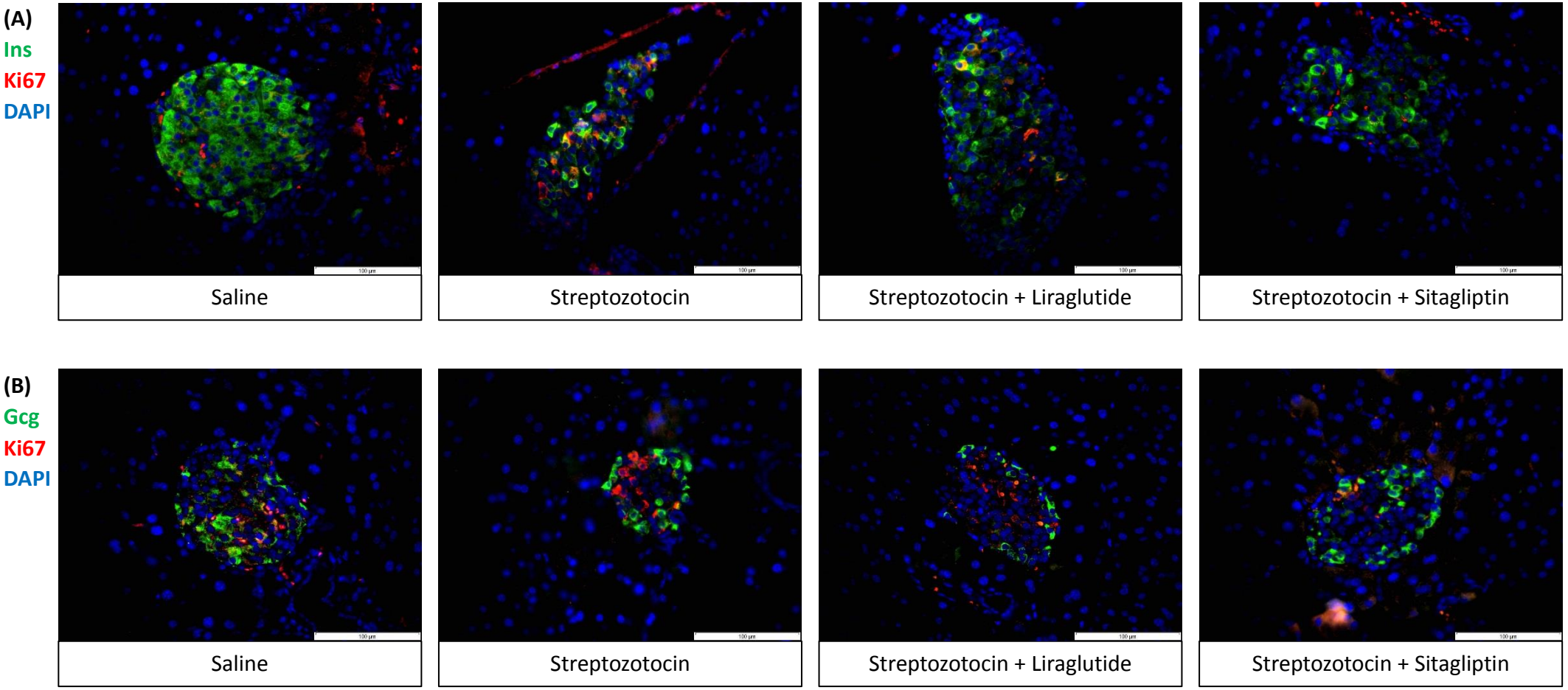

* Legend overleaf

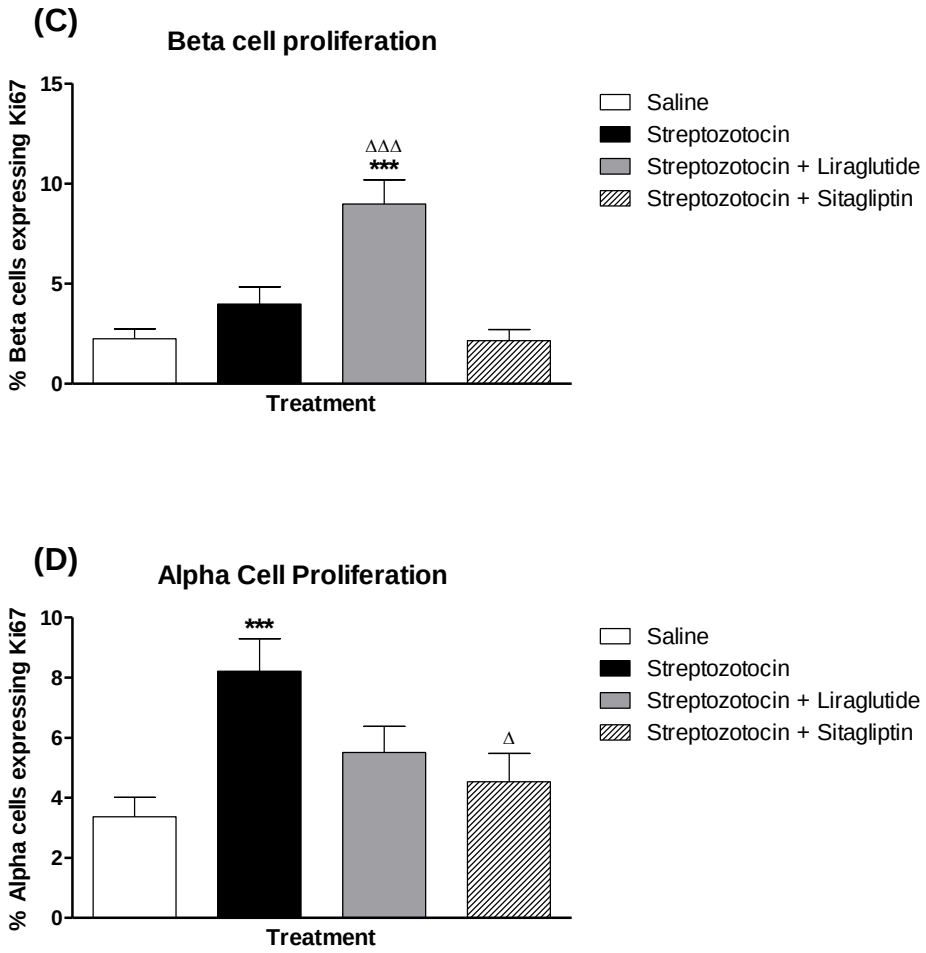

Proliferation Analysis

Representative images of islets from mice treated with saline, streptozotocin, streptozotocin plus liraglutide and streptozotocin plus sitagliptin stained for (A) insulin and ki-67 or (B) glucagon and ki-67. Beta cell and alpha cell proliferation determined by populations of (C) insulin positive, ki-67 positive cell and (D) glucagon positive, ki-67 positive cells respectively.

Values are mean ± SEM (n=8 mice/group). Comparisons versus saline control (*) or versus streptozotocin (Δ), significant when */Δp<0.05, **/ΔΔp<0.01 and ***/ΔΔΔp<0.001.

Figure 4.7: Effects of streptozotocin alone or in combination with liraglutide or sitagliptin on beta cell Pdx1 expression

(A)

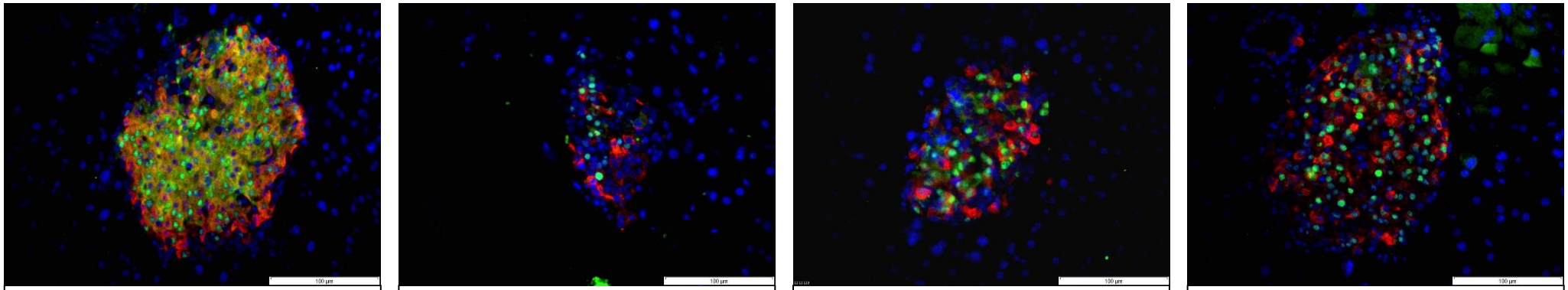

Saline	Streptozotocin	Streptozotocin + Liraglutide	Streptozotocin + Sitagliptin

Insulin / Pdx1 / DAPI

* Legend overleaf

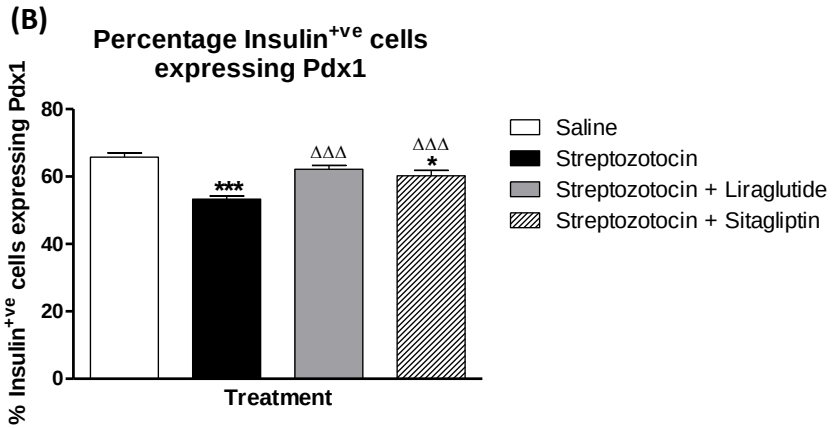

Pdx1 Expression Analysis

(A) Representative images of islets from mice treated with saline, streptozotocin, streptozotocin plus liraglutide and streptozotocin plus sitagliptin on Pdx1 expression (B). Determined by histological analysis of insulin/Pdx1 double immunofluorescence staining showing insulin (red), Pdx1 (green) and DAPI (blue).

Values are mean ± SEM (n=8 mice/group). Comparisons versus saline control (*) or versus streptozotocin (Δ), significant when */Δp<0.05, **/ΔΔp<0.01 and ***p<0.001.

Figure 4.8: Effect of high fat feeding alone or in combination with liraglutide or sitagliptin on body weight, cumulative energy intake and cumulative fluid intake

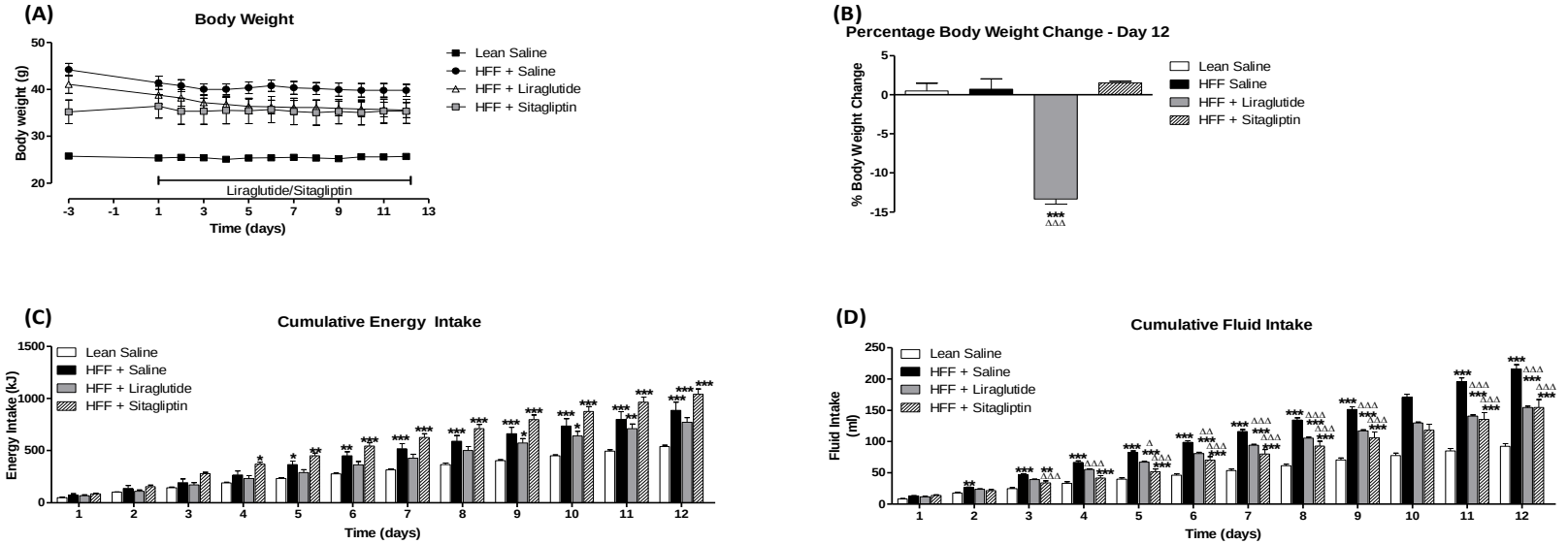

15 week old InsCre;Rosa26-eYFP C57Bl/6 mice kept on a high fat diet for 2 months prior were treatment with liraglutide or sitagliptin by daily ip injections, n=6-8 mice/group. (A) Body weight, (B) percentage body weight change, (C) cumulative energy intake and (D) cumulative fluid intake. Comparisons were made against lean saline (*) or against high fat fed (Δ). Values mean ± SEM, significant when $p<0.05$ */Δ, $p<0.01$ **/ΔΔ and $p<0.001$ ***/ΔΔΔ.

Figure 4.9: Effect of high fat feeding alone or in combination with liraglutide or sitagliptin on blood glucose, plasma insulin, pancreatic insulin content, plasma glucagon, pancreatic glucagon content, GTT and AUC

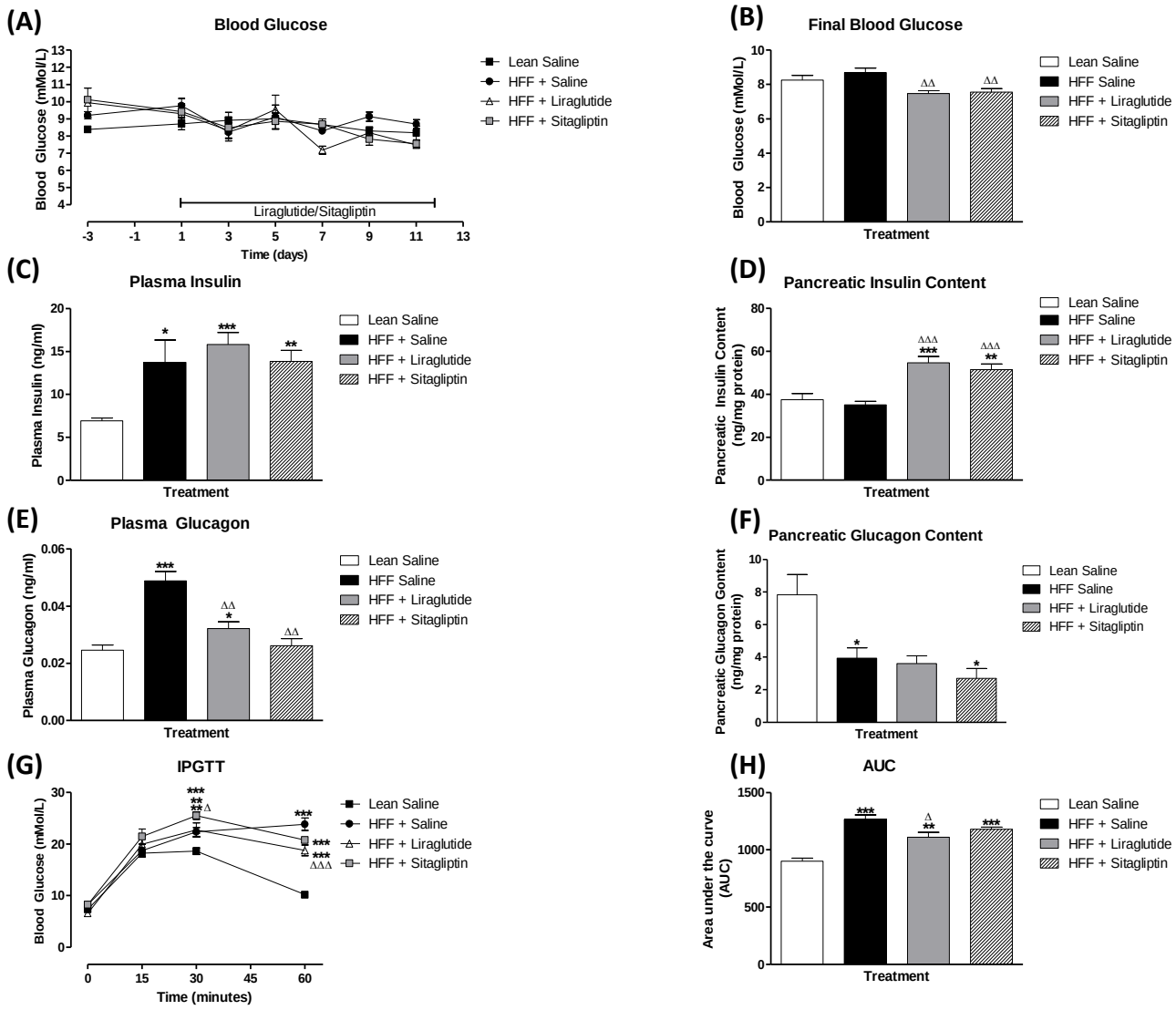

15 week old InsCre;Rosa26-eYFP C57Bl/6 mice kept on a high fat diet for 2 months prior to liraglutide or sitagliptin by daily ip injections, n=6-8 mice/group. (A) Blood glucose, (B) final blood glucose, (C) plasma insulin, (D) pancreatic insulin, (E) plasma glucagon, (F) pancreatic glucagon, (G) ip glucose tolerance test and (H) AUC. Comparisons were made against lean saline (*) or against high fat fed (Δ). Values mean ± SEM, significant when p<0.05 */Δ, p<0.01 **/ΔΔ and p<0.001 ***/ΔΔΔ.

Figure 4.10: Effects of high fat feeding alone or in combination with liraglutide or sitagliptin on pancreatic islet area, beta cell area, alpha cell area, islet size distribution, percentage beta cells and percentage alpha cells

(A)

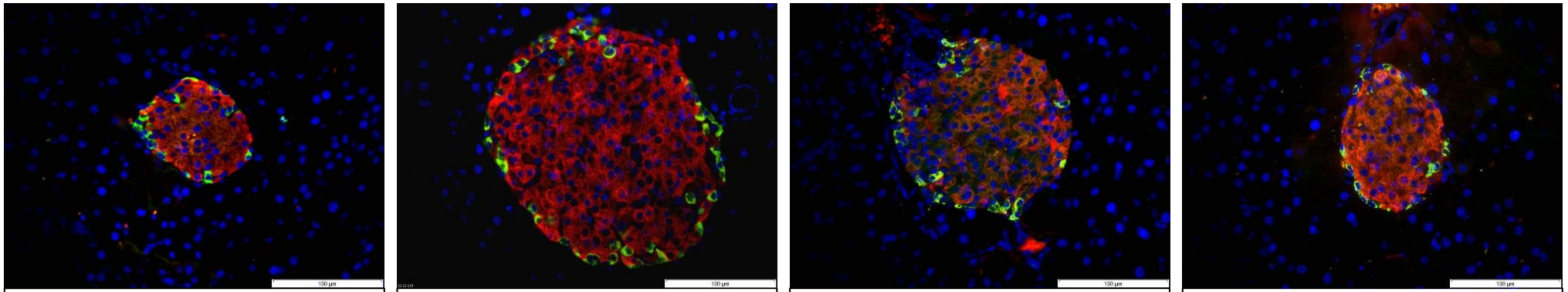

Lean Saline	High-fat Fed Saline	High-fat Fed + Liraglutide	High-fat Fed + Sitagliptin

Insulin / Glucagon / DAPI

* Legend overleaf

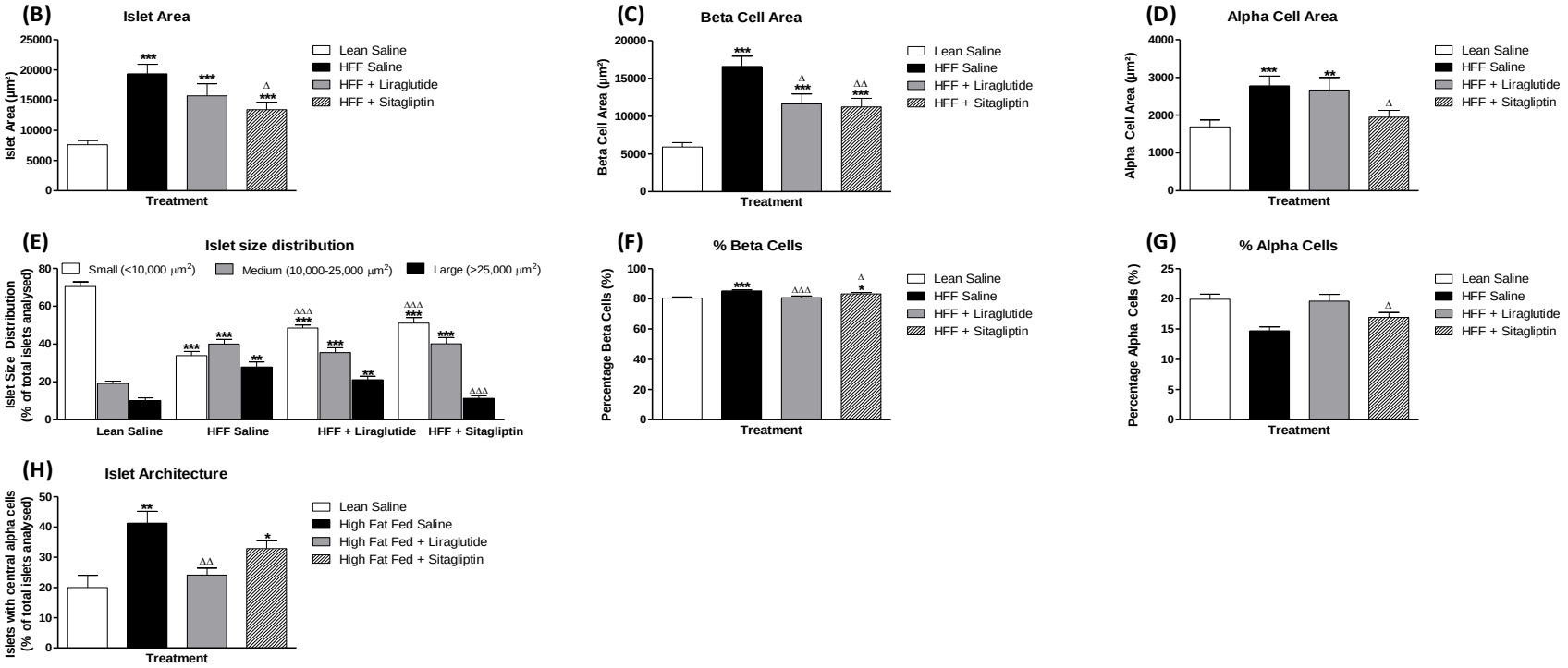

Representative images of islets from (A) lean saline, HFF saline, HFF plus liraglutide and HFF plus sitagliptin mice showing insulin (red), glucagon (green) and DAPI (blue). (B) islet area, (C) beta cell area, (D) alpha cell area, (E) islet size distribution, (F) percentage beta cells, (G) percentage alpha cells and (H) islet architecture. Values are mean ± SEM (n=8 mice/group). Comparisons versus saline control (*) or versus high fat fed (Δ), significant when */Δp<0.05, **/ΔΔp<0.01 and ***/ΔΔΔp<0.001.

Figure 4.11 Effects of high fat feeding alone or in combination with liraglutide or sitagliptin on pancreatic islet beta-to-alpha cell transdifferentiation

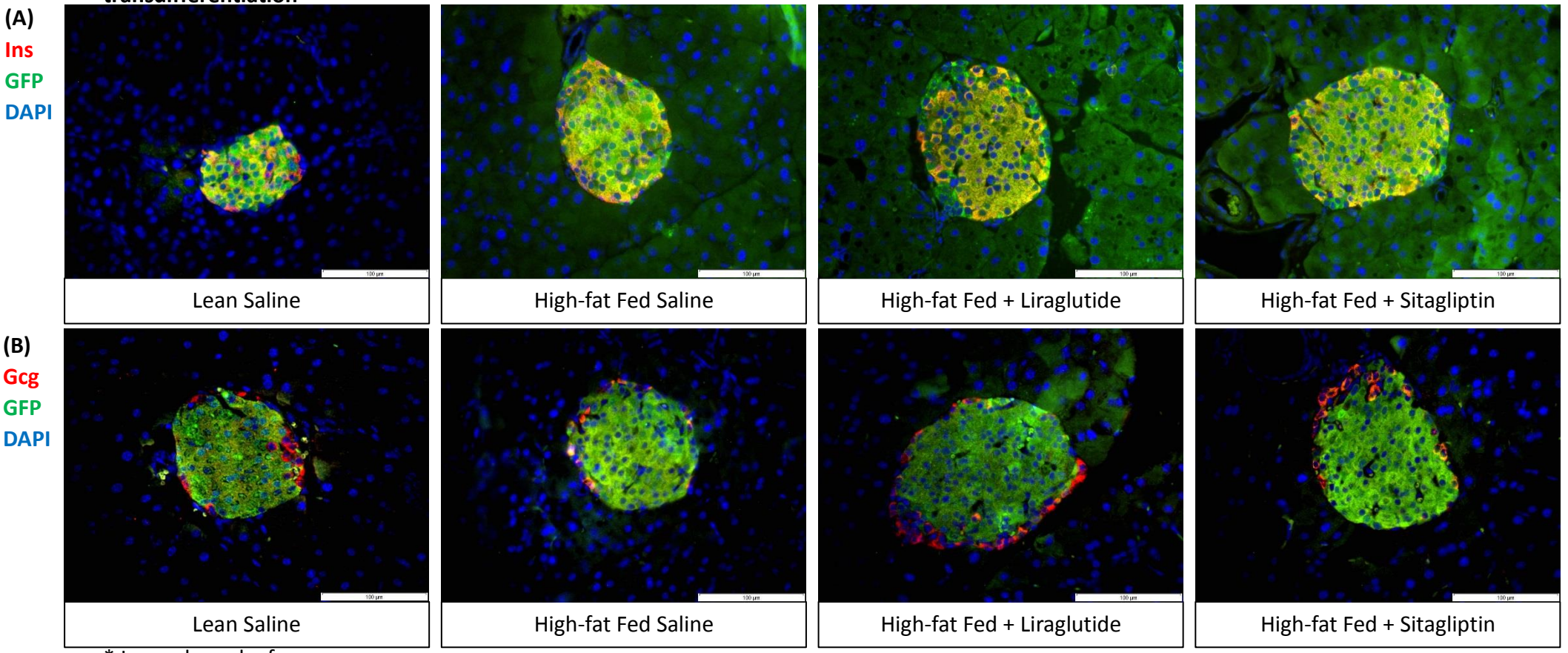

* Legend overleaf

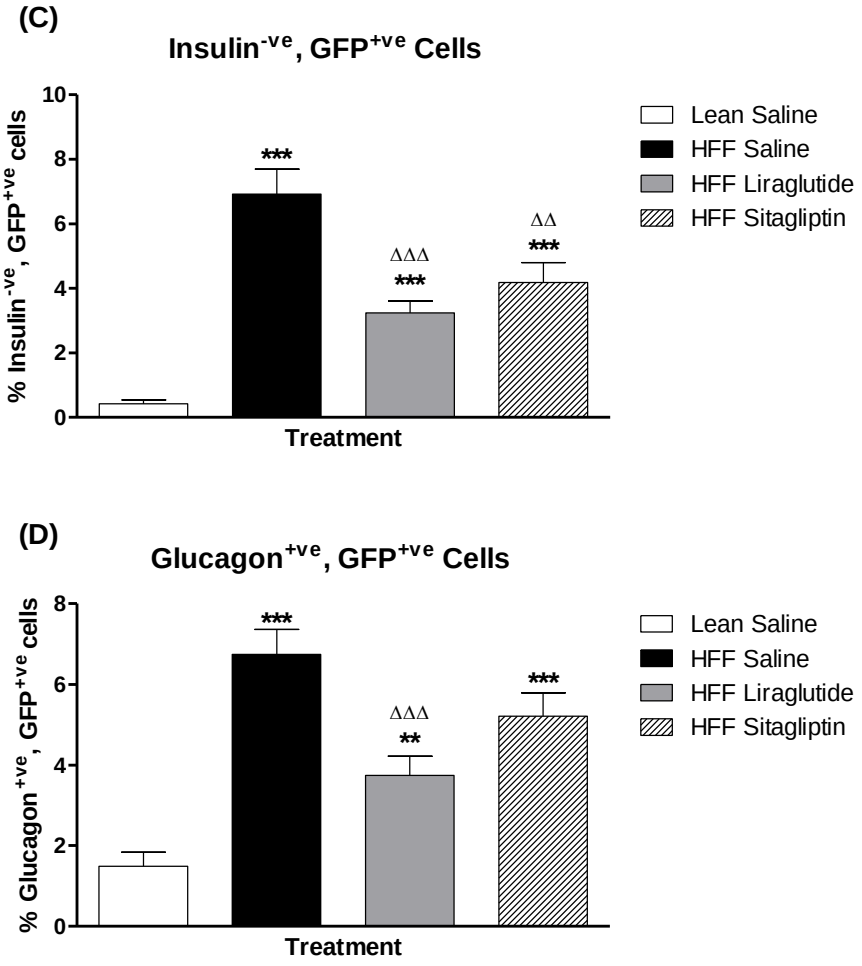

Transdifferentiation Analysis

Representative images of islets from lean saline, high fat fed saline, high fat fed plus liraglutide and high fat fed plus sitagliptin treated mice stained for (A) insulin and GFP or (B) glucagon and GFP. Beta cell transdifferentiation determined by populations of insulin negative, GFP positive cells (C) and glucagon positive, GFP positive cells (D) using double immunofluorescence staining show insulin/glucagon (red), GFP (green). Values are mean ± SEM (n=8 mice/group). Comparisons versus lean saline control (*) or versus high fat fed saline (Δ), significant when */Δp<0.05, **/ΔΔp<0.01 and ***/ΔΔΔp<0.001.

Figure 4.12: Effects of high fat feeding alone or in combination with liraglutide or sitagliptin on beta cell and alpha cell apoptosis

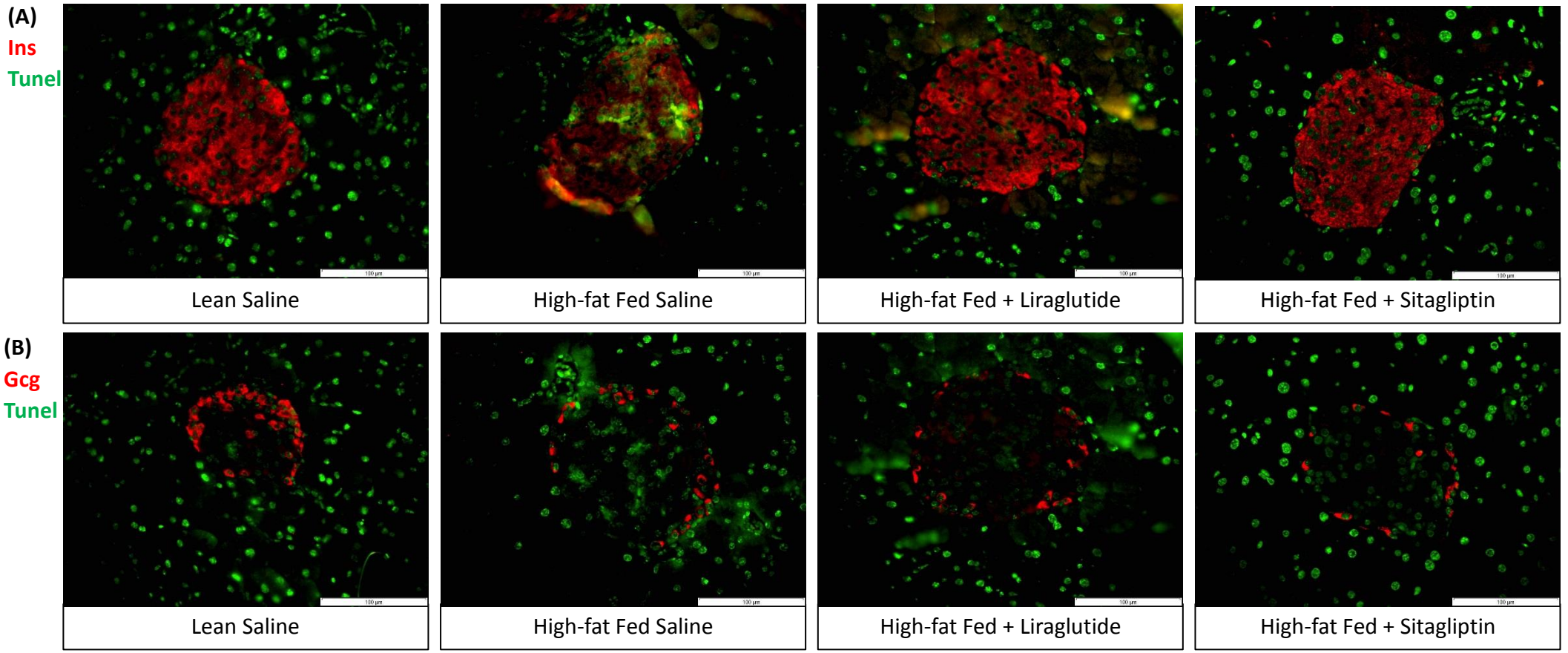

* Legend overleaf

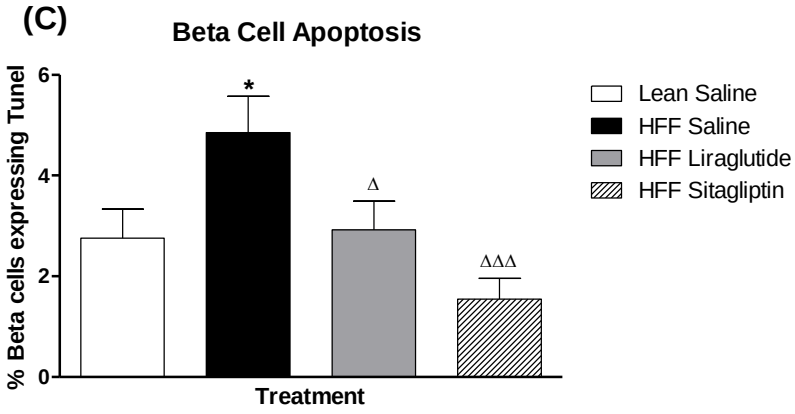

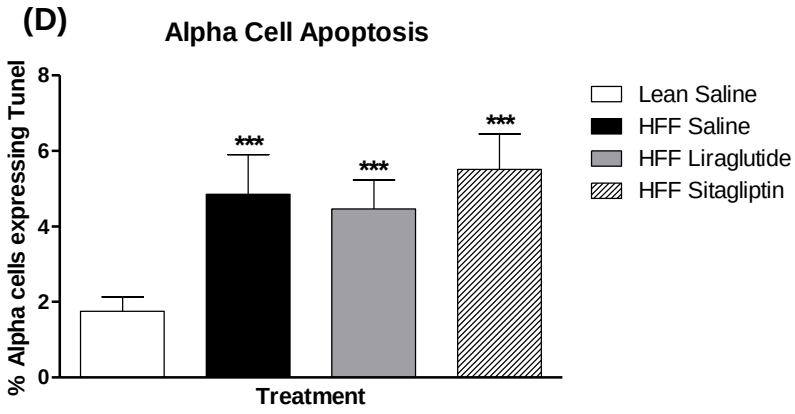

Apoptosis Analysis

Representative images of islets from lean saline, high fat fed saline, high fat fed plus liraglutide and high fat fed plus sitagliptin stained for (A) insulin and TUNEL or (B) glucagon and TUNEL. Beta cell apoptosis and alpha cell apoptosis were quantified by populations of insulin positive, TUNEL positive (C) and glucagon positive, TUNEL positive cells (D) respectively by double immunofluorescence staining.

Values are mean ± SEM (n=8 mice/group). Comparisons versus saline control (*) or versus high fat fed (Δ), significant when */Δp<0.05, **/ΔΔp<0.01 and ***/ΔΔΔp<0.001.

Figure 4.13: Effects of high fat feeding alone or in combination with liraglutide or sitagliptin on beta cell and alpha cell proliferation

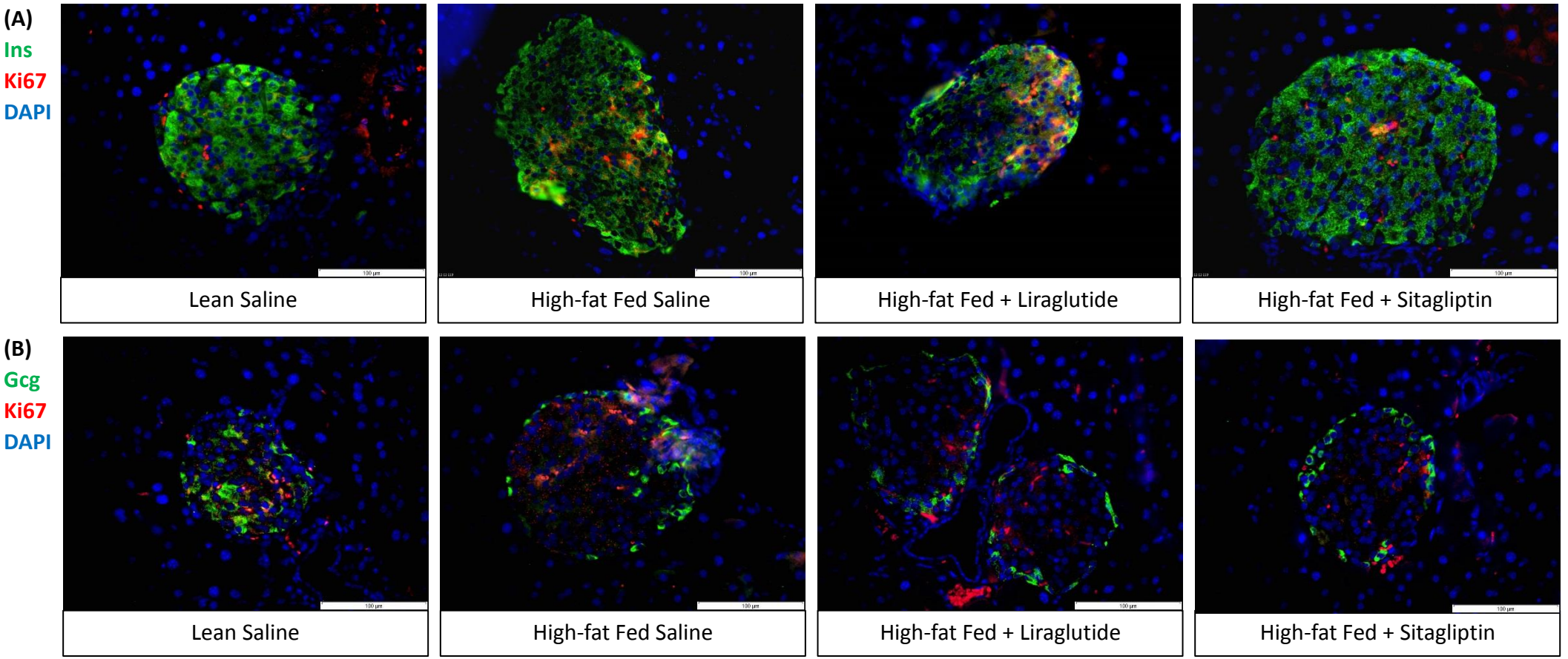

* Legend overleaf

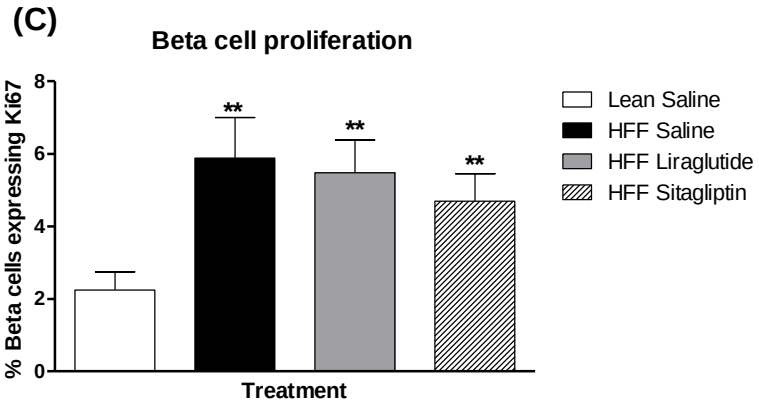

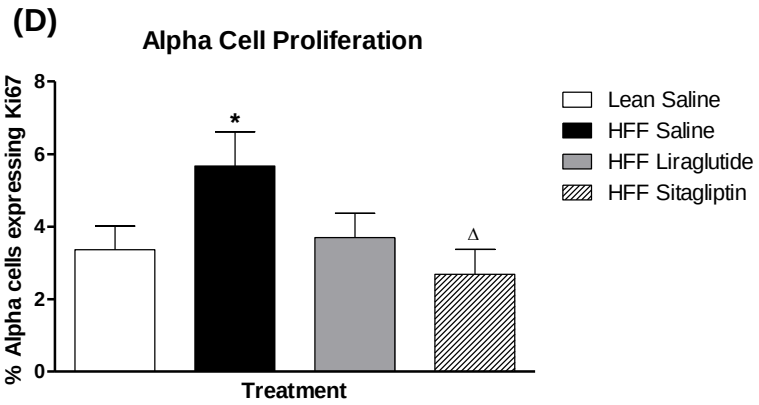

Proliferation Analysis

Representative images of islets lean saline, high fat fed saline, high fat fed plus liraglutide and high fat fed plus sitagliptin stained for (A) insulin and ki-67 or (B) glucagon and ki-67. Beta cell and alpha cell proliferation determined by populations of (C) insulin positive, ki-67 positive cells or (D) glucagon positive, ki-67 positive cells respectively.

Values are mean ± SEM (n=8 mice/group). Comparisons versus saline control (*) or versus high fat fed (Δ), significant when */Δp<0.05, **/ΔΔp<0.01 and ***p<0.001.

Figure 4.14: Effects of high fat feeding alone or in combination with liraglutide or sitagliptin on beta cell Pdx1 expression

(A)

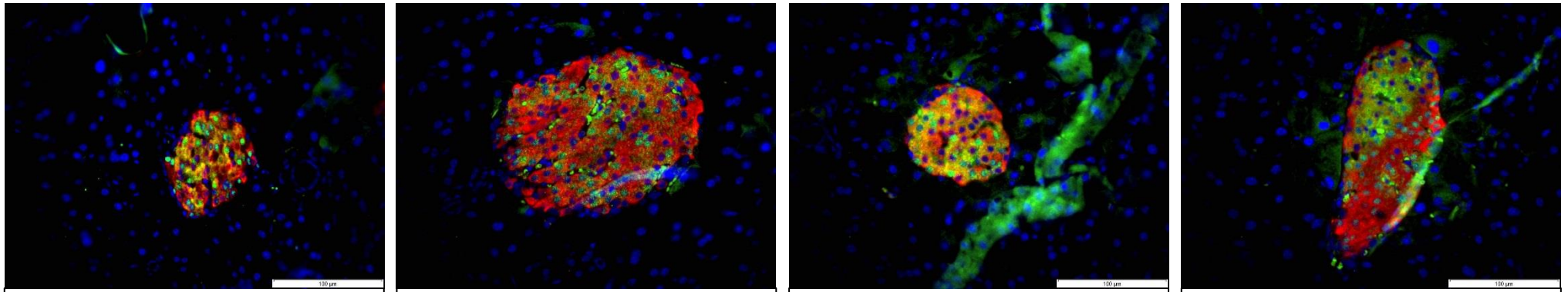

Lean Saline	High-fat Fed Saline	High-fat Fed + Liraglutide	High-fat Fed + Sitagliptin

Insulin / Pdx1 / DAPI

* Legend overleaf

(B)

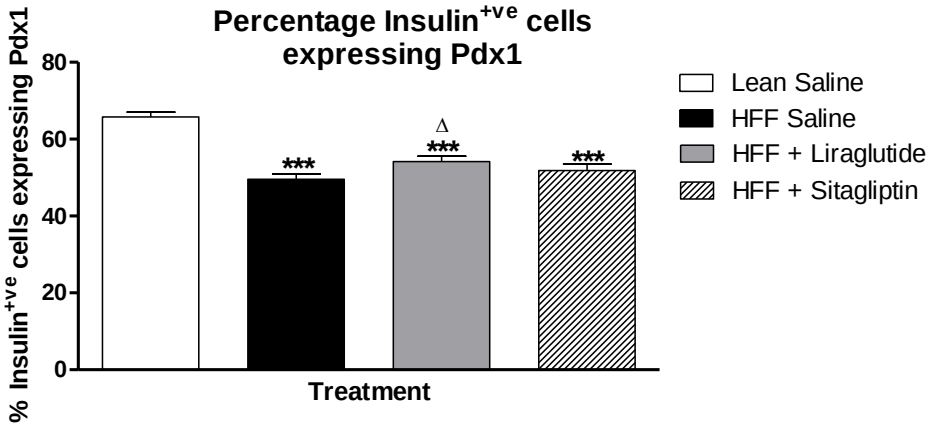

Pdx1 Expression Analysis

(A) Representative images of islets from mice treated with saline, high fat fed saline, high fat fed plus liraglutide and high fat fed plus sitagliptin on Pdx1 expression (B). Determined by histological analysis of insulin/Pdx1 double immunofluorescence staining showing insulin (red), Pdx1 (green) and DAPI (blue).

Values are mean ± SEM (n=8 mice/group). Comparisons versus saline control (*) or versus high fat fed (Δ), significant when */Δp<0.05, **/ΔΔp<0.01 and ***p<0.001.

Figure 4.15: Effect of hydrocortisone alone or in combination with liraglutide or sitagliptin on body weight, cumulative energy intake and cumulative fluid intake

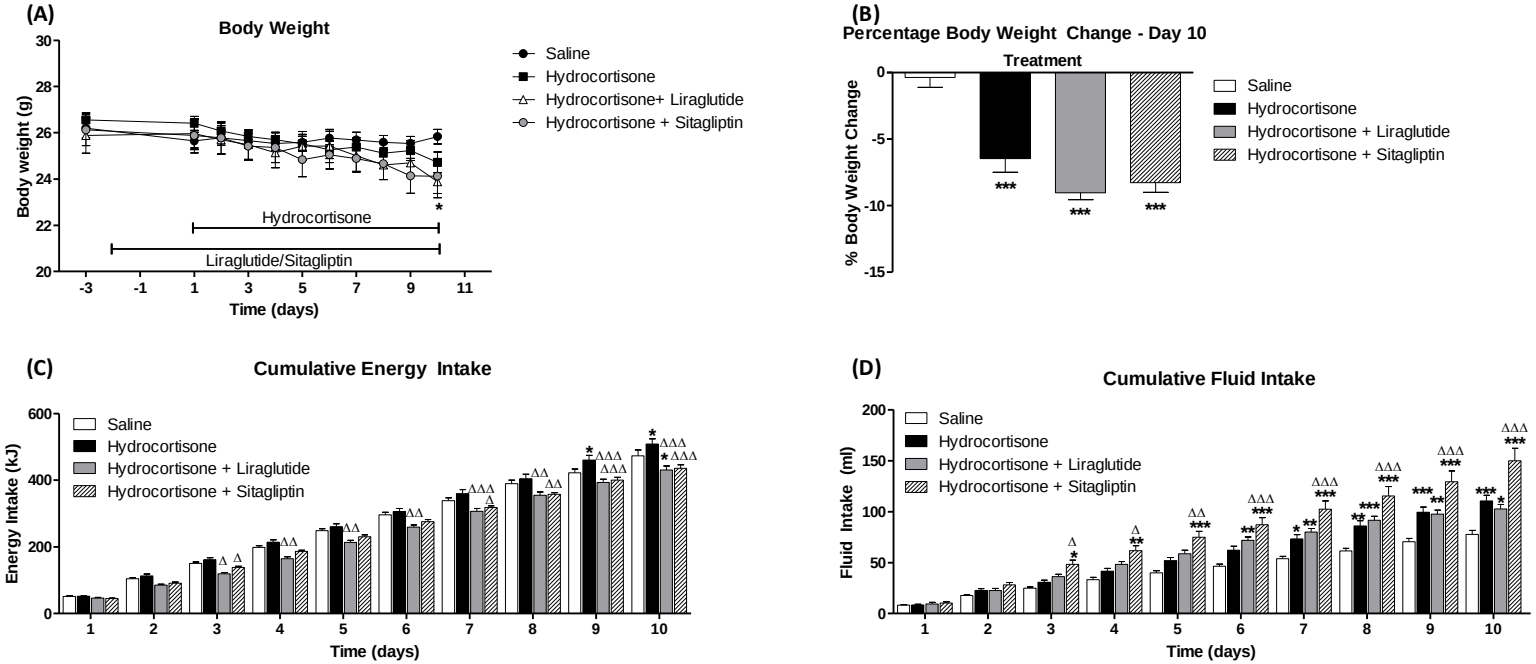

12 week old InsCre;Rosa26-eYFP C57Bl/6 mice were treated with liraglutide or sitagliptin for two days prior to and in conjunction with administration of hydrocortisone (70mg/kg, ip, once daily), n=8 mice/group. (A) Body weight, (B) percentage body weight change, (C) cumulative energy intake and (D) cumulative fluid intake. Comparisons were made against saline (*) or against hydrocortisone treated (Δ). Values were significant when $p<0.05$ */Δ, $p<0.01$ **/ΔΔ and $p<0.001$ ***/ΔΔΔ.

Figure 4.16: Effect of hydrocortisone alone or in combination with liraglutide or sitagliptin on blood glucose, plasma insulin, pancreatic insulin content, plasma glucagon and pancreatic glucagon content

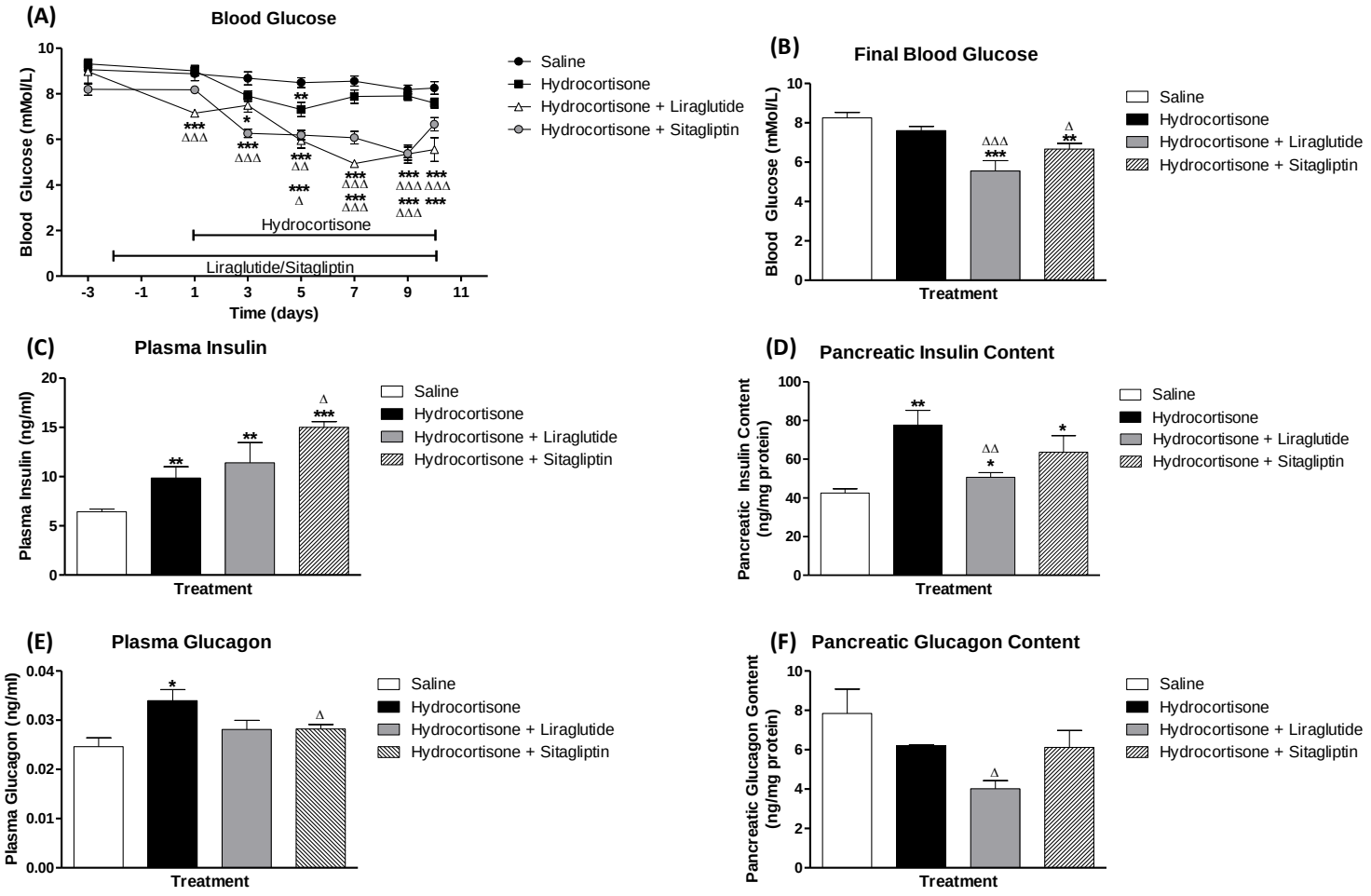

12 week old InsCre;Rosa26-eYFP C57Bl/6 mice were treated with liraglutide or sitagliptin for two days prior to and in conjunction with administration of hydrocortisone (70mg/kg, ip, once daily), n=8 mice/group. Terminal blood was taken to assess plasma insulin and glucagon. (A) Blood glucose, (B) final blood glucose, (C) plasma insulin and (D) pancreatic insulin content. Comparisons were made against saline (*) or against hydrocortisone treated (Δ). Values were significant when $p<0.05$ */Δ, $p<0.01$ **/ΔΔ and $p<0.001$ ***/ΔΔΔ.

Figure 4.17: Effects of hydrocortisone alone or in combination with liraglutide or sitagliptin on pancreatic islet area, beta cell area, alpha cell area, islet size distribution, percentage beta cells and percentage alpha cells

(A)

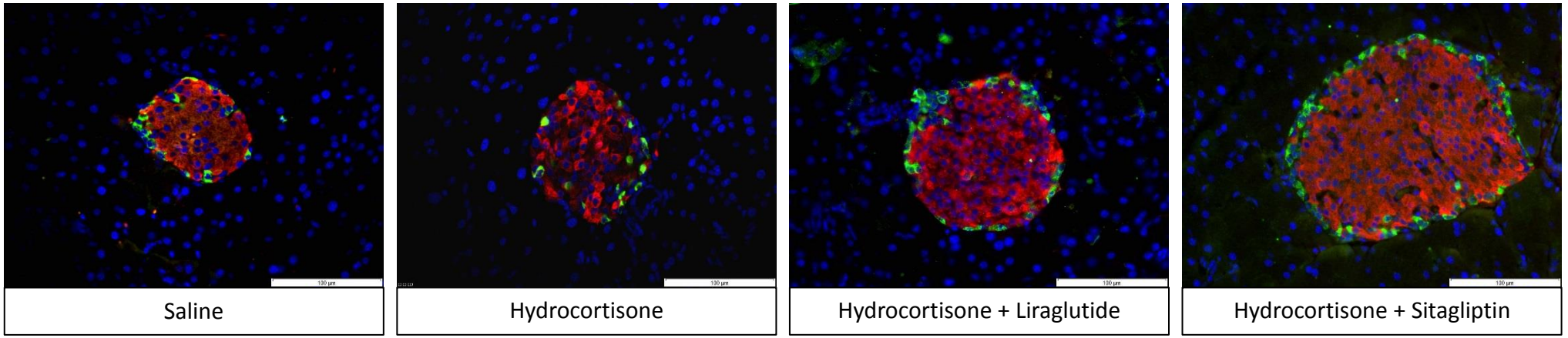

Insulin / Glucagon / DAPI

*Legend overleaf

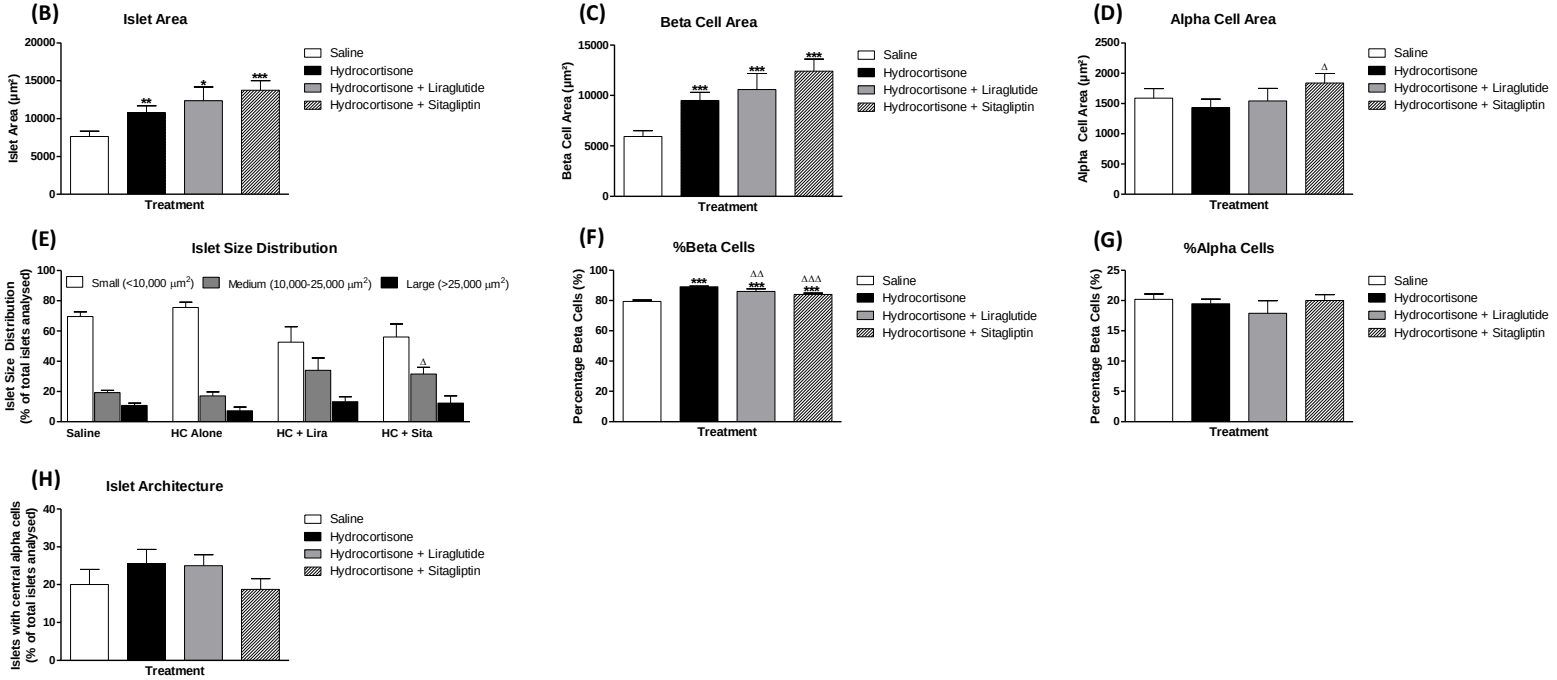

(A) Representative images of islets from saline, hydrocortisone, hydrocortisone plus liraglutide and hydrocortisone plus sitagliptin treated mice showing insulin (red), glucagon (green) and DAPI (blue). (B) islet area (μm^2), (C) beta cell area (μm^2), (D) alpha cell area (μm^2), (E) islet size distribution, (F) percentage beta cells, (G) percentage alpha cells and (H) islet architecture. Values are mean ± SEM(n=8 mice/group). Comparisons versus saline control (*) or versus hydrocortisone (Δ), significant when */Δp<0.05, **/ΔΔp<0.01 and ***/ΔΔΔp<0.001.

Figure 4.18 Effects of hydrocortisone alone or in combination with liraglutide or sitagliptin on pancreatic islet beta-to-alpha cell transdifferentiation

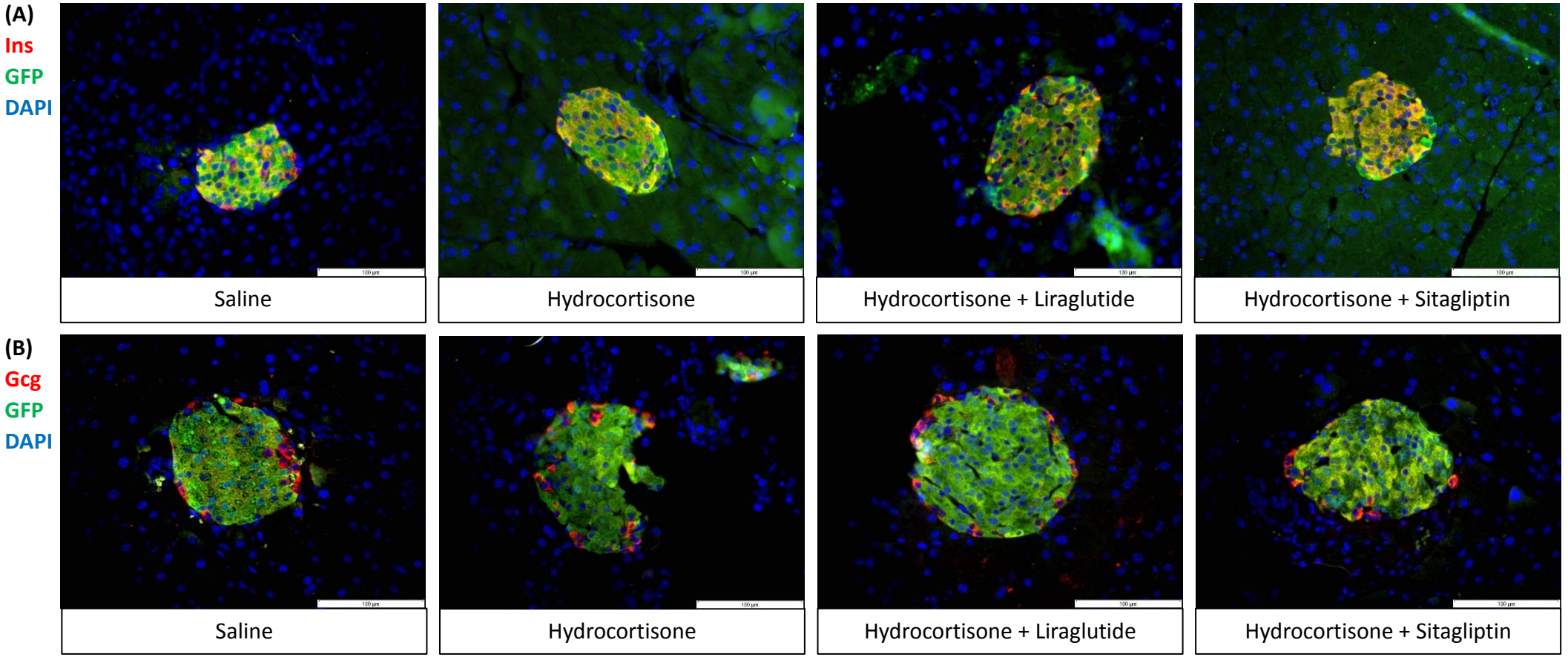

* Legend overleaf

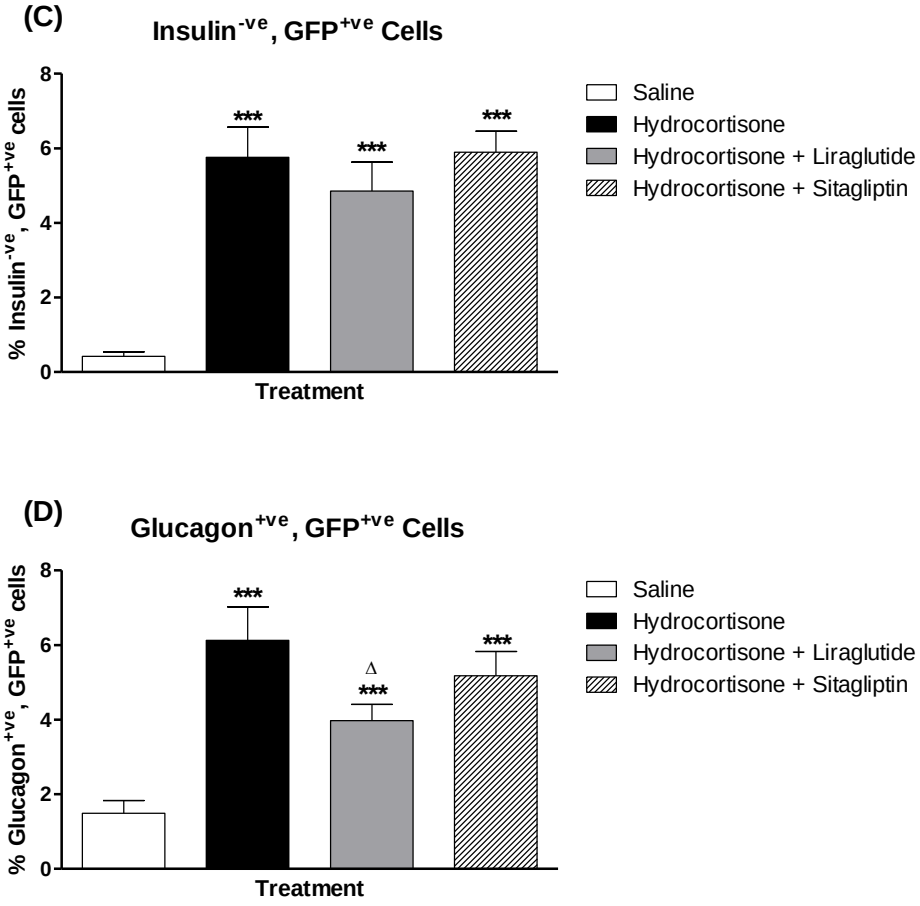

Transdifferentiation Analysis

Representative images of islets from mice treated with saline, hydrocortisone, hydrocortisone plus liraglutide and hydrocortisone plus sitagliptin stained for (A) insulin and GFP or (B) glucagon and GFP. Beta cell transdifferentiation determined by populations of insulin negative, GFP positive cells (C) and glucagon positive, GFP positive cells (D) using double immunofluorescence staining.

Values are mean ± SEM (n=8 mice/group). Comparisons versus saline control (*) or versus hydrocortisone (Δ), significant when */Δp<0.05, **/ΔΔp<0.01 and ***p<0.001.

Figure 4.19 Effects of hydrocortisone alone or in combination with liraglutide or sitagliptin on pancreatic islet beta cell and alpha cell apoptosis

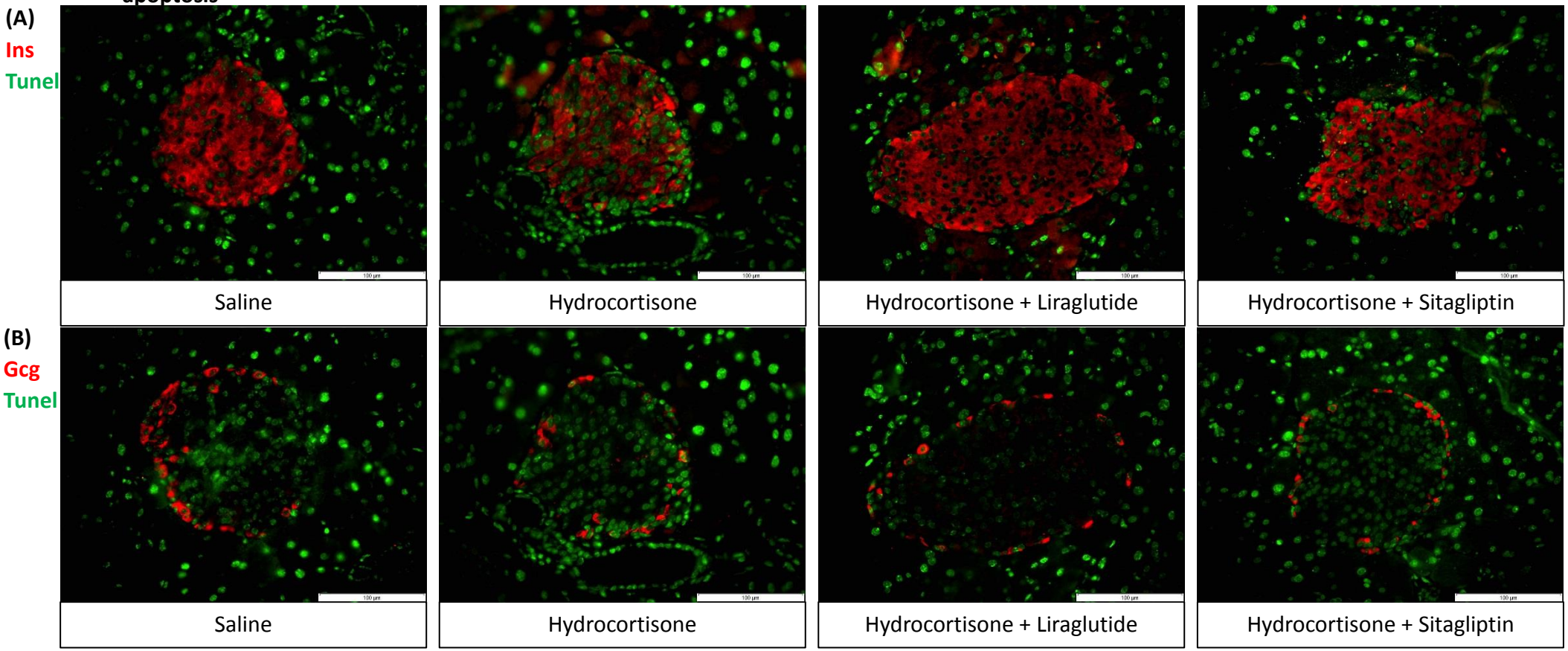

* Legend overleaf

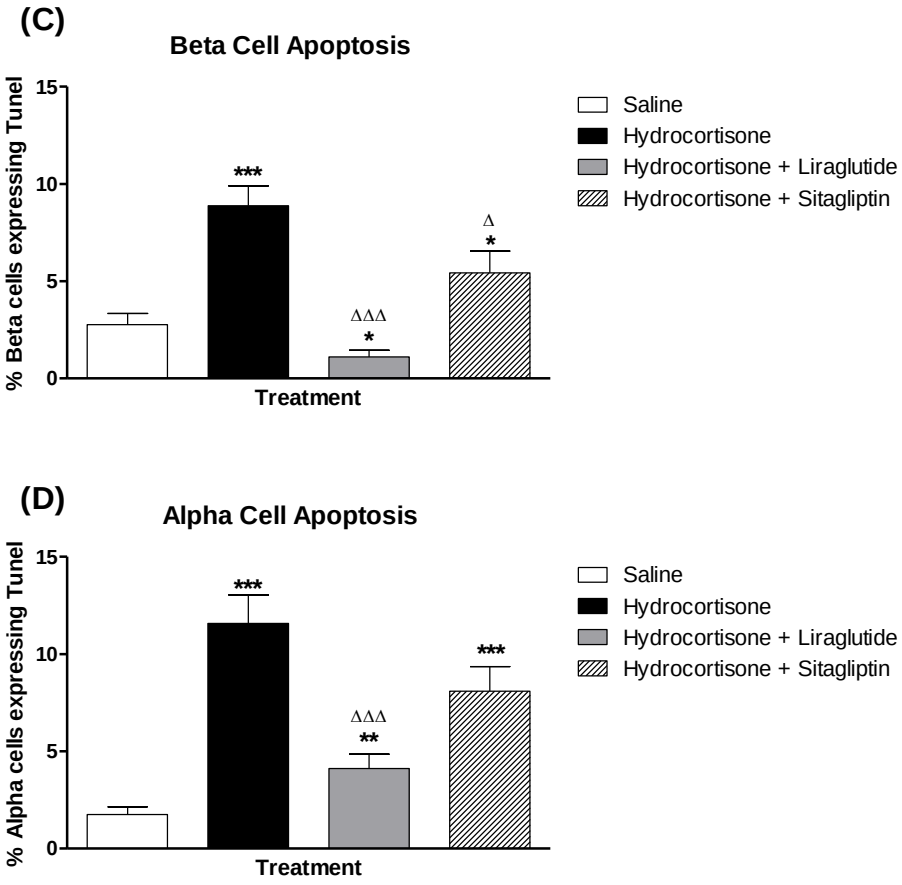

Apoptosis Analysis

Representative images of islets from mice treated with saline, hydrocortisone, hydrocortisone plus liraglutide and hydrocortisone plus sitagliptin stained for (A) insulin and TUNEL or (B) glucagon and TUNEL. Beta cell apoptosis and alpha cell apoptosis determined by populations of (C) insulin positive, TUNEL positive and (D) glucagon positive, TUNEL positive cells respectively by double immunofluorescence staining. Values are mean ± SEM (n=8 mice/group). Comparisons versus saline control (*) or versus hydrocortisone (Δ), significant when */Δp<0.05, **/ΔΔp<0.01 and ***/ΔΔΔp<0.001.

Figure 4.20 Effects of hydrocortisone alone or in combination with liraglutide or sitagliptin on pancreatic islet beta cell and alpha cell proliferation

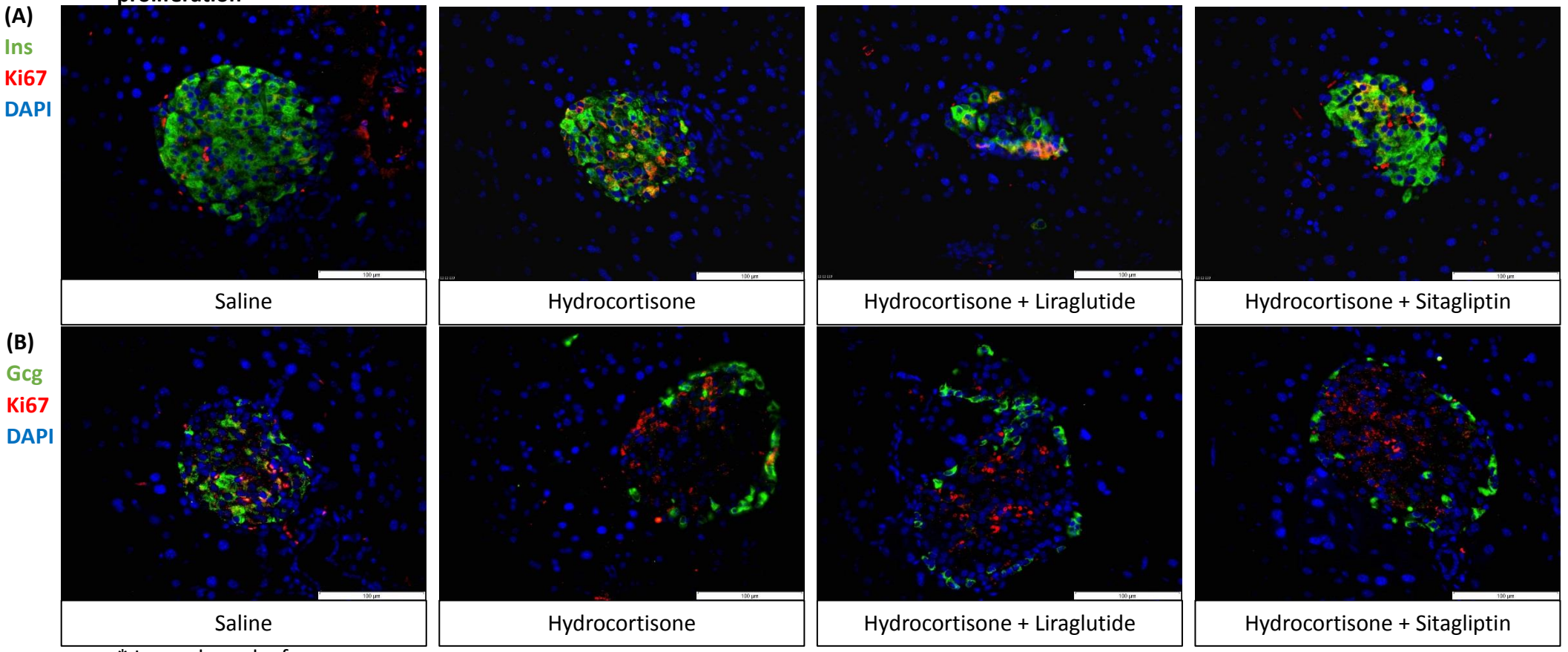

* Legend overleaf

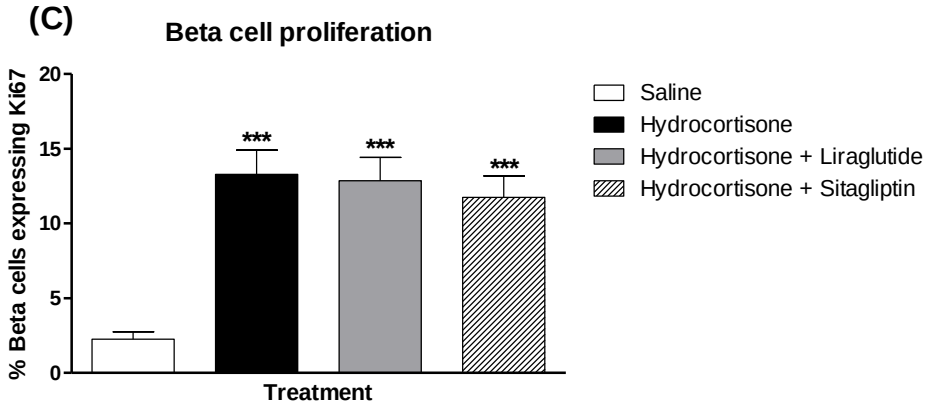

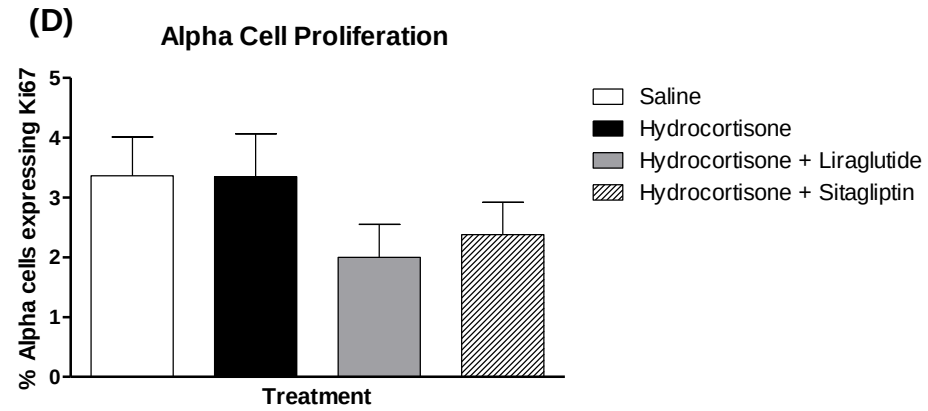

Proliferation Analysis

Representative images of islets from mice treated with saline, hydrocortisone, hydrocortisone plus liraglutide and hydrocortisone plus sitagliptin stained for (A) insulin and ki-67 or (B) glucagon and ki-67. Beta cell and alpha cell proliferation determined by populations of (C) insulin positive, ki-67 positive cells and (D) glucagon positive, ki-67 positive cells respectively.

Values are mean ± SEM (n=8 mice/group). Comparisons versus saline control (*) or versus hydrocortisone (Δ), significant when */Δp<0.05, **/ΔΔp<0.01 and ***p<0.001.

Figure 4.21: Effect of hydrocortisone alone or in combination with liraglutide or sitagliptin on pancreatic islet beta cell Pdx1 expression

(A)

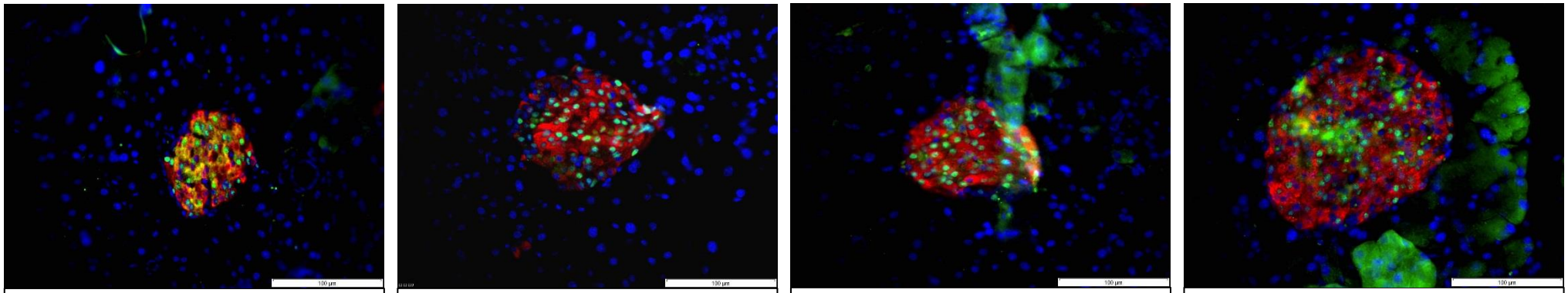

Saline	Hydrocortisone	Hydrocortisone + Liraglutide	Hydrocortisone + Sitagliptin

Insulin / Pdx1 / DAPI

* Legend overleaf

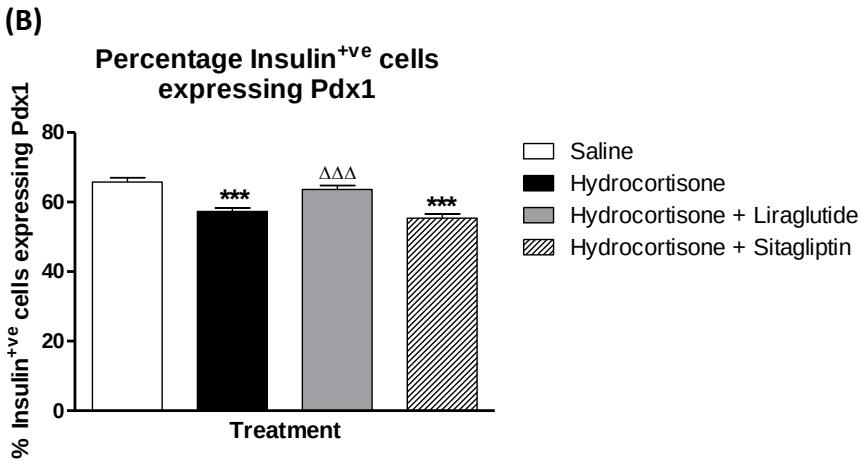

Pdx1 Expression Analysis

(A) Representative images of islets from mice treated with saline, hydrocortisone, hydrocortisone plus liraglutide and hydrocortisone plus sitagliptin on Pdx1 expression (B). Determined by histological analysis of insulin/Pdx1 double immunofluorescence staining showing insulin (red), Pdx1 (green) and DAPI (blue). Values are mean ± SEM (n=8 mice/group). Comparisons versus saline control (*) or versus streptozotocin (Δ), significant when */Δp<0.05, **/ΔΔp<0.01 and ***p<0.001.

Chapter 5

Effects of SGLT2 inhibition and insulin on islet morphology and beta-to-alpha cell transdifferentiation

5.1 Summary

In streptozotocin *Ins1*$^{cre/+}$;Rosa26-eYFP C57Bl/6 treated mice, daily administration of 1mg/kg dapagliflozin for 10 days did not suppress hyperglycaemia despite a mild increase in plasma insulin. Circulating and pancreatic glucagon levels were notably reduced. Within the islet, alpha cell mass expansion was noted with dapagliflozin. This was attributed to notable reduction in alpha cell apoptosis given dapagliflozin had no impact on beta cells transdifferentiation or alpha cell proliferation. A 5mg/kg daily dose of dapagliflozin, for the same period, had similar effects in streptozotocin treated mice albeit also eliciting a glucose lowering effect. In high fat fed mice dapagliflozin expanded both beta cell mass due to increased beta cell proliferation, mildly prevented beta-to-alpha cell transdifferentiation, associated with improved beta cell Pdx1 expression, and alpha cell mass due to inhibition of alpha cell apoptosis. Dapagliflozin worsened islet mass expansion observed in insulin resistant hydrocortisone treated mice. SGLT2 inhibition in this model had no effect on beta cell transdifferentiation however reduced apoptosis of both beta and alpha cells. Insulin countered streptozotocin induced hyperglycaemia, improving circulating and pancreatic insulin and glucagon levels. Histologically insulin also protected against streptozotocin-induced changes in islet morphology and it greatly reduced beta-to-alpha cell transdifferentiation, restoring beta cell Pdx1 expression. These studies suggest that alpha cell expansion seen with SGLT2 inhibitors is not caused by beta-to-alpha cell transdifferentiation but is largely an effect of reduced alpha cell apoptosis. Furthermore in streptozotocin diabetes restoring normoglycaemia is highly beneficial in preventing beta-to-alpha cell transdifferentiation, implying that hyperglycaemia may be an important trigger in this process.

5.2 Introduction

5.2.1 Dapagliflozin

Dapagliflozin belongs to the sodium glucose co-transporter 2 (SGLT2) inhibitor drug class. Inhibition of this transporter prevents reabsorption of glucose within the proximal renal tubules, where 90% of glucose reabsorption occurs, thus increasing excretion and ultimately lowering plasma glucose (Wright, 2001; Kanai et al, 1994; Rossetti et al, 1987). Patients with type-2 diabetes display increased expression of SGLT2 with exaggerated renal glucose reabsorption (Vestri et al, 2001; Freitas et al, 2008). In a Zucker diabetic fatty (ZDF) rat model of type-2 diabetes, dapagliflozin has been shown to produce a sustainable reduction in blood glucose and limit the decline in beta cell mass that occurs in these rats (Macdonald et al, 2010). These authors did not publish data regarding the effect on alpha cell mass however others have reported substantial gains in alpha cell mass with increases in alpha cell glucagon secretion and plasma glucagon levels following dapagliflozin treatment (Millar et al, 2017; Millar et al, 2016; Bonner et al, 2015; Merovci et al, 2014; Zambrowicz et al, 2013). Data also suggests that SGLT2 regulates islet function based on the finding of SGLT2 expression on islet alpha cells (Chen et al, 2012).

How dapagliflozin causes this expansion in alpha cells has yet to be fully determined with beta-to-alpha cell transdifferentiation a potential mechanism. This Chapter aims to explore this aspect by investigating dapagliflozin effects in streptozotocin, high fat fed and hydrocortisone models of diabetes. In *Ins1*$^{cre/+}$;Rosa26-eYFP C57Bl/6 mice were used to track beta cell transdifferentiation as noted in the previous Chapter.

5.2.2 Insulin

Insulin is a 51 amino acid hormone secreted from beta cells. First synthesised as preproinsulin, of 110 amino acids, this protein undergoes cleavage to form proinsulin within the endoplasmic reticulum before being packaged within secretory granules by the golgi apparatus (Orci et al, 1986). Within these granules enzymatic cleavage liberates mature insulin protein from the linking C-peptide (Goodge et al, 2000). Glucose is a key stimulant promoting insulin secretion however interactions between amino acids, fatty acids, neurotransmitters and hormones are all involved in regulating insulin release (Rorsman et al, 2013; Ashcroft et al, 1994). Once secreted the hormone acts on the insulin receptor, expressed on skeletal muscle and adipose tissue, to increase GLUT4 mediated glucose uptake necessary for energy and triglyceride storage respectively. Additionally this anabolic hormone promotes protein synthesis whilst inhibiting protein degradation leading to weight gain (Watson and Pessin, 2001).

Insulin replacement therapy is the primary treatment for type-1 diabetes and makes up late-stage treatment for type-2 diabetes when beta cell function has declined to the point where insulin resistance cannot be overcome by pharmacotherapies. In the present studies insulin will be utilised to examine the effect of glycaemia on beta-to-alpha cell transdifferentiation. Administration of streptozotocin and the resulting hyperglycaemia alters islet morphology dramatically increasing levels of beta-to-alpha cell transdifferentiation. To explore the contribution hyperglycaemia makes to transdifferentiation normogylcaemia will be maintained in streptozotocin treated mice via administration of insulin. This approach should also provide an insight as to whether other anti-diabetic agents are beneficial through their specific mechanisms

of action or whether they limit beta cell transdifferentiation is secondary to their glucose lowering ability.

5.3 Methods

Materials and methods have been briefly summarised below. Full explanations of each method can be found within chapter 2.

5.3.1 Animals

Diabetes was induced in 12 week old male *Ins1*$^{cre/+}$;Rosa26-eYFP C57Bl/6 mice by 5 daily dosing of streptozotocin (50mg/kg body weight). Within the following 5 days mice would present with diabetic symptoms. For hydrocortisone studies mice were dosed by intraperitoneal injections of 70mg/kg body weight hydrocortisone for 10 consecutive days. In both studies mice were dosed by once daily oral administration of 1mg/kg dapagliflozin or 5mg/kg dapagliflozin (where specified), commencing two days prior to streptozotocin/hydrocortisone dosing and continued until the end of the study. For the insulin treatment group streptozotocin-treated mice were dosed with 1 unit of bovine insulin every 8 hours commencing when hyperglycaemia (>15mM) presented. Similarly for diet-induced diabetes studies, high-fat fed mice were dosed with 1mg/kg dapagliflozin by daily oral gavage for 10 days. At the end of this 10 days dosing high-fat fed mice were fasted for a glucose tolerance test using 18.8mmol/kg body weight glucose. For all conducted studies mice were 8 per treatment group with body weight, calorie and fluid consumption recorded at regular

intervals. The dosing regimen was chosen based upon previous work (Millar et al 2017; Millar et al, 2016; Green et al, 2016). At the end of each study, pancreatic tissue was excised and cut longitudinally with one half taken for immunohistochemistry and the other for hormone content. A timeline of conducted studies is presented in Figure 5.0. Data for saline, streptozotocin, high-fat fed and hydrocortisone controls are reused from Chapter 4.

5.3.2 Biochemical Analysis

For hormone content analyses protein was extracted from snap frozen pancreatic tissue following homogenisation in acid ethanol (ethanol (75% (v/v) ethanol, 5% (v/v) distilled water and 1.5% (v/v) 12N HCl). Total protein content was determined by Bradford assay. An in-house radioimmunoassay was used to quantify plasma and pancreatic insulin, whilst glucagon levels were assessed by ELISA.

5.3.3 Immunohistochemistry

Longitudinally cut pancreatic tissue was fixed in 4% PFA for 48 hours at 4°C before dehydration and processing within an automated tissue processor. Processed pancreatic tissue was embedded in wax blocks and sectioned at 5µm thickness. For immunohistochemistry slides were first immersed in xylene to remove wax and then rehydrated through a series of ethanol washes (100-50%). Antigen retrieval was then performed using acidic citrate buffer (pH 6) at 95°C for 20 minutes, followed by 20 minutes at room temperature to cool. Slides were then blocked in a 4% BSA solution before incubation with primary antibodies. Primary antibodies used were as follows: mouse monoclonal anti-insulin antibody (ab6995, 1:1000; Abcam), guinea-pig anti-

glucagon antibody (PCA2/4, 1:200; raised in-house), rabbit anti-Ki67 antibody (ab15580, 1:200; Abcam) and rabbit anti-Pdx1 antibody (ab47267, 1:200; Abcam). After overnight incubation slides were washed in PBS before incubation with fluorescently-linked secondary antibodies used as appropriate: Alexa Fluor488 goat anti-guinea pig IgG — 1:400, Alexa Fluor 594 goat anti-mouse IgG — 1:400, Alexa Fluor 488 goat anti-rabbit IgG — 1:400, Alexa Fluor 594 goat anti-rabbit IgG — 1:400 or Alexa Fluor 488 donkey anti-goat IgG — 1:400. After a further wash in PBS to remove excess antibody before 15 minute incubation with DAPI to stain nuclei. Slides were mounting with cover slips ready for imaging on a fluorescent microscope (Olympus system microscope, model BX51) fitted with DAPI (350nm) FITC (488nm) and TRITC (594nm) filters and a DP70 camera adapter system. To assess apoptosis a TUNEL assay was carried out following manufacturer's guidelines (In situ cell death kit, Fluorescein, Roche Diagnostics, UK).

5.3.4 Image Analysis

Cell^F imaging software (Olympus Soft Imaging Solutions, GmbH) was used to analyse the following islet parameters: islet area, beta cell area, alpha cell area (expressed at μm^2), percentage beta cells and percentage alpha cells. Islets were deemed small (<10,000 μm^2), medium (10,000-25,000 μm^2) or large (>25,000 μm^2) to determine islet size distribution. The number of islets per mm^2 pancreas and proportion of islets with central alpha cells were judged in a blinded fashion. For transdifferentiation analysis beta cells expressing GFP with no insulin were termed "$insulin^{-ve}$, GFP^{+ve} cells" whilst those expressing GFP with glucagon were termed

"glucagon^{+ve}, GFP^{+ve} cells." To quantify apoptosis beta and alpha cells co-expressing TUNEL alongside insulin and glucagon respectively were counted. Similarly for proliferation Ki-67 and insulin/glucagon positive cells were totalled. Beta cell Pdx1 expression was quantified using ImageJ software, counting the total number of insulin positive beta cells within an islet and expressing the number of those expressing Pdx1 as a percentage of that total. All cell counts were determined in a blinded manner with >60 islets analysed per treatment group.

5.3.5 Statistics

All results were generated and analysed using GraphPad PRISM (version 5), with data presented as mean ± SEM. Comparative analyses between groups were carried out using Student's unpaired t-test, one-way ANOVA with a Bonferroni post-hoc test or a two-way repeated measures ANOVA with a Bonferroni post-hoc test where appropriate. Results were deemed significant once $p<0.05$.

5.4 Results

5.4.1 Effects of streptozotocin alone or in combination with low dose dapagliflozin treatment on body weight, energy intake and fluid intake

Mice treated with dapagliflozin presented with body weight loss from day 5 onwards (Figure 5.1A), peaking to 17.1 ± 2.8%, $p<0.001$ percentage weight loss (Figure 5.1B). Similarly, cumulative energy consumption was reduced in dapagliflozin treated mice

(338.7 ± 25.4 vs 445.5 ± 9.0kJ, $p<0.01$, Figure 5.1C), whereas cumulative fluid consumption was raised (109.7 ± 8.2 vs 94.8 ± 3.2ml, $p<0.05$, Figure 5.1D).

5.4.2 Effects of streptozotocin alone or in combination with low dose dapagliflozin treatment on blood glucose, plasma insulin/glucagon and pancreatic insulin/glucagon content

1mg/kg dapagliflozin treatment had no effect on non-fasting blood glucose compared to streptozotocin treatment alone (26.3 ± 1.9 vs 26.3 ± 1.4mM, Figure 5.2A-B). Despite this, dapagliflozin was able to elicit increases in plasma insulin (7.2 ± 0.5 ± 5.2 ± 0.4ng/ml, $p<0.05$, Figure 5.2C) and reductions in plasma glucagon (0.03 ± 0.001 vs 0.08 ± 0.009ng/ml, $p<0.001$, Figure 5.2E) and pancreatic glucagon content (7.3 ± 0.4 vs 18.7 ± 1.2ng/mg protein, $p<0.001$, Figure 5.2F).

5.4.3 Effects of streptozotocin alone or in combination with low dose dapagliflozin treatment on islet parameters

Representative images of islets stained for insulin (red) and glucagon (green) from mice treated with dapagliflozin (Figure 5.3A). Dapagliflozin treatment exacerbated streptozotocin-induced loss of beta cell area (1732 ± 238.4 vs 3309 ± 287.5μm^2, $p<0.001$, Figure 5.3C), whilst alpha cell area remained raised (2897 ± 342.0μm^2, Figure 5.3D). Streptozotocin-induced alterations to percentage beta cells (39.9 ± 2.1 vs 58.9 ± 1.8%, $p<0.001$, Figure 5.3F) and percentage alpha cells (60.1 ± 2.1 vs 43.1 ± 2.1%, $p<0.001$, Figure 5.3G) were worsened by dapagliflozin treatment. Alpha cell

distribution was marginally improved with dapagliflozin treatment (50.0 ± 3.0 vs 70.0 ± 4.4%, p<0.001, Figure 5.3H) but was still impaired compared to non-diabetic mice (20.0 ± 4.0%).

5.4.4 Effects of streptozotocin alone or in combination with low dose dapagliflozin treatment on beta-to-alpha cell transdifferentiation

Representative images of islets stained for (Figure 5.4A) insulin (red) and GFP (green) or (Figure 5.4B) glucagon (red) and GFP (green) from mice treated with dapagliflozin. SGLT2 inhibition had no impact on streptozotocin-induced beta-to-alpha cell transdifferentiation determined by insulin negative, GFP positive cells (6.4 ± 1.0 vs 5.6 ± 0.7%, NS, Figure 5.4C) and glucagon positive, GFP positive cells (4.6 ± 0.6 vs 5.7 ± 0.7%, NS, Figure 5.4D).

5.4.5 Effects of streptozotocin alone or in combination with low dose dapagliflozin treatment on beta and alpha cell apoptosis

Islets stained for insulin (red) and TUNEL (green) or glucagon (red) and TUNEL (green) are displayed Figure 5.5A and B respectively. Dapagliflozin had no impact on streptozotocin induced beta cell apoptosis (6.5 ± 1.3 vs 10.9 ± 1.9%, NS, Figure 5.5C) however reduced alpha cell apoptosis (1.2 ± 0.4 vs 4.7 ± 1.0%, p<0.01, Figure 5.5D).

5.4.6 Effects of streptozotocin alone or in combination with dapagliflozin treatment on beta and alpha cell proliferation

Islets stained for insulin (green) and ki-67 (red) or glucagon (green) and ki-67 (red) are presented in Figure 5.6A and B respectively. Dapagliflozin increased beta cell proliferation (4.8 ± 1.5 vs 2.2 ± 0.5% saline, $p<0.05$, Figure 5.6C) and reduced alpha cell proliferation (3.7 ± 1.6 vs 8.2 ± 1.1%, $p<0.05$, Figure 5.6D).

5.4.7 Effects of streptozotocin alone or in combination with low dose dapagliflozin treatment on beta cell Pdx-1 expression

Representative images of islets stained for insulin (red) and Pdx-1 (green) are found in Figure 5.7A. 1mg/kg body weight dapagliflozin treatment had no effect on streptozotocin-induced reductions in beta cell Pdx-1 expression (50.6 ± 1.7 vs 53.3 ± 1.0%, NS, Figure 5.7B).

5.4.8 Effects of high fat feeding alone or in combination with low dose dapagliflozin treatment on body weight, percentage body weight change, energy and fluid intake

Dapagliflozin treatment reduced percentage body weight (-13.8 ± 0.9 vs 0.7 ± 1.3%, $p<0.001$, Figure 5.8B) but had no notable effect on energy consumption (Figure 5.8C). Fluid consumption was markedly reduced from day 4 of the study onwards (145.0 ± 6.2 vs 215.9 ± 6.9%, $p<0.001$, Figure 5.8D).

5.4.9 Effects of high fat feeding alone or in combination with low dose dapagliflozin treatment on blood glucose, plasma insulin/glucagon and pancreatic insulin/glucagon content

Although variable, dapagliflozin elicited a subtle reduction in non-fasting blood glucose (7.5 ± 0.4 vs 8.7 ± 0.3mM, $p<0.05$, Figure 5.9A-B). Dapagliflozin treatment was able to raise pancreatic insulin content (43.8 ± 3.4 vs 35.1 ± 1.7ng/mg protein, $p<0.05$, Figure 5.9D) whilst reducing plasma glucagon (0.03 ± 0.002 vs 0.05 ± 0.003ng/ml, $p<0.05$, Figure 5.9E). During a glucose tolerance test, dapagliflozin significantly reduced blood glucose at 60 minutes (17.6 ± 1.1 vs 23.8 ± 1.2mM, $p<0.001$, Figure 5.9F) and elicited a reduction in AUC (1066 ± 31.6 vs 1266 ± 38.9, $p<0.01$, Figure 5.9G).

5.4.10 Effects of high fat feeding alone or in combination with low dose dapagliflozin treatment on islet parameters

Figure 5.10A displays representative images of islets stained for insulin (red) and glucagon (green) from mice treated with dapagliflozin. Of note, alpha cell area was markedly increased (3705 ± 392.4 vs 2778 ± 258.0μm^2, $p<0.05$, Figure 5.10D) whilst percentage beta cells was reduced (79.7 ± 1.0 vs 85.3 ± 0.6%, $p<0.001$, Figure 5.10F) by dapagliflozin treatment.

5.4.11 Effects of high fat feeding alone or in combination with low dose dapagliflozin treatment on beta-to-alpha cell transdifferentiation

Representative images of islets stained for (Figure 5.11A) insulin (red) and GFP (green) or (Figure 5.11B) glucagon (red) and GFP (green) from high fat fed mice treated with dapagliflozin. Dapagliflozin treatment reduced the number insulin deficient, GFP positive cells (4.5 ± 0.6 vs 6.9% ± 0.8, $p<0.05$, Figure 5.11C) whilst having no impact on glucagon positive, GFP positive cells.

5.4.12 Effects of high fat feeding alone or in combination with low dose dapagliflozin treatment on beta and alpha cell apoptosis

Representative images of islets stained for insulin or glucagon (red) with TUNEL (green) are displayed in Figure 5.12A and B respectively. Dapagliflozin had no effect on beta cell apoptosis (Figure 5.12C) or alpha cell apoptosis (Figure 5.12D).

5.4.13 Effects of high fat feeding alone or in combination with low dose dapagliflozin treatment on beta and alpha cell proliferation

Islets stained for ki-67 (red) alongside insulin or glucagon (green) are displayed in Figure 5.13A and B respectively. In high fat fed mice dapagliflozin elevated beta cell proliferation (9.4 ± 1.0 vs 5.9 ± 1.1%, $p<0.05$, Figure 5.13C), whilst having no effect on alpha cell proliferation.

5.4.14 Effects of high fat feeding alone or in combination with low dose dapagliflozin treatment on beta cell Pdx-1 expression

Representative images of islets from high fat fed dapagliflozin treated mice stained for insulin (red) and Pdx-1 (green) are displayed in Figure 5.14A. Treatment with SGLT2 inhibitor improved beta cell Pdx-1 expression (53.4 ± 1.0 vs 49.6 ± 1.3%, $p<0.05$, Figure 5.14B), albeit not to levels equivalent to lean mice (65.7 ± 1.3%).

5.4.15 Effects of hydrocortisone alone or in combination with low dose dapagliflozin treatment on body weight, energy and fluid intake

Mice treated with hydrocortisone reduced body weight with dapagliflozin treatment not impacting this change (-8.3 ± 0.6 vs -6.5 ± 1.0%, NS, Figure 5.15B). Of note, dapagliflozin treated mice displayed a reduction in cumulative energy consumption (440.4 ± 13.7 vs 509.0 ± 15.2kJ, $p<0.001$, Figure 5.15C) and cumulative fluid intake (90.8 ± 9.2 vs 110.4 ± 5.6ml, $p<0.05$, Figure 5.15D).

5.4.16 Effects of hydrocortisone alone or in combination with low dose dapagliflozin treatment on blood glucose, plasma insulin/glucagon and pancreatic insulin/glucagon content

Although quite variable dapagliflozin had no profound impact on non-fasting blood glucose levels (Figure 5.16A-B). Similarly both plasma insulin and glucagon were found raised in these mice to similar levels to mice dosed solely with hydrocortisone.

Only pancreatic insulin content was reduced by dapagliflozin treatment (45.1 ± 6.0 vs 77.6 ± 7.7ng/mg protein, $p<0.01$, Figure 5.16D).

5.4.17 Effects of hydrocortisone alone or in combination with low dose dapagliflozin treatment on islet parameters

Representative images of islets stained for insulin (red) and glucagon (green) are displayed in Figure 5.17A. In hydrocortisone treated mice, dapagliflozin markedly increased islet area (17840 ± 2016µm^2 vs 10790 ± 907.4µm^2, $p<0.001$, Figure 5.17B) beta cell area (16930 ± 2215 vs 9499 ± 805.2µm^2, $p<0.001$, Figure 5.17C) and alpha cell area (2477 ± 327.7 vs 1430 ± 141.2, $p<0.001$, Figure 5.17D). Islet size distribution was markedly altered by dapagliflozin treatment with reductions in small sized islets (39.0 ± 9.2 vs 75.5 ± 3.6%, $p<0.05$, Figure 5.17E) in line with an increase in medium sized islets (39.2 ± 5.2 vs 17.1 ± 2.6%, $p<0.01$, Figure 5.17E).

5.4.18 Effects of hydrocortisone alone or in combination with low dose dapagliflozin treatment on beta-to-alpha cell transdifferentiation

GFP staining was carried out to determine transdifferentiation coupled with insulin or glucagon as shown in Figure 5.18A and B respectively. In hydrocortisone treated mice dapagliflozin failed to elicit any discernible changes in insulin negative, GFP positive cells (Figure 5.18C) or glucagon positive, GFP positive cells (Figure 5.18D).

5.4.19 Effects of hydrocortisone alone or in combination with low dose dapagliflozin treatment on beta and alpha cell apoptosis

TUNEL immunohistochemistry was used alongside insulin or glucagon to determine beta and alpha cell apoptosis shown in Figures 5.19A and B respectively. Dapagliflozin treatment protected both beta cells (2.6 ± 0.5 vs 8.9 ± 1.0%, $p<0.001$, Figure 5.19C) and alpha cells (4.8 ± 0.7 vs 11.6 ± 1.5%, $p<0.001$, Figure 5.19D) against hydrocortisone-induced apoptosis.

5.4.20 Effects of hydrocortisone alone or in combination with low dose dapagliflozin treatment on beta and alpha cell proliferation

Representative images of ki-67 staining carried out in conjunction with insulin or glucagon are presented in Figures 5.20A and B respectively. Beta cell proliferation was markedly reduced by dapagliflozin (6.7 ± 1.1 vs 13.2 ± 1.6%, $p<0.001$, Figure 5.20C) whilst alpha cell proliferation was only slightly lowered when compared to saline animals (1.9 ± 0.4 vs 3.4 ± 0.6%, $p<0.05$, Figure 5.20D).

5.4.21 Effects of hydrocortisone alone or in combination with low dose dapagliflozin treatment on beta cell Pdx-1 expression

Islets stained for insulin (red) and Pdx-1 (green) are presented in Figure 5.21A. Dapagliflozin had no discernible impact on beta cell Pdx-1 expression (57.9 ± 1.2 vs 57.2 ± 1.0%, NS, Figure 5.21B).

5.4.22 Effects of streptozotocin alone or in combination with high dose dapagliflozin treatment on body weight, percentage body weight change, energy and fluid intake

High dose dapagliflozin [5mg/kg body weight] caused a reduction in percentage weight change in streptozotocin treated animals (-13.0 ± 1.1 vs -7.6 ± 0.3%, $p<0.001$, Figure 5.22B). This dose had no effect on energy consumption however it increased fluid consumption (109.2 ± 5.7 vs 94.8 ± 3.1ml, $p<0.05$, Figure 5.22D).

5.4.23 Effects of streptozotocin alone or in combination with high dose dapagliflozin treatment on blood glucose, plasma insulin/glucagon and pancreatic insulin/glucagon content

Treatment with dapagliflozin protected against streptozotocin-induced hyperglycaemia (18.8 ± 0.9 vs 26.3 ± 1.4mM, $p<0.01$, Figure 5.23A-B). Streptozotocin reduced plasma insulin with dapagliflozin having not further effect. Pancreatic insulin content however was dramatically increased by dapagliflozin treatment (53.9 ± 1.3 vs 29.1 ± 2.0, $p<0.001$, Figure 5.23D). Glucagon levels both within plasma (0.03 ± 0.001 vs 0.08 ± 0.009ng/ml, $p<0.001$, Figure 5.23E) and pancreas (12.7 ± 1.0 vs 18.7 ± 1.2ng/mg protein, $p<0.05$, Figure 5.23F) were substantially reduced with a high dose of dapagliflozin.

5.4.24 Effects of streptozotocin alone or in combination with high dose dapagliflozin treatment on islet parameters

Representative images of islets stained for insulin (red) and glucagon (green) are displayed in Figure 5.24A. High dose dapagliflozin exacerbated streptozotocin-induced beta cell loss (2088 ± 203.3 vs 3309 ± 287.5μm^2, p<0.001, Figure 5.24C). Islet size distribution was altered with an increase in the number of small islets (90.6 ± 1.5 vs 68.3 ± 1.7%, p<0.001, Figure 5.24E) and a reciprocal reduction in the number of medium sized islets (8.1 ± 1.9 vs 31.7 ± 1.7%, p<0.001, Figure 24E). Similarly high dose dapagliflozin exacerbated streptozotocin- induced reductions and gains in percentage beta cells (42.1 ± 1.5 vs 58.9 ± 1.8%, p<0.001, Figure 5.24F) and percentage alpha cells (58.0 ± 1.5 vs 43.1 ± 2.1%, p<0.001, Figure 5.24G) respectively. Islet architecture was improved by dapagliflozin treatment (52.2 ± 3.2 vs 70.0 ± 4.4%, p<0.01, Figure 5.24H) however was still notably impaired compared to non-diabetic mice.

5.4.25 Effects of streptozotocin alone or in combination with high dose dapagliflozin treatment on beta-to-alpha cell transdifferentiation

Representative images of islets stained for GFP (green) in conjunction with insulin or glucagon (red) are presented in Figure 5.25A and B respectively. A 5mg/kg dose of dapagliflozin elicited a reduction in insulin negative, GFP positive cells (3.7 ± 0.6 vs 5.6 ± 0.7%, p<0.05, Figure 5.25C) however had no effect on glucagon, GFP expression.

5.4.26 Effects of streptozotocin alone or in combination with high dose dapagliflozin treatment on beta and alpha cell apoptosis

Characteristic images of TUNEL (green) staining alongside insulin or glucagon (red) are shown in Figure 5.26A and B respectively. Dapagliflozin had no discernible effect on streptozotocin-induced beta cell apoptosis, however it exacerbated alpha cell apoptosis (7.9 ± 0.9 vs 4.7 ± 1.0%, $p<0.05$, Figure 5.26D).

5.4.27 Effects of streptozotocin alone or in combination with high dose dapagliflozin treatment on beta and alpha cell proliferation

Ki-67 (red) staining was carried out in conjunction with insulin or glucagon (green) as shown in Figures 5.27A and B respectively. A high dose of dapagliflozin notably elevated beta cell proliferation (7.1 ± 1.0 vs 4.0 ± 0.9%, $p<0.05$, Figure 5.27C) whilst having no impact on proliferation of alpha cells.

5.4.28 Effects of streptozotocin alone or in combination with high dose dapagliflozin treatment on beta cell Pdx-1 expression

Representative images of islets stained for insulin (red) and Pdx-1 (green) are presented in Figure 5.28A. 5mg/kg dose dapagliflozin improved beta cell Pdx-1 expression (66.4 ± 0.9 vs 53.3 ± 1.0%, $p<0.001$, Figure 5.28B) to levels comparable to non-diabetic mice.

5.4.29 Effects of streptozotocin alone or with insulin treatment on body weight, energy and fluid intake

Administration of insulin protected against streptozotocin-induced weight loss (-3.7 ± 0.5 vs -7.6 ± 0.3%, $p<0.001$, Figure 5.29B) whilst increasing cumulative energy intake (516.9 ± 25.1 vs 445.5 ± 9.0kJ, $p<0.01$, Figure 5.29C) and reducing water consumption (64.4 ± 3.7 vs 94.8 ± 3.2ml, $p<0.001$, Figure 5.29D).

5.4.30 Effects of streptozotocin alone or with insulin treatment on blood glucose, plasma insulin/glucagon and pancreatic insulin/glucagon content

Predictably administration of insulin reduced streptozotocin-induced hyperglycaemia (13.6 ± 1.2 vs 26.3 ± 1.4mM, $p<0.001$, Figure 5.30A-B). Similarly, bovine insulin administration restored normal plasma insulin (8.3 ± 0.4 vs 5.2 ± 0.4ng/ml, $p<0.001$, Figure 5.30C), pancreatic insulin levels (41.3 ± 4.5 vs 29.1 ± 2.0 ng/mg protein, $p<0.01$, Figure 5.30D) as well as plasma glucagon (0.04 ± 0.004 vs 0.08 ± 0.009ng/ml, $p<0.01$, Figure 5.30E) and pancreatic glucagon content (7.6 ± 2.3 vs 18.7 ± 1.2 ng/mg protein, $p<0.05$, Figure 5.30F).

5.4.31 Effects of streptozotocin alone or with insulin treatment on islet parameters

Representative images of islets showing insulin (red) and glucagon (green) immunohistochemistry are presented in Figure 5.31A). Islet area was improved by insulin treatment (6733 ± 823.7 vs 4407 ± 393.3μm^2, $p<0.05$, Figure 5.31B) despite changes in beta cell area and alpha cell area failing to reach significance. Insulin

therapy profoundly raised percentage beta cells (65.7 ± 1.7 vs 58.9 ± 1.8%, p<0.01, Figure 5.31F) with a reciprocal reduction in percentage alpha cells (34.3 ± 1.7 vs 43.1 ± 2.1, p<0.01, Figure 5.31G). Likewise islet architecture was improved by insulin therapy (31.0 ± 4.0 vs 70.0 ± 4.4%, p0.001, Figure 5.31H).

5.4.32 Effects of streptozotocin alone or with insulin treatment on beta-to-alpha cell transdifferentiation

Immunohistochemistry of GFP (green) with insulin or glucagon (red) is presented in Figure 5.32A and B respectively. Administration of insulin resulted in a marked reduction in the number insulin negative, GFP positive cells (1.2 ± 0.4 vs 5.6 ± 0.7%, p<0.001, Figure 5.32C) and glucagon positive, GFP positive cells (2.8 ± 0.5 vs 5.7 ± 0.7%, p<0.01, Figure 5.32D).

5.4.33 Effects of streptozotocin alone or with insulin treatment on beta and alpha cell apoptosis

Immunohistochemistry images for TUNEL (green) in conjunction with insulin or glucagon (red) are presented in Figure 5.33A and B respectively. Insulin therapy caused a reduction in beta cell apoptosis (5.8 ± 1.0 vs 10.9 ± 1.9%, p<0.05, Figure 5.33C) and alpha cell apoptosis (1.1 ± 0.4 vs 4.7 ± 1.0%, p<0.001, Figure 5.33D).

5.4.34 Effects of streptozotocin alone or with insulin treatment on beta and alpha cell proliferation

Representative images of islets stained for ki-67 (red) alongside insulin or glucagon (green) are presented in Figure 5.34A and B respectively. Insulin treatment caused a notable reduction in alpha cell proliferation (2.8 ± 0.6 vs 8.2 ± 1.1%, $p<0.001$, Figure 5.34D) whilst having no significant effect on beta cell proliferation.

5.4.35 Effects of streptozotocin alone or with insulin treatment on beta cell Pdx-1 expression

Immunohistochemistry for insulin (red) and Pdx-1 (green) was carried out and presented in Figure 5.35A. Streptozotocin-treated mice given insulin showed improved beta cell Pdx-1 expression (68.3 ± 2.4 vs 53.3 ± 1.0%, $p<0.001$, Figure 5.35B) to levels comparable to non-diabetic mice.

5.5 Discussion

As noted in the previous Chapter, beta-to-alpha cell transdifferentiation is observed in diet-induced diabetes, multiple dose hydrocortisone and multiple low-dose streptozotocin models, the greatest extent found in the latter model. The presented studies have explored the effect of dapagliflozin, a SGLT2 inhibitor, on islet morphology and this beta-to-alpha cell transdifferentiation process. Based upon previous studies showing favourable anti-diabetic effects, a 1mg/kg oral dose was selected for the use within these studies (Millar et al, 2016; Millar et al, 2017). This dose of dapagliflozin in streptozotocin-treated *Ins1*$^{cre/+;}$Rosa26-eYFP C57Bl/6 mice

had no effect on reducing the number of islets showing transdifferentiated beta cells, with reduced beta cell Pdx-1 expression helping to confirm loss of beta cell maturity. Alpha cell apoptosis however was reduced by dapagliflozin treatment. This suggests that the increase in alpha cell area noted in these mice was due to reduced alpha cell apoptosis. Alpha cell proliferation does not contribute to this increased alpha cell area given that it was not observed within these mice.

Unexpectedly this 1mg/kg dose of dapagliflozin did not produce the expected glucose lowering effect. This suggests that the observed islet changes were not a consequence of improved diabetes control, but a direct action of SGLT2 inhibition. To prove this further, a higher dose of 5mg/kg dapagliflozin was selected and administered to streptozotocin-diabetic *Ins1*$^{cre/+}$;Rosa26-eYFP C57Bl/6 mice. This dose showed a more profound glucose-lowering effect, as widely stated within the literature, however it was insufficient to restore normoglycaemia (Macdonald et al, 2010). Within the pancreas, the islets showed similar changes compared to mice treated with a lower dose of dapagliflozin, with increased alpha cell mass largely attributable reduced apoptosis of alpha cells.

In diet-induced high fat fed mice, the low dose of dapagliflozin had a slight effect on reducing the number of islets showing transdifferentiated beta cells. This was supported by improved beta cell maturity as denoted by improved beta cell Pdx-1 expression. Despite this reduction in beta cell transdifferentiation, alpha cell mass was still raised in high fat fed dapagliflozin treated mice. Given that alpha cell apoptosis and proliferation was unchanged the cause of this increase in alpha cell

mass is still undetermined. Beta cell proliferation was upregulated and may contribute to marked the increase in large islets (>25,000μm^2) observed.

Dapagliflozin therapy had no impact on beta cell transdifferentiation levels in hydrocortisone-treated animals, with lowered Pdx-1 expression equivalent to hydrocortisone alone. Much like before, the increase in alpha cell mass seen in these mice was due to a reduction in alpha cell apoptosis. In this model, beta cell mass was also elevated with our data showing that this was due to a combination of increased beta cell proliferation and reduction in beta cell apoptosis. Beta cell mass was notably increased by dapagliflozin treatment, an effect largely attributable to beta cell hypertrophy and reduced beta cell apoptosis. Interestingly, in this model of diabetes, dapagliflozin elicited a reduction in beta cell proliferation compared with both streptozotocin and high fat fed models where proliferation increased.

These results show that dapagliflozin had little impact regarding beta cell transdifferentiation, however it acted to lower alpha cell apoptosis. Despite the kidney being the primary target of SGLT2 inhibitors, evidence is growing regarding effects within the brain (Millar et al, 2017) and within the pancreas as shown here and by others (Chen et al, 2012; Bonner et al, 2015). Nonetheless use of SGLT2 inhibitors should be promoted due to their ability to lower blood glucose independent of insulin, increase insulin sensitivity and promote weight loss (List et al, 2009; Han et al, 2008). Their ability to reduce glucose reabsorption complements the action of other anti-diabetic agents and has been shown when combined with

DPPIV inhibitors of GLP-1 receptor agonists (Scheen et al, 2016; Jabbour et al, 2014; Rosenstock et al, 2015; Millar et al, 2017).

Streptozotocin elicits both a direct chemical insult on the pancreatic islet, likely due to DNA alkylation and insulitis, as well as an indirect insult due to prolonged hyperglycaemia (Srinivasan and Ramaro, 2007). Administration of insulin post streptozotocin insult to counteract hyperglycaemia should provide insight on whether beta cell transdifferentiation is impacted directly by anti-diabetic agents or whether this may be a secondary action due to their glucose lowering effect. Administration of 1 unit insulin every 8 hours was effective at reducing non-fasting hyperglycaemia however glucose was still elevated suggesting a stricter dosing regimen may be more beneficial. Nonetheless insulin therapy severely stunted streptozotocin-induced changes in islet morphology; reduced beta cell mass and increased alpha cell mass. Islet architecture was markedly improved with most islets showing regular peripheral distribution of alpha cells. By preventing prolonged elevations in blood glucose beta cell maturity as determined by Pdx-1 expression was restored with beta-to-alpha cell transdifferentiation markedly reduced to levels comparable to non-diabetic mice (Gao et al, 2014). This supports the theory suggested by Cinti et al, 2014 whereby beta cells transdifferentiate to protect themselves from apoptosis and that when favourable metabolic conditions return (normoglycaemia for streptozotocin diabetes) readily revert back to mature beta cells.

This hyperglycaemic stress mediated transdifferentiation is supported by others that used pancreatectomy, or K_{ATP}-GOF mice to induce hyperglycaemia and induce beta cell dedifferentiation (Jonas et al, 1999; Wang et al, 2014). Similarly both these authors also observed that restoration of normoglycaemia, either by phlorizin or insulin, was sufficient to reverse this dedifferentiation (Jonas, et al, 1999; Wang et al, 2014). Opposing findings have also been observed in db/db mice whereby insulin therapy was insufficient to reduce beta cell dedifferentiation (Ishida et al, 2017). In this instance reductions in alpha cell proliferation and beta cell transdifferentiation work synergistically to counteract reduced alpha cell apoptosis to limit the extent of alpha cell mass expansion. Likewise conservation of mature beta cells and potentially insulin-stimulated beta cell proliferation, albeit not significant, collectively limited beta cell loss observed in streptozotocin-induced diabetes. As expected administration of insulin protected against hyperglycaemia-induced metabolic changes in calorie consumption and fluid intake. Increasing circulating insulin exogenously appears to trigger a negative feedback on glucagon limiting both circulating levels and pancreatic production of this hormone.

This Chapter has shed light on the source of the increased alpha cells noted in diabetic animal models and patients. Beta-to-alpha cell transdifferentiation in streptozotocin diabetes was substantially reduced by administration of insulin and restoration of normoglycaemia. This finding strongly suggests that removal of beta cell stressors, in this model hyperglycaemia, is sufficient for the restoration of transdifferentiated beta cells back to functional insulin producing cells. Whether this

runs true for insulin resistant models for diabetes remains to be seen, but is highly plausible.

Figure 5.0 Timeline of *Ins1*$^{cre/+}$;Rosa26-eYFP C57Bl/6 Studies

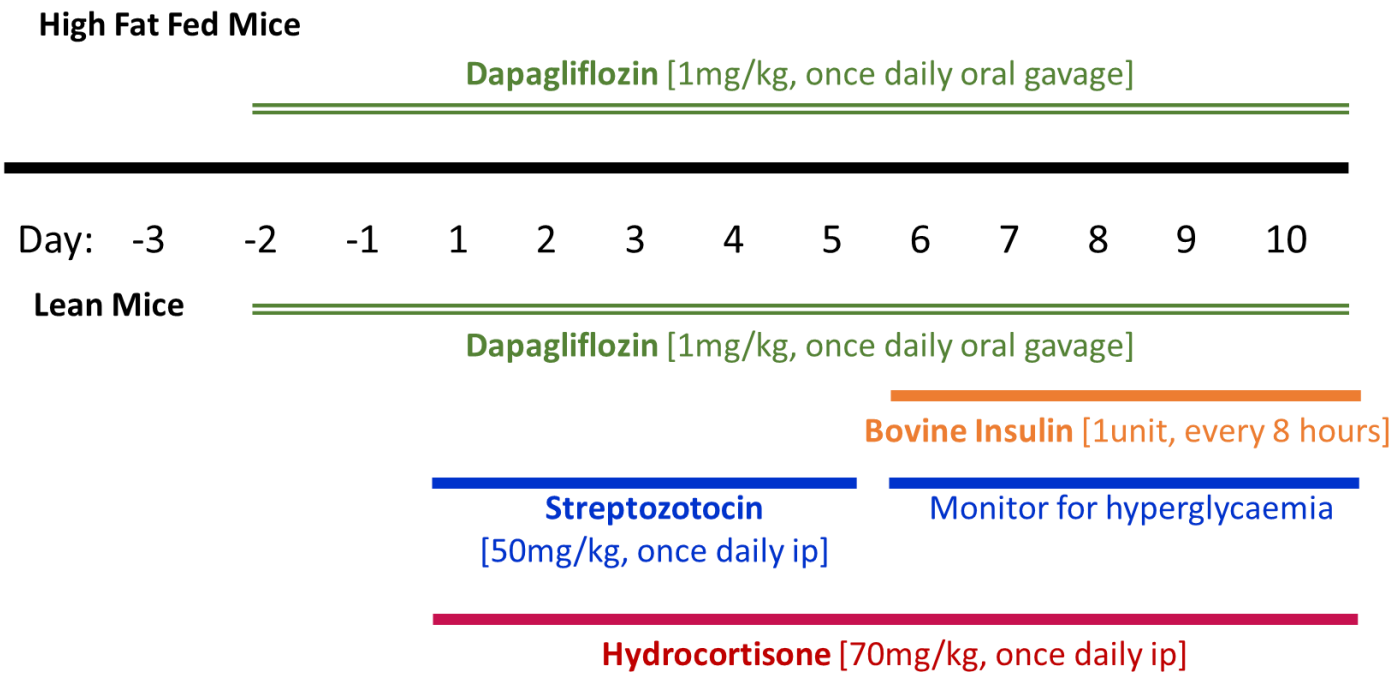

Figure 5.1 Effects of streptozotocin alone or in combination with dapagliflozin on body weight, cumulative energy intake and cumulative fluid intake

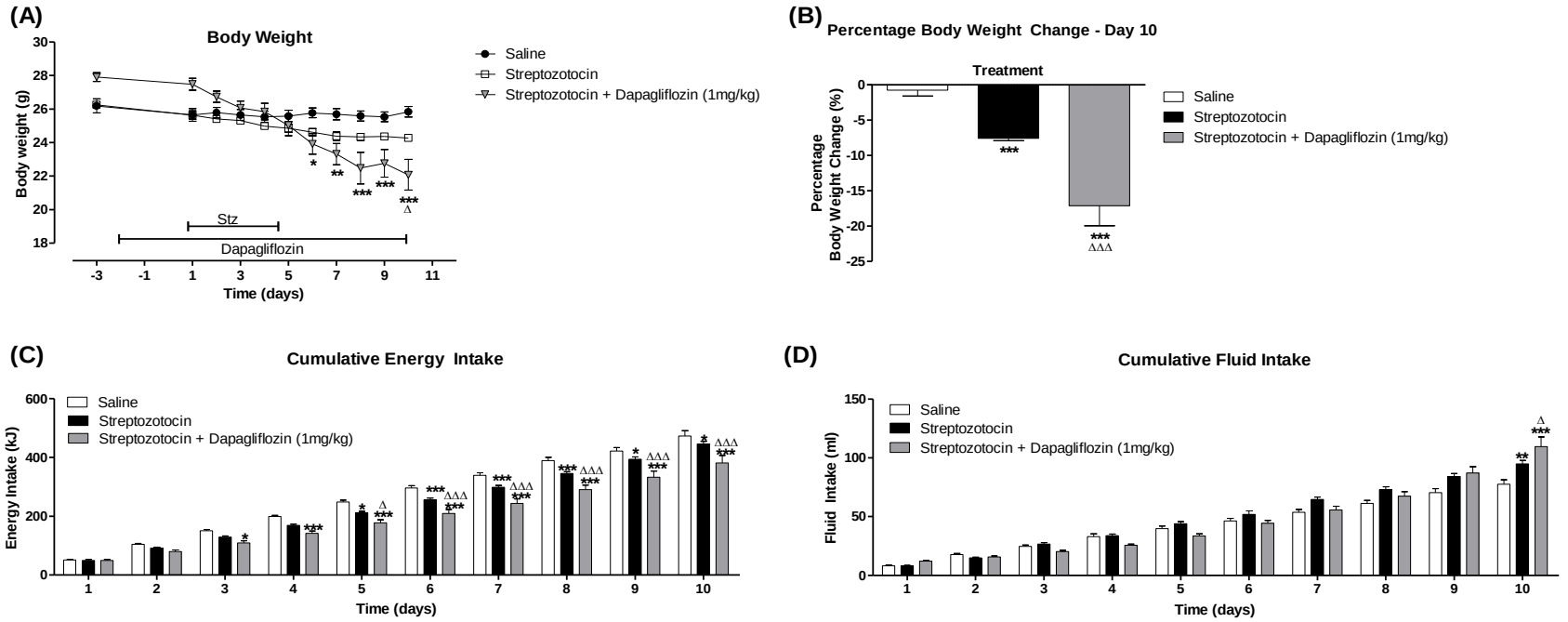

12 week old InsCre;Rosa26-eYFP C57Bl/6 mice were treated with 1mg/kg dapagliflozin for two days prior to and in conjunction with administration of streptozotocin (50mg/kg, ip, once daily), n=8 mice/group. (A) Body weight, (B) percentage body weight change, (C) cumulative energy intake and (D) cumulative fluid intake. Comparisons were made against saline (*) or against streptozotocin treated (Δ). Values were significant when $p<0.05$ */Δ, $p<0.01$ **/ΔΔ and $p<0.001$ ***/ΔΔΔ.

Figure 5.2: Effect of streptozotocin alone or in combination with dapagliflozin on blood glucose, plasma insulin, pancreatic insulin content, plasma glucagon and pancreatic glucagon content

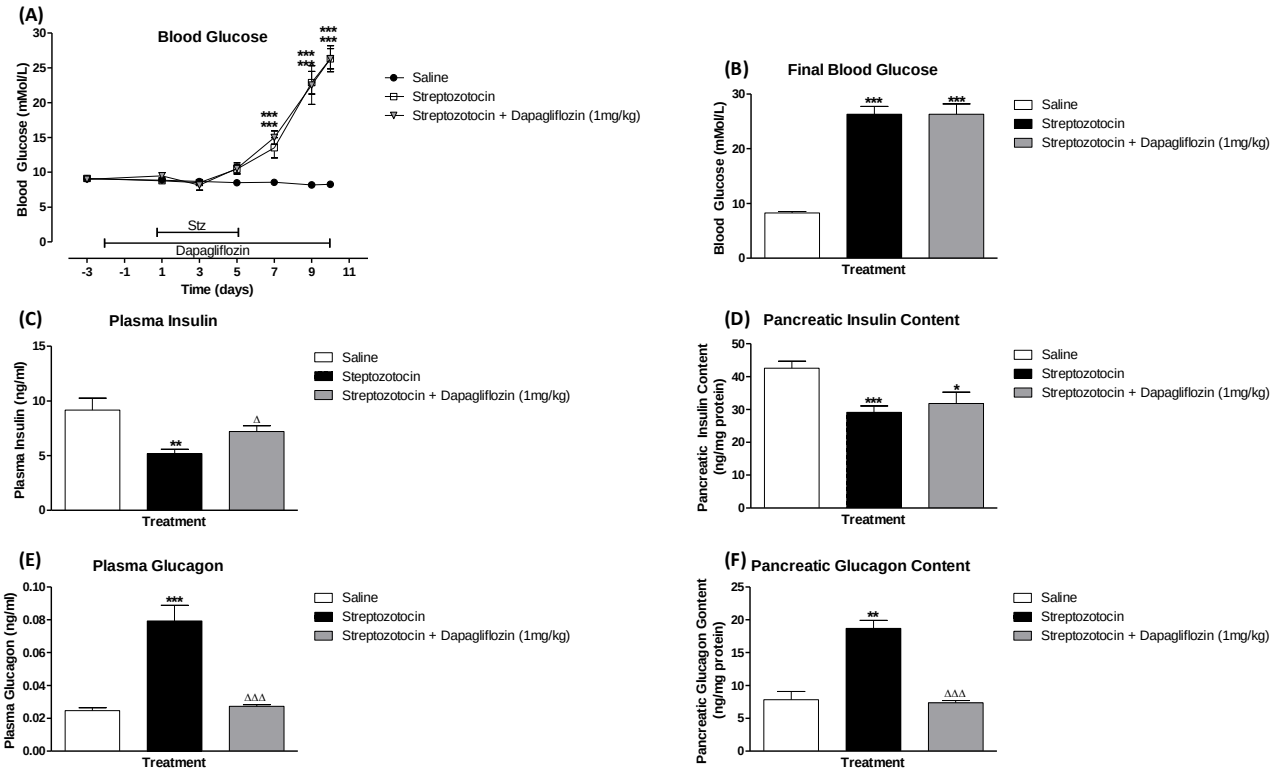

12 week old InsCre;Rosa26-eYFP C57Bl/6 mice were treated with 1mg/kg dapagliflozin for two days prior to and in conjunction with administration of streptozotocin (50mg/kg, ip, once daily), n=8 mice/group. Terminal blood was taken to assess plasma insulin and glucagon. (A) Blood glucose, (B) final blood glucose, (C) plasma insulin, (D) pancreatic insulin content, (E) plasma glucagon and (F) pancreatic glucagon content.

Comparisons were made against saline (*) or against streptozotocin treated (Δ). Values were significant when p<0.05 */Δ, p<0.01 **/ΔΔ and p<0.001 ***/ΔΔΔ.

Figure 5.3 Effects of streptozotocin alone or in combination dapagliflozin on pancreatic islet area, beta cell area, alpha cell area, islet size distribution, percentage beta cells and percentage alpha cells

(A)

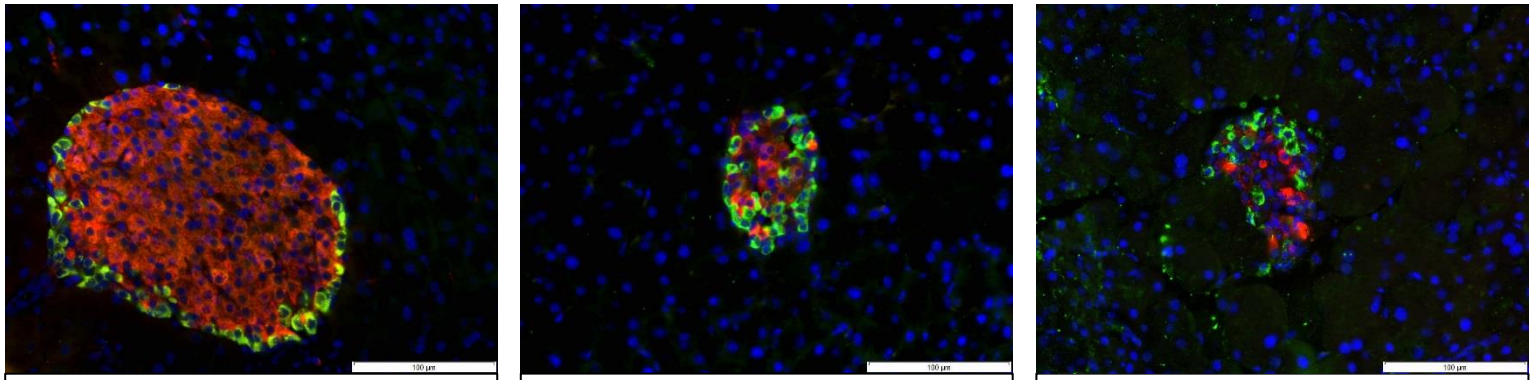

Saline	Streptozotocin	Streptozotocin + Dapagliflozin

Insulin / Glucagon / DAPI

* Legend overleaf

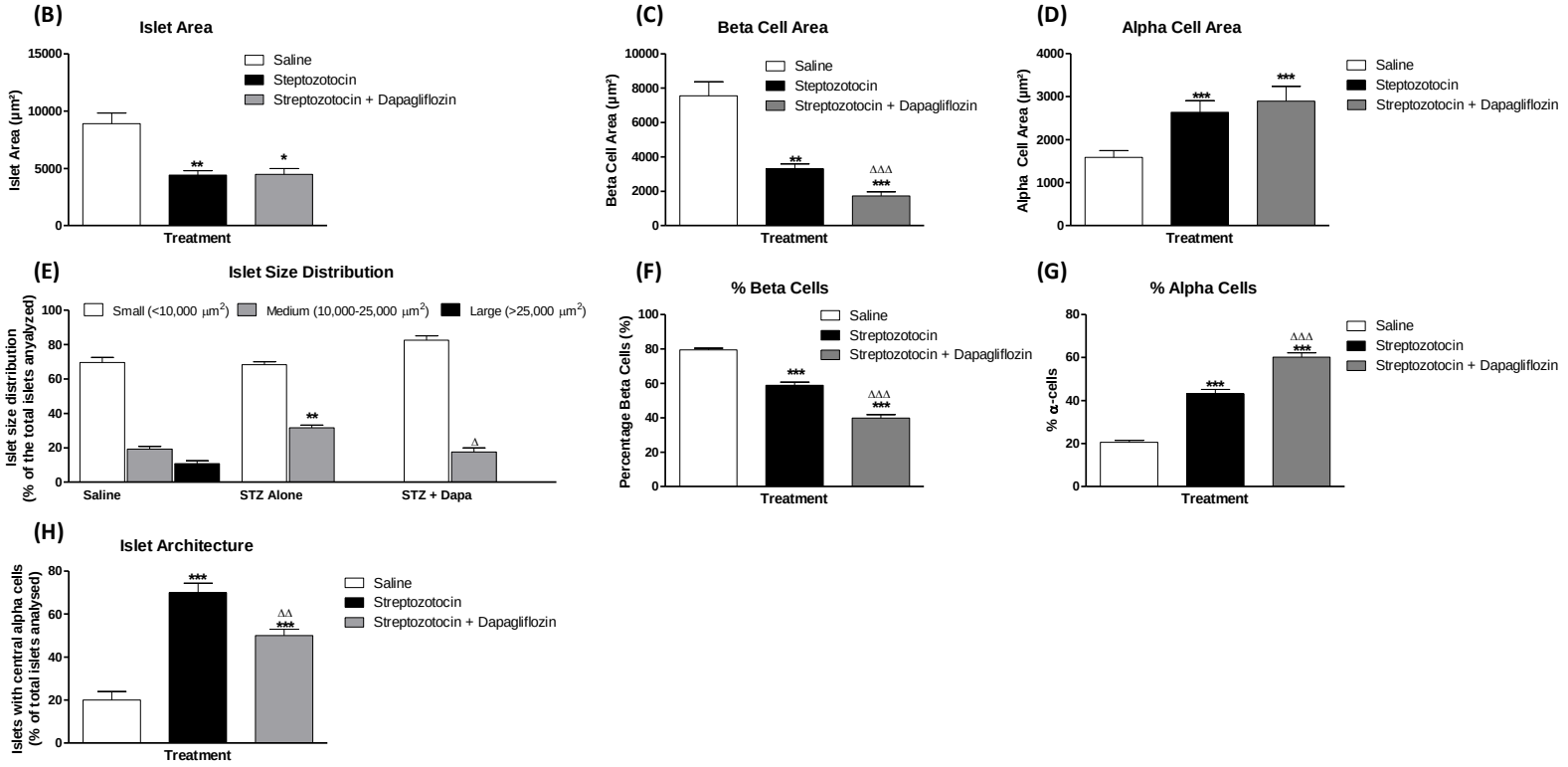

Representative images of islets from saline, streptozotocin and streptozotocin plus 1mg/kg dapagliflozin treated mice showing insulin (red), glucagon (green) and DAPI (blue). (B) islet area, (C) beta cell area, (D) alpha cell area, (E) islet size distribution, (F) percentage beta cells, (G) percentage alpha cells and (H) islet architecture. Values are mean ± SEM(n=8 mice/group). Comparisons versus saline control (*) or versus streptozotocin (Δ), significant when */Δp<0.05, **/ΔΔp<0.01 and ***/ΔΔΔp<0.001.

Figure 5.4: Effects of streptozotocin alone or in combination dapagliflozin on pancreatic islet beta-to-alpha cell transdifferentiation

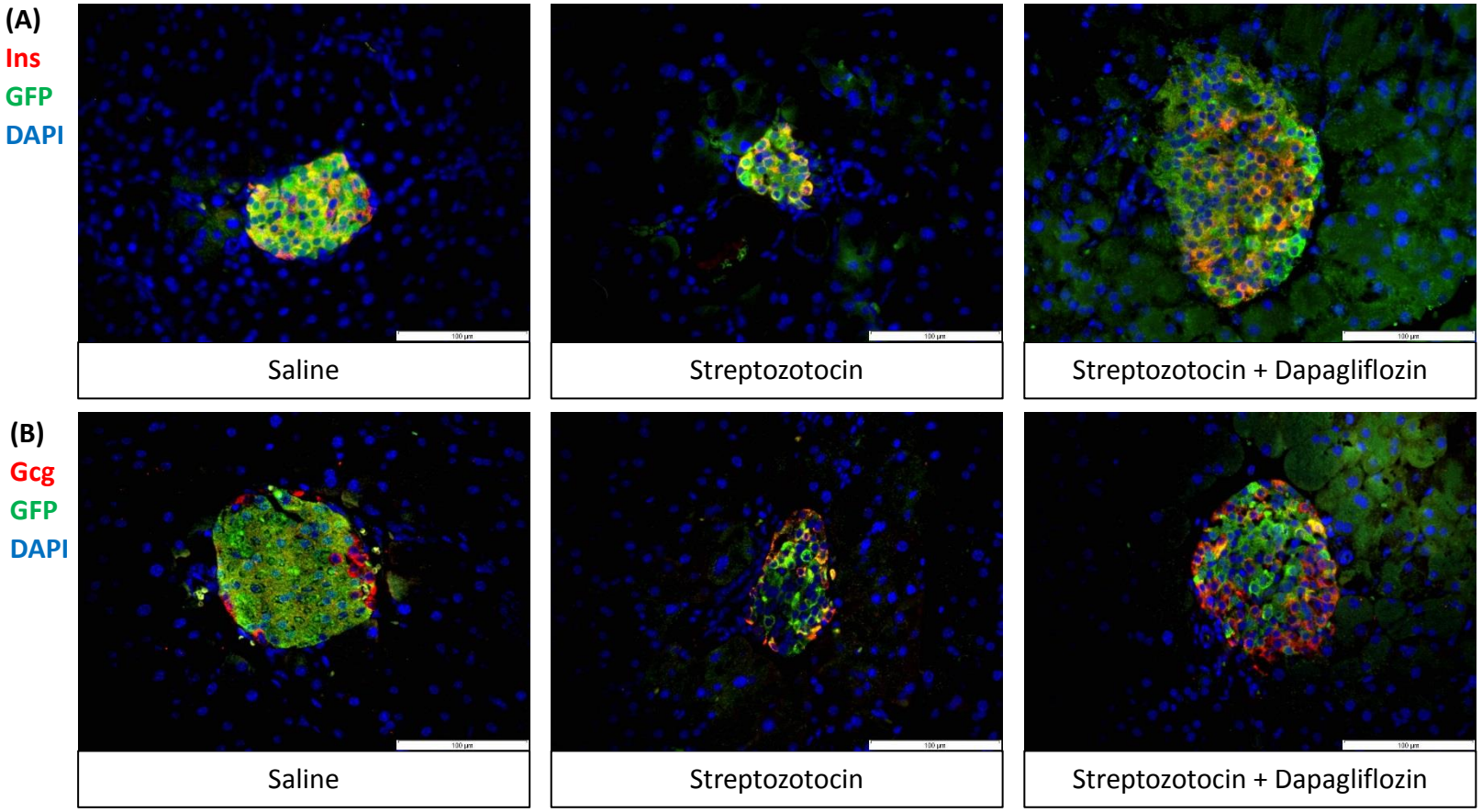

* Legend overleaf

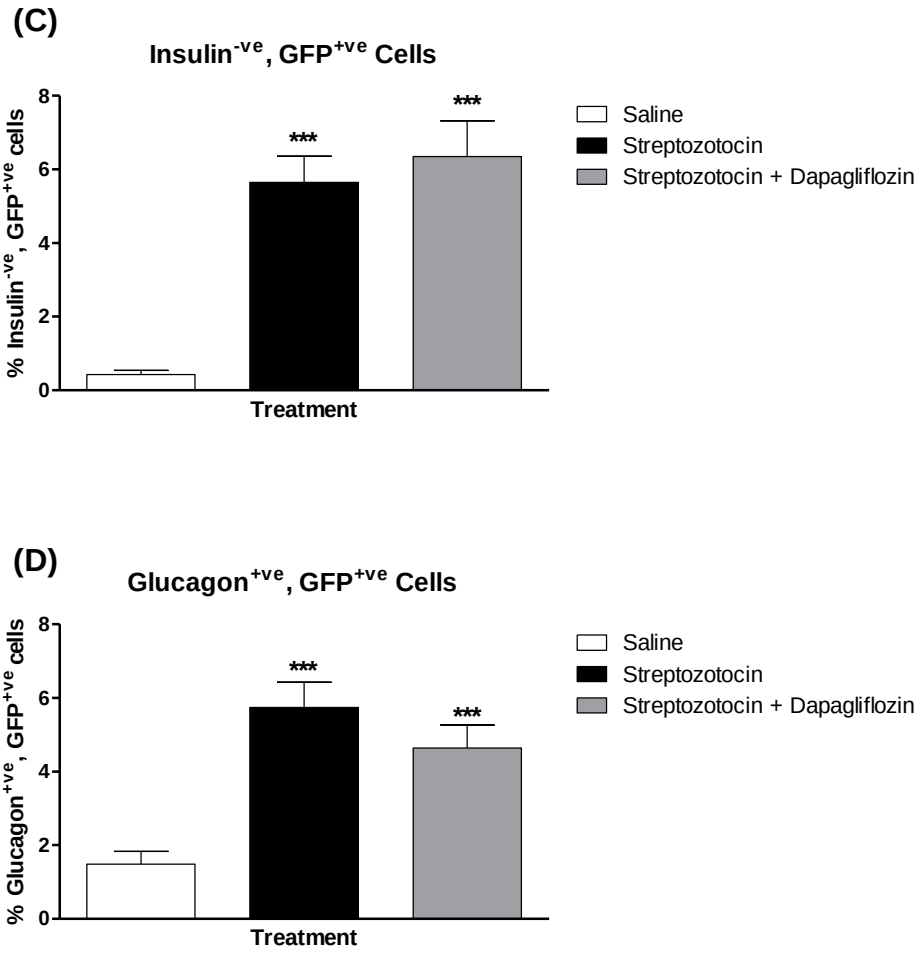

Transdifferentiation Analysis

Representative images of islets from mice treated with saline, streptozotocin and streptozotocin plus dapagliflozin (1mg/kg) stained for (A) insulin and GFP or (B) glucagon and GFP. Beta cell transdifferentiation determined by populations of insulin negative, GFP positive cells (C) and glucagon positive, GFP positive cells (D) using double immunofluorescence staining showing insulin/glucagon (red) and GFP (green).

Values are mean ± SEM (n=8 mice/group). Comparisons versus saline control (*) or versus streptozotocin (Δ), significant when */Δp<0.05, **/ΔΔp<0.01 and ***p<0.001.

Figure 5.5: Effects of streptozotocin alone or in combination dapagliflozin on beta cell and alpha cell apoptosis

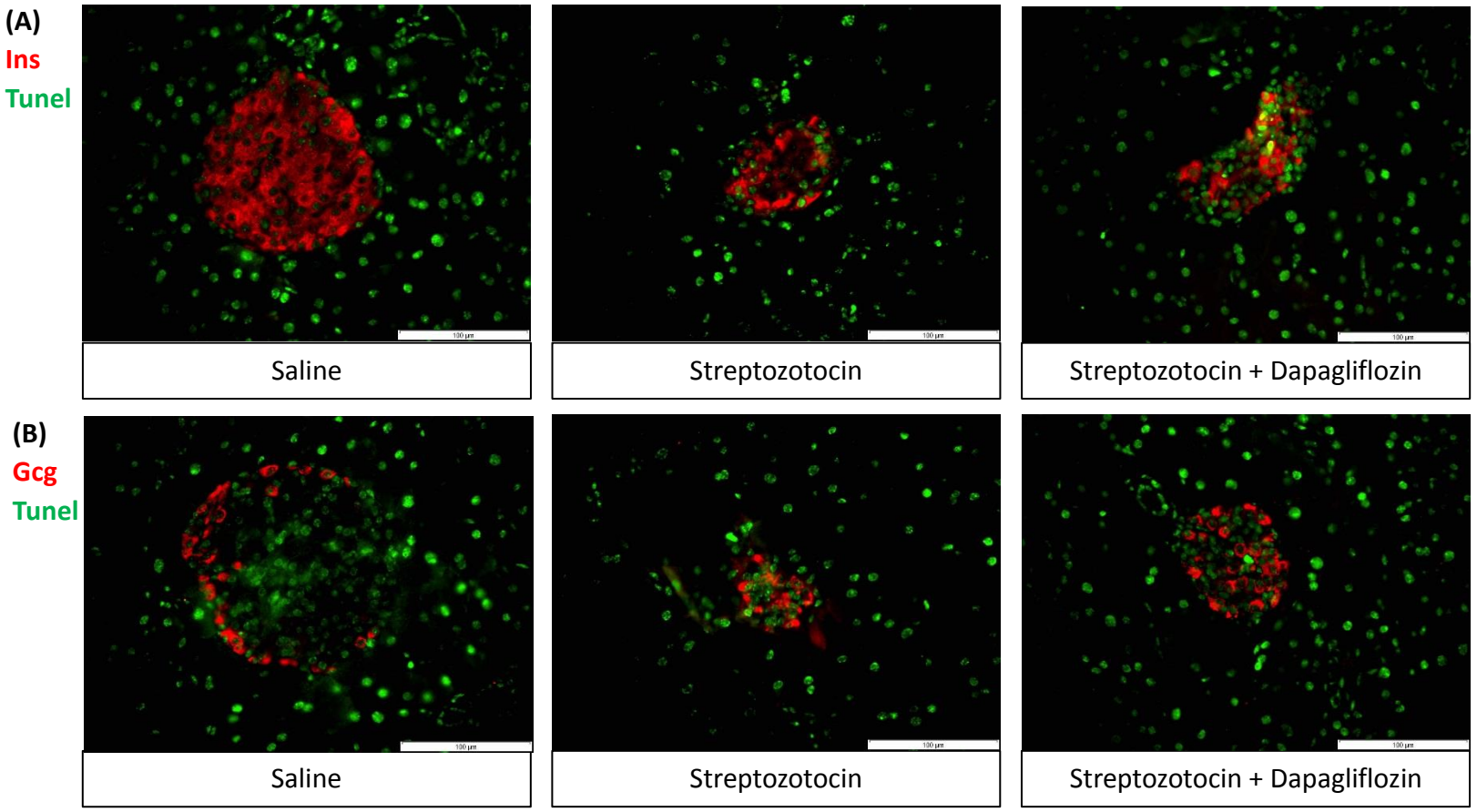

* Legend overleaf

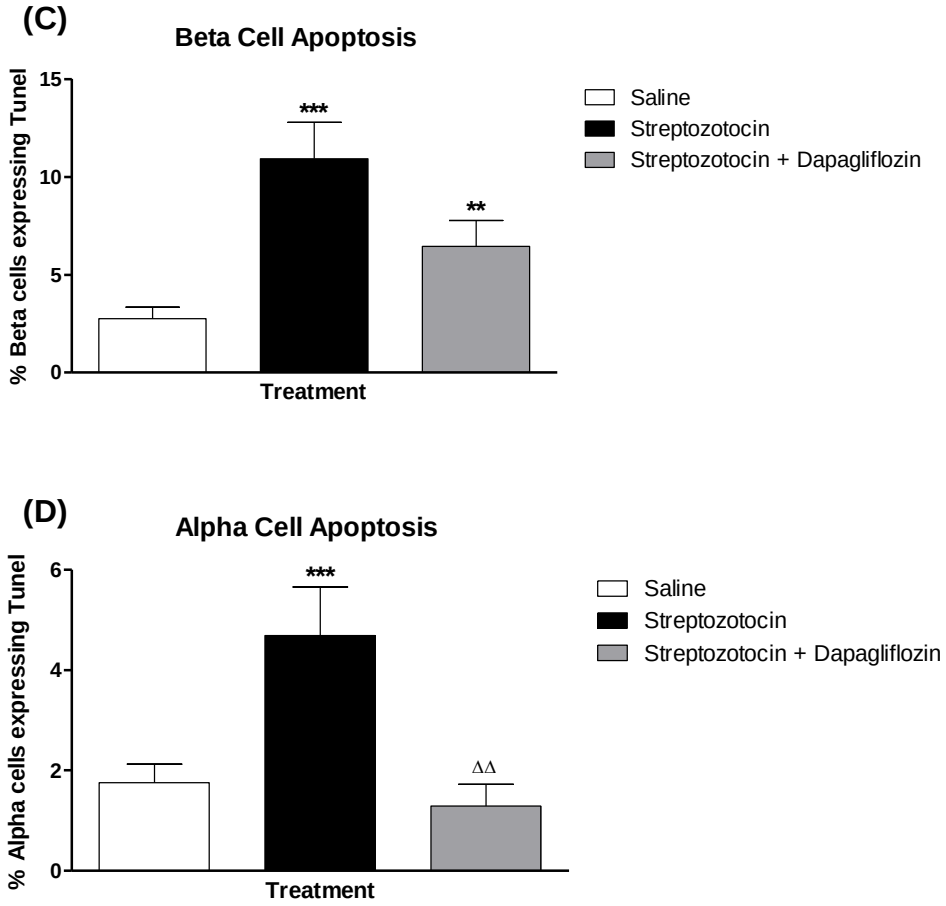

Apoptosis Analysis

Representative images of islets from mice treated with saline, streptozotocin and streptozotocin plus dapagliflozin (1mg/kg) stained for (A) insulin and TUNEL or (B) glucagon and TUNEL. Beta cell apoptosis and alpha cell apoptosis determined by populations of insulin positive, TUNEL positive (C) and glucagon positive, TUNEL positive (D) cells respectively by double immunofluorescence staining.

Values are mean ± SEM (n=8 mice/group). Comparisons versus saline control (*) or versus streptozotocin (Δ), significant when */Δp<0.05, **/ΔΔp<0.01 and ***p<0.001.

Figure 5.6: Effects of streptozotocin alone or in combination dapagliflozin on beta cell and alpha cell proliferation

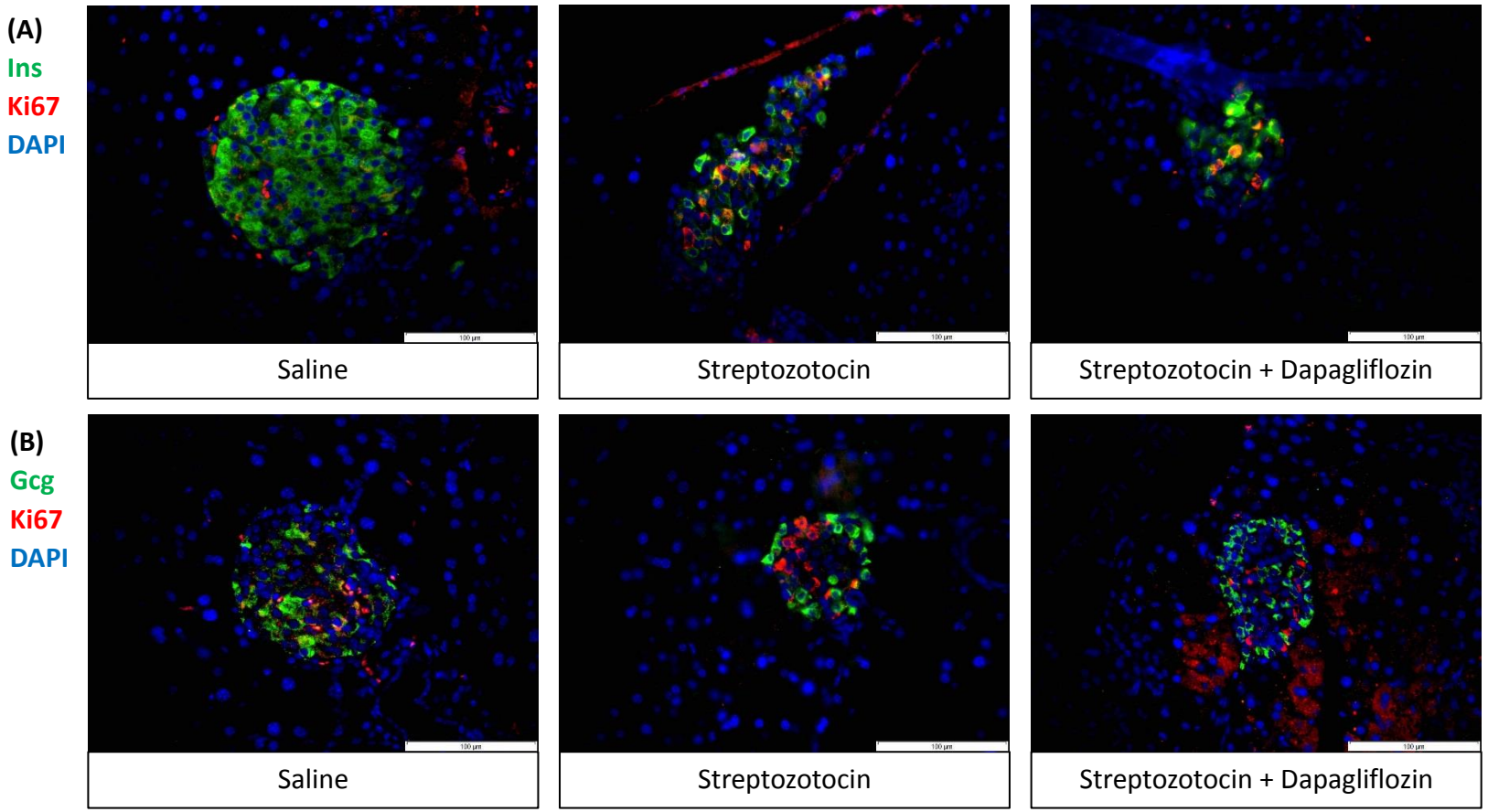

* Legend overleaf

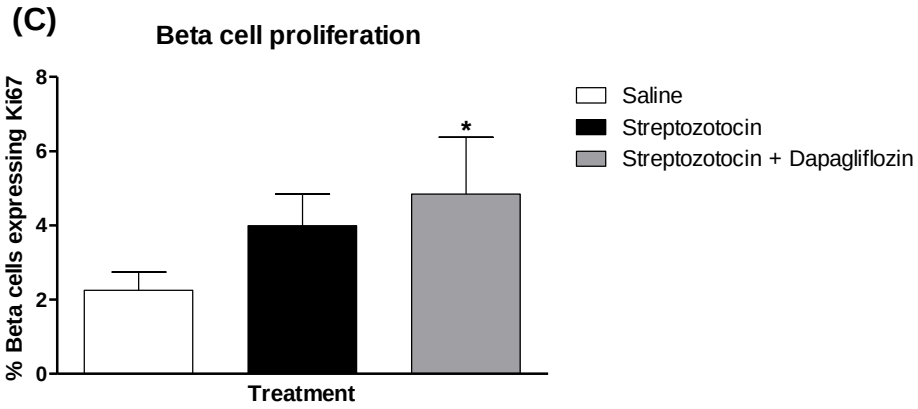

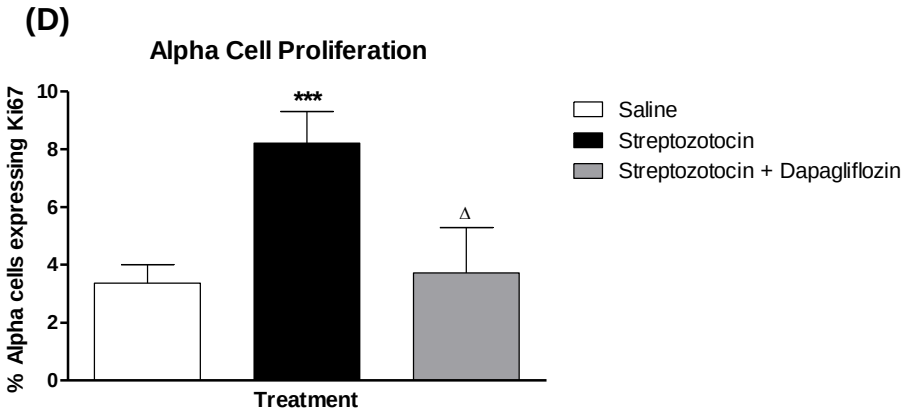

Proliferation Analysis

Representative images of islets from mice treated with saline, streptozotocin and streptozotocin plus dapagliflozin (1mg/kg) stained for (A) insulin and ki-67 or (B) glucagon and ki-67. Beta cell and alpha cell proliferation determined by populations of (C) insulin positive, ki-67 positive cell and (D) glucagon positive, ki-67 positive cells respectively.

Values are mean ± SEM (n=8 mice/group). Comparisons versus saline control (*) or versus streptozotocin (Δ), significant when */Δp<0.05, **/ΔΔp<0.01 and ***p<0.001.

Figure 5.7 Effects of streptozotocin alone or in combination dapagliflozin on beta cell Pdx1 expression

(A)

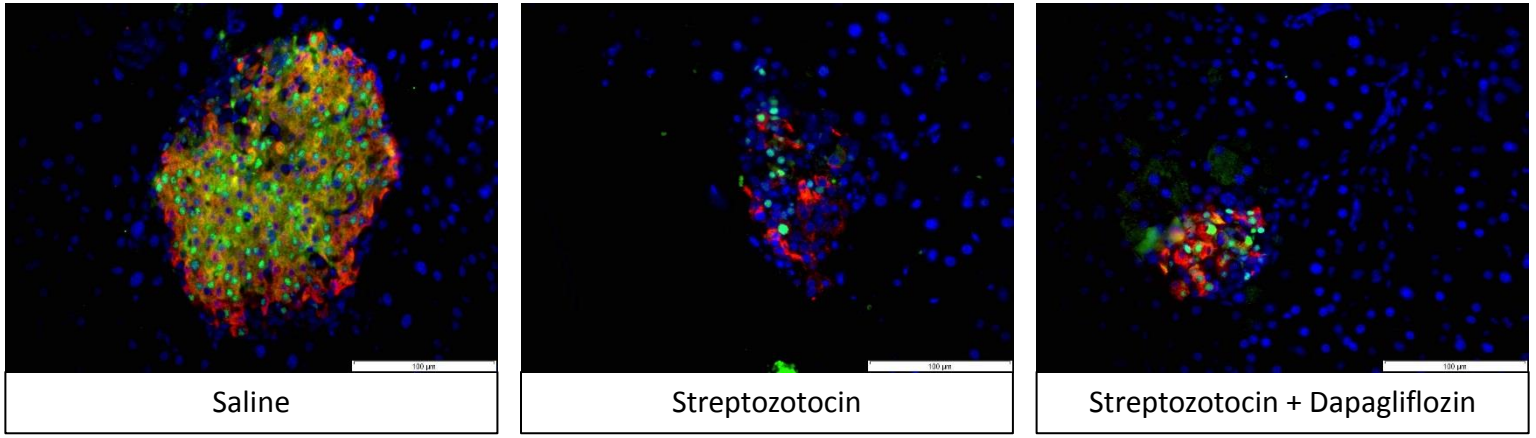

* Legend overleaf

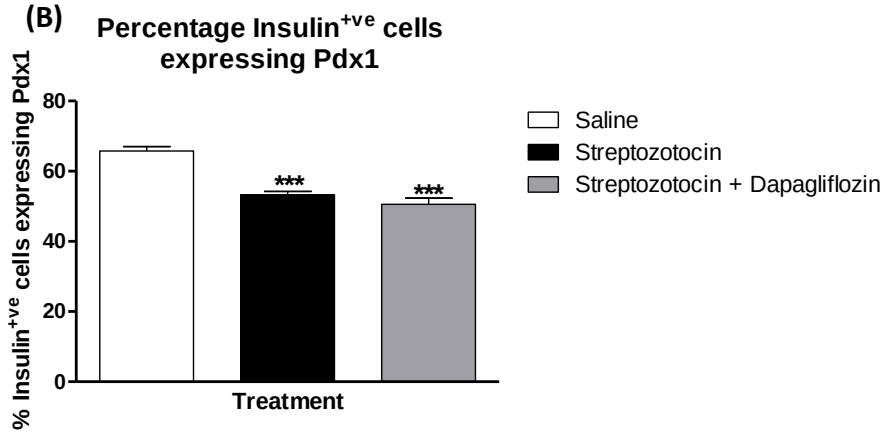

Pdx1 Expression Analysis

(A) Representative images of islets from mice treated with saline, streptozotocin and streptozotocin plus dapagliflozin (1mg/kg) on Pdx1 expression (B). Determined by histological analysis of insulin/Pdx1 double immunofluorescence staining showing insulin (red), Pdx1 (green) and DAPI (blue).

Values are mean ± SEM (n=8 mice/group). Comparisons versus saline control (*) or versus streptozotocin (Δ), significant when */Δp<0.05, **/ΔΔp<0.01 and ***p<0.001.

Figure 5.8: Effects of high fat feeding alone or in combination with dapagliflozin on body weight, cumulative energy intake and cumulative fluid intake

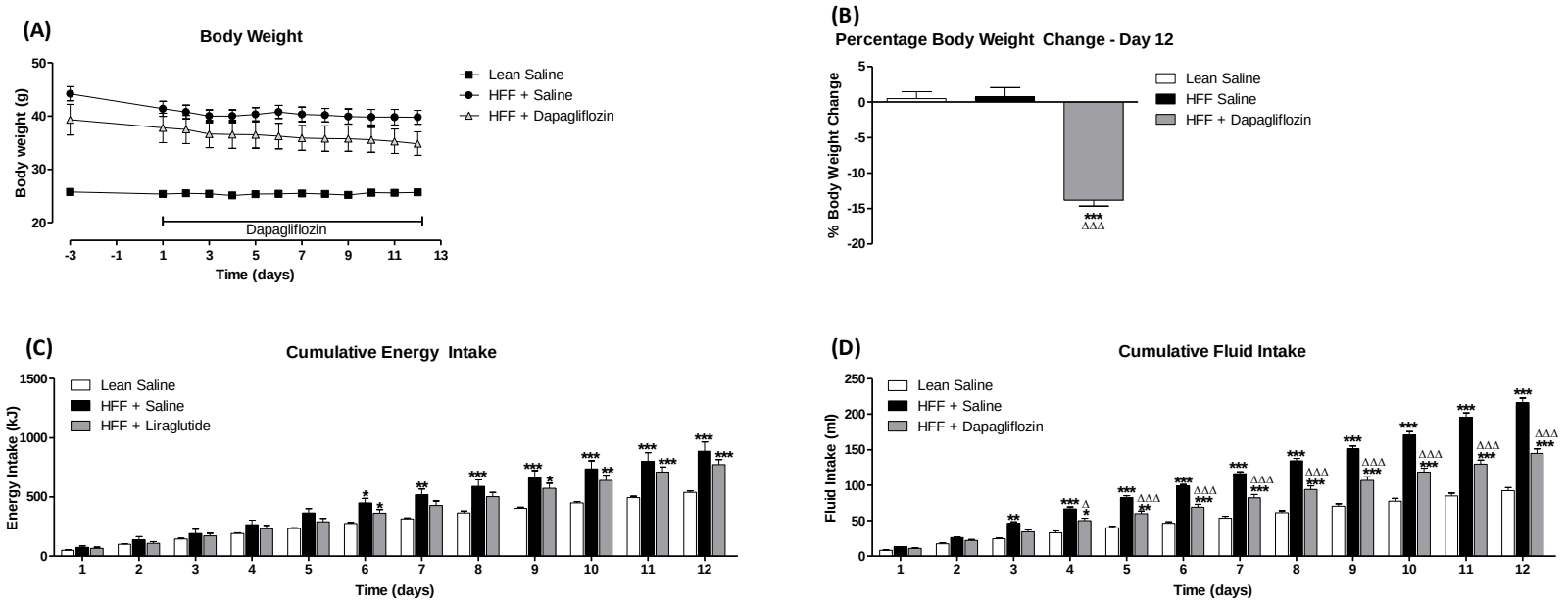

15 week old InsCre;Rosa26-eYFP C57Bl/6 mice kept on a high fat diet for 2 months prior were treatment with dapagliflozin (1mg/kg) by daily oral gavage, n=6-8 mice/group. (A) body weight, (B) percentage body weight change, (C) cumulative energy intake and (D) cumulative fluid intake.

Comparisons were made against lean saline (*) or against high fat fed (Δ). Values mean ± SEM, significant when $p<0.05$ */Δ, $p<0.01$ **/ΔΔ and $p<0.001$ ***/ΔΔΔ.

Figure 5.9: Effects of high fat feeding alone or in combination with dapagliflozin on blood glucose, plasma insulin, pancreatic insulin content, plasma glucagon, pancreatic glucagon content, GTT and AUC

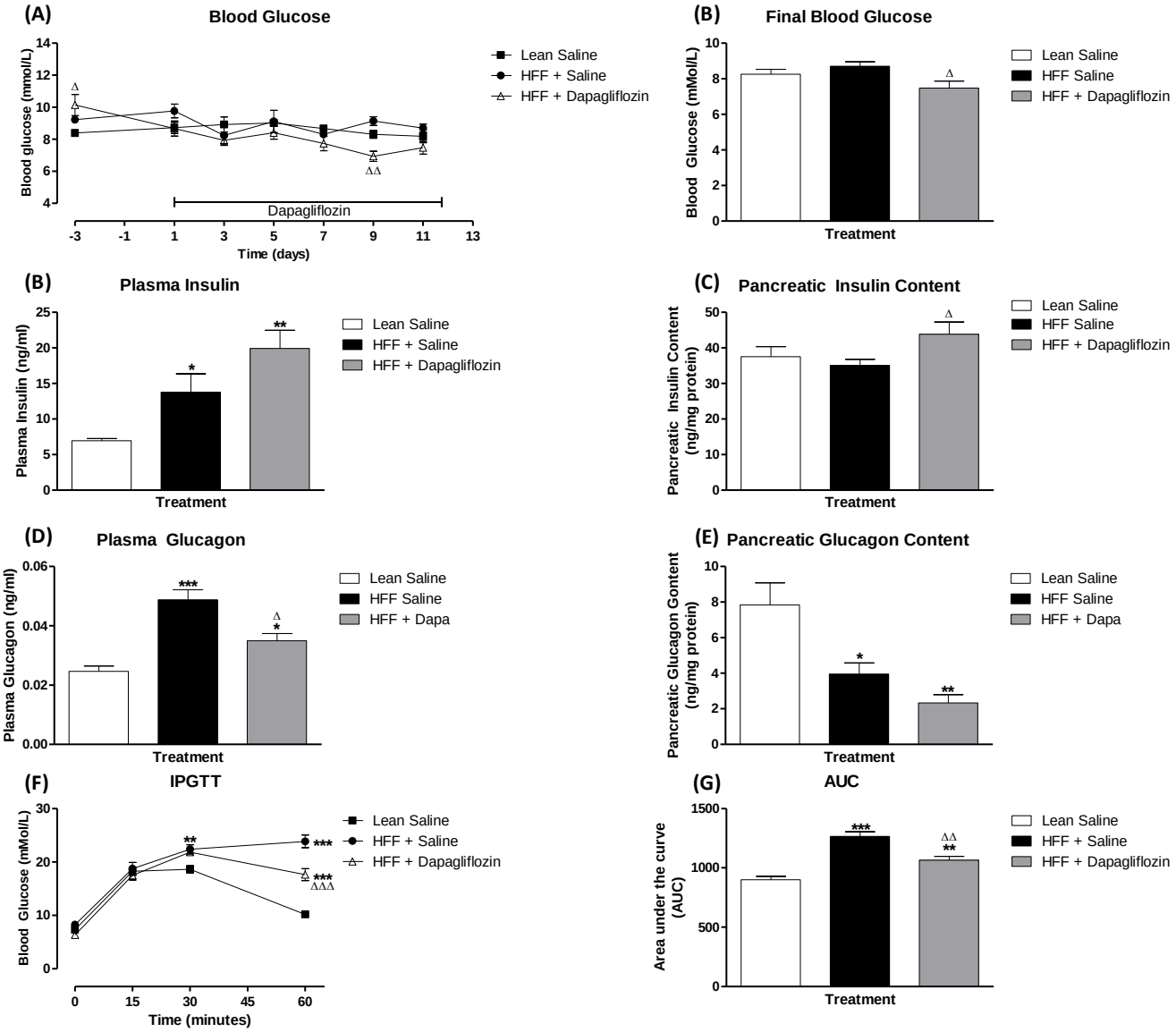

15 week old InsCre;Rosa26-eYFP C57Bl/6 mice kept on a high fat diet for 2 months prior were treatment dapagliflozin (1mg/kg) by daily oral gavage, n=6-8 mice/group. (A) Blood glucose, (B) final blood glucose, (C) plasma insulin, (D) pancreatic insulin, (E) plasma glucagon, (F) pancreatic glucagon, G) ip glucose tolerance test and (F) AUC. Comparisons were made against lean saline (*) or against high fat fed (Δ). Values mean ± SEM, significant when p<0.05 */Δ, p<0.01 **/ΔΔ and p<0.001 ***/ΔΔΔ.

Figure 5.10: Effects of high fat feeding alone or in combination dapagliflozin on pancreatic islet area, beta cell area, alpha cell area, islet size distribution, percentage beta cells and percentage alpha cells

(A)

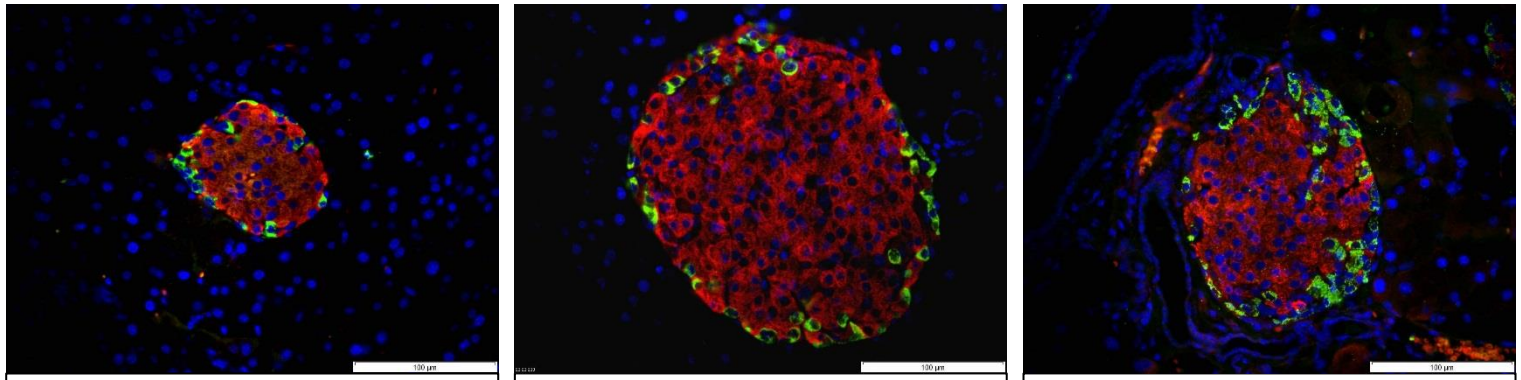

Lean Saline	High-fat Fed Saline	High-fat Fed + Dapagliflozin

Insulin / Glucagon / DAPI

* Legend overleaf

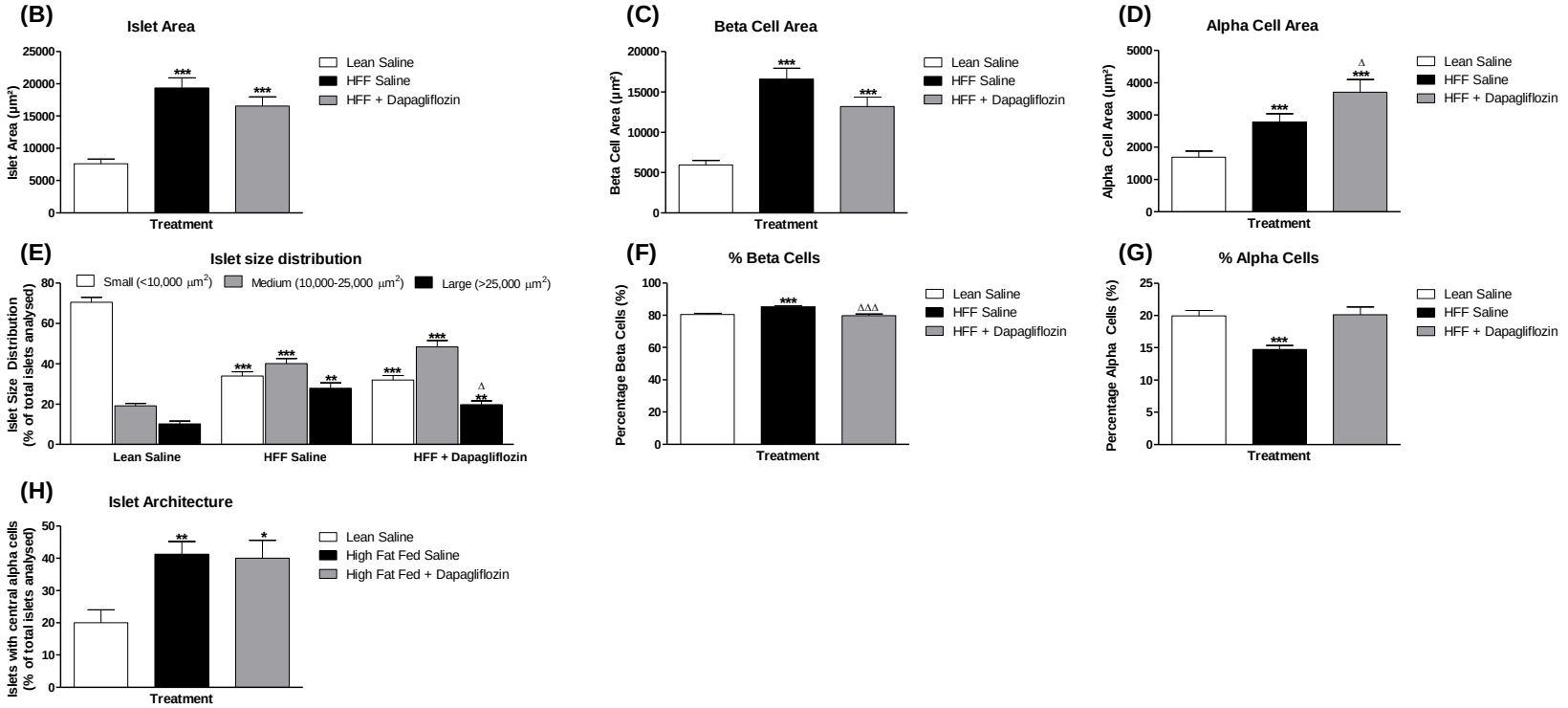

Representative images of islets from (A) lean saline, high fat fed saline and high fat fed plus dapagliflozin (1mg/kg) mice showing insulin (red), glucagon (green) and DAPI (blue). (B) islet area, (C) beta cell area, (D) alpha cell area, (E) islet size distribution, (F) percentage beta cells, (G) percentage alpha cells and (H) islet architecture. Values are mean ± SEM (n=8 mice/group). Comparisons versus saline control (*) or versus high fat fed (Δ), significant when */Δp<0.05, **/ΔΔp<0.01 and ***/ΔΔΔp<0.001.

Figure 5.11: Effects of high fat feeding alone or in combination with dapagliflozin on pancreatic islet beta-to-alpha cell transdifferentiation

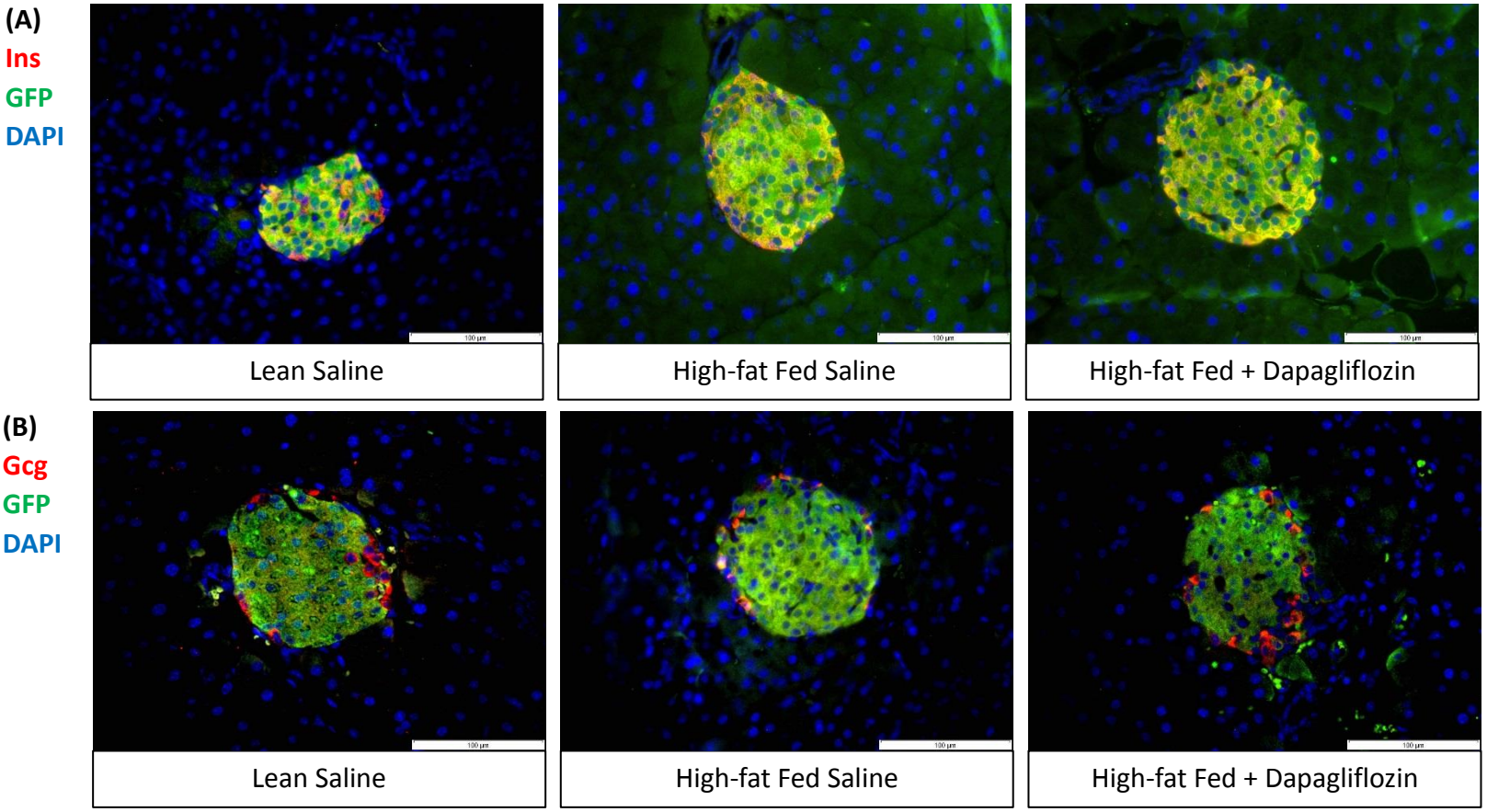

* Legend overleaf

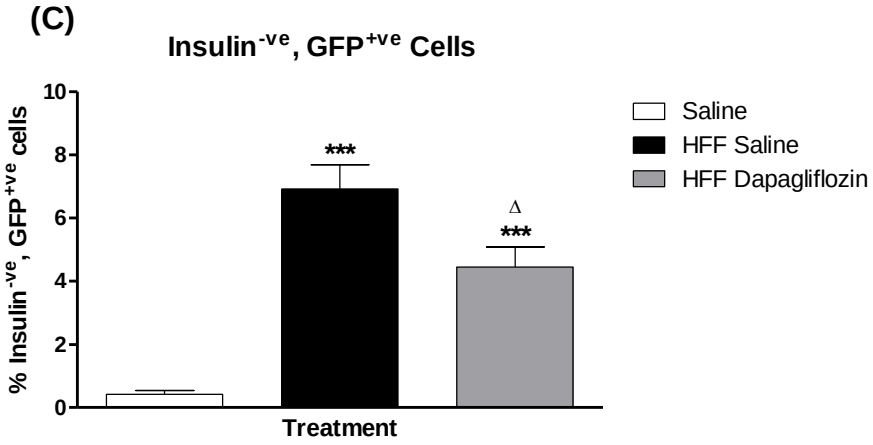

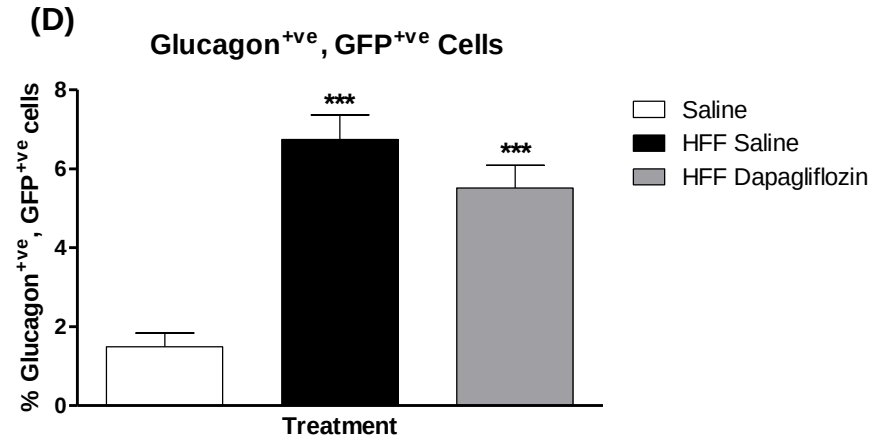

Transdifferentiation Analysis

Representative images of islets from lean saline, high fat fed saline and high fat fed plus dapagliflozin (1mg/kg) treated mice stained for (A) insulin and GFP or (B) glucagon and GFP. Beta cell transdifferentiation determined by populations of insulin negative, GFP positive cells (C) and glucagon positive, GFP positive cells (D) using double immunofluorescence staining show insulin/glucagon (red), GFP (green). Values are mean ± SEM (n=8 mice/group). Comparisons versus lean saline control (*) or versus high fat fed saline (Δ), significant when */Δp<0.05, **/ΔΔp<0.01 and ***p<0.001.

Figure 5.12: Effects of high fat feeding alone or in combination with dapagliflozin on pancreatic islet beta cell and alpha cell apoptosis

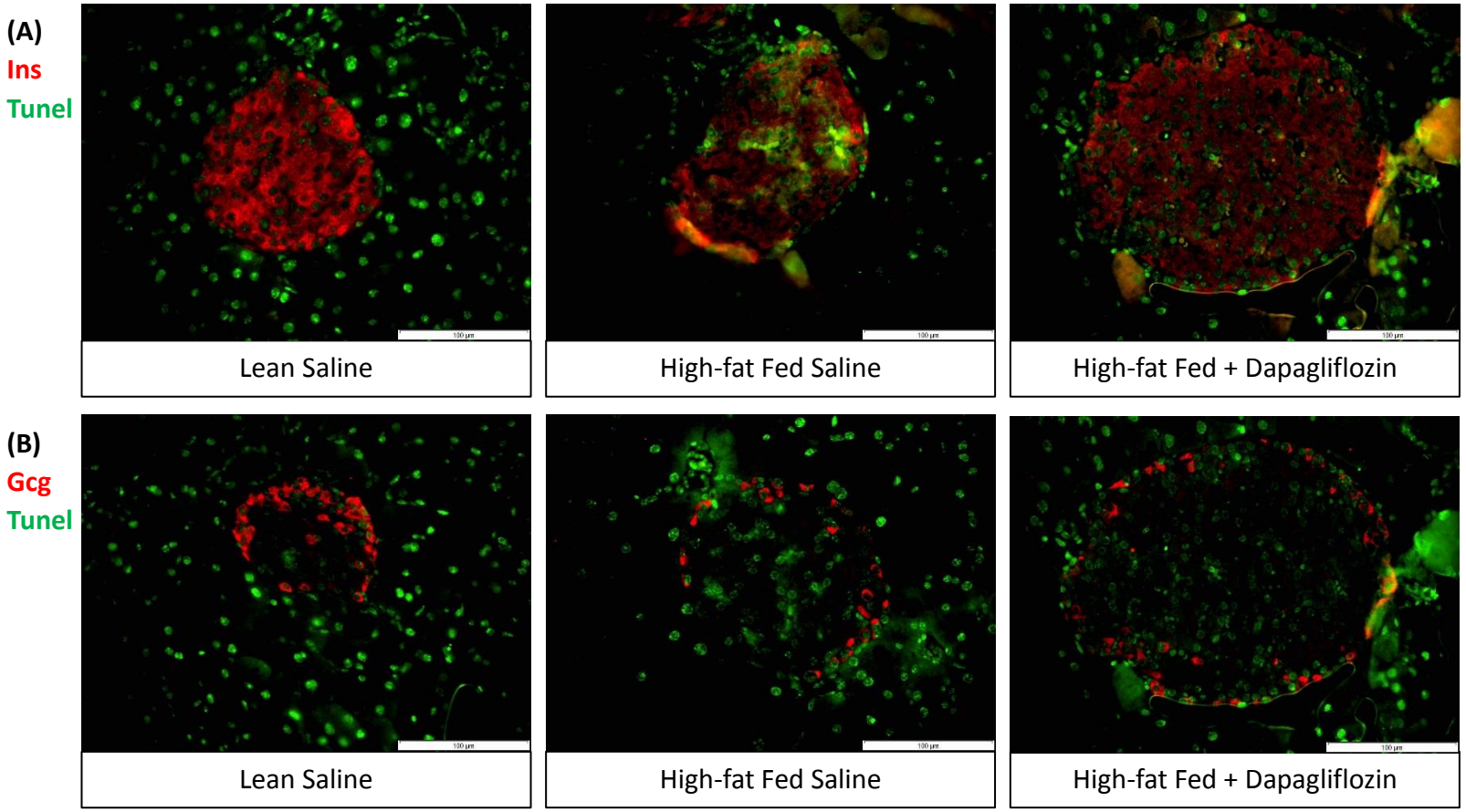

* Legend overleaf

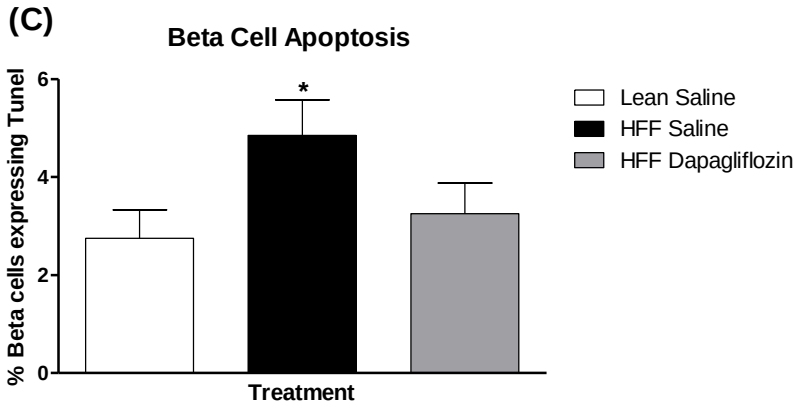

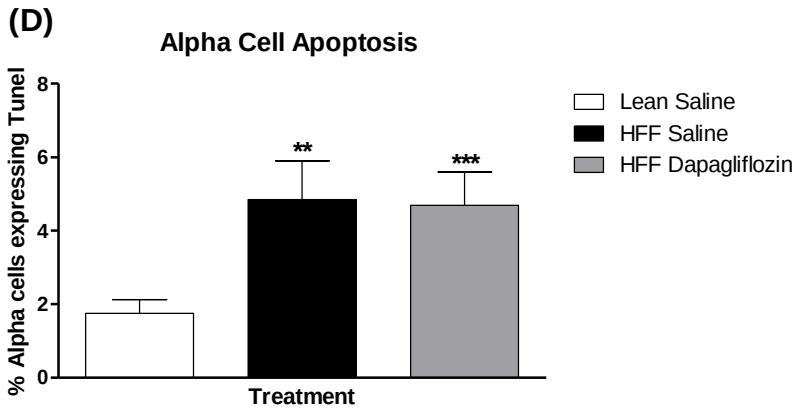

Apoptosis Analysis

Representative images of islets from lean saline, high fat fed saline and high fat fed plus dapagliflozin (1mg/kg) stained for (A) insulin and TUNEL or (B) glucagon and TUNEL. Beta cell apoptosis and alpha cell apoptosis were quantified by populations of insulin positive, TUNEL positive (C) and glucagon positive, TUNEL positive cells (D) respectively by double immunofluorescence staining.

Values are mean ± SEM (n=8 mice/group). Comparisons versus saline control (*) or versus high fat fed (Δ), significant when */Δp<0.05, **/ΔΔp<0.01 and ***p<0.001.

Figure 5.13: Effects of high fat feeding alone or in combination with dapagliflozin on pancreatic islet beta cell and alpha cell proliferation

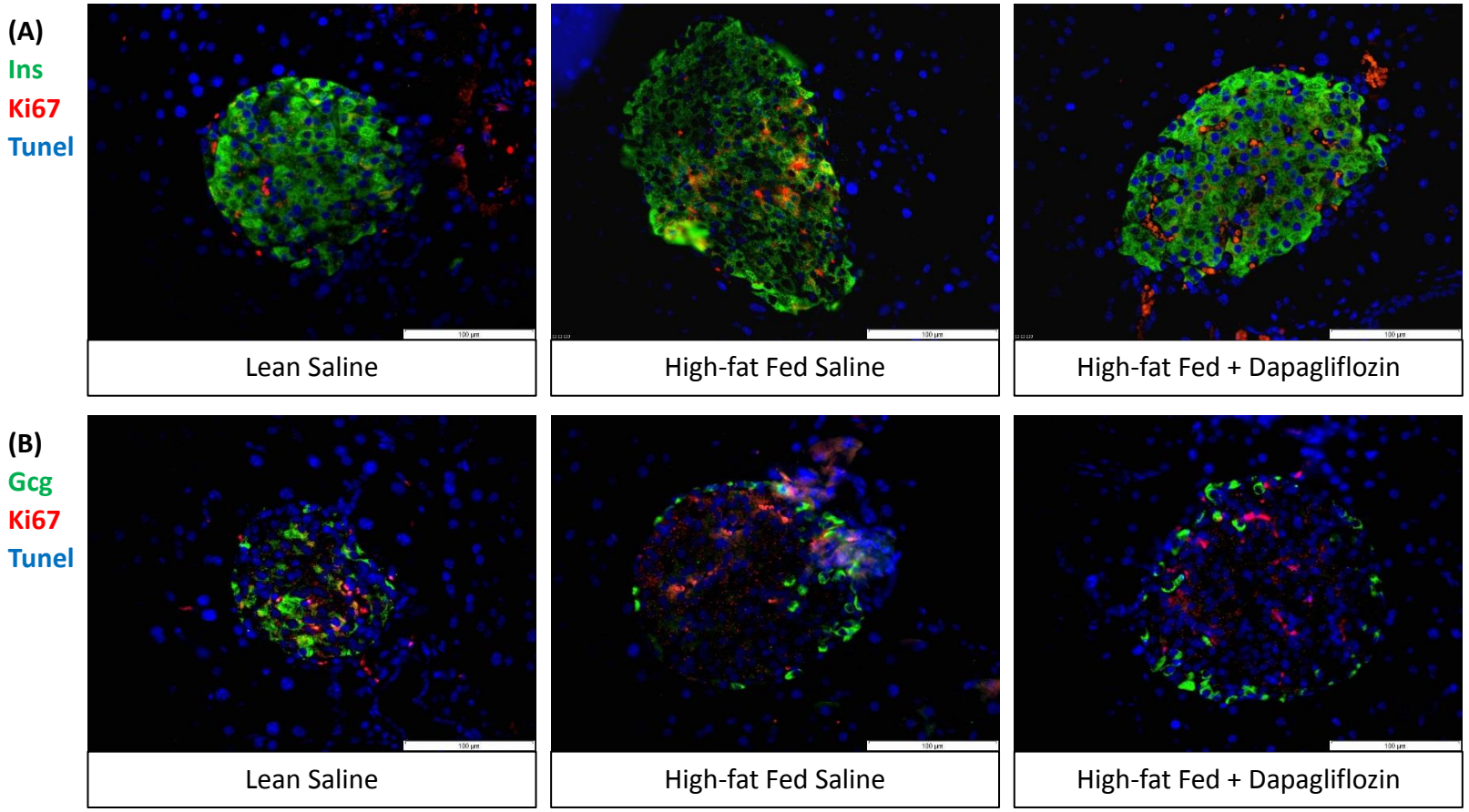

* Legend overleaf

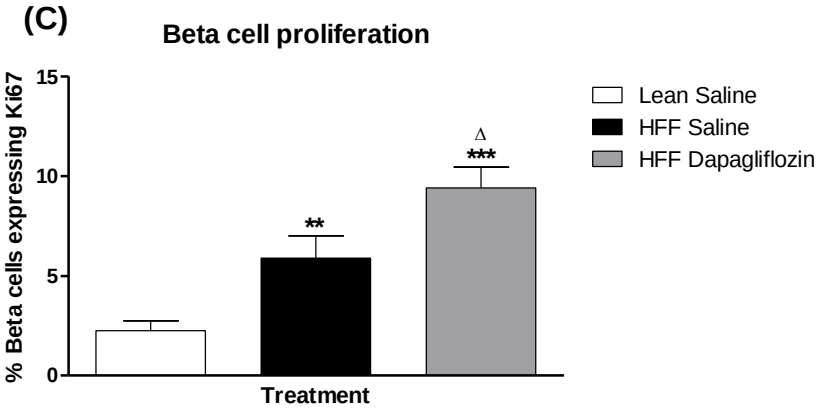

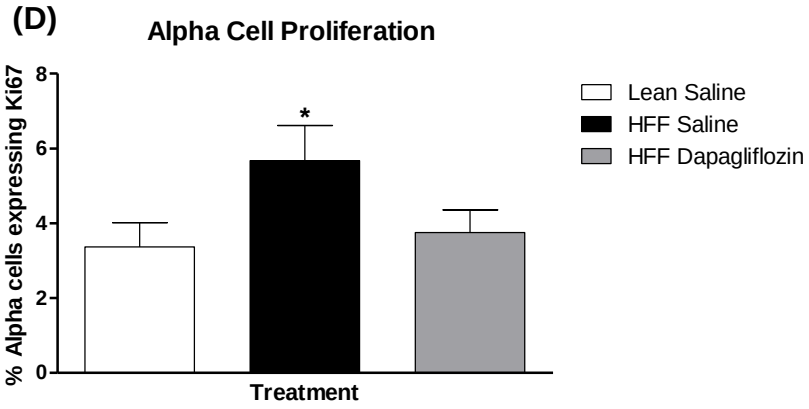

Proliferation Analysis

Representative images of islets lean saline, high fat fed saline and high fat fed plus dapagliflozin (1mg/kg) stained for (A) insulin and ki-67 or (B) glucagon and ki-67. Beta cell and alpha cell proliferation determined by populations of (C) insulin positive, ki-67 positive cells or (D) glucagon positive, ki-67 positive cells respectively.

Values are mean ± SEM (n=8 mice/group). Comparisons versus saline control (*) or versus high fat fed (Δ), significant when */Δp<0.05, **/ΔΔp<0.01 and ***p<0.001.

Figure 5.14: Effects of high fat feeding alone or in combination with dapagliflozin on pancreatic islet beta cell Pdx1 expression

(A)

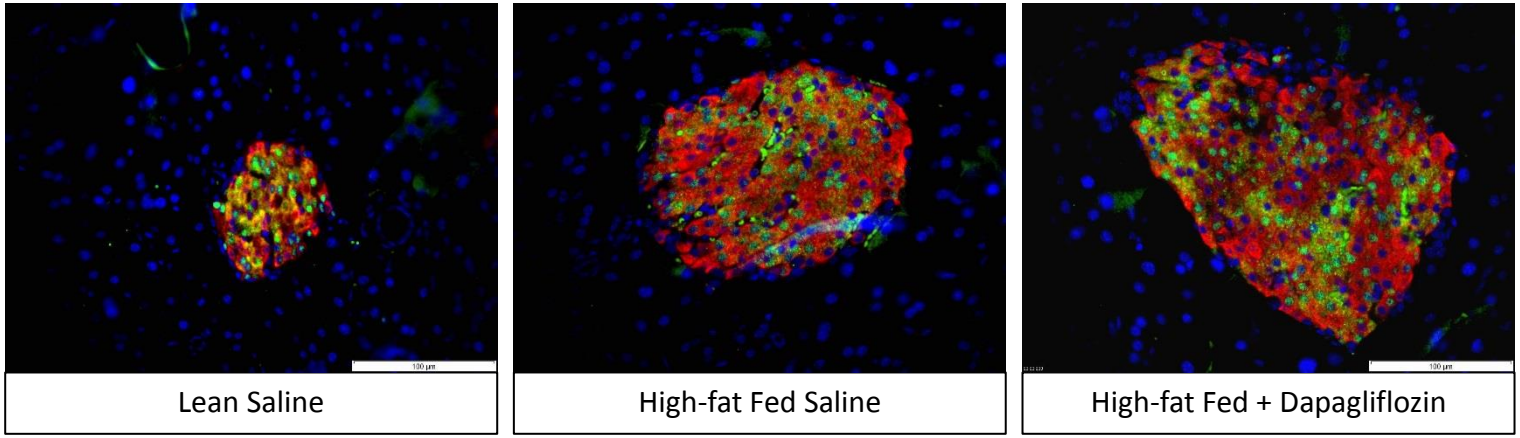

* Legend overleaf

(B)

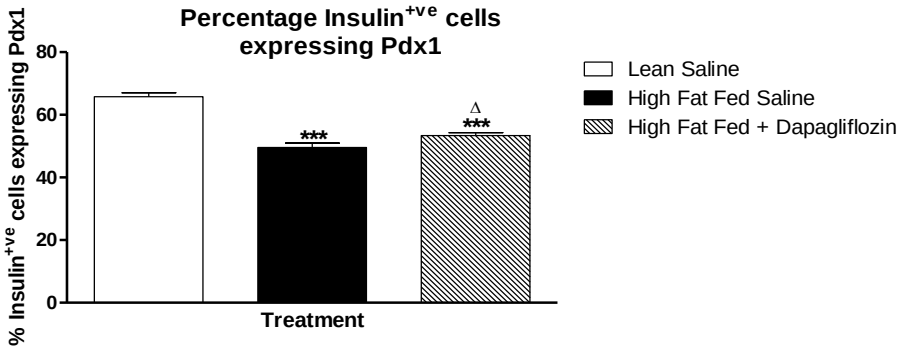

Pdx1 Expression Analysis

(A) Representative images of islets from mice treated with saline, high fat fed saline and high fat fed plus dapagliflozin (1mg/kg) on Pdx1 expression (B). Determined by histological analysis of insulin/Pdx1 double immunofluorescence staining showing insulin (red), Pdx1 (green) and DAPI (blue).

Values are mean ± SEM (n=8 mice/group). Comparisons versus saline control (*) or versus high fat fed (Δ), significant when */Δp<0.05, **/ΔΔp<0.01 and ***p<0.001.

Figure 5.15: Effects of hydrocortisone alone or in combination with dapagliflozin on body weight, cumulative energy intake and cumulative fluid intake

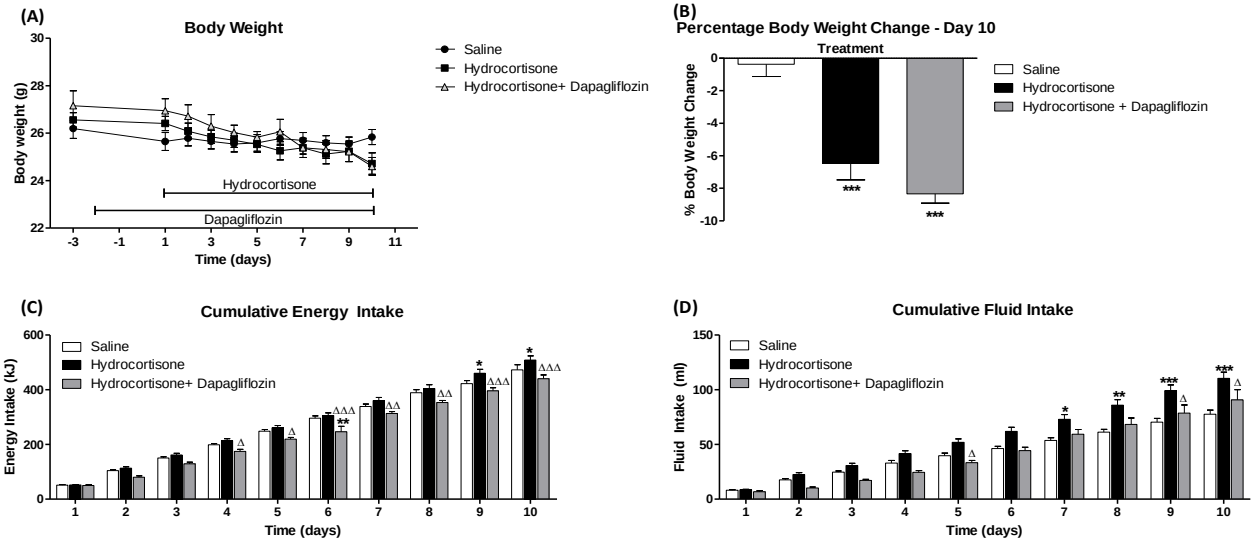

12 week old InsCre;Rosa26-eYFP C57Bl/6 mice were treated with dapagliflozin for two days prior to and in conjunction with administration of hydrocortisone (70mg/kg, ip, once daily), n=8 mice/group. (A) Body weight, (B) percentage body weight change, (C) cumulative energy intake and (D) cumulative fluid intake. Comparisons were made against saline (*) or against hydrocortisone treated (Δ). Values were significant when $p<0.05$ */Δ, $p<0.01$ **/ΔΔ and $p<0.001$ ***/ΔΔΔ.

Figure 5.16: Effect of hydrocortisone alone or in combination with dapagliflozin on blood glucose, plasma insulin, pancreatic insulin content, plasma glucagon and pancreatic glucagon content

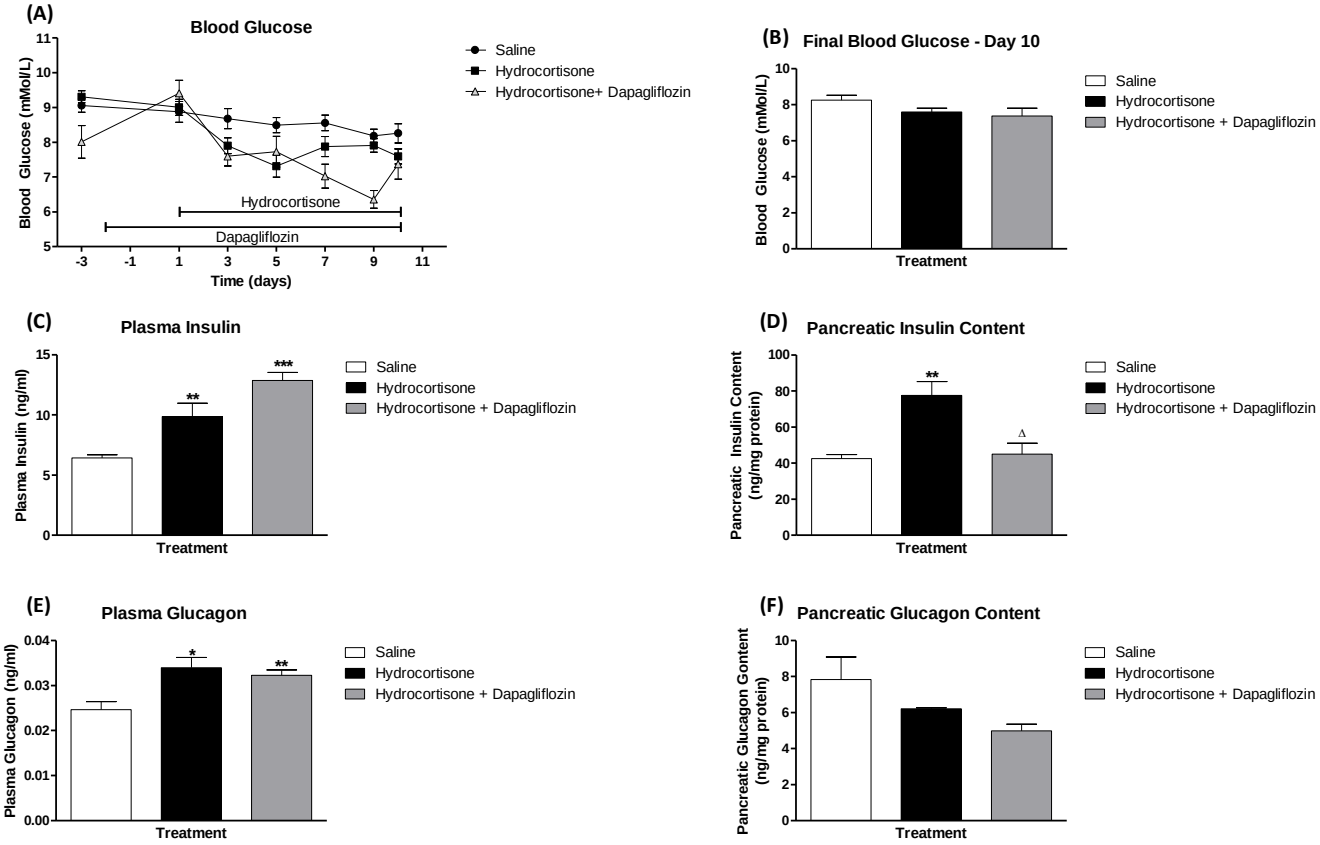

12 week old InsCre;Rosa26-eYFP C57Bl/6 mice were treated with dapagliflozin for two days prior to and in conjunction with administration of hydrocortisone (70mg/kg, ip, once daily), n=8 mice/group. Terminal blood was taken to assess plasma insulin and glucagon. (A) Blood glucose, (B) final blood glucose, (C) plasma insulin, (D) pancreatic insulin content (E) plasma glucagon and (F) pancreatic glucagon content.

Comparisons were made against saline (*) or against hydrocortisone treated (Δ). Values were significant when $p<0.05$ */Δ, $p<0.01$ **/ΔΔ and $p<0.001$ ***/ΔΔΔ.

Figure 5.17 Effects of hydrocortisone alone or in combination dapagliflozin on pancreatic islet area, beta cell area, alpha cell area, islet size distribution, percentage beta cells and percentage alpha cells

(A)

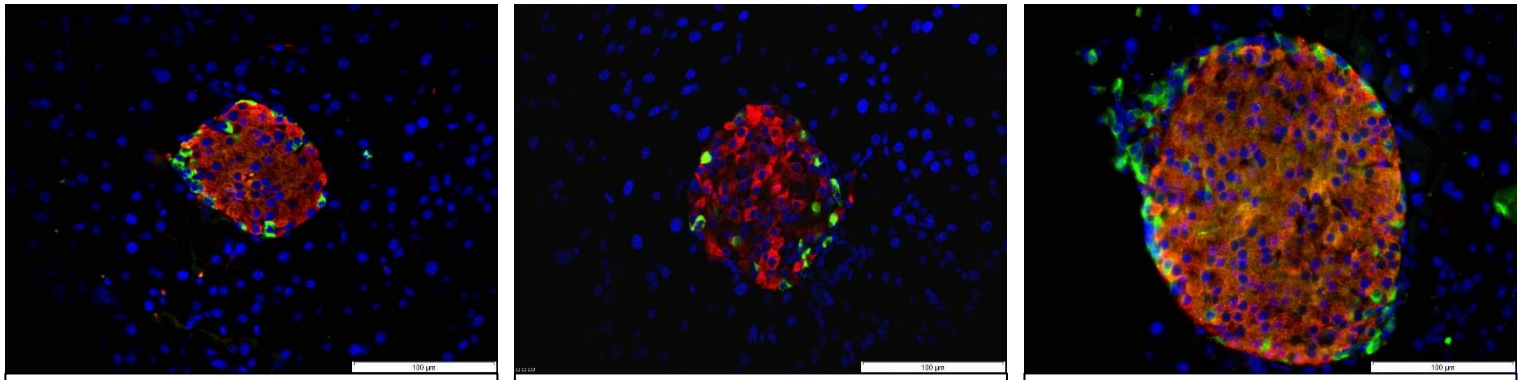

* Legend overleaf

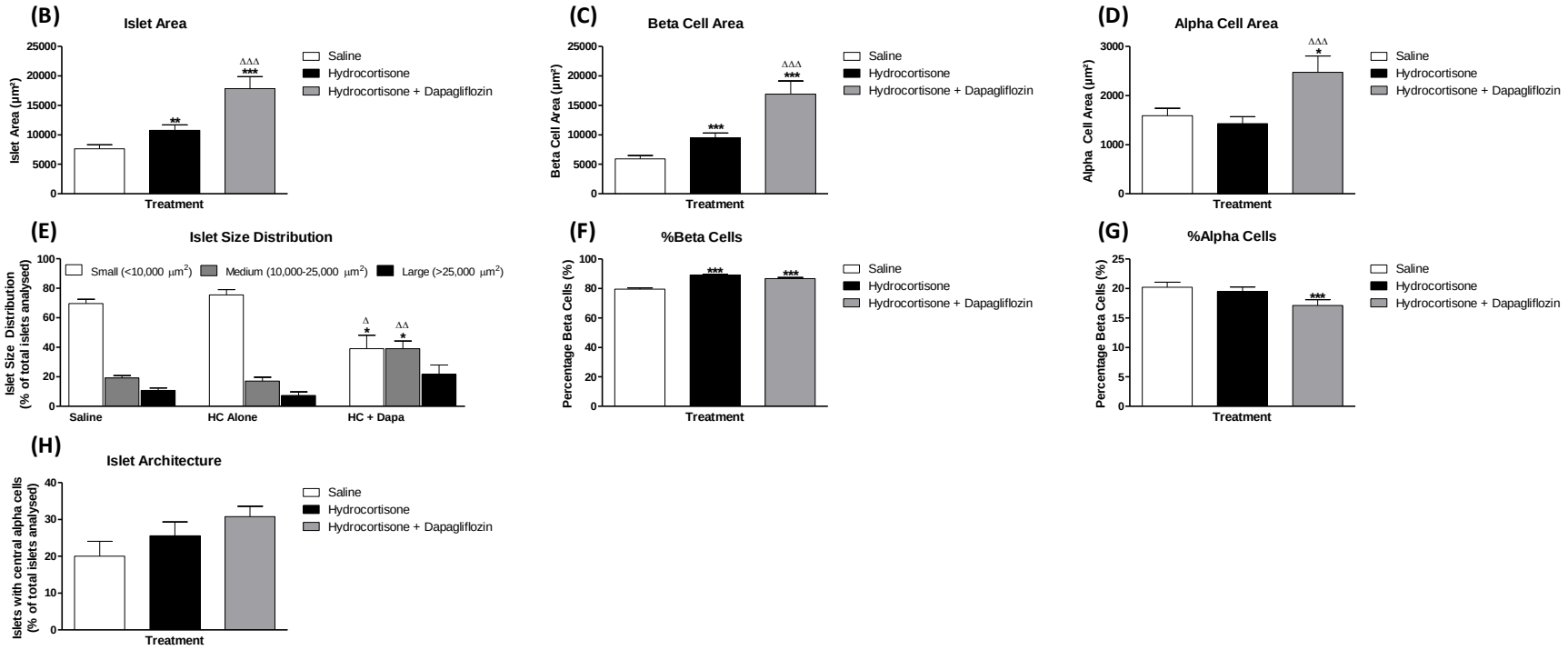

(A) Representative images of islets from saline, hydrocortisone and hydrocortisone plus dapagliflozin treated mice showing insulin (red), glucagon (green) and DAPI (blue). (B) Islet area, (C) beta cell area, (D) alpha cell area, (E) islet size distribution, (F) percentage beta cells, (G) percentage alpha cells and (H) islet architecture. Values are mean ± SEM(n=8 mice/group). Comparisons versus saline control (*) or versus hydrocortisone (Δ), significant when */Δp<0.05, **/ΔΔp<0.01 and ***/ΔΔΔp<0.001.

Figure 5.18: Effects of hydrocortisone alone or in combination with dapagliflozin on pancreatic islet beta-to-alpha cell transdifferentiation

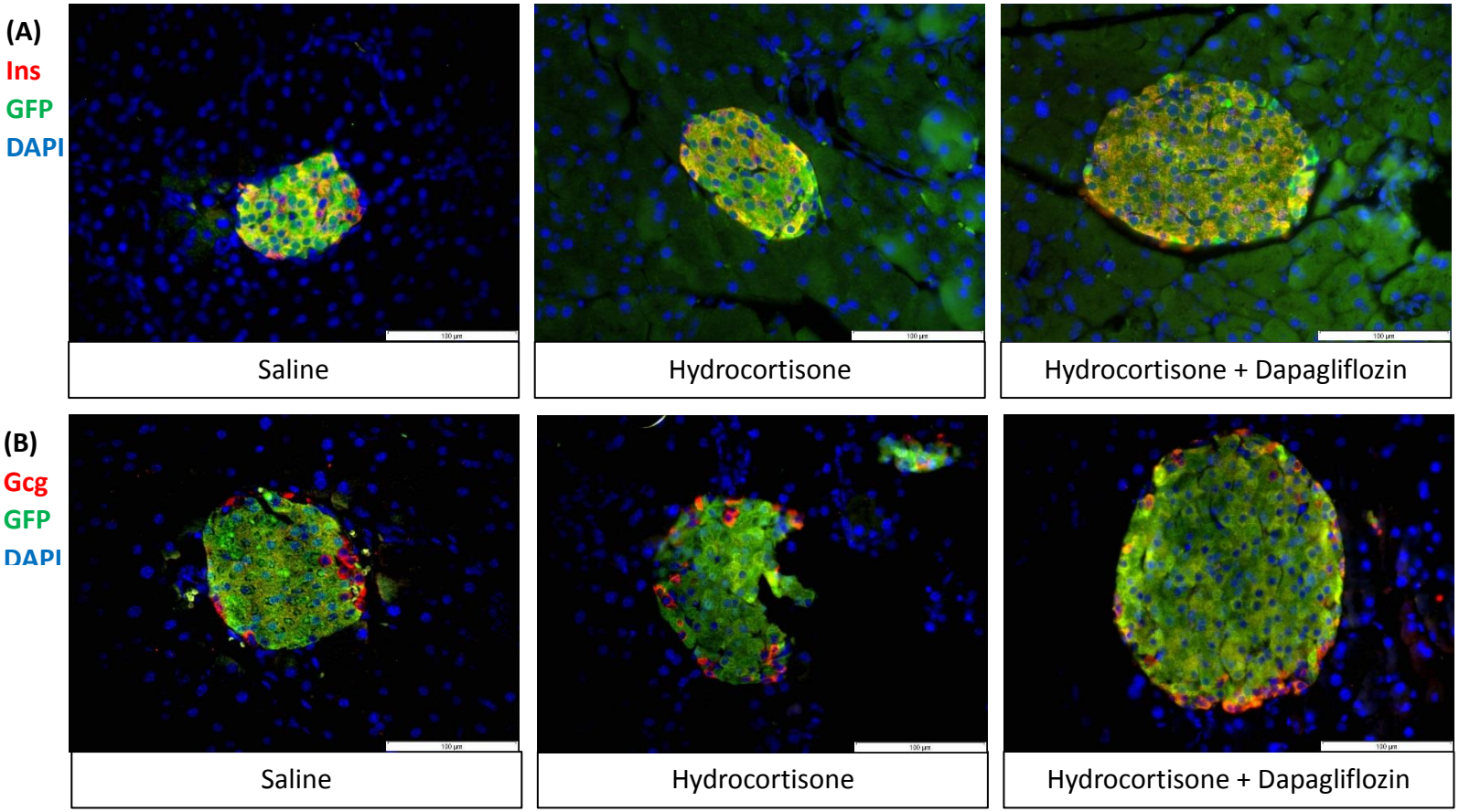

* Legend overleaf

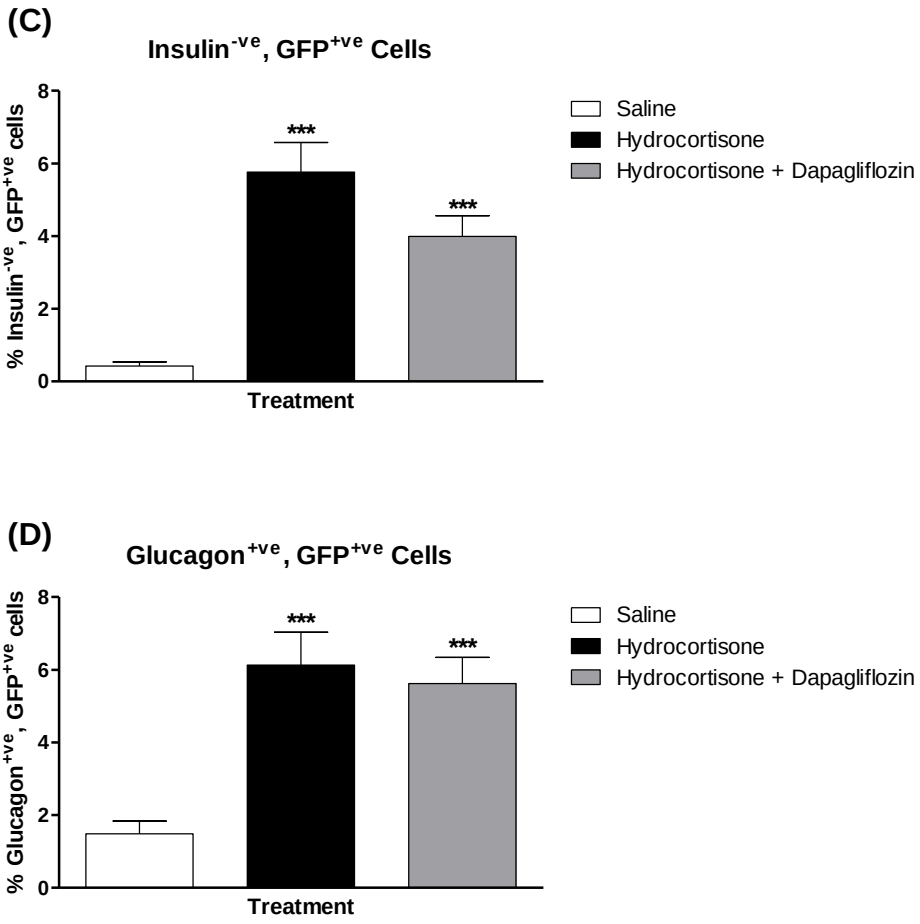

Transdifferentiation Analysis

Representative images of islets from mice treated with saline, hydrocortisone and hydrocortisone plus dapagliflozin (1mg/kg) stained for (A) insulin and GFP or (B) glucagon and GFP. Beta cell transdifferentiation determined by populations of insulin negative, GFP positive cells (C) and glucagon positive, GFP positive cells (D) using double immunofluorescence staining showing insulin/glucagon (red) and GFP (green).

Values are mean ± SEM (n=8 mice/group). Comparisons versus saline control (*) or versus hydrocortisone (Δ), significant when */Δp<0.05, **/ΔΔp<0.01 and ***p<0.001.

Figure 5.19: Effects of hydrocortisone alone or in combination with dapagliflozin on pancreatic islet beta cell and alpha cell apoptosis

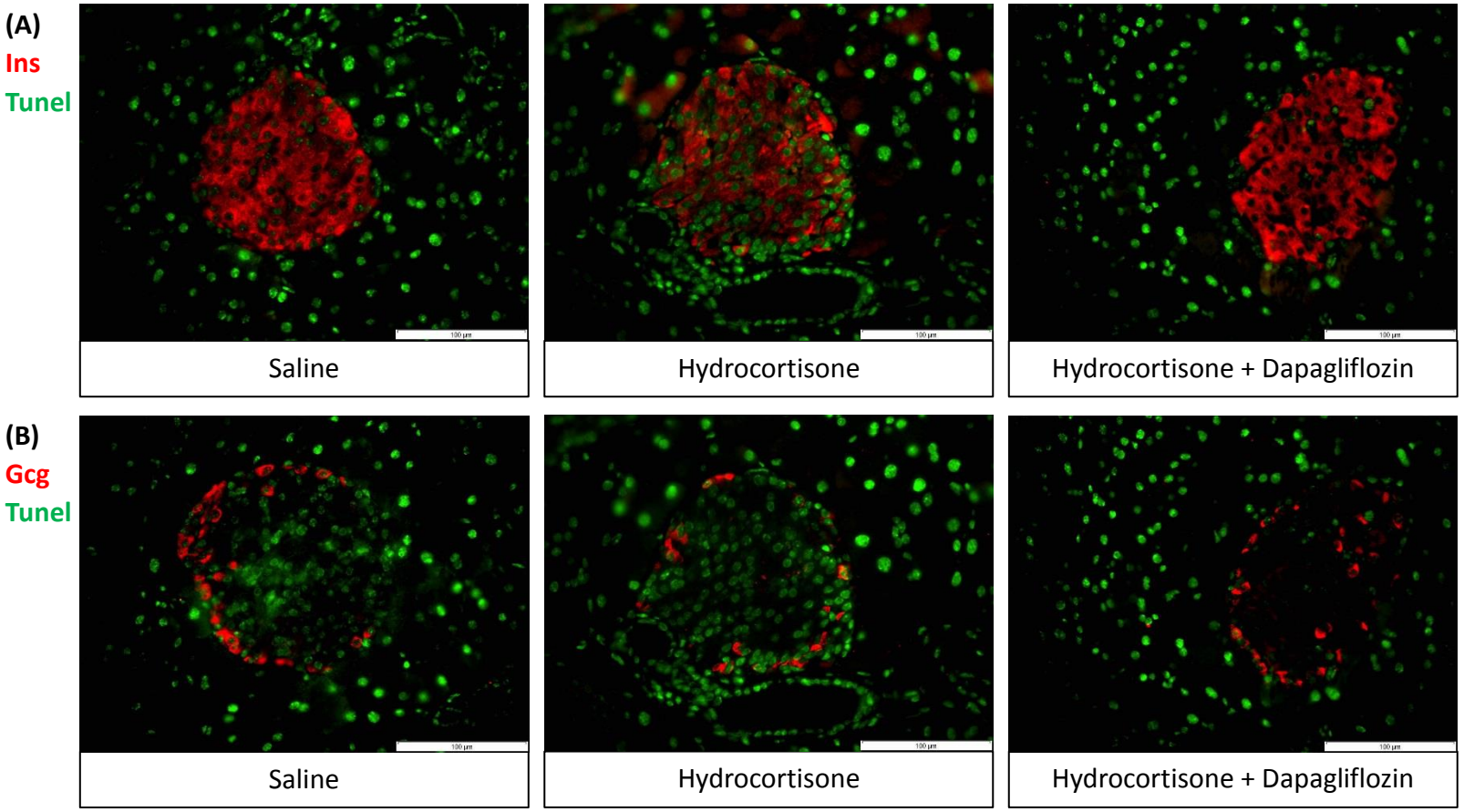

* Legend overleaf

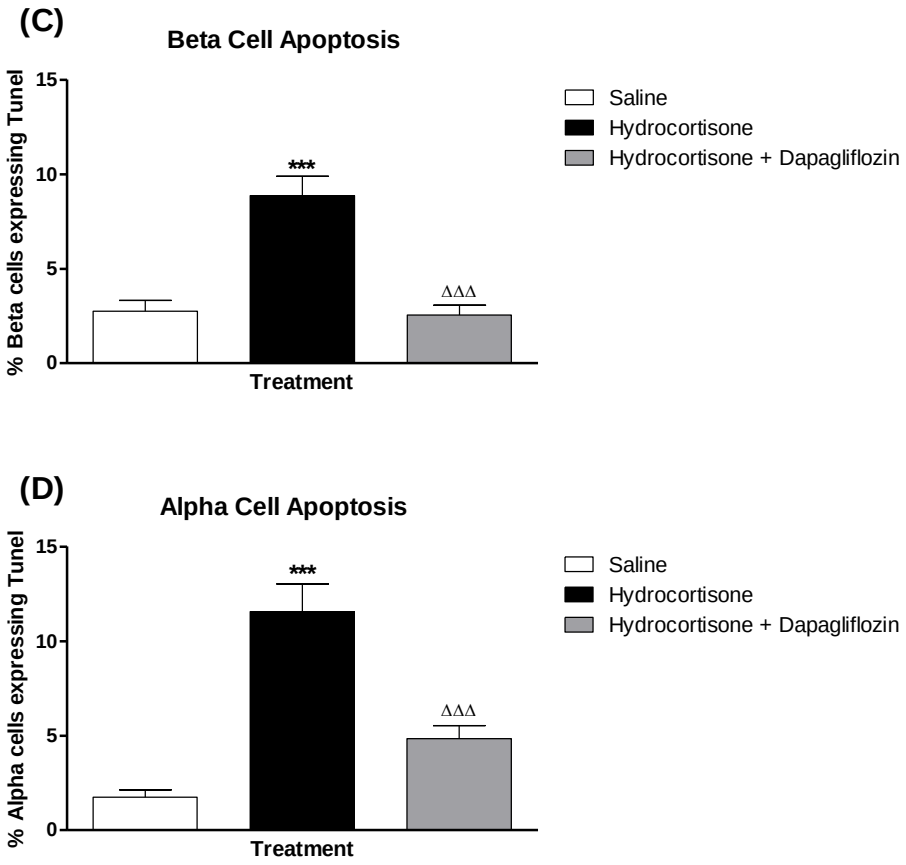

Apoptosis Analysis

Representative images of islets from mice treated with saline, hydrocortisone and hydrocortisone plus dapagliflozin (1mg/kg) stained for (A) insulin and TUNEL or (B) glucagon and TUNEL. Beta cell apoptosis and alpha cell apoptosis determined by populations of insulin positive, TUNEL positive (C) and glucagon positive, TUNEL positive (D) cells respectively by double immunofluorescence staining.

Values are mean ± SEM (n=8 mice/group). Comparisons versus saline control (*) or versus hydrocortisone (Δ), significant when */Δp<0.05, **/ΔΔp<0.01 and ***/ΔΔΔp<0.001.

Figure 5.20: Effects of hydrocortisone alone or in combination with dapagliflozin on pancreatic islet beta cell and alpha cell proliferation

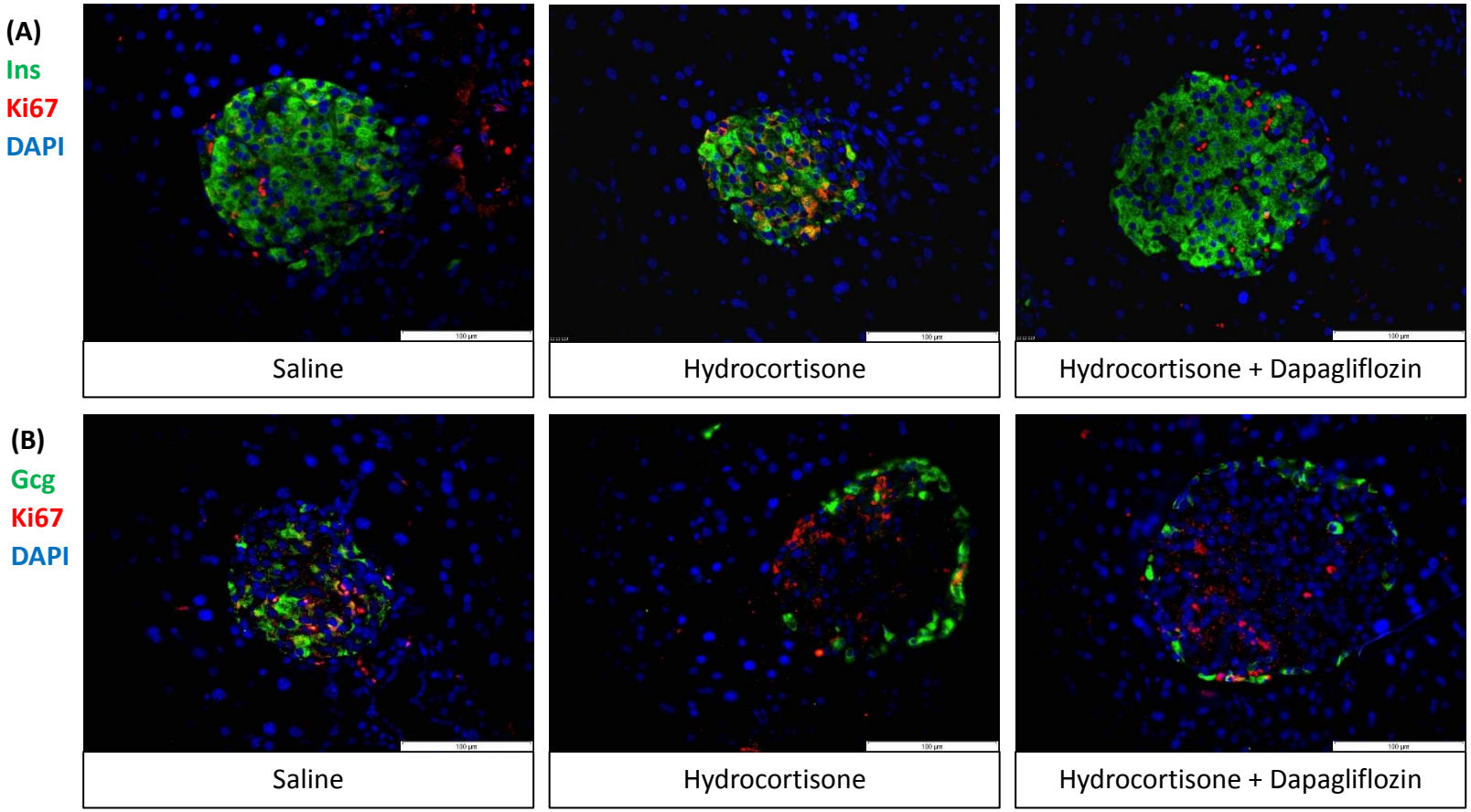

* Legend overleaf

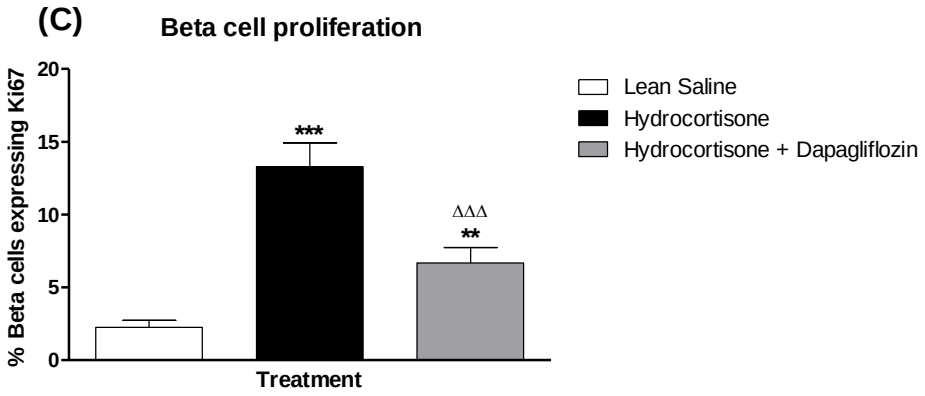

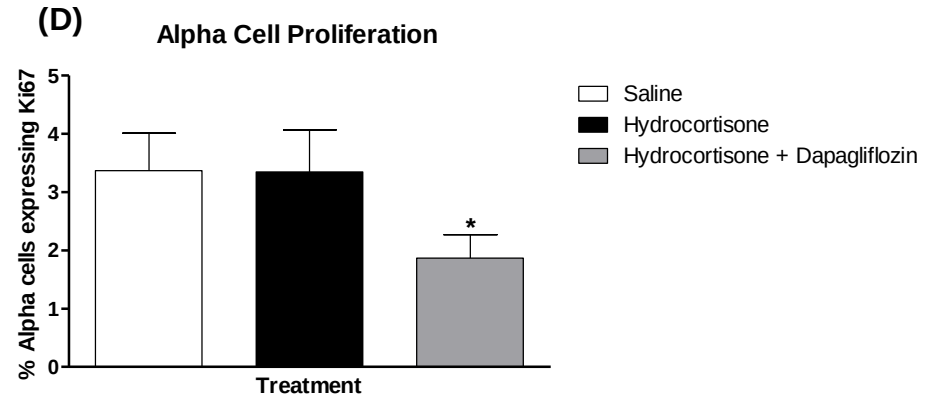

Proliferation Analysis

Representative images of islets from mice treated with saline, hydrocortisone and hydrocortisone plus dapagliflozin (1mg/kg) stained for (A) insulin and ki-67 or (B) glucagon and ki-67. Beta cell and alpha cell proliferation determined by populations of (C) insulin positive, ki-67 positive cell and (D) glucagon positive, ki-67 positive cells respectively.

Values are mean ± SEM (n=8 mice/group). Comparisons versus saline control (*) or versus hydrocortisone (Δ), significant when */Δp<0.05, **/ΔΔp<0.01 and ***/ΔΔΔp<0.001

.**Figure 5.21: Effects of hydrocortisone alone or in combination with dapagliflozin on pancreatic islet beta cell Pdx1 expression**

(A)

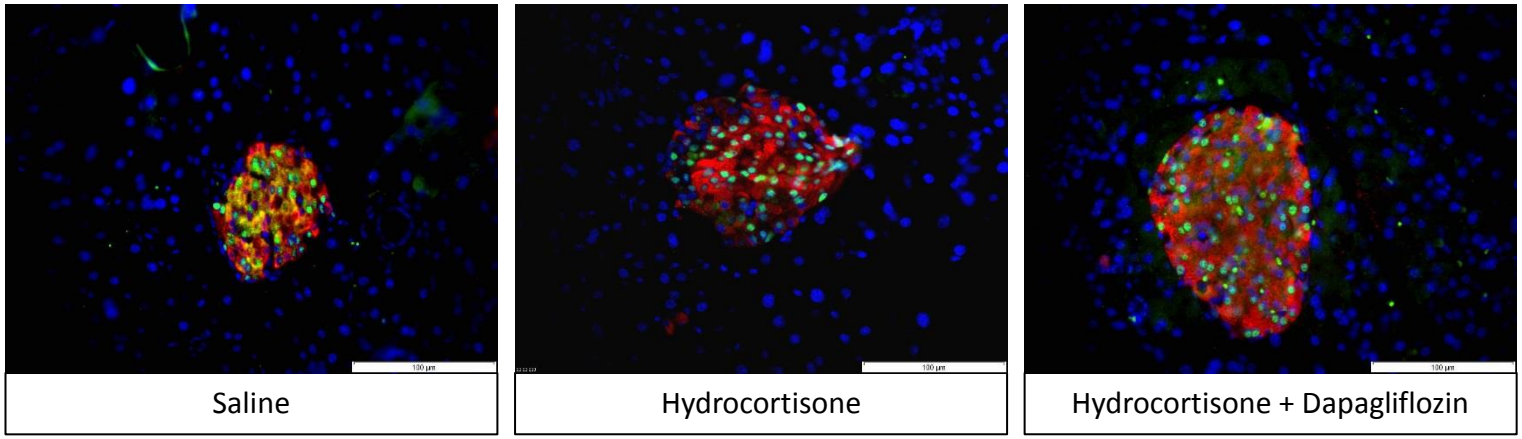

* Legend overleaf

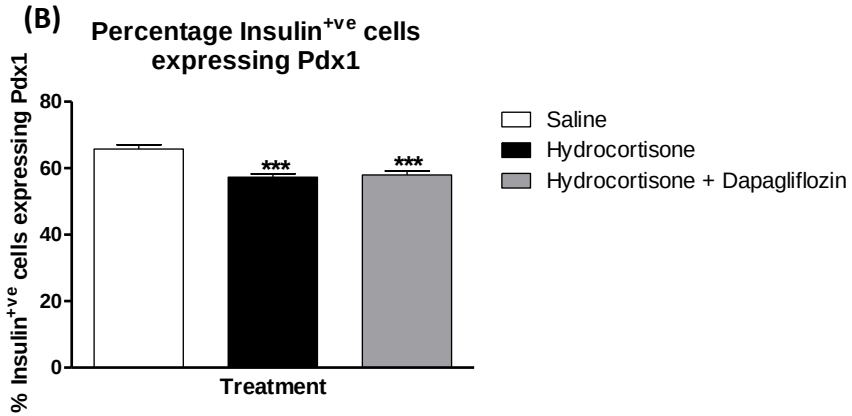

Pdx1 Expression Analysis

Representative images of islets from mice treated with (A) saline, hydrocortisone alone and hydrocortisone plus dapagliflozin on Pdx1 expression. (B) Determined by histological analysis of insulin/Pdx1 double immunofluorescence staining showing insulin (red), Pdx1 (green) and DAPI (blue).

Values are mean ± SEM (n=8 mice/group). Comparisons versus saline control (*) or versus hydrocortisone (Δ), significant when */Δp<0.05, **/ΔΔp<0.01 and ***p<0.001.

Figure 5.22: Effects of streptozotocin alone or in combination with dapagliflozin on body weight, cumulative energy intake and cumulative fluid intake

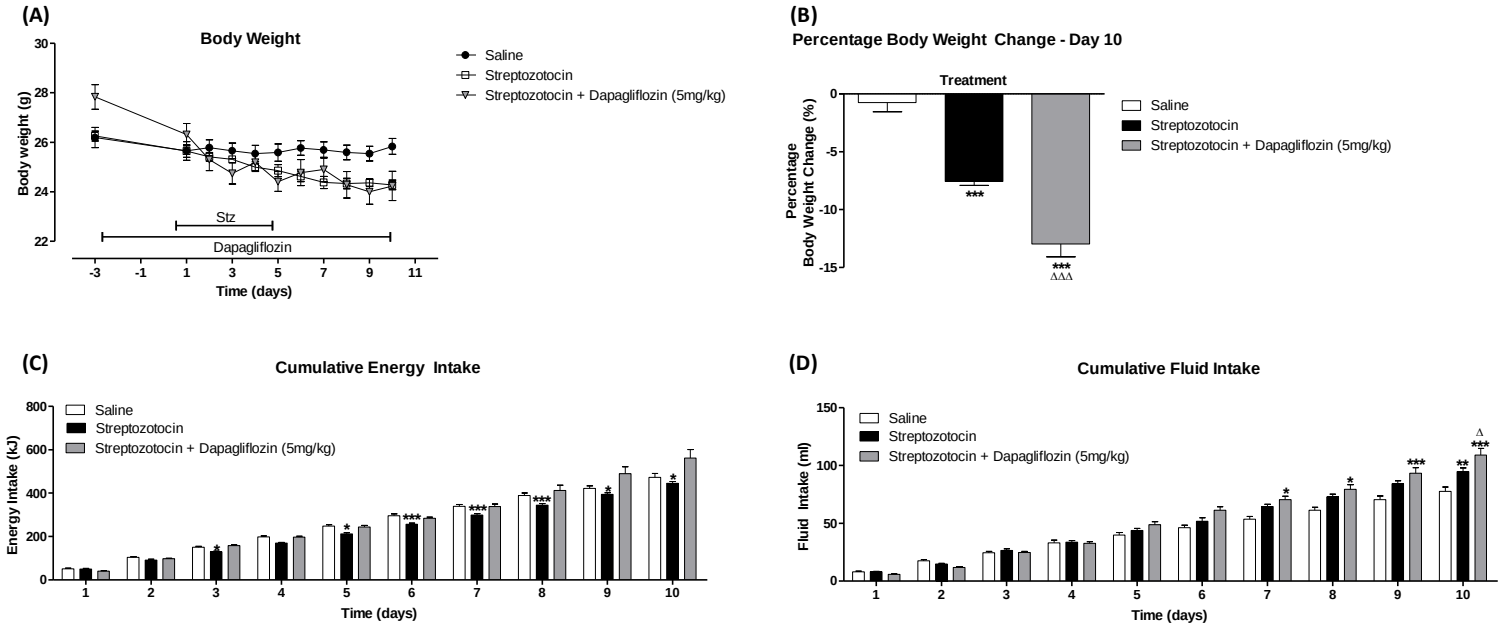

12 week old InsCre;Rosa26-eYFP C57Bl/6 mice were treated with 5mg/kg dapagliflozin for two days prior to and in conjunction with administration of streptozotocin (50mg/kg, ip, once daily), n=8 mice/group. (A) Body weight, (B) percentage body weight change, (C) cumulative energy intake and (D) cumulative fluid intake. Comparisons were made against saline (*) or against streptozotocin treated (Δ). Values were significant when $p<0.05$ */Δ, $p<0.01$ **/ΔΔ and $p<0.001$ ***/ΔΔΔ.

Figure 5.23 Effect of streptozotocin alone or in combination with dapagliflozin on blood glucose, plasma insulin, pancreatic insulin content, plasma glucagon and pancreatic glucagon content

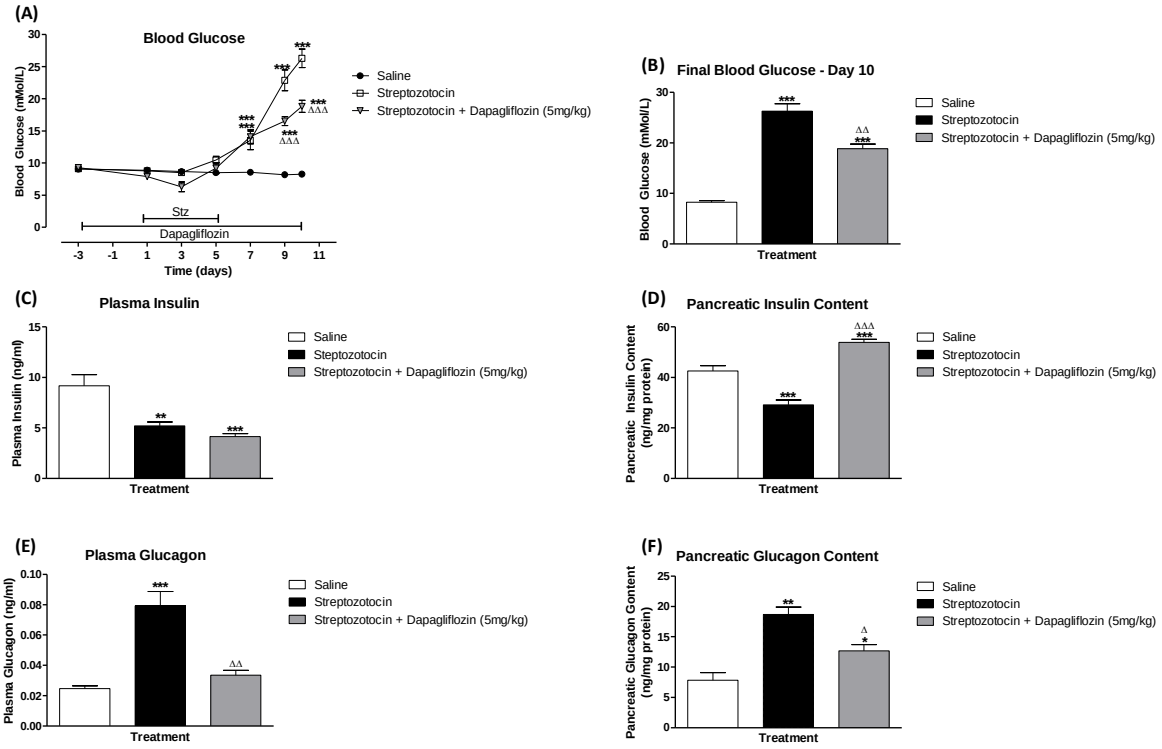

12 week old InsCre;Rosa26-eYFP C57Bl/6 mice were treated with 5mg/kg dapagliflozin for two days prior to and in conjunction with administration of streptozotocin (50mg/kg, ip, once daily), n=8 mice/group. Terminal blood was taken to assess plasma insulin and glucagon. Blood glucose, (B) final blood glucose, (C) plasma insulin, (D) pancreatic insulin content, (E) plasma glucagon and (F) pancreatic glucagon content.

Comparisons were made against saline (*) or against streptozotocin treated (Δ). Values were significant when $p<0.05$ */Δ, $p<0.01$ **/ΔΔ and $p<0.001$ ***/ΔΔΔ.

Figure 5.24: Effects of streptozotocin alone or in combination dapagliflozin on pancreatic islet area, beta cell area, alpha cell area, islet size distribution, percentage beta cells, percentage alpha cells and islet architecture

(A)

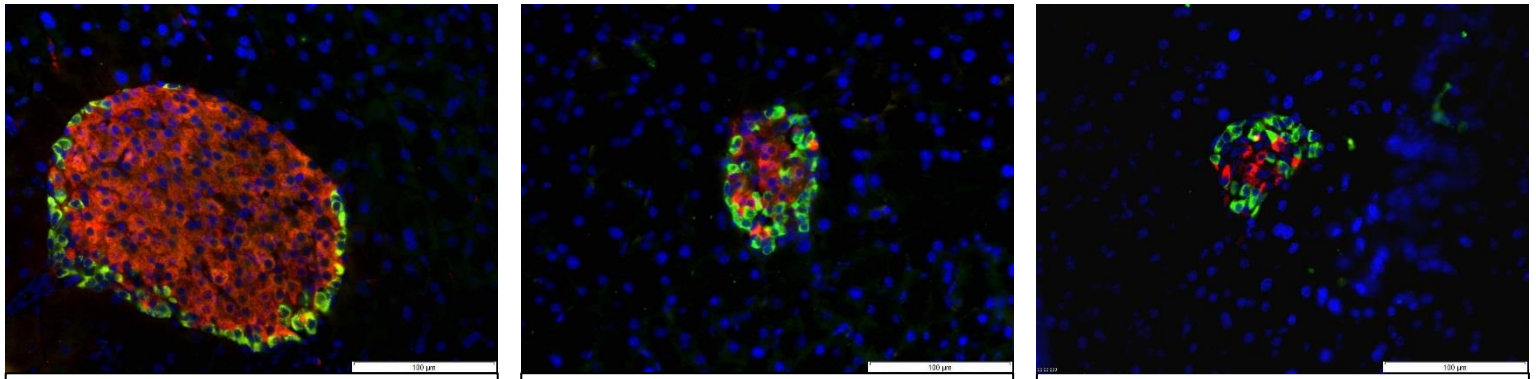

Saline	Streptozotocin	Streptozotocin + Dapagliflozin

Insulin / Glucagon / DAPI

* Legend overleaf

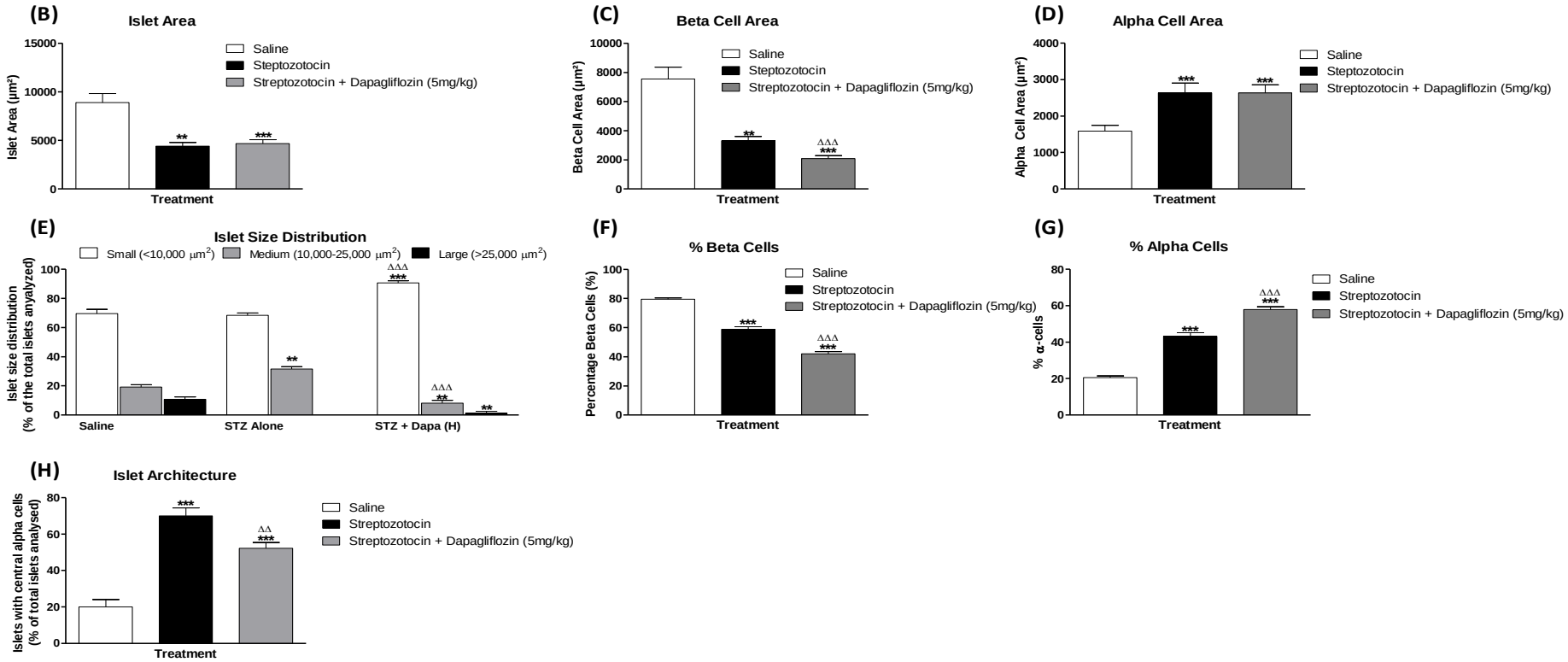

(A) Representative images of islets from saline, streptozotocin and streptozotocin plus 5mg/kg dapagliflozin treated mice showing insulin (red), glucagon (green) and DAPI (blue). (B) islet area, (C) beta cell area, (D) alpha cell area, (E) islet size distribution, (F) percentage beta cells, (G) percentage alpha cells and (H) islet architecture. Values are mean ± SEM (n=8 mice/group). Comparisons versus saline control (*) or versus streptozotocin (Δ), significant when */Δp<0.05, **/ΔΔp<0.01 and ***/ΔΔΔp<0.001.

Figure 5.25: Effects of streptozotocin alone or in combination dapagliflozin on pancreatic islet beta-to-alpha cell transdifferentiation

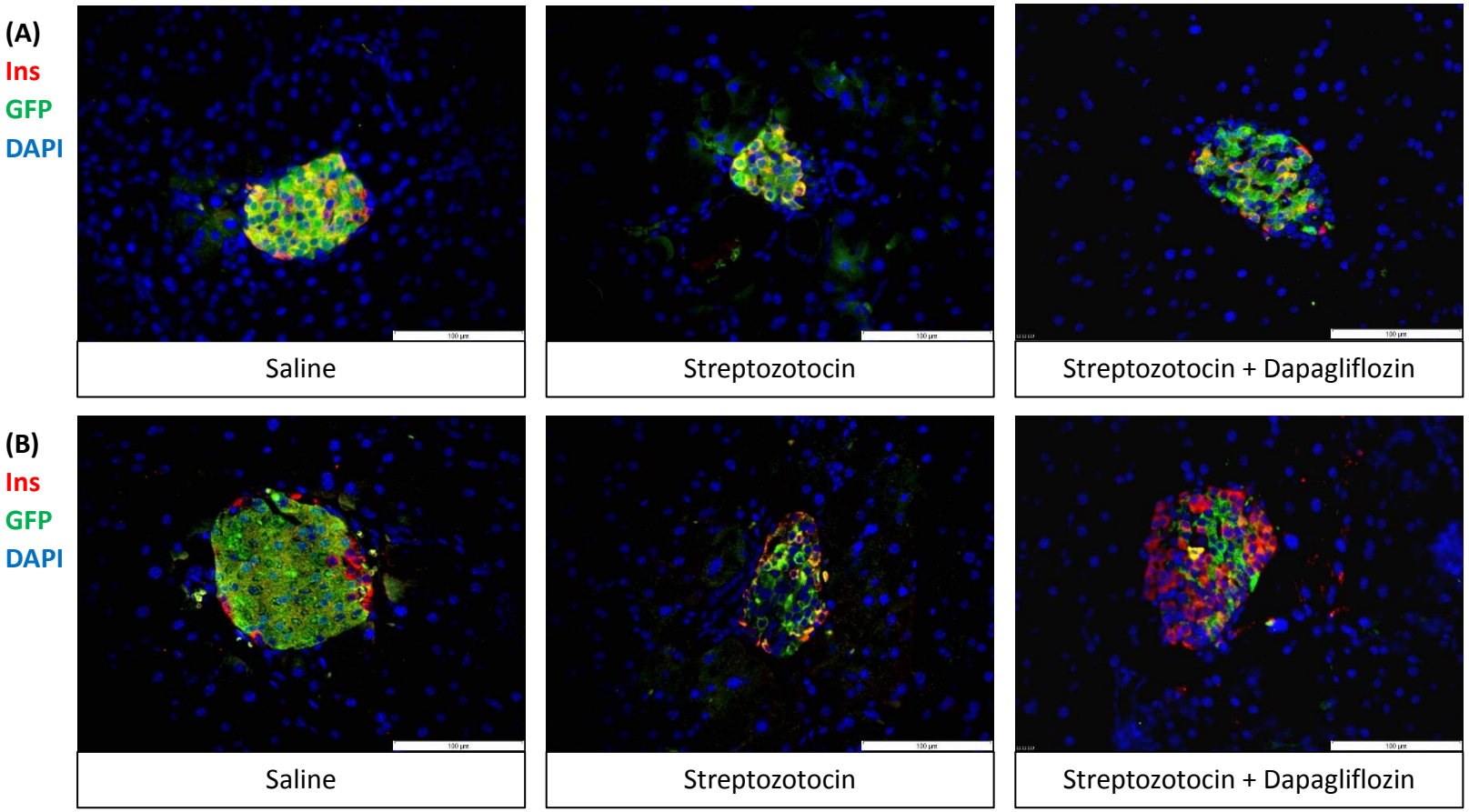

* Legend overleaf

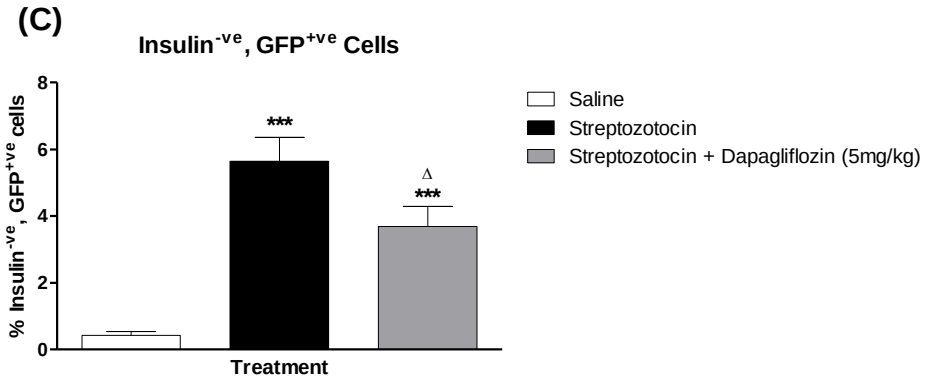

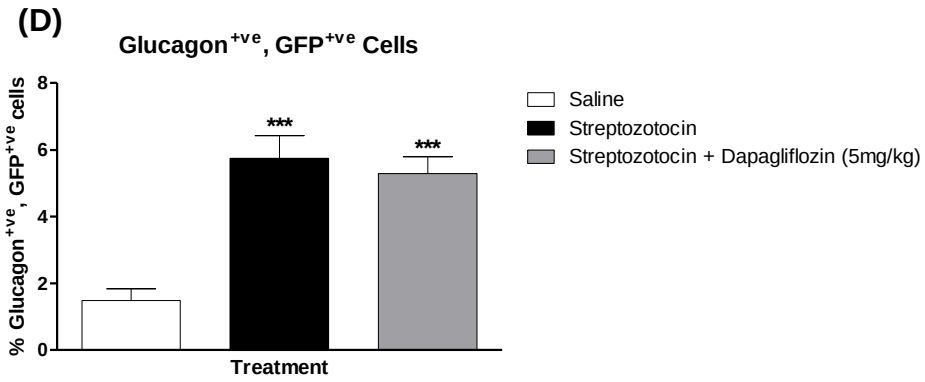

Transdifferentiation Analysis

Representative images of islets from mice treated with saline, streptozotocin and streptozotocin plus dapagliflozin (5mg/kg) stained for (A) insulin and GFP or (B) glucagon and GFP. Beta cell transdifferentiation determined by populations of insulin negative, GFP positive cells (C) and glucagon positive, GFP positive cells (D) using double immunofluorescence staining showing insulin/glucagon (red) and GFP (green).

Values are mean ± SEM (n=8 mice/group). Comparisons versus saline control (*) or versus streptozotocin (Δ), significant when */Δp<0.05, **/ΔΔp<0.01 and ***/ΔΔΔp<0.001.

Figure 5.26: Effects of streptozotocin alone or in combination dapagliflozin on beta cell and alpha cell apoptosis

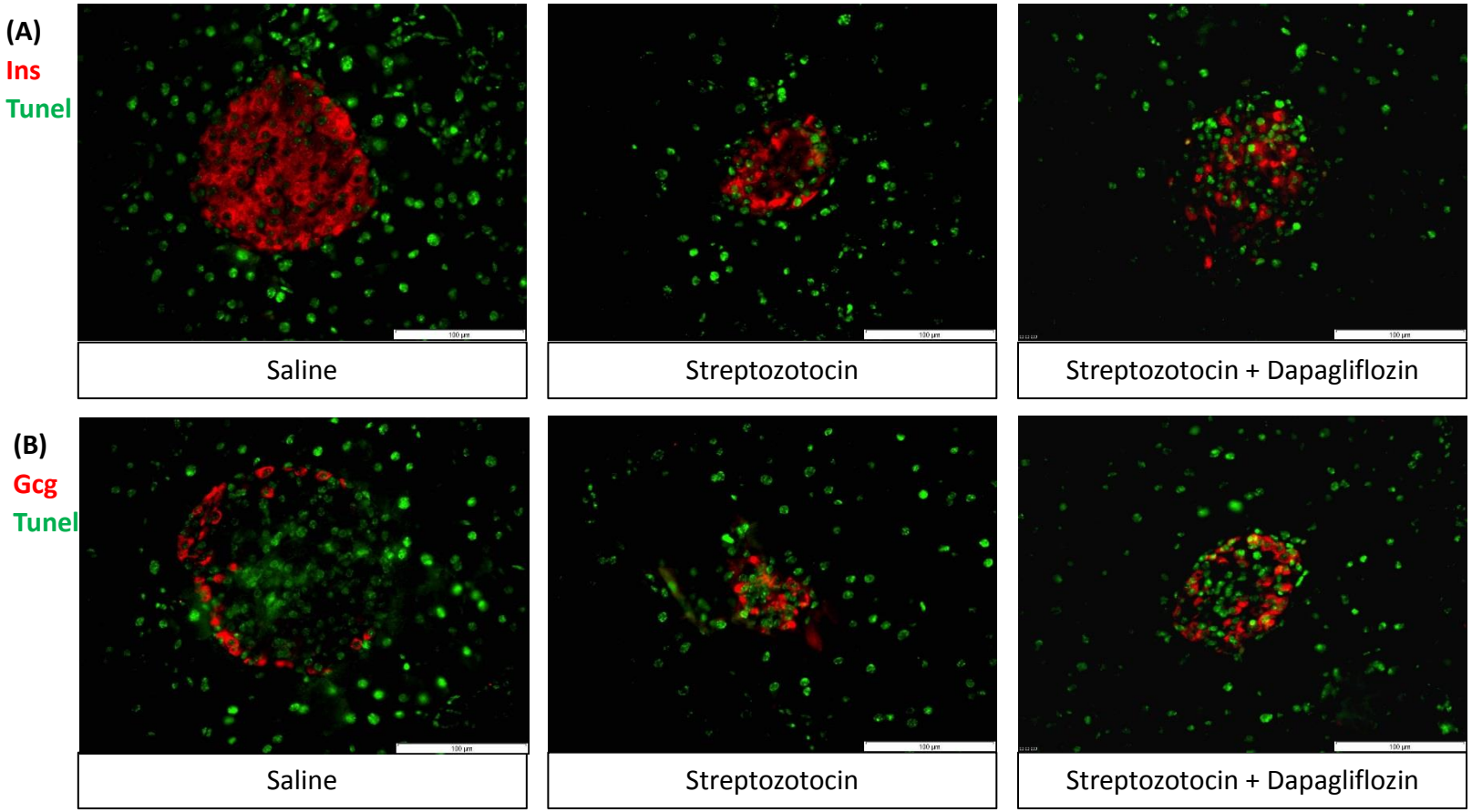

* Legend overleaf

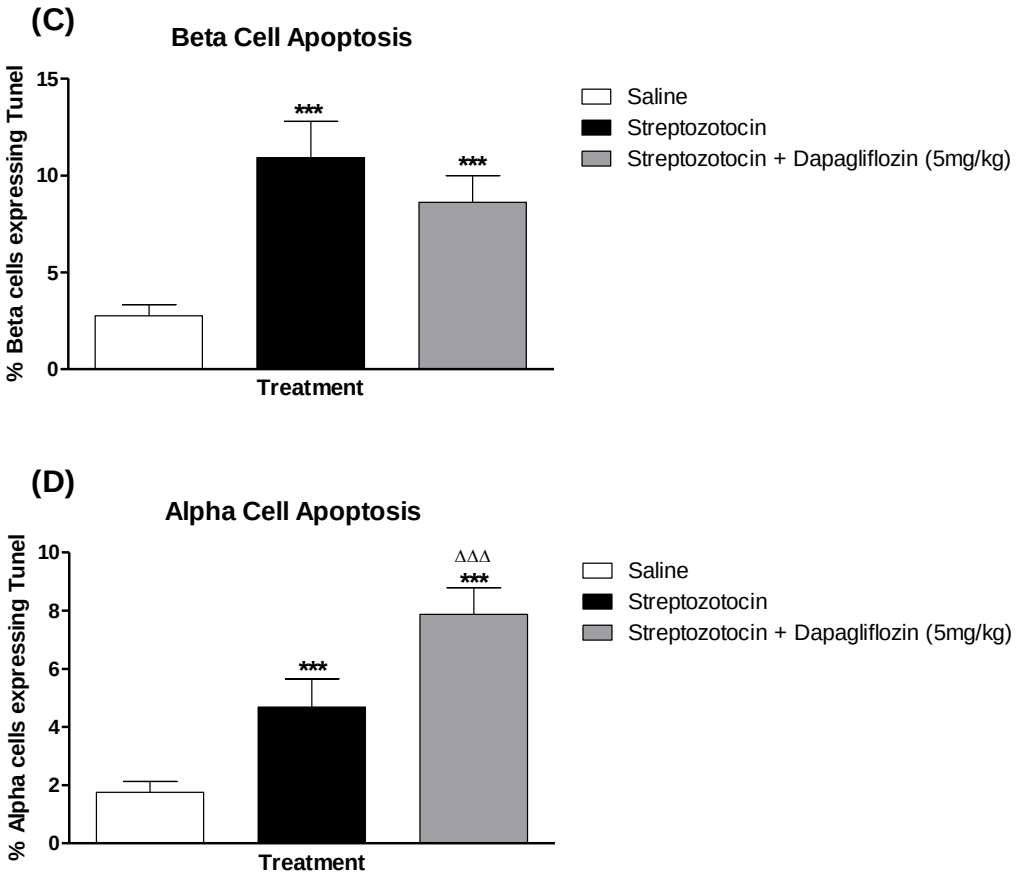

Apoptosis Analysis

Representative images of islets from mice treated with saline, streptozotocin and streptozotocin plus dapagliflozin (5mg/kg) stained for (A) insulin and TUNEL or (B) glucagon and TUNEL. Beta cell apoptosis and alpha cell apoptosis determined by populations of insulin positive, TUNEL positive (C) and glucagon positive, TUNEL positive (D) cells respectively by double immunofluorescence staining.

Values are mean ± SEM (n=8 mice/group). Comparisons versus saline control (*) or versus streptozotocin (Δ), significant when */Δp<0.05, **/ΔΔp<0.01 and ***/ΔΔΔp<0.001.

Figure 5.27: Effects of streptozotocin alone or in combination dapagliflozin on beta cell and alpha cell proliferation

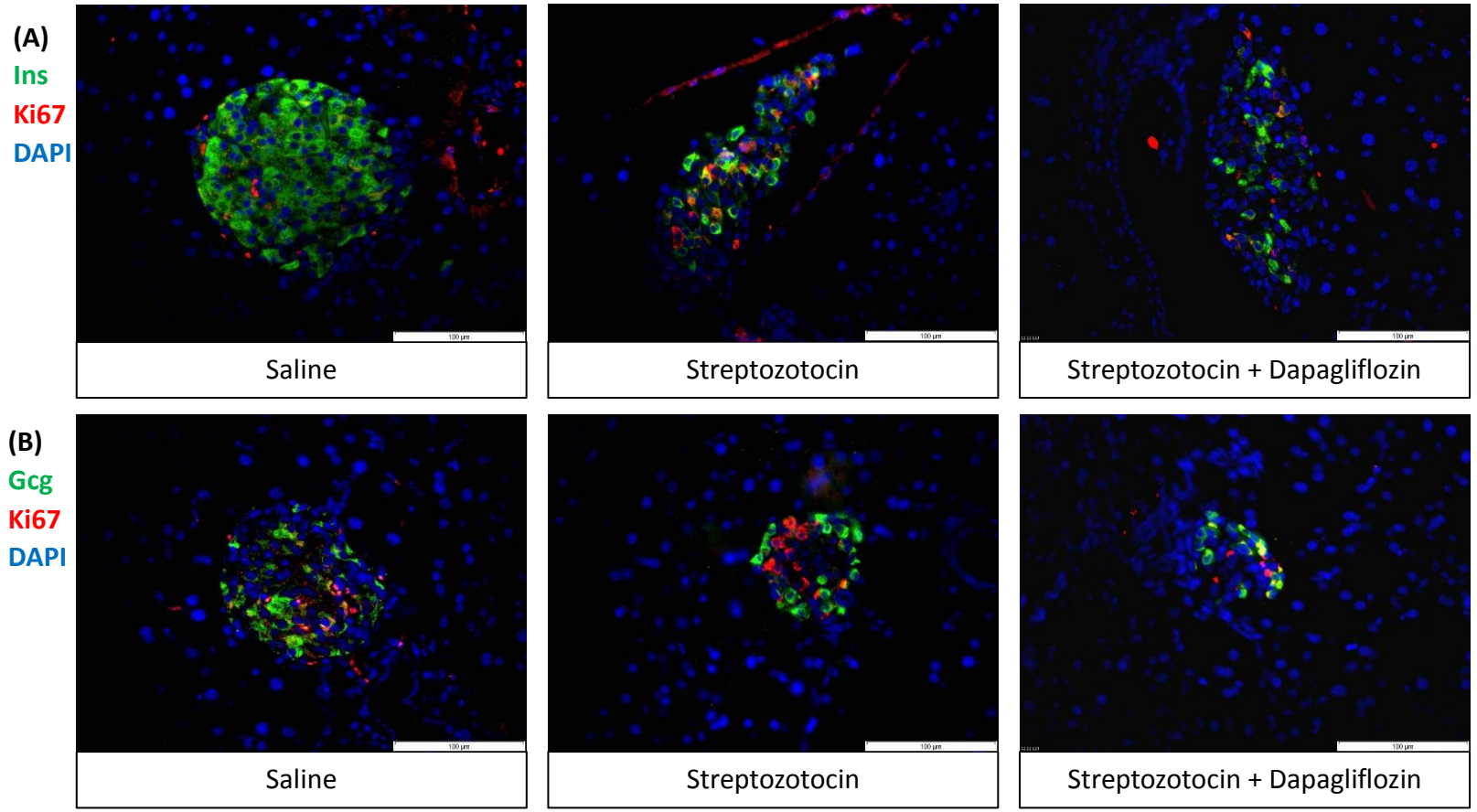

* Legend overleaf

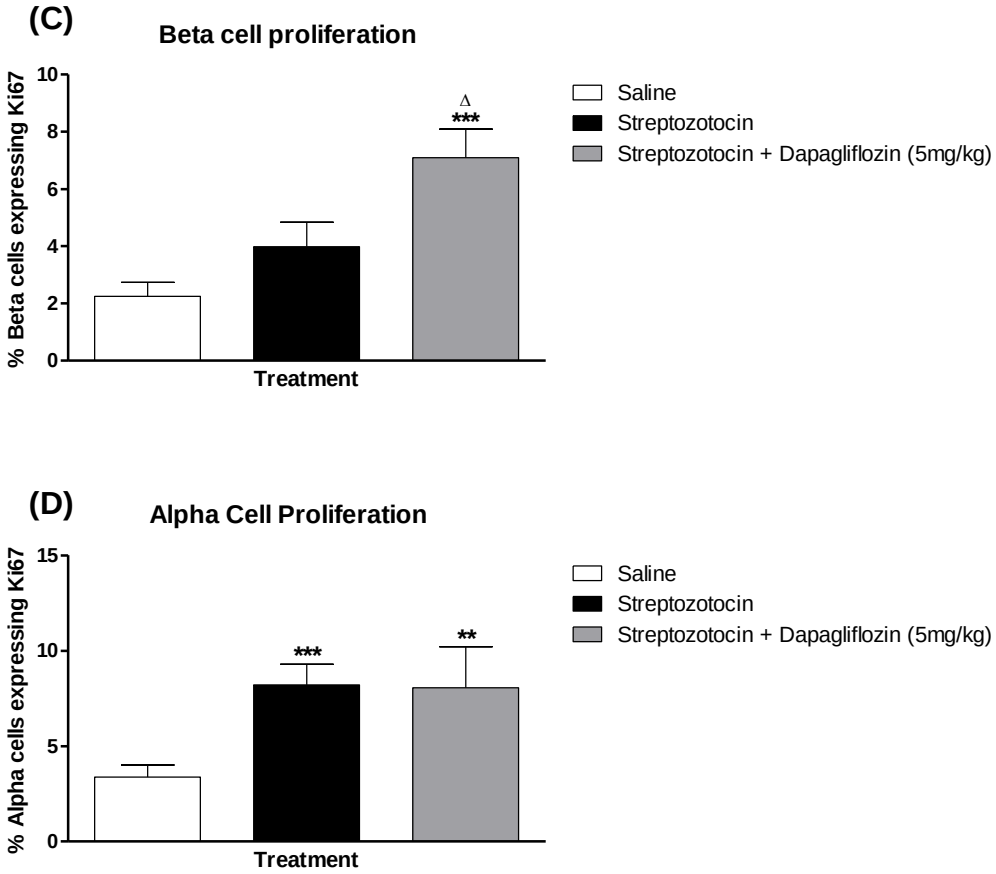

Proliferation Analysis

Representative images of islets from mice treated with saline, streptozotocin and streptozotocin plus dapagliflozin (5mg/kg) stained for (A) insulin and ki-67 or (B) glucagon and ki-67. Beta cell and alpha cell proliferation determined by populations of (C) insulin positive, ki-67 positive cell and (D) glucagon positive, ki-67 positive cells respectively.

Values are mean ± SEM (n=8 mice/group). Comparisons versus saline control (*) or versus streptozotocin (Δ), significant when */Δp<0.05, **/ΔΔp<0.01 and ***p<0.001.

Figure 5.28: Effects of streptozotocin alone or in combination dapagliflozin on beta cell Pdx1 expression

(A)

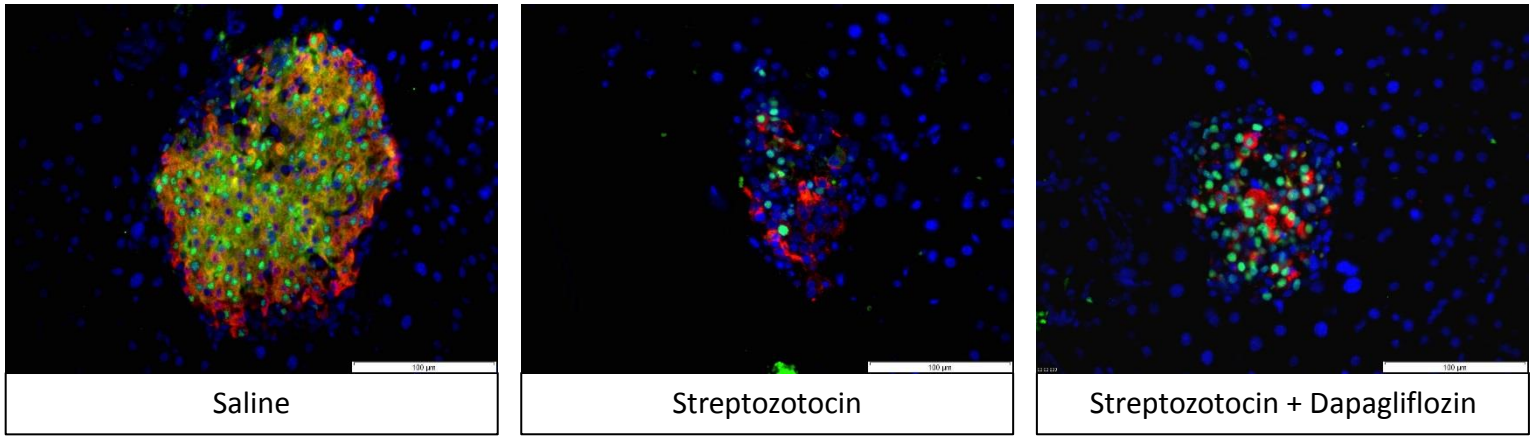

* Legend overleaf

Pdx1 Expression Analysis

(A) Representative images of islets from mice treated with saline, streptozotocin and streptozotocin plus dapagliflozin (5mg/kg) on Pdx1 expression (B). Determined by histological analysis of insulin/Pdx1 double immunofluorescence staining showing insulin (red), Pdx1 (green) and DAPI (blue).

Values are mean ± SEM (n=8 mice/group). Comparisons versus saline control (*) or versus streptozotocin (Δ), significant when */Δp<0.05, **/ΔΔp<0.01 and ***p<0.001.

Figure 5.29: Effects of streptozotocin alone or with insulin treatment on body weight, cumulative energy intake and cumulative fluid intake

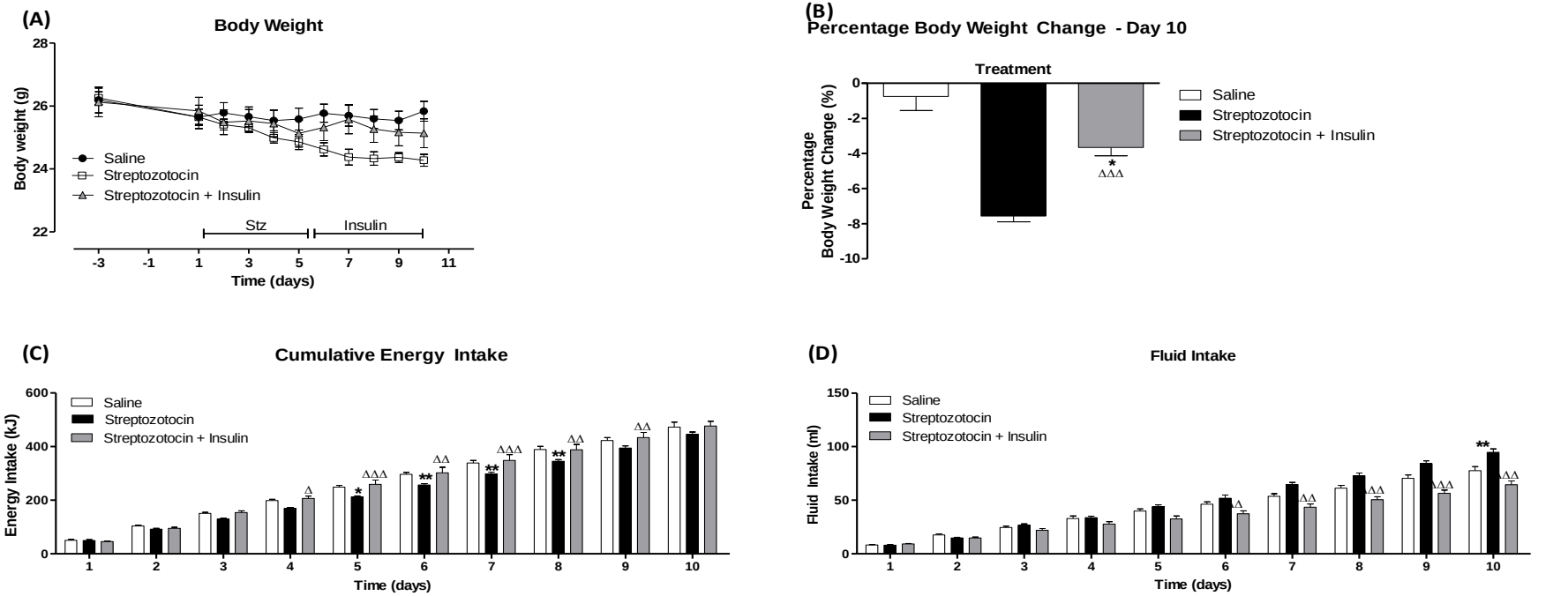

12 week old InsCre;Rosa26-eYFP C57Bl/6 mice were administered streptozotocin (50mg/kg, ip, once daily) and treated with insulin (1unit every 8 hours) when hyperglycaemia presented, n=8 mice/group. (A) Body weight, (B) percentage body weight change, (C) cumulative energy intake and (D) cumulative fluid intake. Comparisons were made against saline (*) or against streptozotocin treated (Δ). Values were significant when $p<0.05$ */Δ, $p<0.01$ **/ΔΔ and $p<0.001$ ***/ΔΔΔ.

Figure 5.30: Effects of streptozotocin alone or with insulin treatment on blood glucose, plasma insulin, pancreatic insulin content, plasma glucagon and pancreatic glucagon content

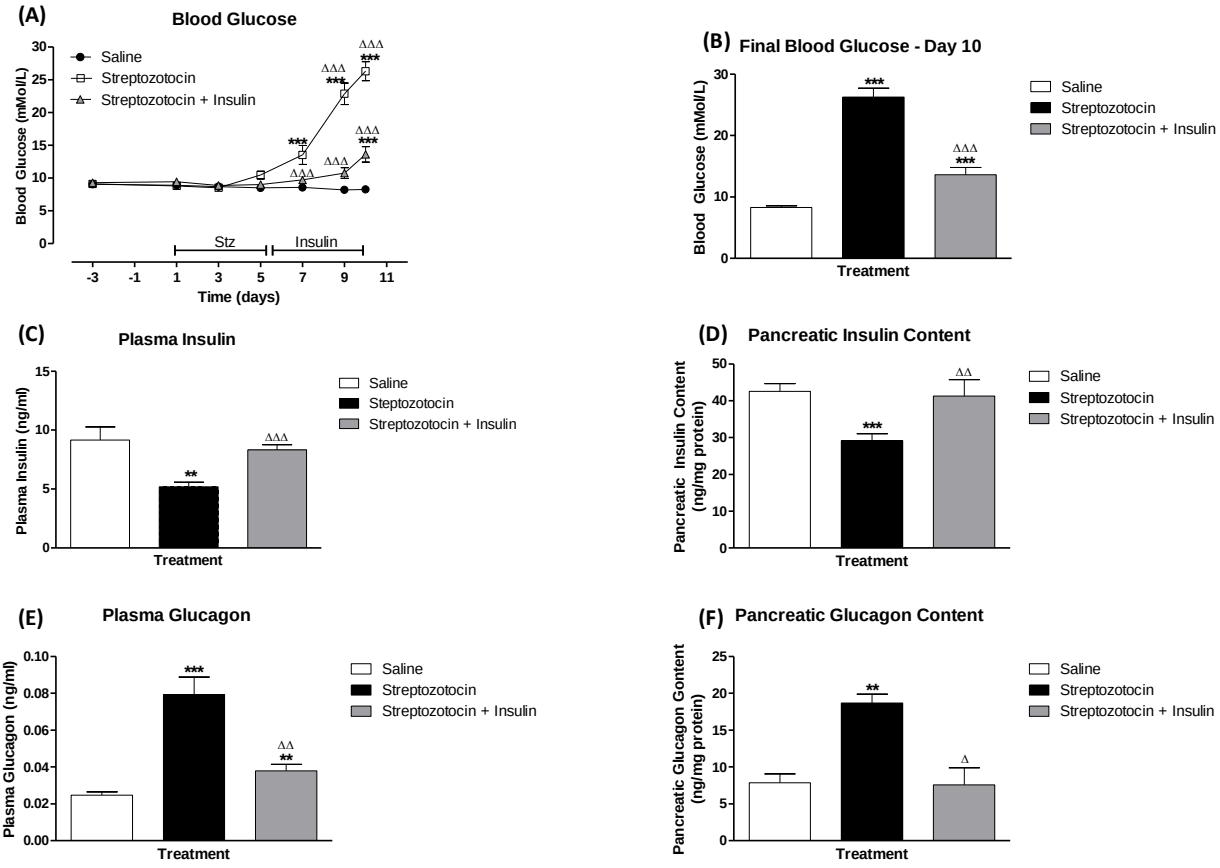

12 week old InsCre;Rosa26-eYFP C57Bl/6 mice were administered streptozotocin (50mg/kg, ip, once daily) and treated with insulin (1unit every 8 hours) when hyperglycaemia presented, n=8 mice/group. Terminal blood was taken to assess plasma insulin and glucagon. (A) Blood glucose, (B) final blood glucose, (C) plasma insulin, (D) pancreatic insulin content, (E) plasma glucagon and (F) pancreatic glucagon content.

Comparisons were made against saline (*) or against streptozotocin treated (Δ). Values were significant when $p<0.05$ */Δ, $p<0.01$ **/ΔΔ and $p<0.001$ ***/ΔΔΔ.

Figure 5.31: Effects of streptozotocin alone or insulin treatment on pancreatic islet area, beta cell area, alpha cell area, islet size distribution, percentage beta cells and percentage alpha cells

(A)

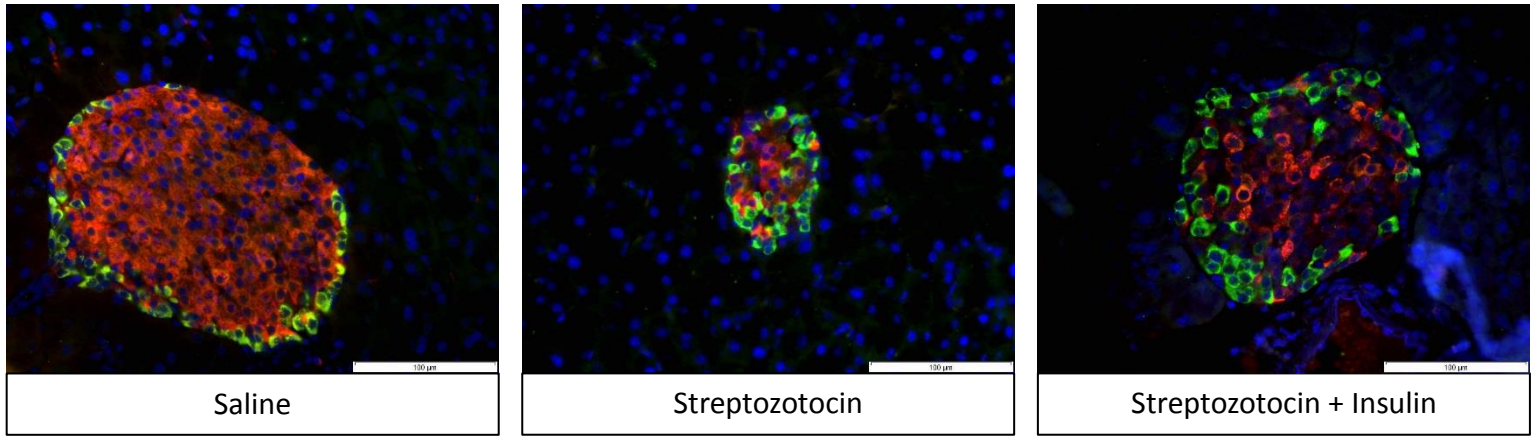

* Legend overleaf

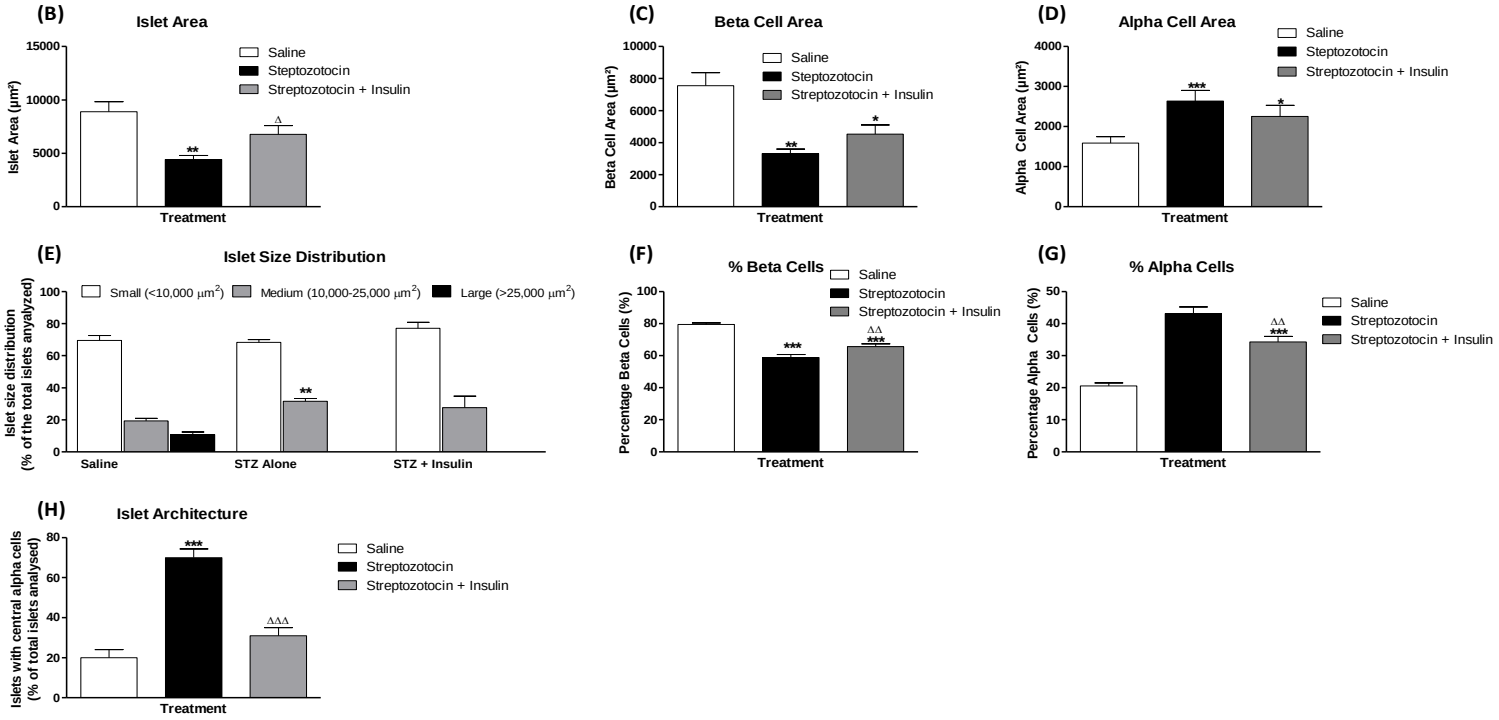

(A) Representative images of islets from saline, streptozotocin and streptozotocin plus insulin treated mice showing insulin (red), glucagon (green) and DAPI (blue). (B) islet area, (C) beta cell area, (D) alpha cell area, (E) islet size distribution, (F) percentage beta cells, (G) percentage alpha cells and (H) islet architecture. Values are mean ± SEM(n=8 mice/group). Comparisons versus saline control (*) or versus streptozotocin (Δ), significant when */Δp<0.05, **/ΔΔp<0.01 and ***/ΔΔΔp<0.001.

Figure 5.32: Effects of streptozotocin alone or with insulin treatment on pancreatic islet beta-to-alpha cell transdifferentiation

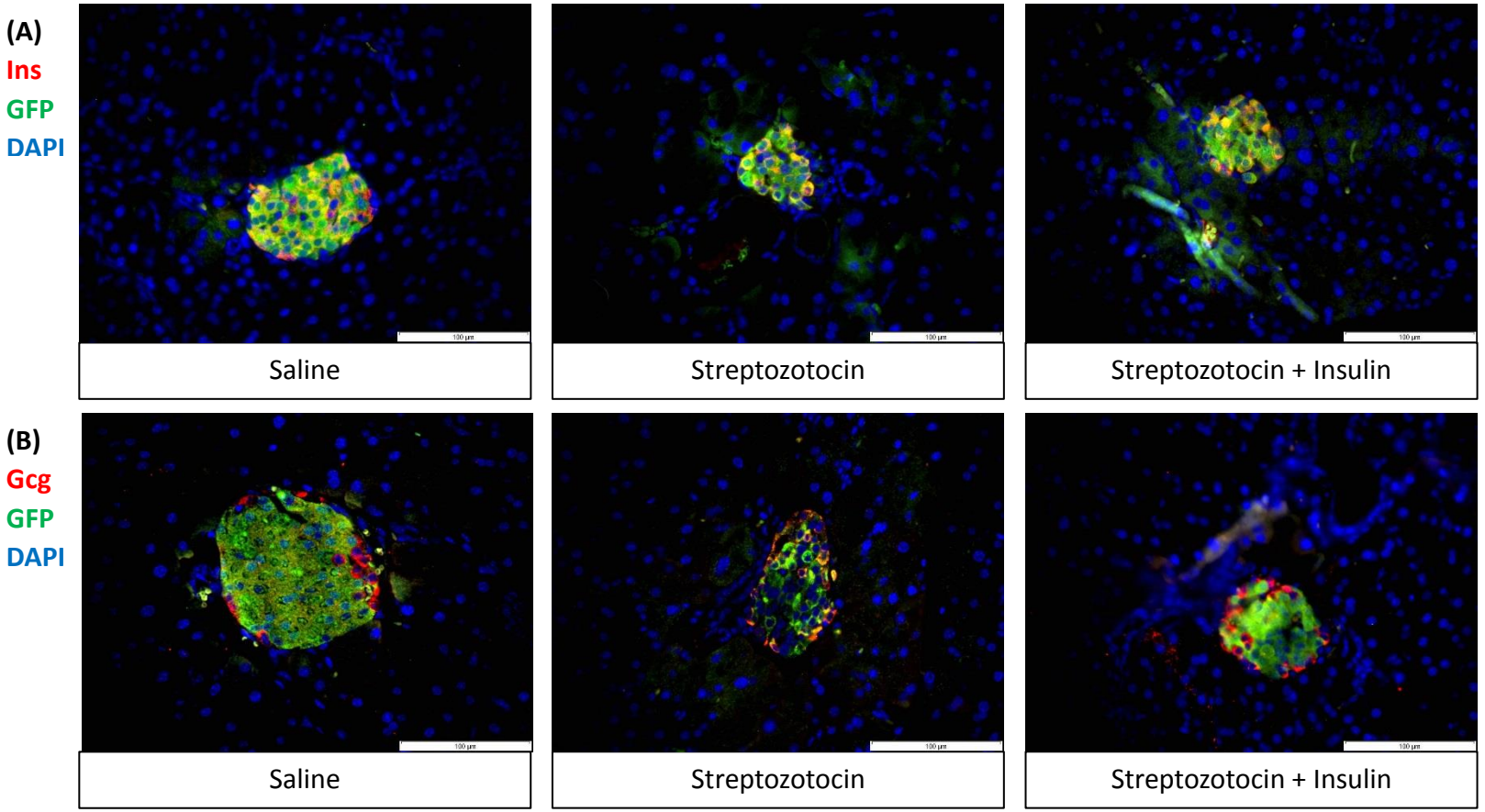

*Legend overleaf

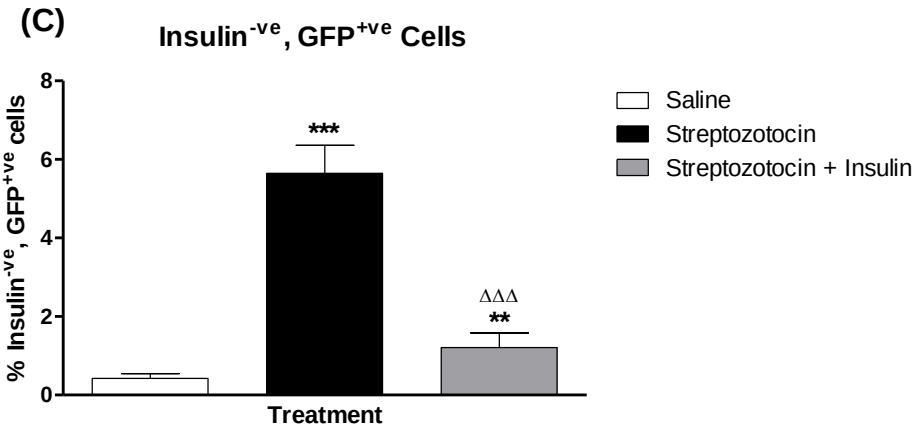

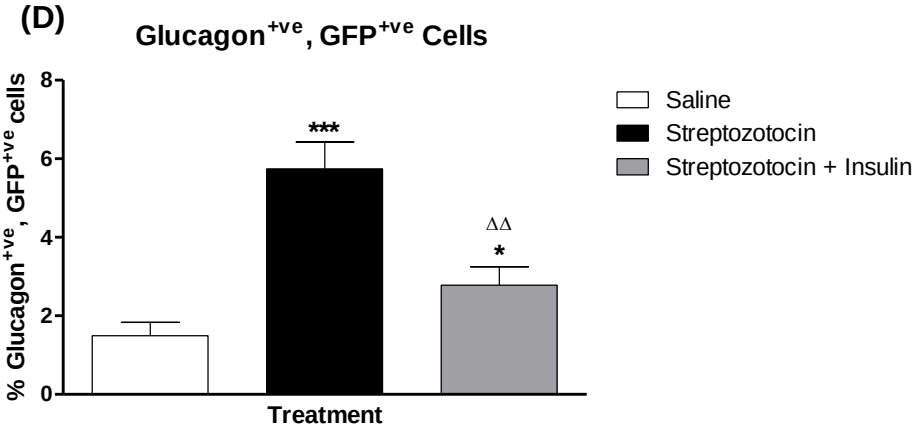

Transdifferentiation Analysis

Representative images of islets from mice treated with saline, streptozotocin and streptozotocin plus insulin stained for (A) insulin and GFP or (B) glucagon and GFP. Beta cell transdifferentiation determined by populations of insulin negative, GFP positive cells (C) and glucagon positive, GFP positive cells (D) using double immunofluorescence staining showing insulin/glucagon (red) and GFP (green).

Values are mean ± SEM (n=8 mice/group). Comparisons versus saline control (*) or versus streptozotocin (Δ), significant when */Δp<0.05, **/ΔΔp<0.01 and ***/ΔΔΔp<0.001.

Figure 5.33: Effects of streptozotocin alone or with insulin treatment on pancreatic beta cell and alpha cell apoptosis

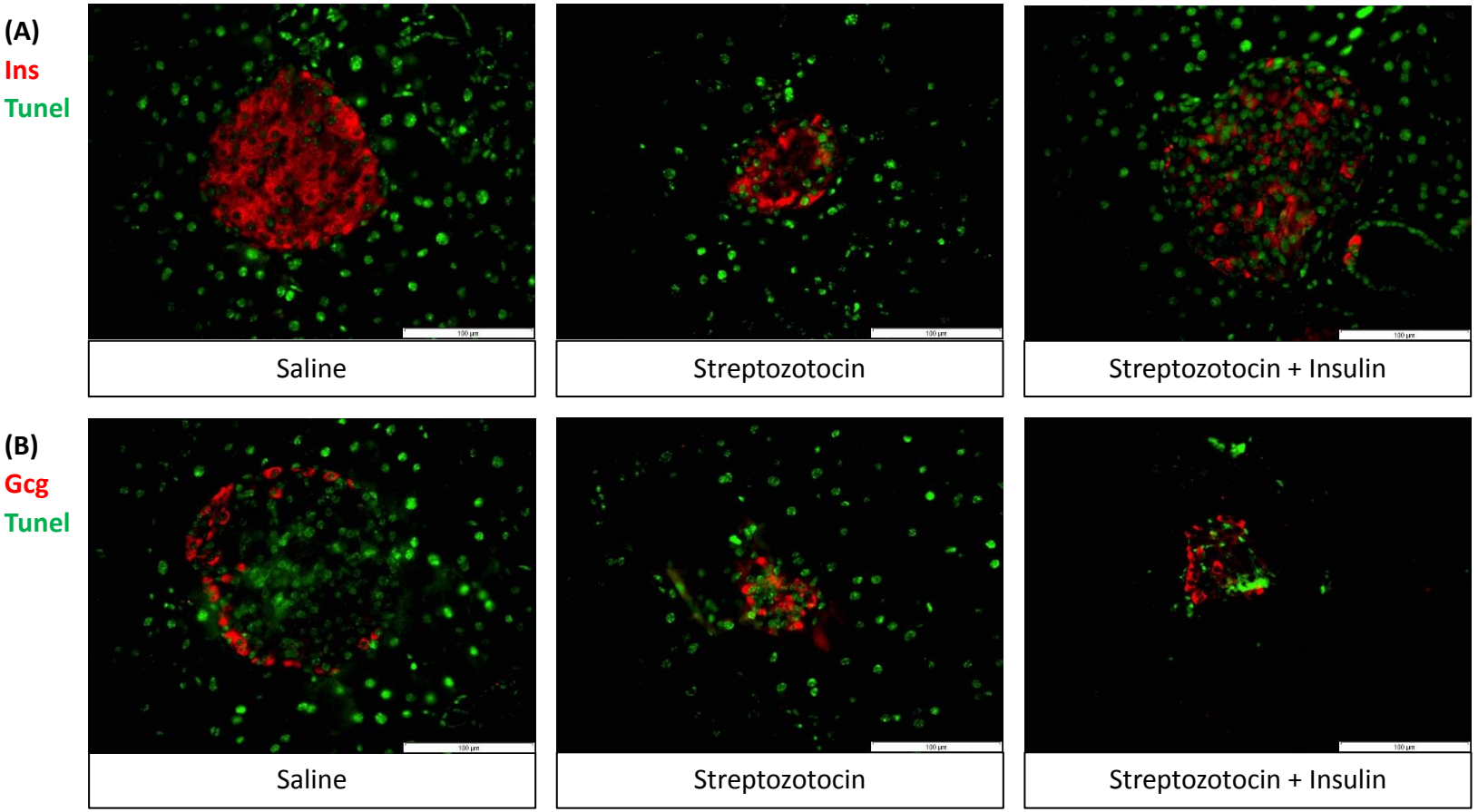

* Legend overleaf

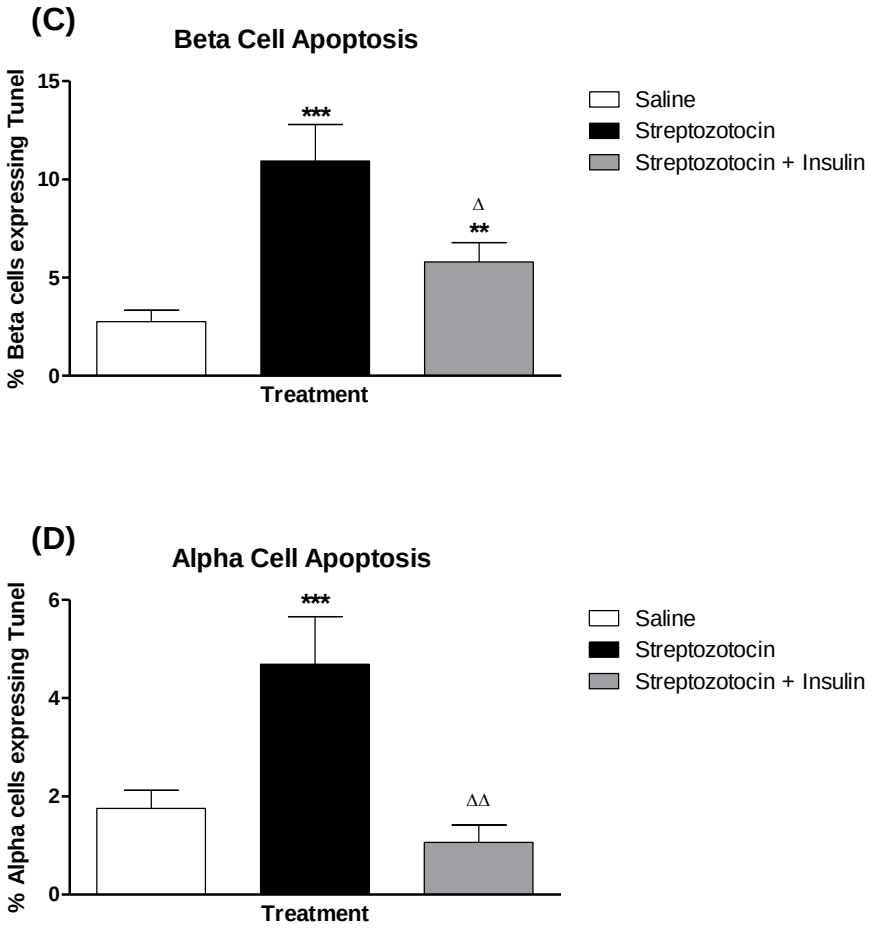

Apoptosis Analysis

Representative images of islets from mice treated with saline, streptozotocin and streptozotocin plus insulin stained for (A) insulin and TUNEL or (B) glucagon and TUNEL. Beta cell apoptosis and alpha cell apoptosis determined by populations of insulin positive, TUNEL positive (C) and glucagon positive, TUNEL positive (D) cells respectively by double immunofluorescence staining.

Values are mean ± SEM (n=8 mice/group). Comparisons versus saline control (*) or versus streptozotocin (Δ), significant when */Δp<0.05, **/ΔΔp<0.01 and ***p<0.001.

Figure 5.34: Effects of streptozotocin alone or with insulin treatment on pancreatic beta cell and alpha cell proliferation

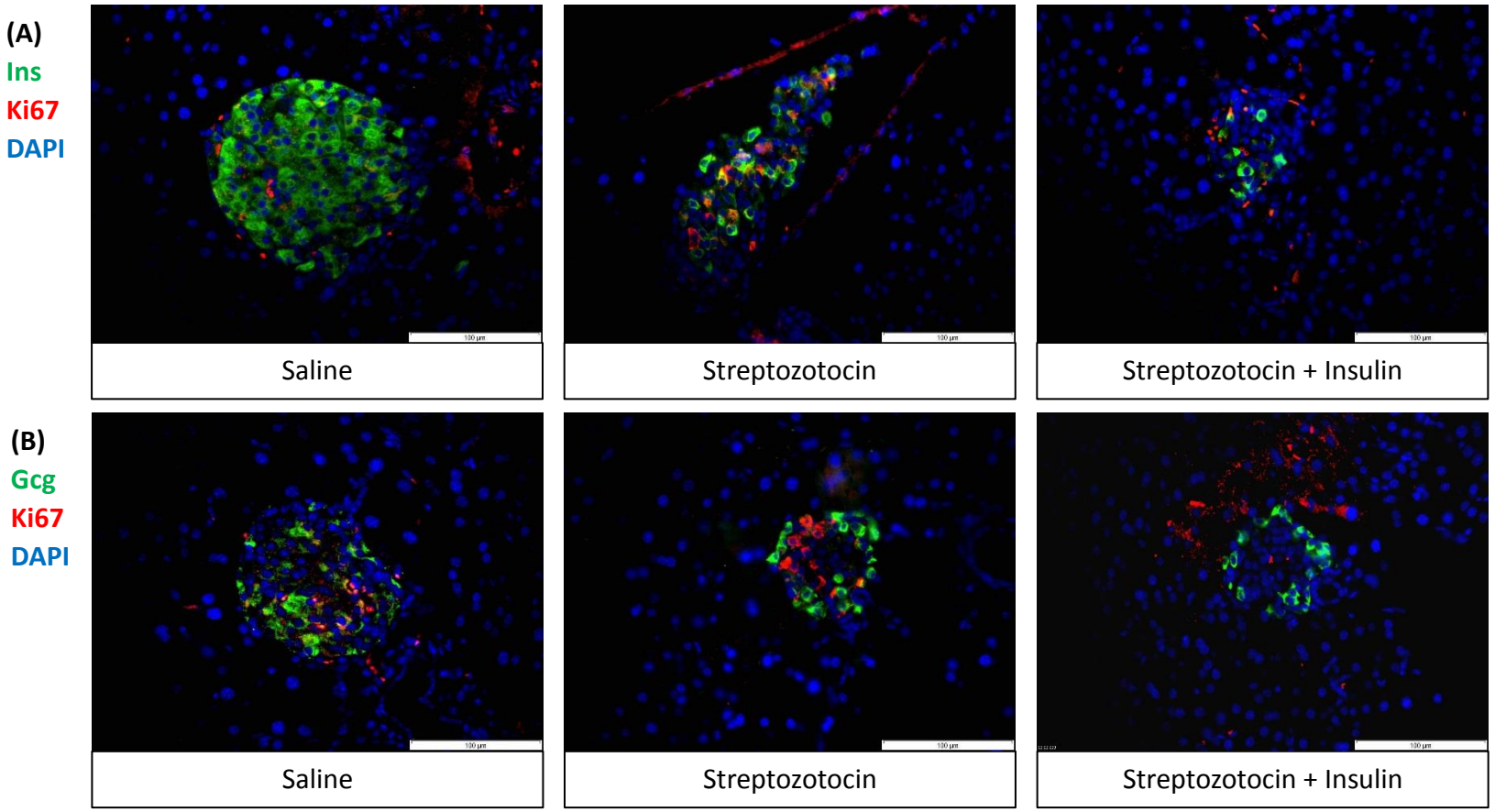

* Legend overleaf

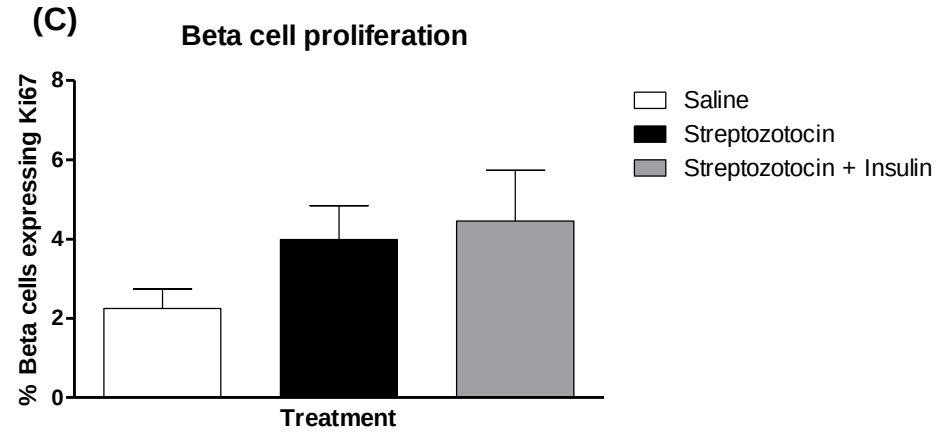

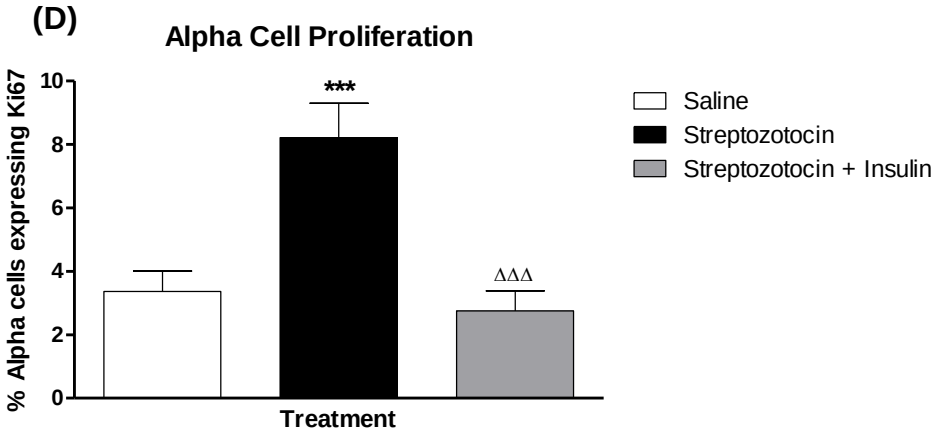

Proliferation Analysis

Representative images of islets from mice treated with saline, streptozotocin and streptozotocin plus insulin stained for (A) insulin and ki-67 or (B) glucagon and ki-67. Beta cell and alpha cell proliferation determined by populations of (C) insulin positive, ki-67 positive cell and (D) glucagon positive, ki-67 positive cells respectively.

Values are mean ± SEM (n=8 mice/group). Comparisons versus saline control (*) or versus streptozotocin (Δ), significant when */Δp<0.05, **/ΔΔp<0.01 and ***//ΔΔΔp<0.001.

Figure 5.35: Effects of streptozotocin alone or with insulin treatment on pancreatic beta cell Pdx1 expression

(A)

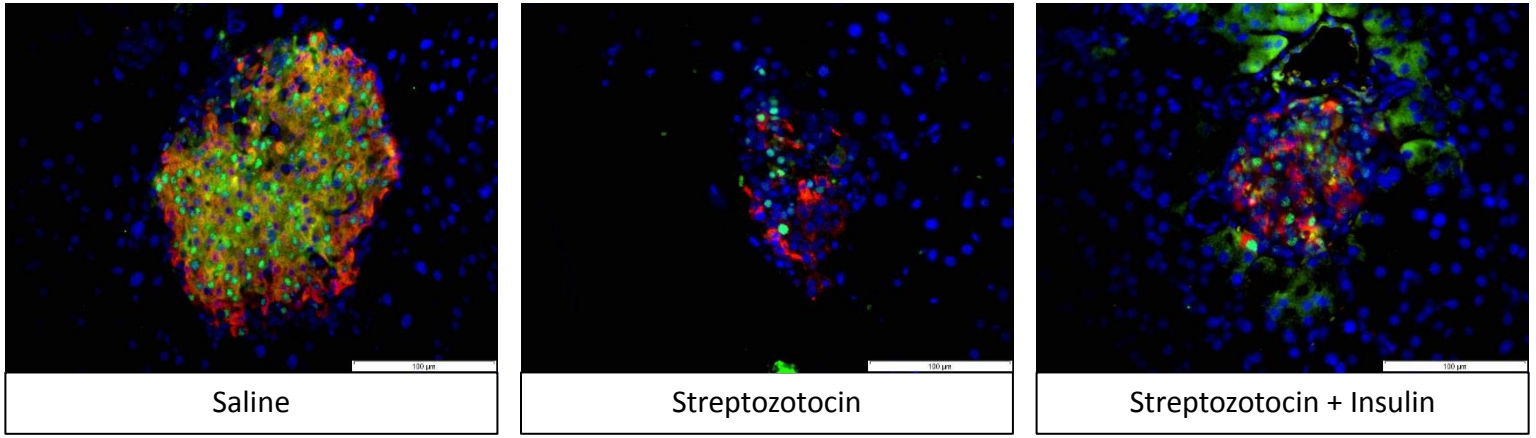

* Legend overleaf

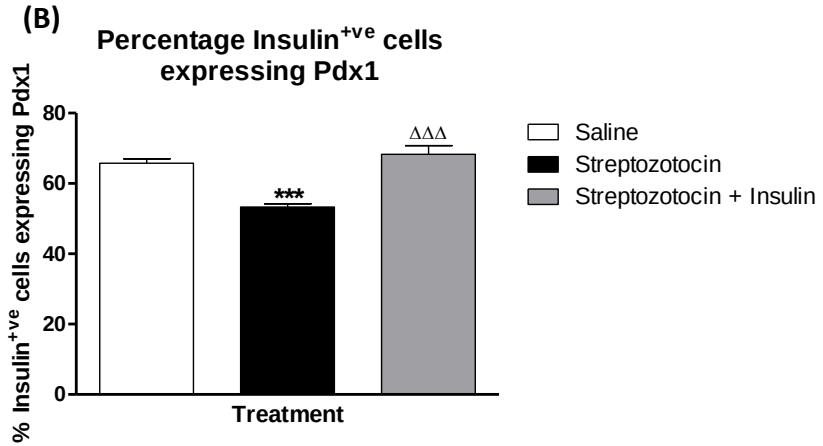

Pdx1 Expression Analysis

(A) Representative images of islets from mice treated with saline, streptozotocin and streptozotocin plus insulin on Pdx1 expression (B). Determined by histological analysis of insulin/Pdx1 double immunofluorescence staining showing insulin (red), Pdx1 (green) and DAPI (blue).

Values are mean ± SEM (n=8 mice/group). Comparisons versus saline control (*) or versus streptozotocin (Δ), significant when */Δp<0.05, **/ΔΔp<0.01 and ***p<0.001.

Chapter 6

Effect of apelin and xenin on islet morphology and beta-to-alpha cell transdifferentiation

6.1 Summary

Apelin and xenin are both peptides that have been shown to improve insulin secretion and beta cell function, survival and proliferation. Chemically modified versions of these peptides extend their biological half-life making them potential novel anti-diabetic agents for the future. In the present study, 10 days once daily treatment with 25nmol/kg pGlu-apelin-(Glut-pal)-amide or xenin-25-GluPal effectively reducing beta-to-alpha cell transdifferentiation in both streptozotocin and high fat feeding induced diabetes. Both agents displayed improved metabolic parameters and improvements in islet function showcasing their potential as anti-diabetic agents. Of note in streptozotocin-induced diabetes, both peptides were able to reduce circulating glucagon whilst elevating circulating insulin levels and increasing beta cell proliferation. Xenin in particular was as effective as liraglutide in suppressing streptozotocin induced hyperglycaemia whist conserving beta cell mass and limiting expansion of alpha cells. Similarly in diet-induced obese diabetic mice, both peptide agents were able to suppress circulating glucagon levels, improve glucose tolerance, limit islet beta and alpha cell expansion, and reduce beta cell apoptosis and alpha cell proliferation. Apelin in particular further suppressed alpha cell mass expansion by increasing alpha cell apoptosis. These studies outline the many beneficial properties both apelin and xenin based peptides elicit in diabetic animal models, including suppression of beta cell transdifferentiation.

6.2 Introduction

6.2.1 Apelin

Apelin was first discovered and isolated from adipose extracts. The 36 amino acid adipokine, either whole or truncated to apelin-13, binds to the APJ receptor expressed within the central nervous system and peripheral tissues to regulate angiogenesis, water homeostasis and energy homeostasis (Hu et al, 2016). The latter would implicate apelin's involvement in metabolic disorders such as diabetes and obesity. Apelin knock-out mice display impaired metabolism exhibiting hyperglycaemia, reduced glucose tolerance and insulin insensitivity. These were all improved by exogenous administration of apelin, strongly linking this adipokine in regulation of insulin sensitivity (Yu et al, 2010). Apelin levels are notably raised in both obese rodents and humans implicating its involvement in metabolism (Dray et al, 2008; Boucher et al, 2005). Central actions of apelin within the hypothalamus have been attributed to the peptide's ability to reduce appetite and food intake in mice (O'Harte et al, 2017) and rats (Sunter et al, 2003).

Apelin is degraded by ACE2 (angiotensin converting enzyme-2) which cleaves phenylalanine from the C-terminus, permitted further enzymatic degradation and loss of bioactivity (Murza et al, 2014). Previous research investigating peptide modifications have found that acylation of apelin-13 analogues resulted in significant extension of half-life without altering insulin stimulating ability (O'Harte et al, 2017). These author's concluded that beneficial effects of pGlu(Lys8GluPAL)apelin-13 amide in a diet-induced obese-diabetic mouse model were as effective as liraglutide in reducing blood glucose, normalising insulin levels, enhancing glucose tolerance and

insulin sensitivity (O'Harte et al, 2018). Notably apelin outperformed liraglutide in terms of reducing percentage body fat and improving bone mineral density (O'Harte et al, 2018). In akita mice apelin-13 has been shown to act within the pancreas to preserve islet mass and insulin content potentially by alleviating diabetes-induced endoplasmic reticulum (ER) stress (Chen et al, 2011).

6.2.2 Xenin

Xenin is a 25 amino acid peptide hormone secreted alongside GIP from the enteroendocrine K cells within the digestive tract (Anlauf et al, 2000; Feurle et al, 1992). Its actions within the body range from potentiating GIP's insulinotropic action, reducing gastric emptying, increasing gallbladder contractions and promoting breakdown of lipids and reducing lipogenesis (Martin et al, 2012; Wice et al, 2010). Xenin has been shown to suppress appetite, a feat attributed to its gastric effects as well as its central actions within the hypothalamus (Alexiou et al, 1998; Cooke et al, 2009) once xenin crosses the blood-brain barrier. With rapid degradation within 30 minutes, xenin has only been shown to potentiate glucose-stimulated insulin secretion when injected shortly before the glucose load is administered (Taylor et al, 2010). As a result, peptide modifications involving the addition of fatty acids have been carried out to improve enzymatic stability and extend pharmacokinetic ability (Martin et al, 2012; Irwin et al, 2006).

Xenin-25 has been shown to potentiate glucose-stimulated insulin release whilst promoting beta cell resistance against apoptosis both within pancreatic beta cell lines (BRIN-BD11) and isolated mouse islets (Taylor et al, 2010). Furthermore xenin-25 has

been demonstrated to potentiate the action of the incretin hormone GIP, making it a promising candidate for an anti-diabetic agent. In high fat fed mice modified xenin-25 has been shown to improve glucose tolerance and significantly reduce alpha cell area whilst increasing beta cell area (Parthsarathy et al, 2016).

Both of these non-classical peptides show great potential for consideration as next generation anti-diabetic therapies. They have been vigorously tested within diet-induced models of obesity-diabetes however little has been done investigating their effect on beta cell transdifferentiation in this model or within streptozotocin-induced diabetes. The present Chapter aims to investigate this utilising transgenic *Ins1*$^{cre/+}$;Rosa26-eYFP C57Bl/6 mice.

6.3 Methods

A brief summary of the methods implemented are outlined below. For full descriptions of methods and materials used please refer to Chapter 2.

6.3.1 Animals

12 week old male *Ins1*$^{cre/+}$;Rosa26-eYFP C57Bl/6 mice had diabetes induced via 5 daily intraperitoneal injections of 50mg/kg streptozotocin, freshly dissolved in citrate buffer. Mice presented with clear diabetic symptoms within the following 5 days post dosing. Modified apelin (pGlu-apelin-(Glut-pal)-amide) or modified xenin-25 (xenin-25-GluPal) were both administered at 25nmol/kg by once daily intraperitoneal injections for two days prior to administration of streptozotocin and this was

continued for each day until the end of the study at day 10. For high-fat fed studies, mice were kept on a 45% fat content high fat diet from the time of weaning at 4 weeks old for 11 weeks by which time mice were obese. Experiments were conducted with these high fat fed mice at 15 weeks of age. In line with the other models, mice were dosed with 25nmol/kg pGlu-apelin-(Glut-pal)-amide or 25nmol/kg xenin-25-GluPal by daily intraperitoneal injections for 10 days. Prior to the end of the study, a glucose tolerance test was conducted on high-fat fed mice. Following an overnight fast, mice were subjected to an 18.8mMol/kg glucose load with blood glucose assessed regularly for the following hour. A timeline outlining these studies is displayed in Figure 6.0. For all studies, mice were 8 per treatment group, or 6 where stated. Body weight, blood glucose, calorie and fluid consumption were monitored as stated. Peptide modification, dose and dosing schedule was chosen based on established literature and previous studies carried out within the lab (Martin et al, 2012; Parthsarathy et al, 2017; Parthsararthy et al, 2018; O'Harte et al, 2018; O'Harte et al, 2017). Data for saline, streptozotocin, high-fat fed and hydrocortisone controls are reused from Chapter 4.

All mice were kept individually housed during the time of experiments within holding rooms maintained at 22±2°C kept on a 12 hour light/dark cycle. Mice had free access to drinking water and standard chow or high fat chow, where appropriate. All breeding and studies were approved by Ulster University Animal Ethics Review Committee and conducted in accordance to UK Animals (Scientific Procedures) Act 1986.

6.3.2 Biochemical Analysis

Longitudinally sectioned pancreatic tissue was snap frozen within liquid nitrogen at the end of each study and stored at -70°C before processing. Tissues were homogenised in acid ethanol and centrifuged at 3000rpm for 15 minutes at 4°C. The supernatant was transferred to fresh tube and TRIS buffer was added to extract protein. Protein homogenates were put though an in-house radioimmunoassay to determine insulin content, a Bradford assay to determine total protein content and an ELISA to determine glucagon levels. Non-fasting plasma insulin was also determined by radioimmunoassay whilst plasma glucagon was assessed by ELISA. Both Bradford and ELISA were performed in line with the manufacturer's guidelines.

6.3.3 Immunohistochemistry

Longitudinally cut pancreatic tissue was collected from mice at the end of each study and fixed in 4% paraformaldehyde for 48 hours. Fixed tissues were then processed using a Leica automated tissue processor before embedding in wax blocks and sectioned into 5µm slices onto polysine coated slides. To begin immunohistochemistry slides were immersed in xylene to remove wax and rehydrated in a series of ethanol solutions (100 – 50%). Antigen retrieval was carried out in citrate buffer heated to 95°C, followed by blocking in a 4% BSA solution. Slides were incubated with primary antibodies overnight at 4°C, with the following antibodies used: mouse monoclonal anti-insulin antibody (ab6995, 1:1000; Abcam), guinea-pig anti-glucagon antibody (PCA2/4, 1:200; raised in-house), rabbit anti-Ki67 antibody (ab15580, 1:200; Abcam) and rabbit anti-Pdx1 antibody (ab47267, 1:200;

Abcam). The next day slides were washed in PBS before incubating with secondary antibody at 37°C**.** The following secondary antibodies were used where appropriate: Alexa Fluor488 goat anti-guinea pig IgG — 1:400, Alexa Fluor 594 goat anti-mouse IgG — 1:400, Alexa Fluor 488 goat anti-rabbit IgG — 1:400, Alexa Fluor 594 goat anti-rabbit IgG — 1:400 or Alexa Fluor 488 donkey anti-goat IgG — 1:400. To stain nuclei a final incubation was carried out at 37°C with 300nM DAPI. To assess apoptosis a TUNEL assay was carried out following manufacturer's guidelines (In situ cell death kit, Fluorescein, Roche Diagnostics, UK). Stained slides were mounted and kept at 4°C, covered from light until ready to image. Imaging was carried out using an Olympus fluorescent microscope fitted with DAPI (350nm) FITC (488nm) and TRITC (594nm) filters and a DP70 camera adapter system.

6.3.4 Image Analysis

Images were analysed by an experienced user on Cell^F imaging software to assess: islet area, beta cell area, alpha cell area (expressed at μm^2), percentage beta cells and percentage alpha cells. For islet size distribution islets were defined as small, medium or large if they were <10,000μm^2, 10,000-25,000μm^2 or 25,000μm^2 respectively. Islet architecture was defined by the proportion of islets displaying central alpha cells. To define beta cell transdifferentiation insulin, GFP staining was assessed by quantifying the number of insulin negative, GFP positive staining cells, whilst glucagon, GFP staining was assessed by quantifying glucagon positive, GFP positive staining cells. Beta cell and alpha cell apoptosis was quantified by counting the number of insulin positive or glucagon positive, TUNEL positive cells respectively.

Similarly this was done to analyse proliferation in beta and alpha cells using ki-67 co-stained with insulin or glucagon respectively. ImageJ software was used to quantify beta cell Pdx1 expression, expressed as a percentage of the number of insulin positive cells expressing Pdx1. All counts were determined in a blinded manner with >60 islets analysed per treatment group.

6.3.5 Statistics

GraphPad PRISM v.5 software was used to generate and analyse all figures, with data presented as mean ± SEM. Comparative analysis between two groups was carried out using Student's unpaired t-test. To compare multiple groups one-way ANOVA tests were conducted using a Bonferroni post-hoc test. Similarly to compare multiple groups over various time points a repeated measures two-way ANOVA test was conducted using a Bonferroni post-hoc test. Results were classed significant when $p<0.05$.

6.4 Results

6.4.1 Effect of streptozotocin alone or in combination with pGlu-apelin-(Glut-pal)-amide or xenin-25-GluPal treatment on body weight, energy intake and fluid intake

Compared to the streptozotocin treated group, mice additionally given apelin and xenin showed reduced percentage body weight change (apelin -3.3 ± 1.0%, $P<0.001$ and xenin -2.0 ± 0.9%, $P<0.001$ vs STZ -7.6 ± 0.6%, Figure 6.1B). Cumulative energy

intake was similarly reduced in apelin treated mice compared to streptozotocin alone (407.7 ± 7.6 vs 445.5 ± 9.0kJ, P<0.01, Figure 6.1C). Xenin treated mice however displayed energy consumption equivalent to streptozotocin treated mice. Peculiarly, cumulative fluid consumption was greatly increased by both apelin and xenin treatments from as early as day 4 of the study, ultimately peaking at the final day (day 10 apelin 140.6 ± 8.7ml, P<0.001 and day 10 xenin 148.8 ± 8.5ml vs day 10 STZ 94.9 ± 3.4ml, P<0.001, Figure 6.1D).

6.4.2 Effects of streptozotocin alone or in combination with pGlu-apelin-(Glut-pal)-amide or xenin-25-GluPal treatment on blood glucose, plasma insulin/glucagon and pancreatic insulin/glucagon content

Both apelin and xenin treated groups of mice exhibited characteristic streptozotocin induced hyperglycaemia, albeit onset of this was delayed (Figure 6.2A). Xenin treatment in particular reduced final blood glucose comparative to streptozotocin (21.3 ± 1.5 vs 26.3 ± 1.4mM, P<0.05, Figure 6.2B). Plasma insulin was restored by both apelin (9.1 ± 1.0ng/ml) and xenin (7.6 ± 0.9ng/ml) treatments to levels comparable to non-diabetic mice (9.2 ± 1.1ng/ml, Figure 6.2C). Pancreatic insulin content was reduced by streptozotocin treatment, with apelin and xenin groups having no additional impact on this parameter (Figure 6.2D). Plasma glucagon was considerably reduced by both apelin and xenin compared to streptozotocin (apelin 0.029 ± 0.003ngml, p<0.01 and xenin 0.025 ± 0.004ng/ml vs 0.080 ± 0.009ng/ml, p<0.001, Figure 6.2E) to levels equivalent to non-diabetic mice. Similar to pancreatic

insulin content, glucagon content was unchanged by apelin and xenin treatments compared to streptozotocin alone (Figure 6.2F).

6.4.3 Effects of streptozotocin alone or in combination with pGlu-apelin-(Glut-pal)-amide or xenin-25-GluPal treatment on islet parameters

Representative images of saline, streptozotocin, streptozotocin plus pGlu-apelin-(Glut-pal)-amide and streptozotocin plus xenin-25-GluPal treated islets stained for insulin (red) and glucagon (green) with nuclei (blue) are shown in Figure 6.3A. Treatment with apelin resulted in a reduction in islet area (5344 ± 600.5µm^2 vs 8893 ± 942.5µm^2, $p<0.01$, Figure 6.3B) and beta cell area (3479 ± 413.2µm^2 vs 7546 ± 814.0µm^2, $p<0.01$, Figure 6.3C) equivalent to that found in streptozotocin alone however alpha cell area was not raised (Figure 6.3D). Xenin however protected against streptozotocin induced changes increasing islet area (6870 ± 889.5 vs 4407 ± 393.3µm, $p<0.05$, Figure 6.3B) and beta cell area (4875 ± 656.0 vs 3309 ± 287.5µm^2, $p<0.05$, Figure 6.3C) whilst reducing alpha cell area (1776 ± 161.8 vs 2635 ± 271.8µm^2, $p<0.01$, Figure 6.3D). Islet size distribution was similar between apelin and xenin groups with both treatments increasing the proportion of small and large-sized islets whilst reducing medium-sized islets (figure 6.3E). Similar to previous changes only xenin treatment was able to elicit increases in percentage beta cells (63.8 ± 1.5 vs 58.9 ± 1.8%, $p<0.05$, Figure 6.3F) and reductions in percentage alpha cells (36.2 ± 1.5 vs 43.1 ± 2.1%, $p<0.01$, Figure 6.3G). Islet architecture determined by the percentage of islets with central alpha cells was improved by apelin and xenin (apelin 42.7 ± 4.0%,

p<0.001 and xenin 45.5 ± 3.7% vs 70.0 ± 4.4%, p<0.001, Figure 6.3H) but still disrupted compared to non-diabetic islets (20.0 ± 4.0%, Figure 6.3H).

6.4.4 Effects of streptozotocin alone or in combination with pGlu-apelin-(Glut-pal)-amide or xenin-25-GluPal treatment on beta-to-alpha cell transdifferentiation

Representative images of islets stained for insulin (red) and GFP (green) or glucagon (red) and GFP (green) are shown in Figure 6.4A and B respectively. Both apelin and xenin were able to reduce both the number insulin negative, GFP positive cells (apelin 1.6 ± 0.3%, p<0.001 and xenin 1.7 ± 0.4% vs STZ 5.6 ± 0.7%, p<0.001, Figure 6.4C) and those showing glucagon positive, GFP positive cells (apelin 2.8 ± 0.4%, p<0.001 and xenin 2.7 ± 0.5% vs STZ 5.7 ± 0.7%, p<0.001, Figure 6.4D).

6.4.5 Effects of streptozotocin alone or in combination with pGlu-apelin-(Glut-pal)-amide or xenin-25-GluPal treatment on beta cell and alpha cell apoptosis

Beta cell and alpha cell apoptosis were determined by insulin and glucagon plus TUNEL staining, with representative islets shown in Figure 6.5A and B respectively. Beta cell apoptosis was raised by treatment with streptozotocin with apelin and xenin preventing this (apelin 6.3 ± 1.2%, p<0.05 and xenin 3.8 ± 0.7%, p<0.001 vs STZ 10.9 ± 1.9%, Figure 6.5C). Similarly alpha cell apoptosis was found to be raised by streptozotocin, however treatment with xenin was able to reduce this (2.5 ± 0.6 vs 4.7 ± 1.0%, p<0.05, Figure 6.5D).

6.4.6 Effect of streptozotocin alone or in combination with pGlu-apelin-(Glut-pal)-amide or xenin-25-GluPal treatment on beta cell and alpha cell proliferation

Representative images of islets stained for ki-67 with either insulin (Figure 6.6A) or glucagon (Figure 6.6B) were used to assess beta cell and alpha cell proliferation respectively. Both apelin and xenin were able to elicit substantial elevations in beta cell proliferation (apelin 9.1 ± 1.1%, $p<0.01$ and xenin 9.0 ± 1.4%, $p<0.01$ vs STZ 4.0 ± 0.9%, Figure 6.6C), whilst alpha cell proliferation remained unchanged (Figure 6.6D).

6.4.7 Effects of streptozotocin alone or in combination with pGlu-apelin-(Glut-pal)-amide or xenin-25-GluPal treatment on beta cell Pdx1 expression

Figure 6.7A displays representative images of islets stained for insulin (red) and Pdx-1 (green) counterstained with dapi (blue). Apelin and xenin were able to significantly increase the percentage of beta cells expressing Pdx-1 against streptozotocin treated mice (apelin 63.0 ± 1.4%, $p<0.001$ and xenin 58.4 ± 1.7% vs 53.3 ± 1.0%, $p<0.001$, Figure 6.7B) with only the former restoring Pdx-1 expression to levels similar to non-diabetic mice.

6.4.8 Effect of high fat feeding alone or in combination with liraglutide or sitagliptin treatment on body weight, energy intake and fluid intake

Neither peptide impacted body weight or cumulative energy intake. Cumulative fluid intake however was reduced in both treatment groups as early as day 5 of the study

until the final day (day 12 apelin 134.6 ± 6.3ml, p<0.001 and day 12 xenin 129.9 ± 3.2ml vs day 12 high fat fed saline 215.9 ± 6.9ml, p<0.001, Figure 6.8D).

6.4.9 Effects of high fat feeding alone or in combination with apelin or xenin treatment on blood glucose, plasma insulin/glucagon, pancreatic insulin/glucagon and glucose tolerance test

Non-fasting blood glucose levels were largely unaltered throughout the study (Figure 6.9A) however on the final day mice within the xenin group displayed a mild reduction in blood glucose (7.9 ± 0.2 vs 8.7 ± 0.3mM, p<0.05, figure 6.9B). Circulating insulin levels were unchanged by these peptide treatments (figure 6.9C) although pancreatic insulin content was found raised by apelin and xenin (apelin 65.9 ± 8.8ng/ml, p<0.001 and xenin 73.8 ± 3.6 vs 54.6 ± 3.0ng/ml, p<0.001, Figure 6.9D). As seen previously, apelin and xenin also exerted a plasma glucagon lowering effect in high fat fed mice (apelin 0.022 ± 0.003ng/ml, p<0.001 and xenin 0.020 ± 0.007 vs 0.05 ± 0.003ng/ml, p<0.001, Figure 6.9E) despite having no effect on pancreatic glucagon content (Figure 6.F). At the end of the study an ip GTT was carried out with only xenin treated mice showing a reduction in blood glucose at 60 minutes (19.3 ± 1.1 vs 23.8 ± 1.2mM, p<0.05, Figure 6.9G), despite overall AUC being unchanged (Figure 6.9H).

6.4.10 Effects of high fat feeding alone or in combination with pGlu-apelin-(Glut-pal)-amide or xenin-25-GluPal treatment on islet parameters

Representative images of islets from each treatment group are displayed in Figure 6.10A. Treatment with modified apelin resulted in a significant reduction in islet area

(14160 ± 1480 vs 19360 ± 1567μm^2, p<0.05, Figure 6.10B) due to reductions in both beta cell (12300 ± 1314 vs 16590 ± 1347μm^2, p<0.05, Figure 6.10C) and alpha cell (1863 ± 196.6 vs 2778 ± 258.0μm^2, p<0.05, Figure 6.10D) areas. Modified xenin elicited similar reductions in islet area, beta cell area and alpha cell area (14280 ± 1257μm^2, p<0.05, 12330 ± 1125μm^2, p<0.05 and 1945 ± 156.7μm^2, p<0.05, Figure 6.10B-D respectively) within high fat fed mice. Similarly both apelin and xenin elicited a change in islet size, with smaller islets predominating (Figure 6.10E). Percentage beta and alpha cells were unaltered by these treatment groups (Figure 6.10F-G). Number of islets displaying irregular central alpha cells was reduced by apelin treatment only (29.2 ± 2.3 vs 41.3 ± 3.9%, p<0.05, Figure 6.10H).

6.4.11 Effects of high fat feeding alone or in combination with pGlu-apelin-(Glut-pal)-amide or xenin-25-GluPal treatment on beta-to-alpha cell transdifferentiation

Representative images of islets stained for insulin with GFP and glucagon with GFP are presented in Figure 6.11A-B respectively. Modified apelin and xenin both markedly reduced the number of insulin deficient beta cells (apelin 2.9 ± 0.3%, p<0.001 and xenin 2.5 ± 0.3%, p<0.001, vs STZ 6.9 ± 0.8%, Figure 6.11C). Similarly these treatments were able to significantly reduce the number of glucagon positive beta cells (apelin 3.3 ± 0.5%, p<0.001 and xenin 2.1 ± 0.3%, p<0.001 vs STZ 6.7 ± 0.6%, Figure 6.11D).

6.4.12 Effects of high fat feeding alone or in combination with pGlu-apelin-(Glut-pal)-amide or xenin-25-GluPal treatment on beta and alpha cell apoptosis

Representative images of islets stained with TUNEL to determine in beta cell and alpha cell apoptosis are shown in Figure 6.12A and B respectively. Remarkably apelin and xenin treatments were both able to markedly reduce beta cell apoptosis to levels comparable to non-diabetic mice (apelin 2.2 ± 0.5%, $p<0.01$ and xenin 1.7% ± -0.4%, $p<0.001$ vs HFF 4.9 ± 0.7%, Figure 6.12C). alpha cell death was unaffected by either peptide treatment.

6.4.13 Effects of high fat feeding alone or in combination with pGlu-apelin-(Glut-pal)-amide or xenin-25-GluPal treatment on beta and alpha cell proliferation

Representative images of islets stained for ki-67 used to determine beta cell and alpha cell proliferation are shown in Figure 6.13A-B respectively. In high fat fed mice apelin and xenin had no effect on beta cell proliferation compared to high fat feeding alone. In regards to alpha cell proliferation, both treatments elicited a substantial reduction (apelin 2.4 ± 0.5%, $p<0.01$ and xenin 2.5 ± 0.7%, $p<0.05$ vs HFF 5.7 ± 0.9%, Figure 6.13D).

6.4.14 Effect of high fat feeding alone or in combination with pGlu-apelin-(Glut-pal)-amide or xenin-25-GluPal treatment on beta cell Pdx1 expression

Representative images showcasing beta cell Pdx1 expression from high fat fed apelin or xenin treated mice are shown in Figure 6.14A. Both treatments were able to

maintain Pdx1 expression within beta cells compared to high fat fed saline treated mice (apelin 54.2 ± 1.1%, $p<0.01$ and xenin 55.8 ± 1.1% vs 49.6 ± 1.3%, $p<0.001$, Figure 6.14B).

6.5 Discussion

Building upon the previous data investigating current anti-diabetic agents on beta cell transdifferentiation, the present study focuses on two relatively novel, non-classical peptides, apelin and xenin. In these studies, both peptides were chemically modified to prolong their circulating half-life as described previously (Martin et al, 2012; Parthsarathy et al, 2018).

In streptozotocin-induced diabetes, both apelin and more profoundly xenin were able to reduce the number of islets showing beta-to-alpha cell transdifferentiation whilst maintaining beta cell maturity by Pdx-1 expression. This may be in part due to their ability to suppress streptozotocin-induced hyperglycaemia, allowing for a healthier metabolic environment in which beta cells were not forced to transdifferentiate (Cinti et al, 2015). Despite eliciting a reduction in alpha cell apoptosis, xenin was able to significantly prevent the streptozotocin-induced increase in alpha cell mass, whereas apelin therapy fell short of significance. Given that alpha cell proliferation was largely unchanged it can be deduced that the ability of xenin to prevent beta-to-alpha cell transdifferentiation is predominantly responsible for conserving beta cell mass and limiting alpha cell expansion. Unlike other tested anti-diabetic agents, apelin and xenin were able to stimulate beta cell proliferation in streptozotocin-treated mice. Similarly both peptides were able to

restore circulating insulin and glucagon levels in these mice. Whether this effect would be similar in humans is undetermined, but such an effect would make these peptides a tempting treatment for diabetes.

Quite consistently modified apelin and xenin were effective at preventing beta-to-alpha cell transdifferentiation in diet-induced diabetes. Both peptides were effective at preventing diet-induced alpha cell proliferation. As a results of these two effects, alpha cell mass was largely reduced to levels comparable to lean non-diabetic mice. In particular, xenin also exerted this effect on alpha cell mass by increasing alpha cell apoptosis. Contrasting with streptozotocin diabetes, these agents had no effect on beta cell proliferation in high fat fed mice but they were highly effective at reducing beta cell apoptosis. In high-fat fed mice both agent suppressed circulating glucagon levels a feat similarly observed in streptozotocin diabetic mice.

Consistent with previous studies, pGlu-apelin-(Glut-pal)-amide and xenin-25-GluPal performed as expected improving pancreatic insulin content, reducing plasma glucagon levels and enhancing glucose tolerance in high-fat fed mice. This apelin analogue performed well in streptozotocin-induced diabetic mice improving plasma insulin and reducing plasma glucagon. The study reported by O'Harte et al (2017), pGlu-apelin-(Glut-pal)-amide did not elicit a reduction in calorie consumption in high-fat fed mice but it did decrease feeding in streptozotocin-treated mice. The lack of effect could be in part due to the short duration of the present studies. Xenin-25-GluPal appeared to outperform apelin in streptozotocin-treated mice by reducing non-fasting blood glucose levels in addition to sharing the beneficial effects exerted by apelin. The efficacy of these peptides in glucose-lowering capability may have

matched that of liraglutide had they been dosed twice daily instead of a single daily dose.

These studies outline the beneficial effects of apelin and xenin as potential anti-diabetic therapies. In many respects, these novel peptide therapeutics have performed as well as the current gold standard incretin therapy, liraglutide.

Figure 6.0: Timeline of *Ins1*$^{cre/+}$;Rosa26-eYFP C57Bl/6 Studies

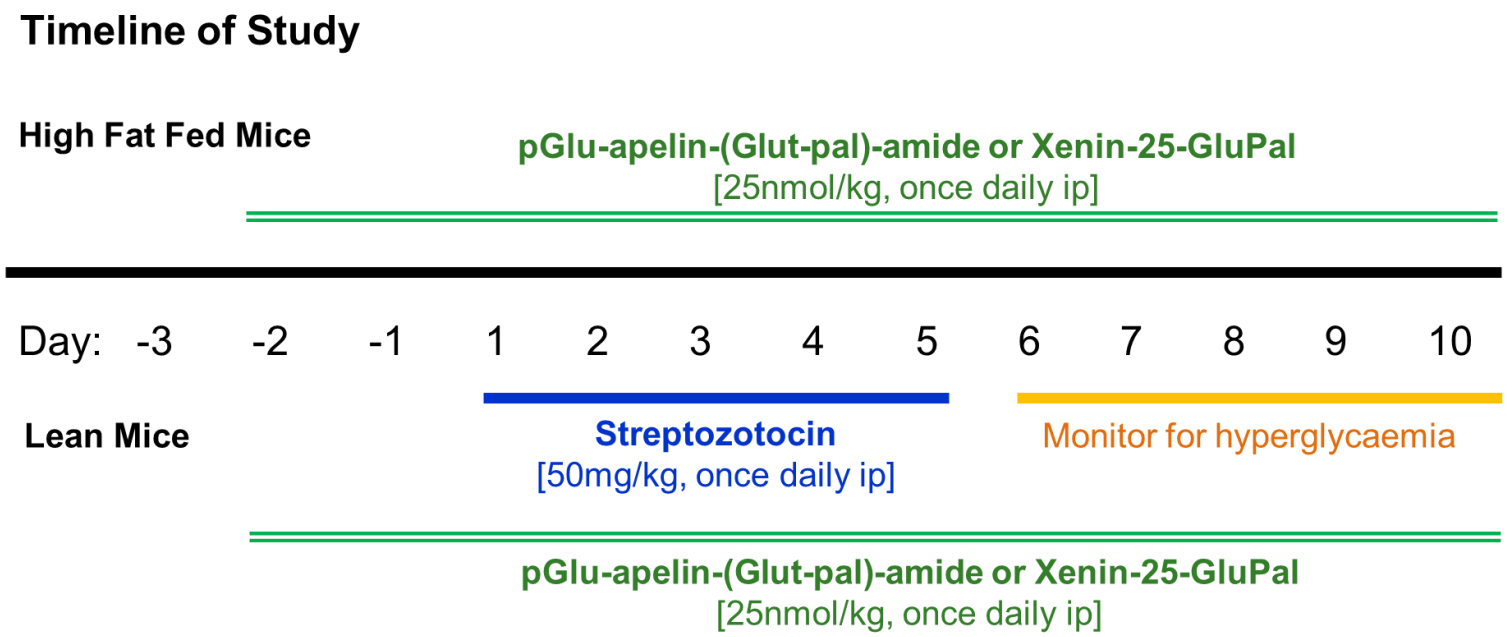

Figure 6.1: Effects of streptozotocin alone or in combination with pGlu-apelin(Glut-pal)-amide or xenin-25-GluPal on body weight, cumulative energy intake and cumulative fluid intake

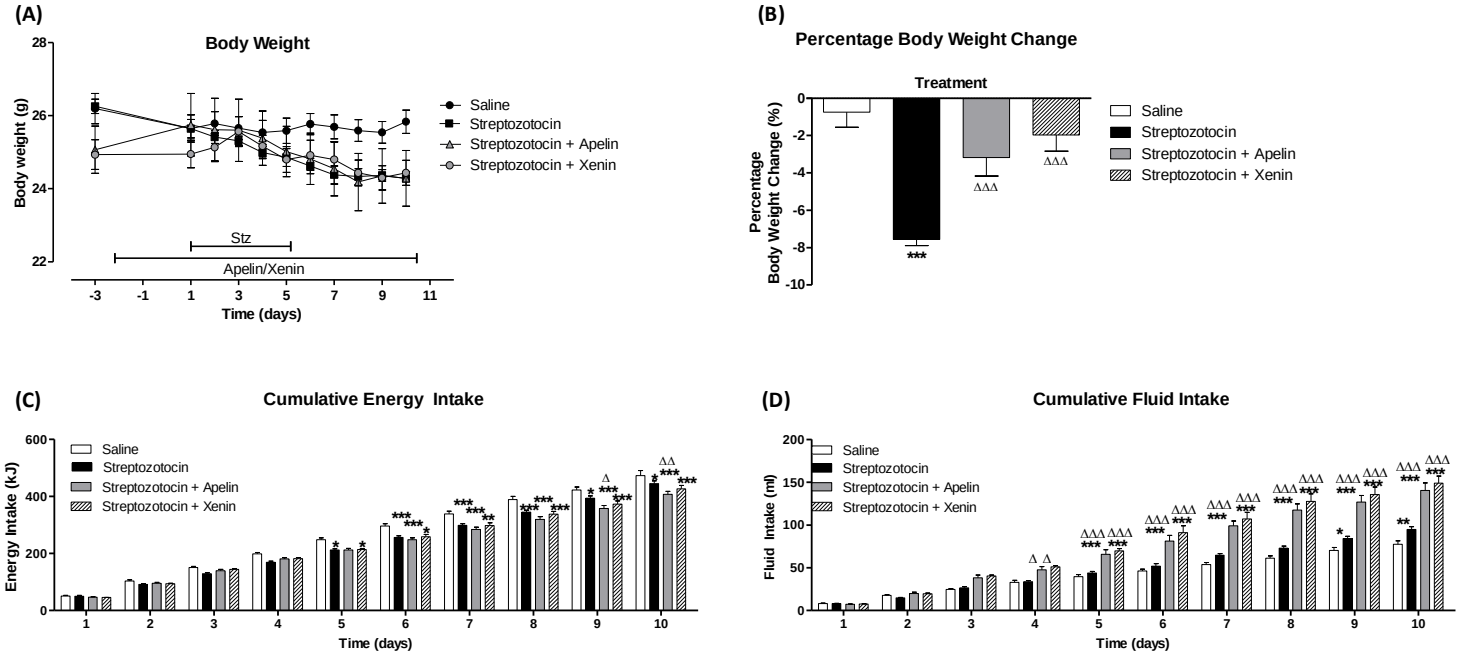

12 week old InsCre;Rosa26-eYFP C57Bl/6 mice were treated with pGlu-Apelin-(Glut-pal)amide or xenin-25-GluPal for two days prior to and in conjunction with administration of streptozotocin (50mg/kg, ip, once daily), n=8 mice/group. (A) Body weight, (B) percentage body weight change, (C) cumulative energy intake and (D) cumulative fluid intake. Comparisons were made against saline (*) or against streptozotocin treated (Δ). Values were significant when $p<0.05$ */Δ, $p<0.01$ **/ΔΔ and $p<0.001$ ***/ΔΔΔ.

Figure 6.2: Effects of streptozotocin alone or in combination with pGlu-apelin(Glut-pal)-amide or xenin-25-GluPal on blood glucose, plasma insulin, pancreatic insulin content, plasma glucagon and pancreatic glucagon content

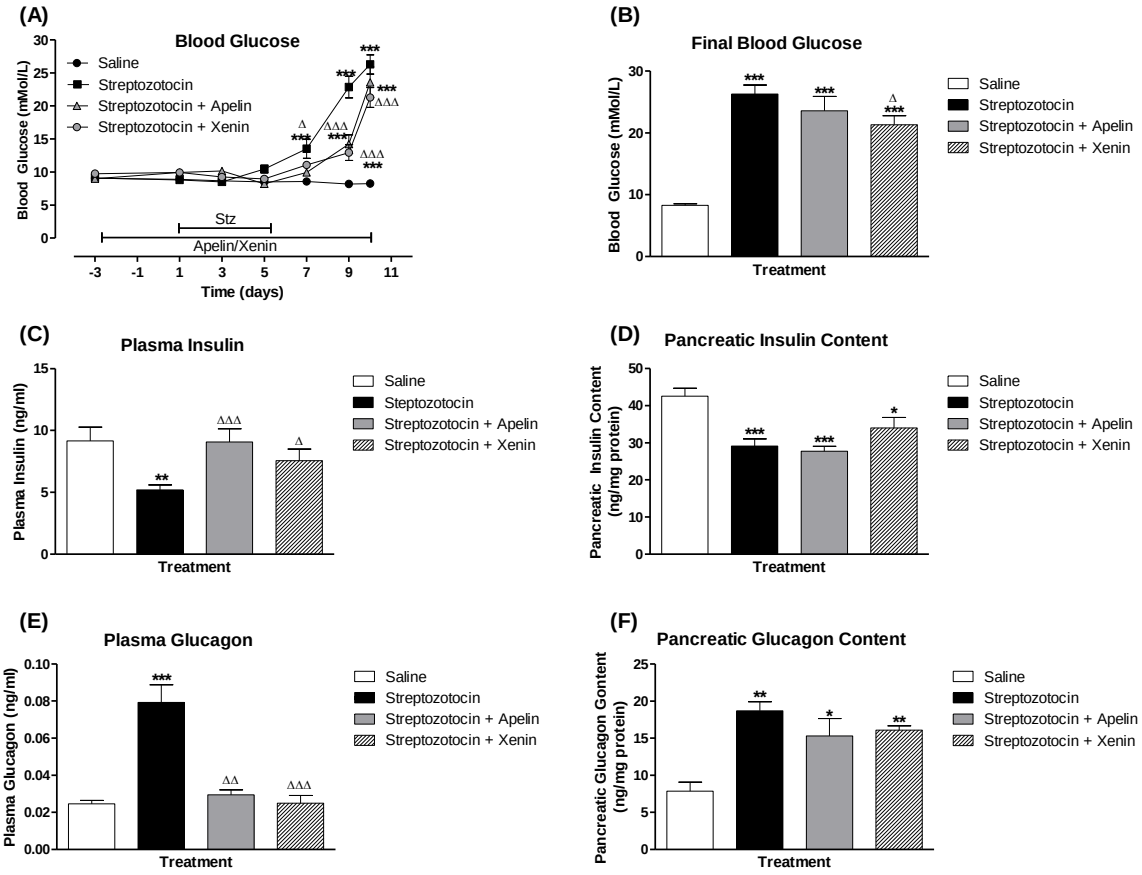

12 week old InsCre;Rosa26-eYFP C57Bl/6 mice were treated with pGlu-Apelin-(Glut-pal)amide or xenin-25-GluPal for two days prior to and in conjunction with administration of streptozotocin (50mg/kg, ip, once daily), n=8 mice/group. Terminal blood was taken to assess plasma insulin and glucagon. (A) Blood glucose, (B) final blood glucose, (C) plasma insulin, (D) pancreatic insulin content, (E) plasma glucagon and (F) pancreatic glucagon content. Comparisons were made against saline (*) or against streptozotocin treated (Δ). Values were significant when $p<0.05$ */Δ, $p<0.01$ **/ΔΔ and $p<0.001$ ***/ΔΔΔ.

Figure 6.3: Effects of streptozotocin alone or in combination pGlu-apelin(Glut-pal)-amide or xenin-25-GluPal on pancreatic islet area, beta cell area, alpha cell area, islet size distribution, percentage beta cells and percentage alpha cells

(A)

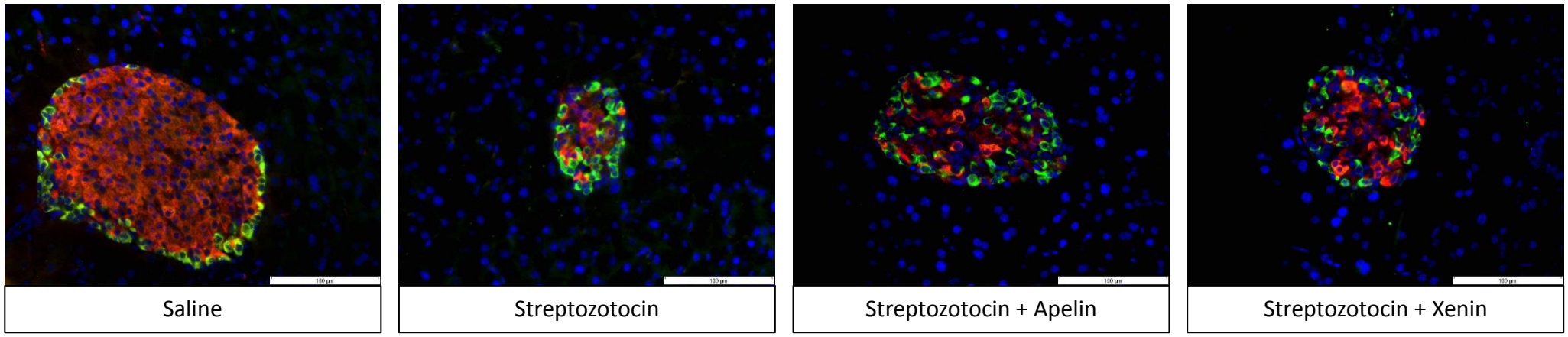

* Legend overleaf

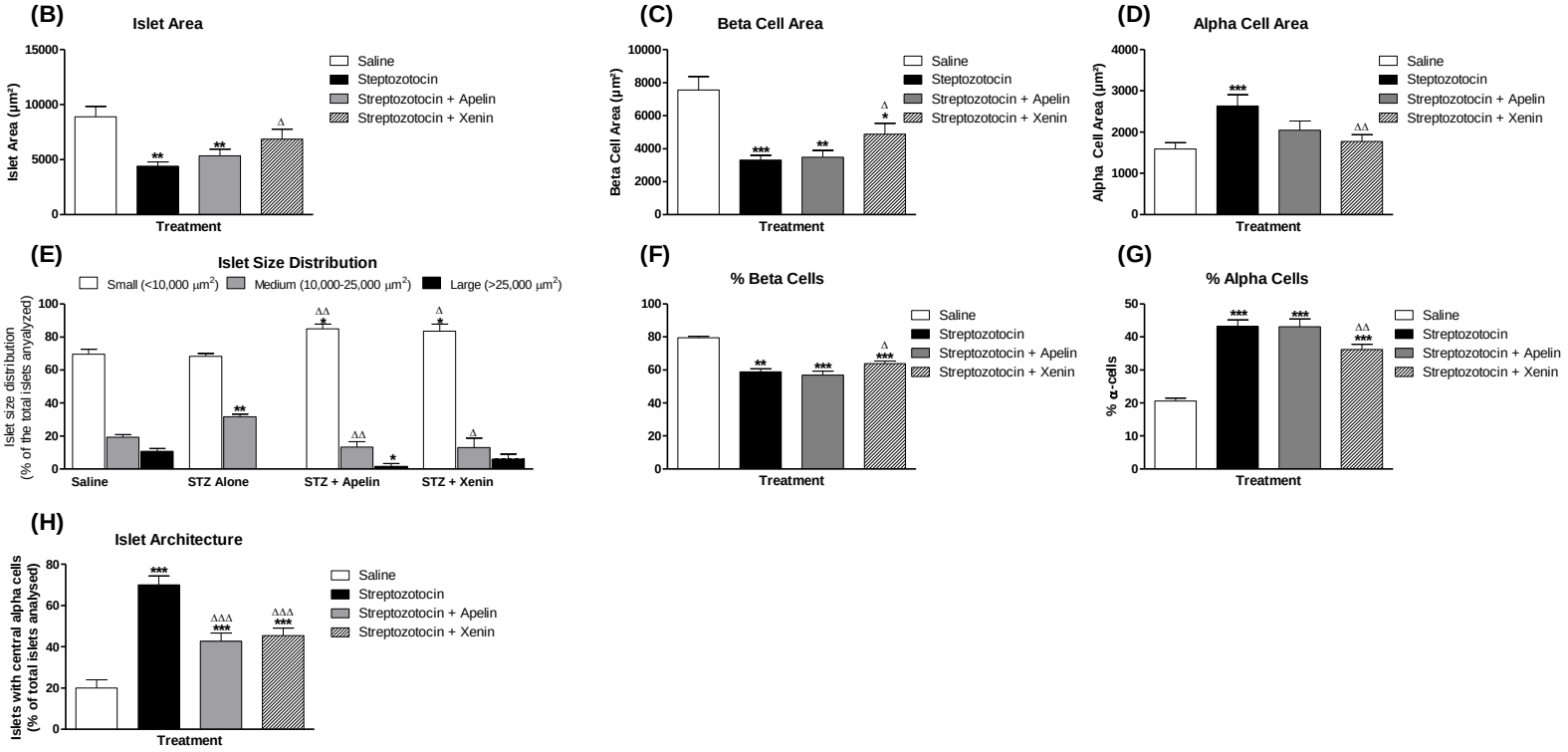

Representative images of islets from (A) streptozotocin plus pGlu-Apelin-(Glut-pal)amide or xenin-25-GluPal treated mice showing insulin (red), glucagon (green) and DAPI (blue). (B) islet area, (C) beta cell area, (D) alpha cell area, (E) islet size distribution, (F) percentage beta cells, (G) percentage alpha cells and (H) islet architecture. Values are mean ± SEM(n=8 mice/group). Comparisons versus saline control (*) or versus streptozotocin (Δ), significant when */Δp<0.05, **/ΔΔp<0.01 and ***/ΔΔΔp<0.001.

Figure 6.4: Effects of streptozotocin alone or in combination pGlu-apelin(Glut-pal)-amide or xenin-25-GluPal on pancreatic islet beta-to-alpha cell transdifferentiation

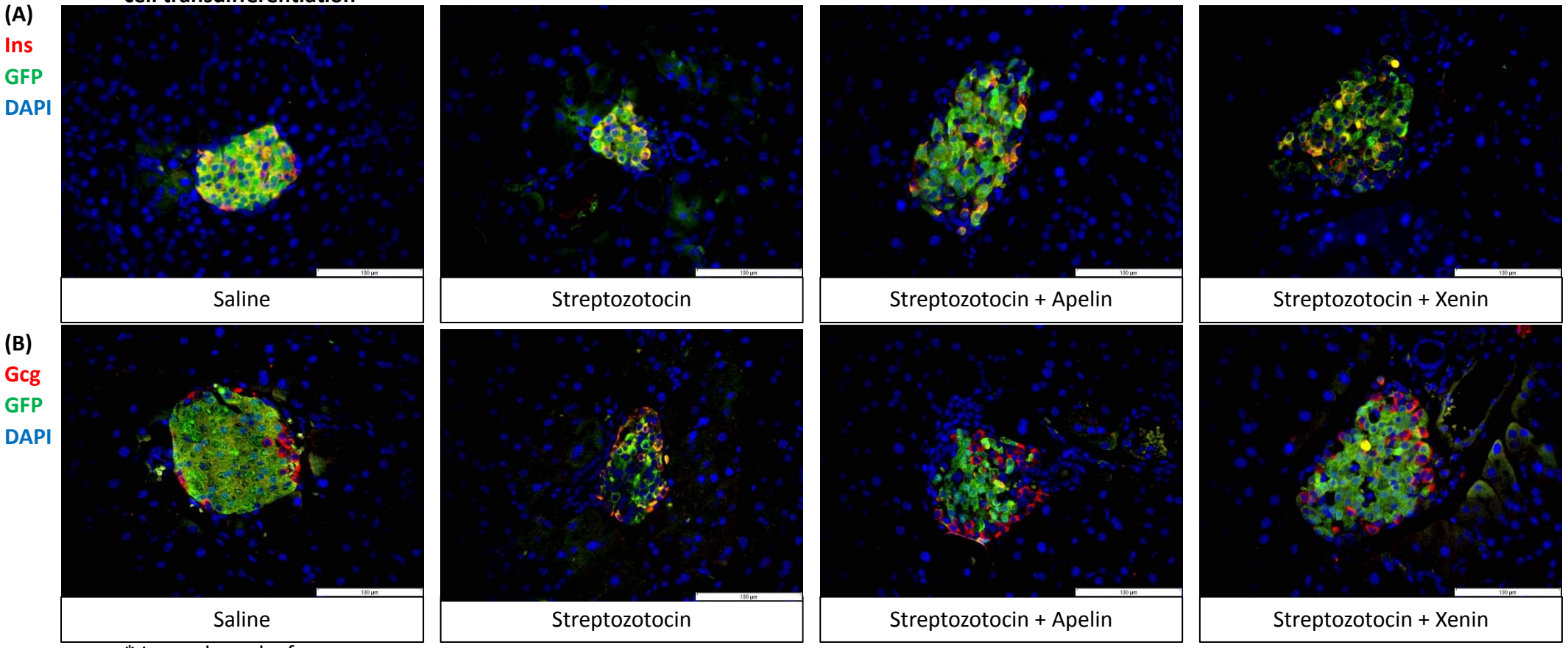

* Legend overleaf

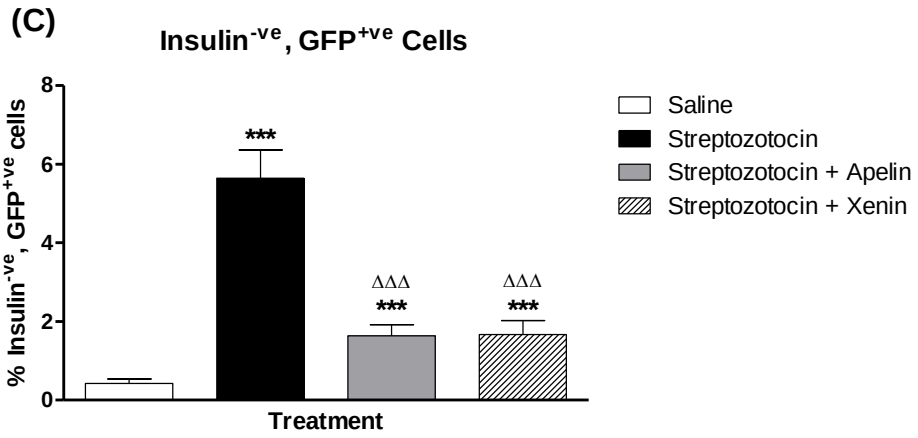

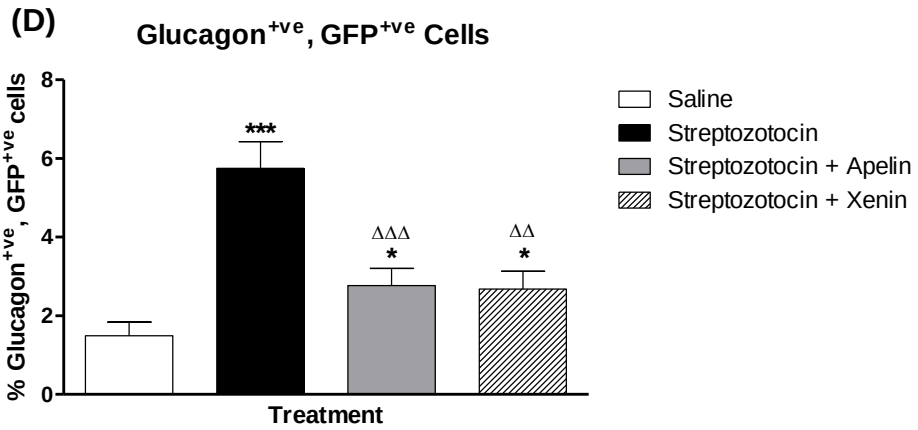

Transdifferentiation Analysis

Representative images of islets from saline, streptozotocin, streptozotocin plus pGlu-apelin-(Glut-pal)--amide or streptozotocin plus xenin-25-GluPal showing (A) insulin (red), GFP (green) and (B) glucagon (red), GFP (green) staining. Beta cell transdifferentiation determined by populations of insulin negative, GFP positive cells (C) and glucagon positive, GFP positive cells (D) using double immunofluorescence staining.

Values are mean ± SEM (n=8 mice/group). Comparisons versus saline control (*) or versus streptozotocin (Δ), significant when */Δp<0.05, **/ΔΔp<0.01 and ***/ΔΔΔp<0.001.

Figure 6.5: Effects of streptozotocin alone or in combination pGlu-apelin(Glut-pal)-amide or xenin-25-GluPal on pancreatic islet beta cell and alpha cell apoptosis

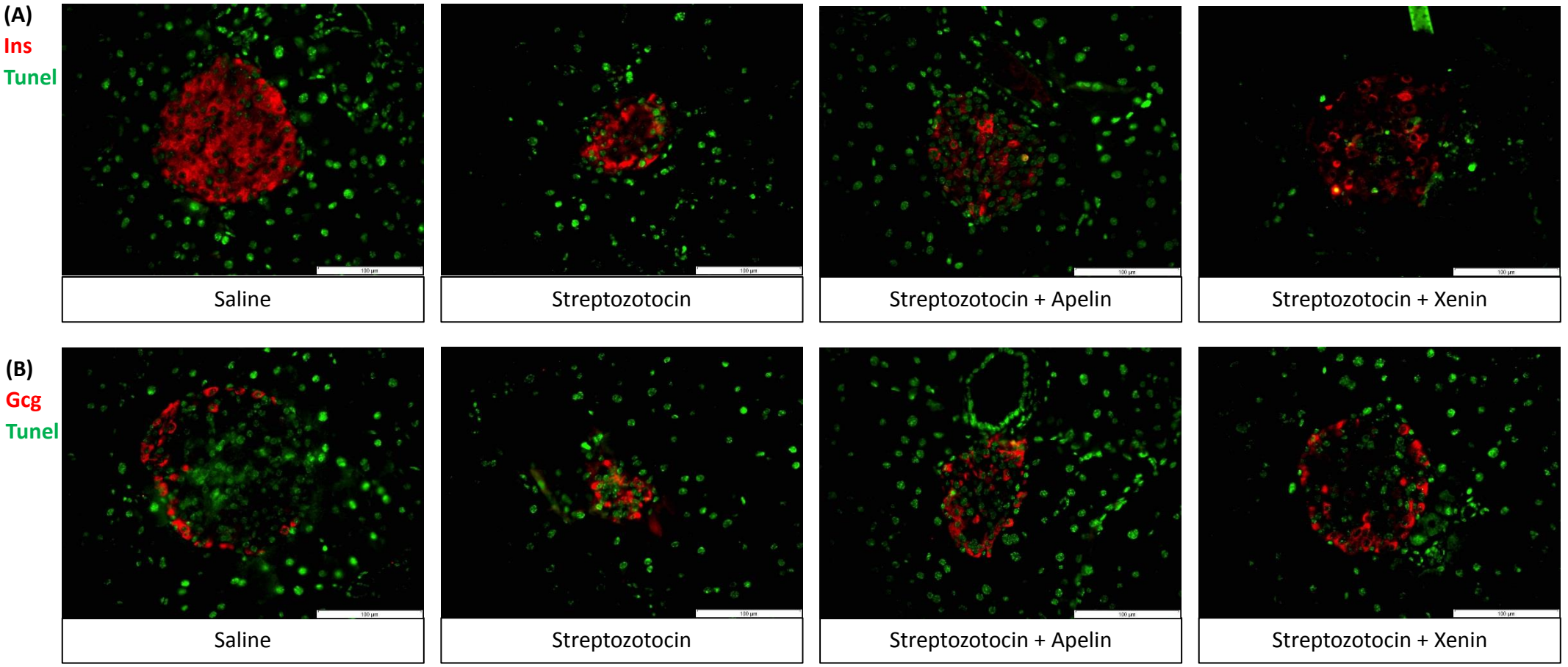

* Legend overleaf

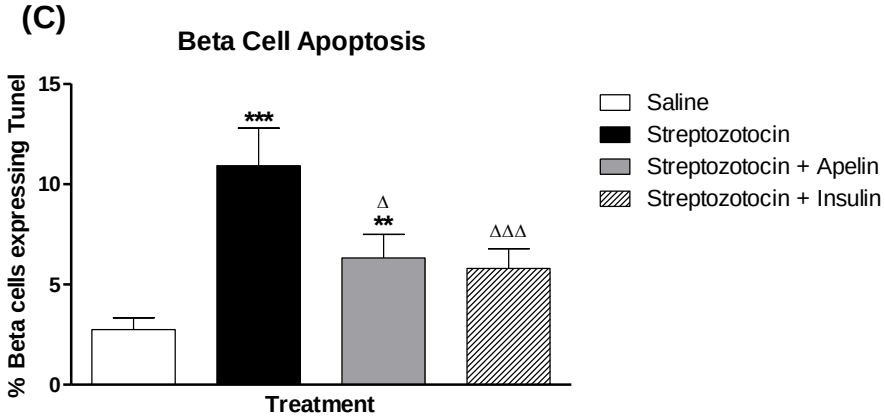

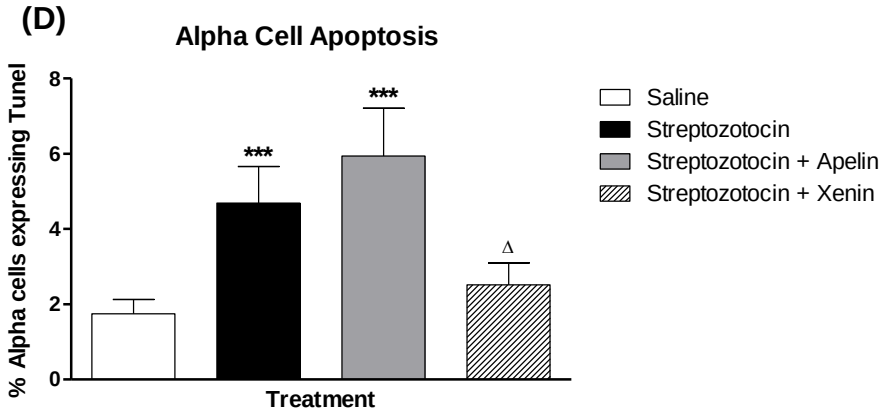

Apoptosis Analysis

Representative images of islets from mice treated with saline, streptozotocin, streptozotocin plus pGlu-apelin-(Glut-pal)-amide or streptozotocin plus xenin-25-GluPal stained for (A) insulin and TUNEL or (B) glucagon and TUNEL. Beta cell apoptosis and alpha cell apoptosis determined by populations of (C) insulin positive, TUNEL positive and (D) glucagon positive, TUNEL positive cells respectively by double immunofluorescence staining.

Values are mean ± SEM (n=8 mice/group). Comparisons versus saline control (*) or versus streptozotocin (Δ), significant when */Δp<0.05, **/ΔΔp<0.01 and ***/ΔΔΔp<0.001.

Figure 6.6: Effects of streptozotocin alone or in combination pGlu-apelin(Glut-pal)-amide or xenin-25-GluPal on pancreatic islet beta cell and alpha cell proliferation

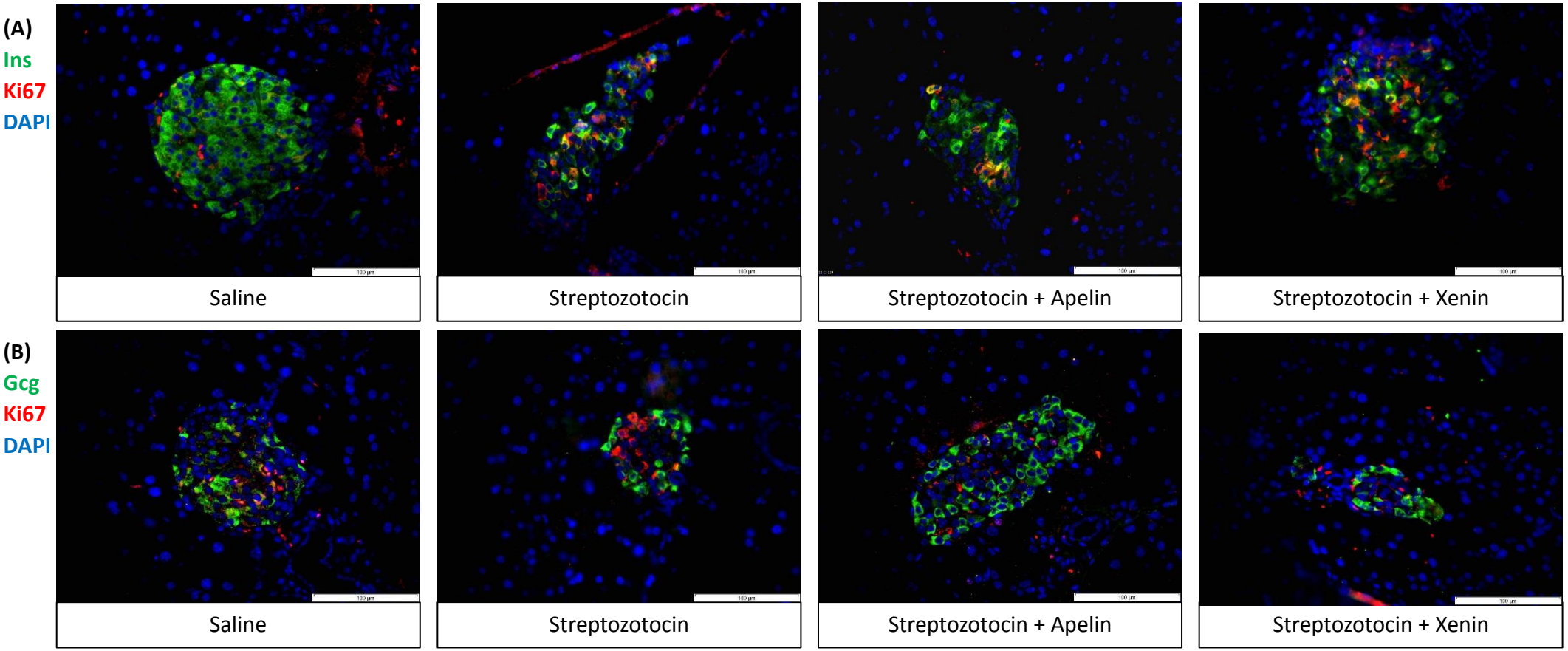

* Legend overleaf

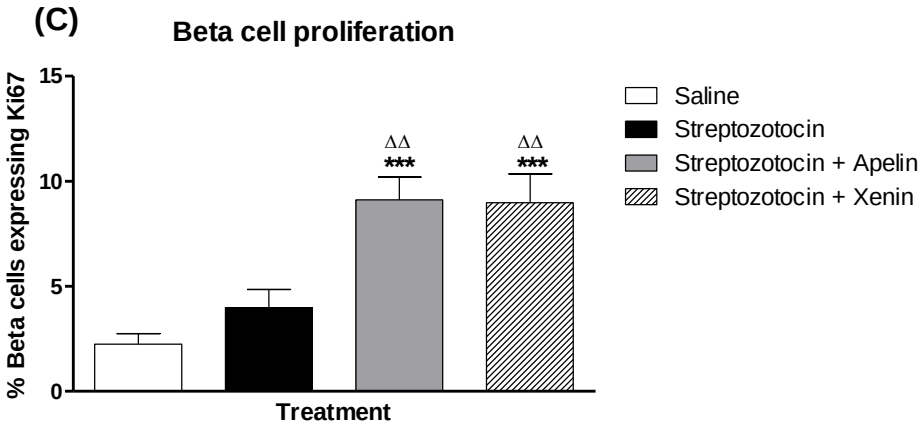

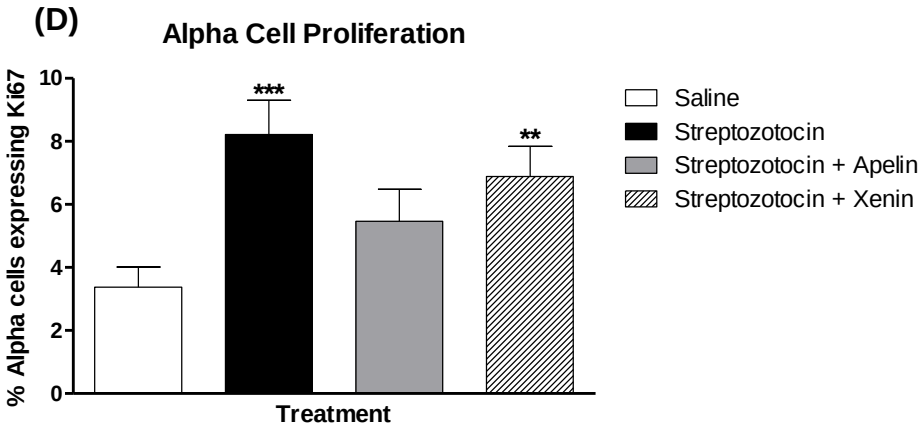

Proliferation Analysis

Representative images of islets from mice treated with saline, streptozotocin, streptozotocin plus pGlu-apelin-(Glut-pal)-amide and streptozotocin plus xenin-25-GluPal stained for (A) insulin and ki-67 or (B) glucagon and ki-67. Beta cell and alpha cell proliferation determined by populations of (C) insulin positive, ki-67 positive cells or (D) glucagon positive, ki-67 positive cells respectively by double immunofluorescence staining.

Values are mean ± SEM (n=8 mice/group). Comparisons versus saline control (*) or versus streptozotocin (Δ), significant when */Δp<0.05, **/ΔΔp<0.01 and ***p<0.001.

Figure 6.7: Effects of streptozotocin alone or in combination pGlu-apelin (Glut-pal)-amide or xenin-25-GluPal on pancreatic beta cell Pdx1 expression

(A)

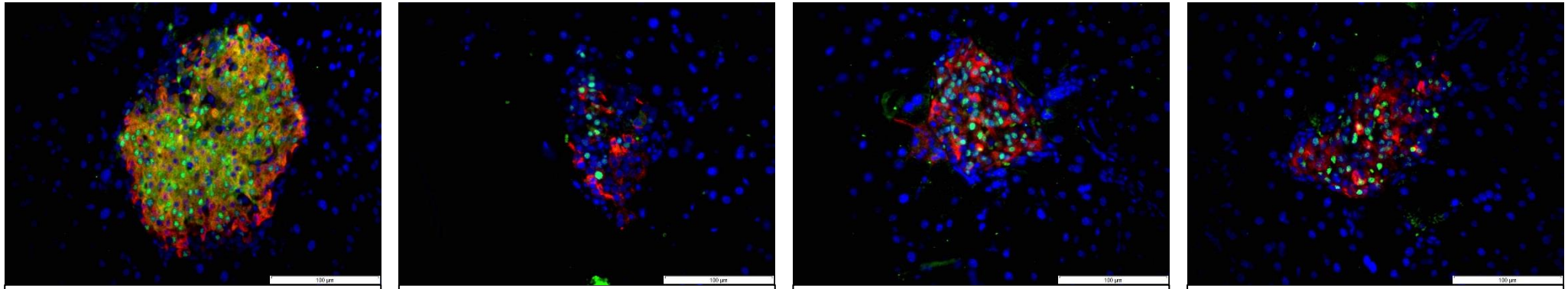

Saline	Streptozotocin	Streptozotocin + Apelin	Streptozotocin + Xenin

Insulin / Pdx1 / DAPI

* Legend overleaf

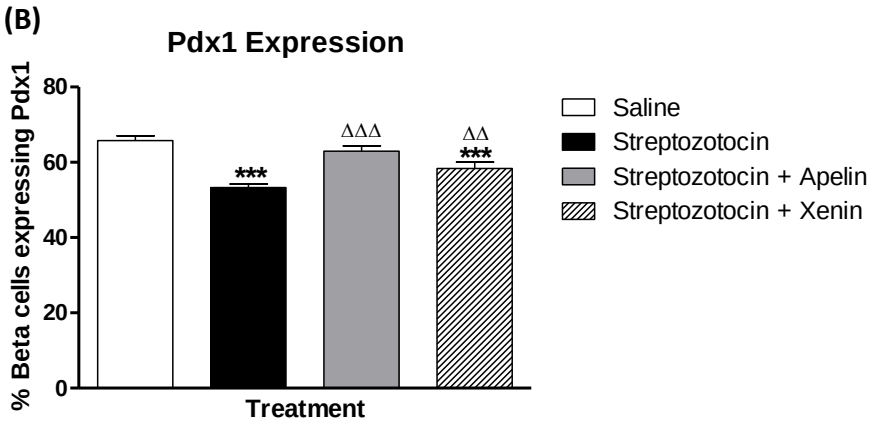

Pdx1 Expression Analysis

(A) Representative images of islets from mice treated with saline, streptozotocin, streptozotocin plus pGlu-apelin-(Glut-pal)-amide and streptozotocin plus xenin-25-GluPal on Pdx1 expression (B). Determined by histological analysis of insulin/Pdx1 double immunofluorescence staining showing insulin (red), Pdx1 (green) and DAPI (blue).

Values are mean ± SEM (n=8 mice/group). Comparisons versus saline control (*) or versus streptozotocin (Δ), significant when */Δp<0.05, **/ΔΔp<0.01 and ***p<0.001.

Figure 6.8: Effects of high fat feeding alone or in combination pGlu-apelin(Glut-pal)-amide or xenin-25-GluPal on body weight, cumulative energy intake and cumulative fluid intake

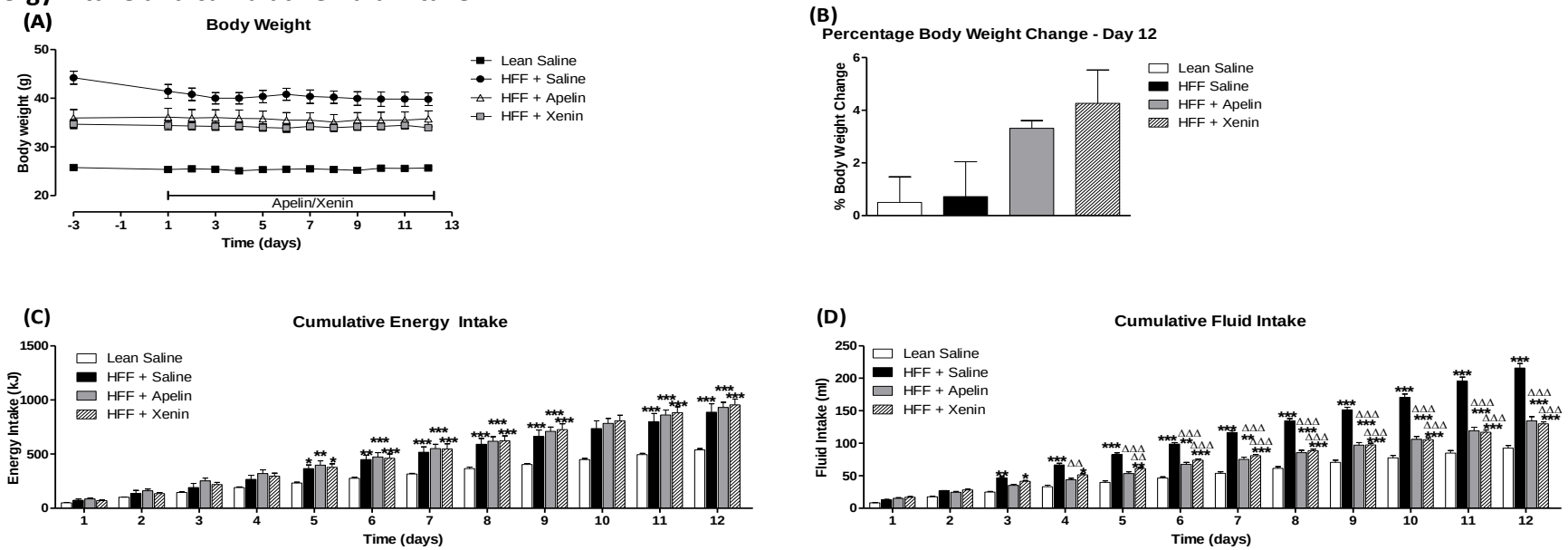

15 week old InsCre;Rosa26-eYFP C57Bl/6 mice kept on a high fat diet for 2 months prior were treatment with pGlu-apelin-(Glut-pal)-amide or xenin-25-GluPal by daily ip injections, n=6-8 mice/group. (A) body weight, (B) percentage body weight change, (C) cumulative energy intake and (D) cumulative fluid intake. Comparisons were made against lean saline (*) or against high fat fed (Δ). Values mean ± SEM, significant when $p<0.05$ */Δ, $p<0.01$ **/ΔΔ and $p<0.001$ ***/ΔΔΔ.

Figure 6.9: Effects of high fat feeding alone or in combination with pGlu-apelin(Glut-pal)-amide or xenin-25-GluPal on blood glucose, plasma insulin, pancreatic insulin content, plasma glucagon, pancreatic glucagon content, GTT and AUC

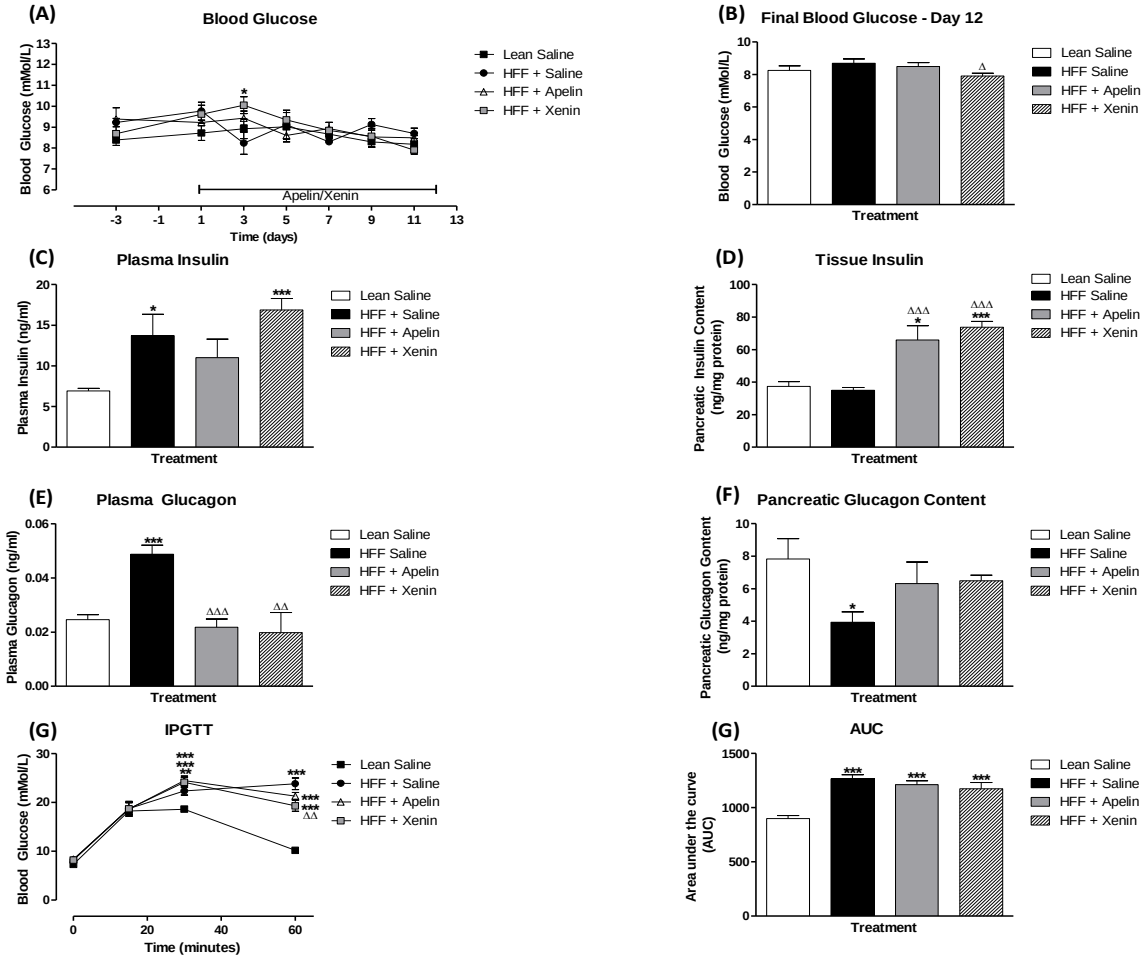

15 week old InsCre;Rosa26-eYFP C57Bl/6 mice kept on a high fat diet for 2 months prior were treatment with pGlu-apelin-(Glut-pal)-amide or xenin-25-GluPal by daily ip injections, n=6-8 mice/group. Blood glucose, (B) final blood glucose, (C) plasma insulin, (D) pancreatic insulin, (E) plasma glucagon, (F) pancreatic glucagon, (G) ip glucose tolerance test and (H) AUC. Comparisons were made against lean saline (*) or against high fat fed (Δ). Values mean ± SEM, significant when $p<0.05$ */Δ, $p<0.01$ **/ΔΔ and $p<0.001$ ***/ΔΔΔ

Figure 6.10: Effects of high fat feeding alone or in combination with pGlu-apelin(Glut-pal)-amide or xenin-25-GluPal on pancreatic islet area, beta cell area, alpha cell area, islet size distribution, percentage beta cells and percentage alpha cells

(A)

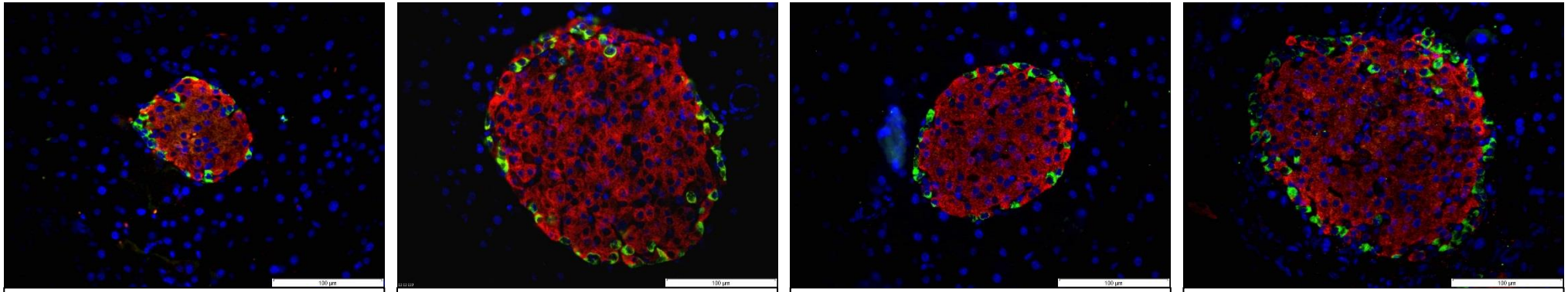

Lean Saline	High-fat Fed Saline	High-fat Fed + Apelin	High-fat Fed + Xenin

Insulin / Glucagon / DAPI

* Legend overleaf

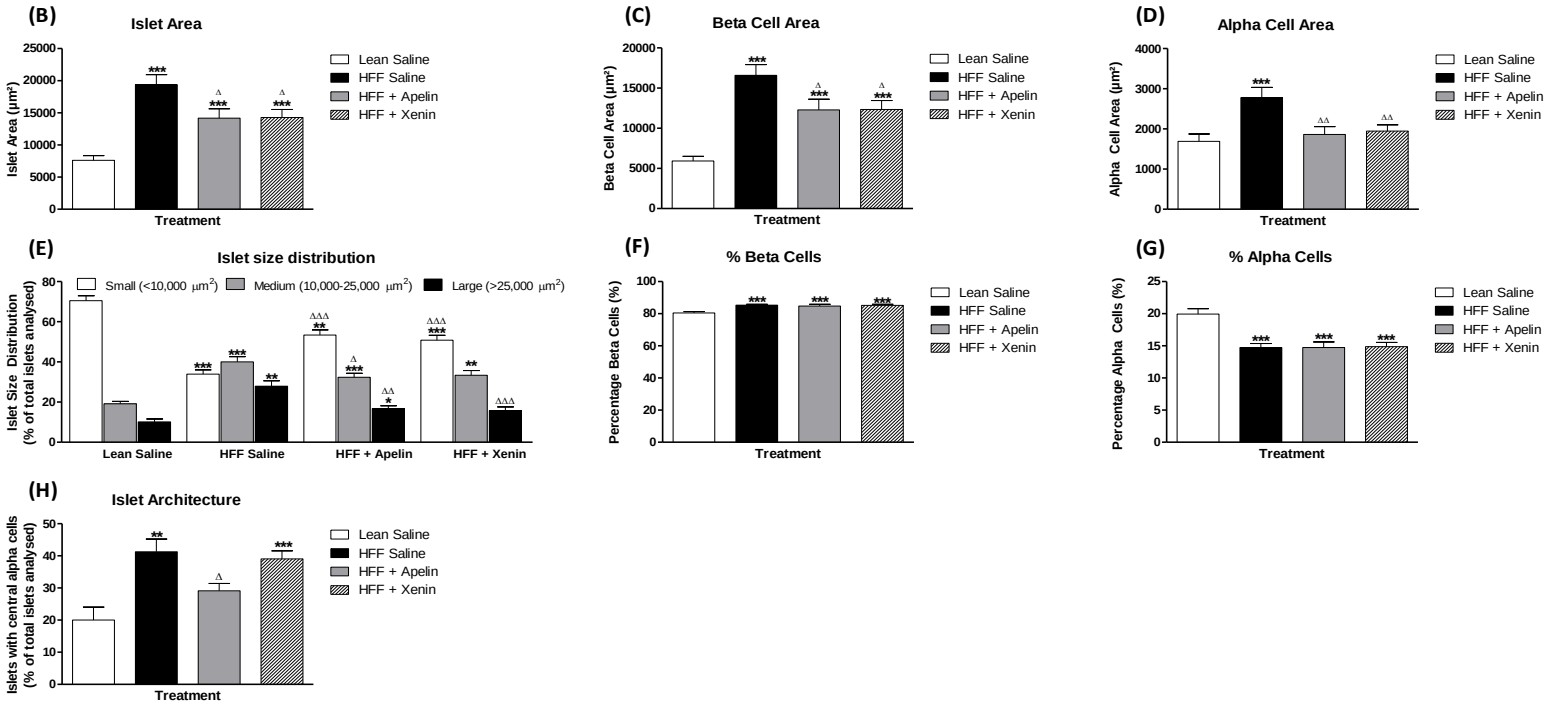

(A) Representative images of islets from high fat fed plus pGlu-apelin-(Glut-pal)-amide or xenin-25-GluPal mice showing insulin (red), glucagon (green) and DAPI (blue). (B) islet area, (C) beta cell area, (D) alpha cell area, (E) islet size distribution (F) percentage beta cells, (G) percentage alpha cells and (H) islet architecture. Values are mean ± SEM (n=8 mice/group). Comparisons versus saline control (*) or versus high fat fed (Δ), significant when */Δp<0.05, **/ΔΔp<0.01 and ***/ΔΔΔp<0.001.

Figure 6.11: Effects of high fat feeding alone or in combination with pGlu-apelin(Glut-pal)-amide or xenin-25-GluPal on pancreatic islet beta-to-alpha cell transdifferentiation

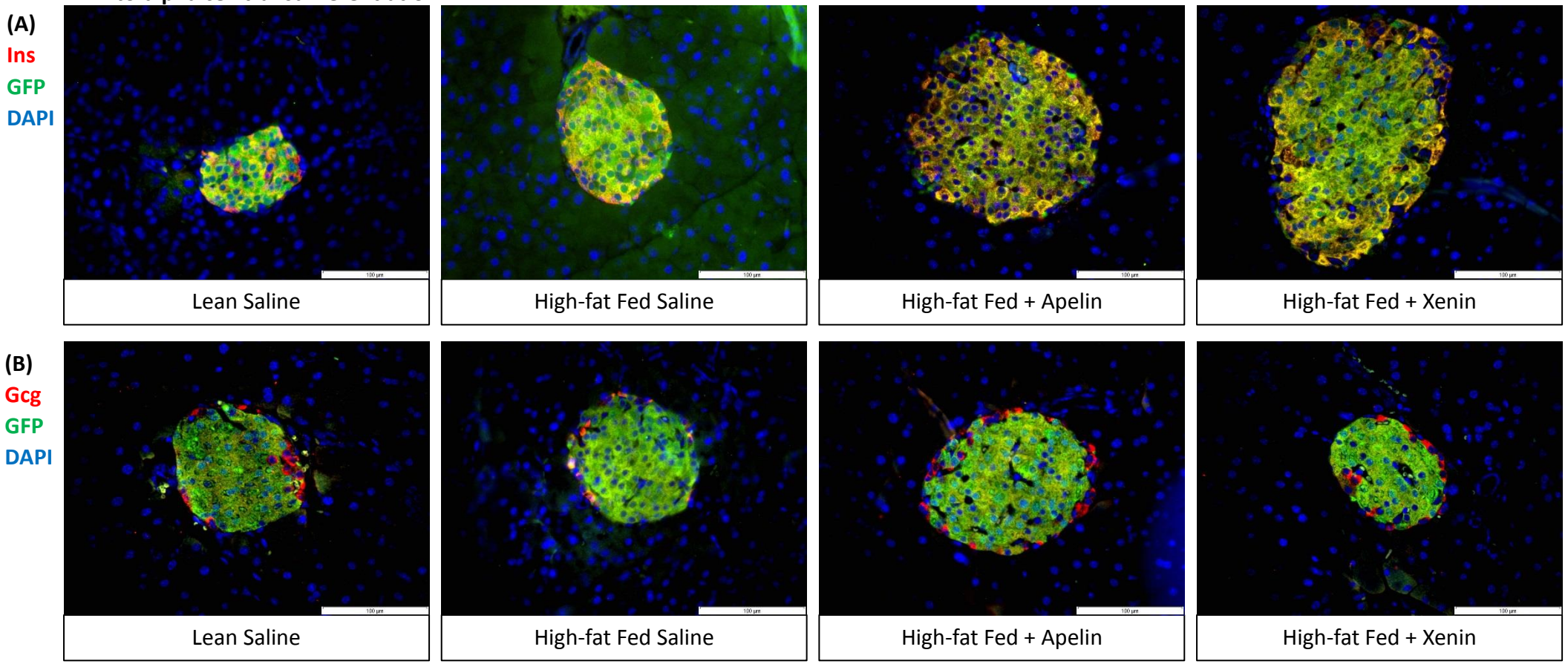

* Legend overleaf

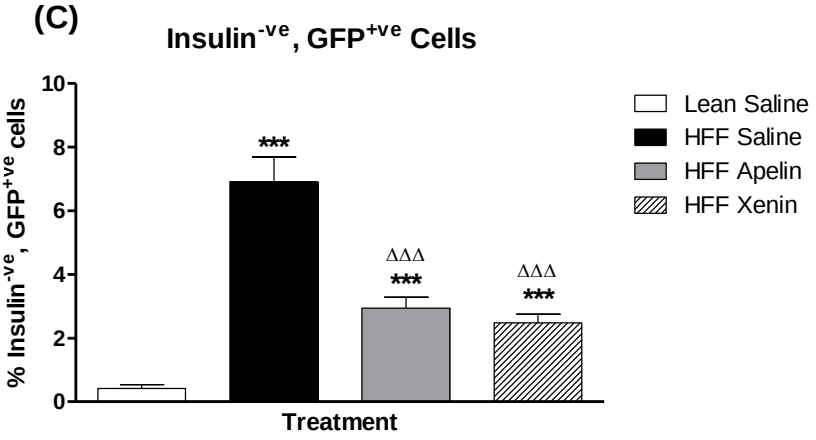

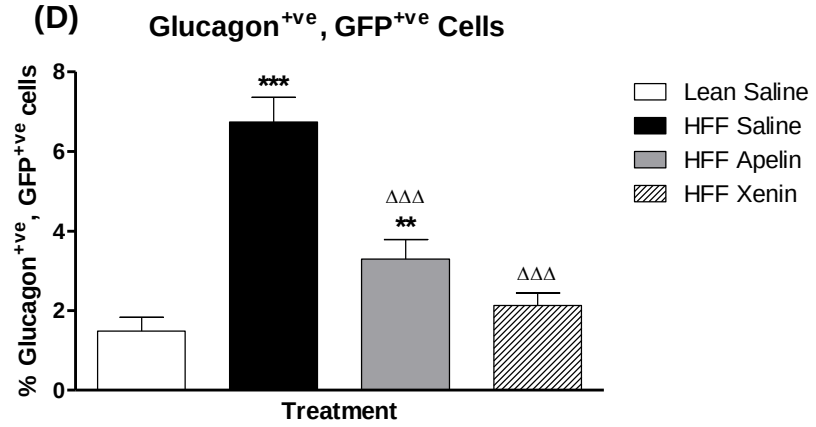

Transdifferentiation Analysis

Representative images of islets from lean saline, high fat fed saline, high fat fed plus pGlu-apelin-(Glut-pal)-amide and high fat fed plus xenin-25-GluPal treated mice stained for (A) insulin and GFP or (B) glucagon and GFP. Beta cell transdifferentiation determined by populations of (C) insulin negative, GFP positive cells and (D) glucagon positive GFP positive cells using double immunofluorescence staining. Values are mean ± SEM (n=8 mice/group). Comparisons versus lean saline control (*) or versus high fat fed saline (Δ), significant when */Δp<0.05, **/ΔΔp<0.01 and ***/ΔΔΔp<0.001.

Figure 6.12: Effects of high fat feeding alone or in combination with pGlu-apelin(Glut-pal)-amide or xenin-25-GluPal on pancreatic islet beta cell and alpha cell apoptosis

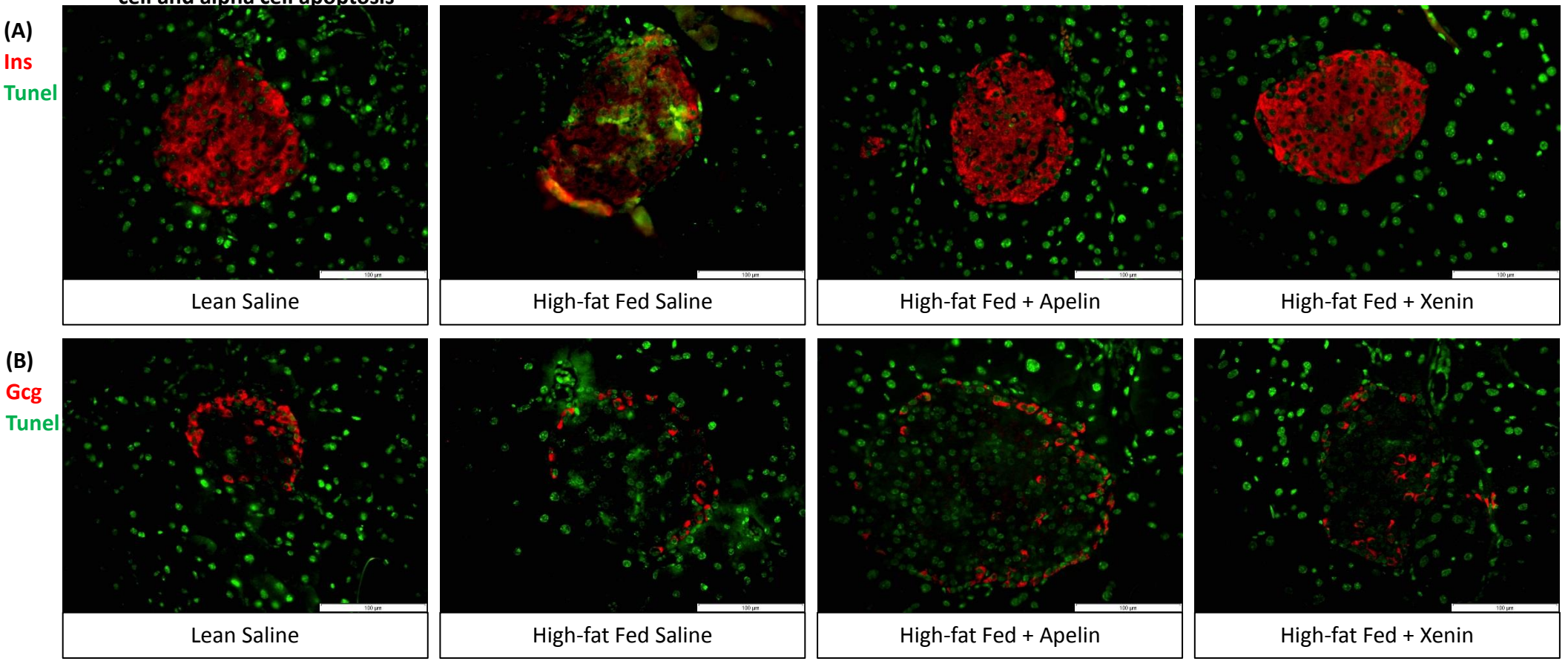

* Legend overleaf

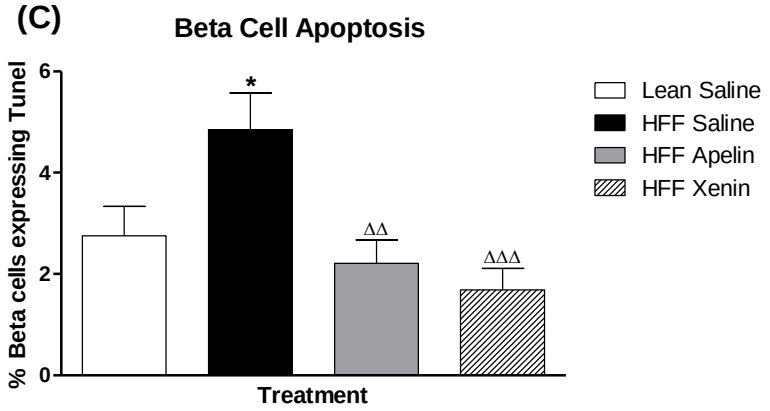

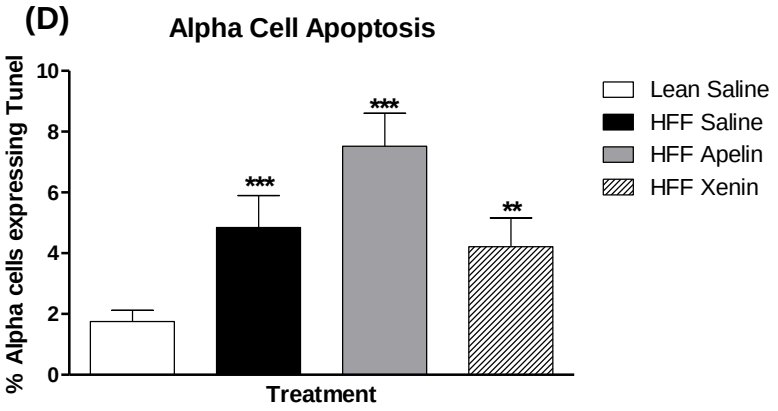

Apoptosis Analysis

Representative images of islets from lean saline, high fat fed saline, high fat fed plus pGlu-apelin-(Glut-pal)-amide and high fat fed plus xenin-25-GluPal treated mice stained for (A) insulin and TUNEL or (B) glucagon and TUNEL. Beta cell apoptosis and alpha cell apoptosis determined by populations of (C) insulin positive, TUNEL positive and (D) glucagon positive, TUNEL positive cells respectively by double immunofluorescence staining.

Values are mean ± SEM (n=8 mice/group). Comparisons versus saline control (*) or versus high fat fed (Δ), significant when */Δp<0.05, **/ΔΔp<0.01 and ***/ΔΔΔp<0.001.

Figure 6.13: Effects of high fat feeding alone or in combination with pGlu-apelin(Glut-pal)-amide or xenin-25-GluPal on pancreatic islet beta cell and alpha cell proliferation

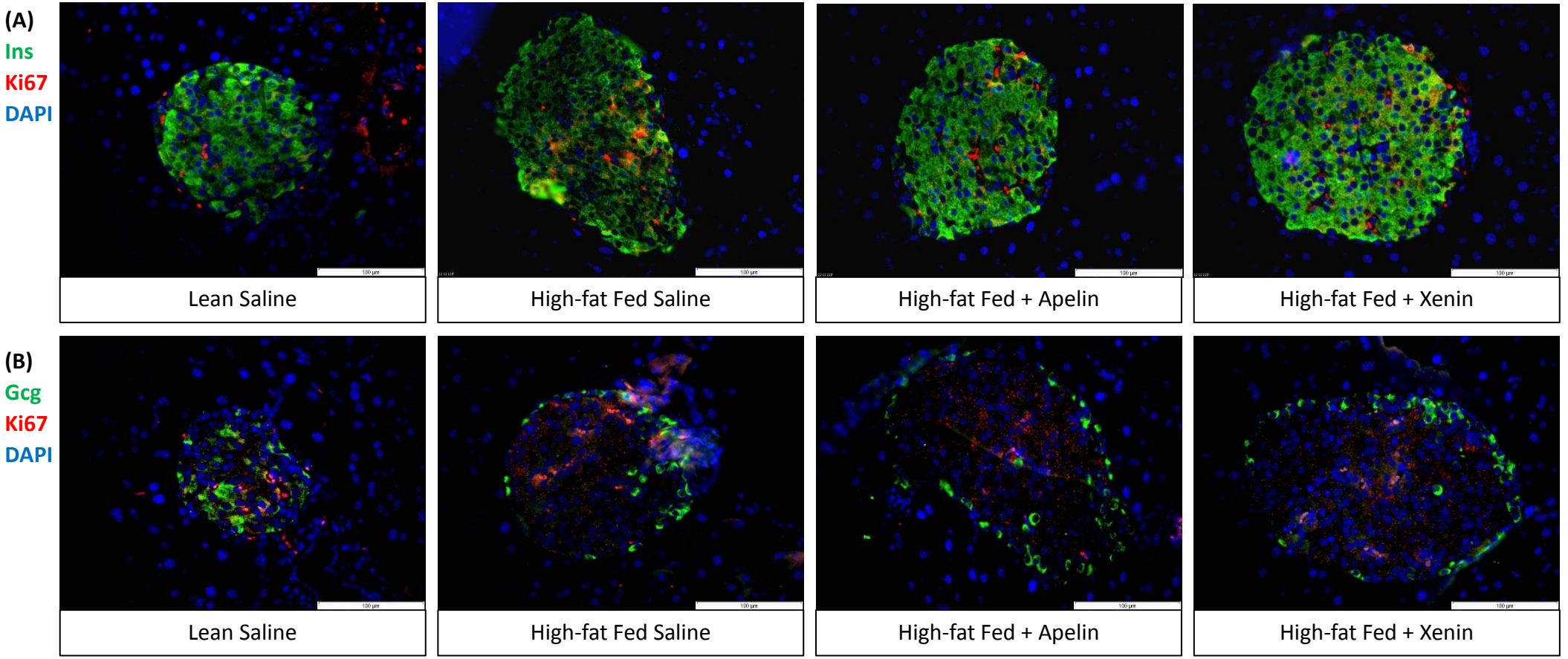

* Legend overleaf

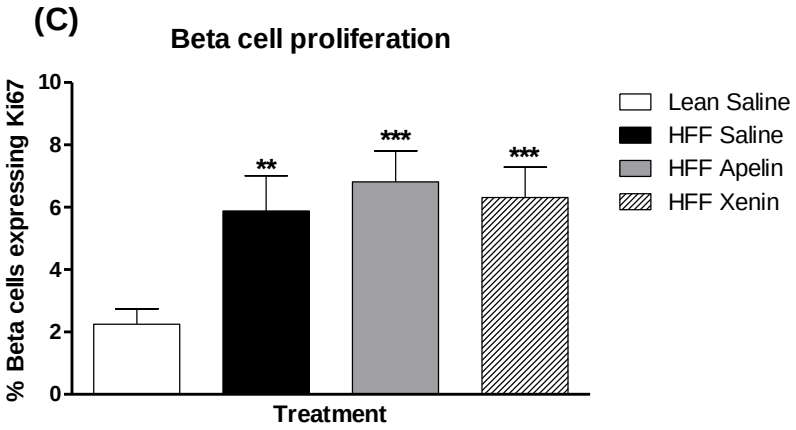

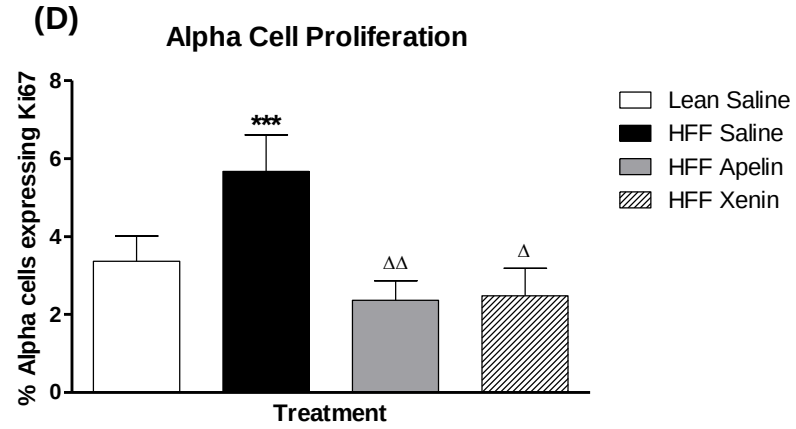

Proliferation Analysis

Representative images of islets lean saline, high fat fed saline, high fat fed plus pGlu-apelin-(Glut-pal)-amide and high fat fed plus xenin-25-GluPal stained for (A) insulin and ki-67 or (B) glucagon and ki-67. Beta cell and alpha cell proliferation determined by populations of (C) insulin positive, ki-67 positive cells and (D) glucagon positive, ki-67 positive cells respectively by double immunofluorescence staining.

Values are mean ± SEM (n=8 mice/group). Comparisons versus saline control (*) or versus high fat fed (Δ), significant when */Δp<0.05, **/ΔΔp<0.01 and ***p<0.001.

Figure 6.14: Effects of high fat feeding alone or in combination with pGlu-apelin(Glut-pal)-amide or xenin-25-GluPal on pancreatic islet beta cell Pdx1 expression

(A)

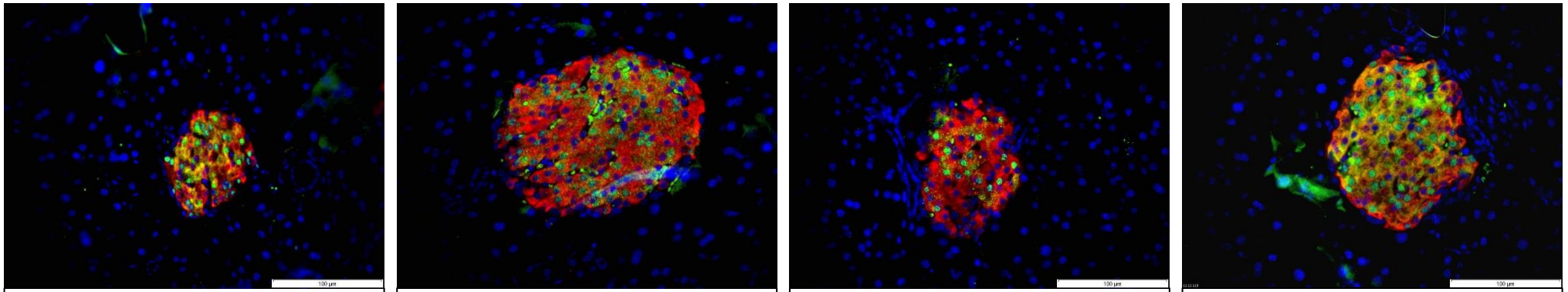

Lean Saline	High-fat Fed Saline	High-fat Fed + Apelin	High-fat Fed + Xenin

Insulin / Pdx1 / DAPI

* Legend overleaf

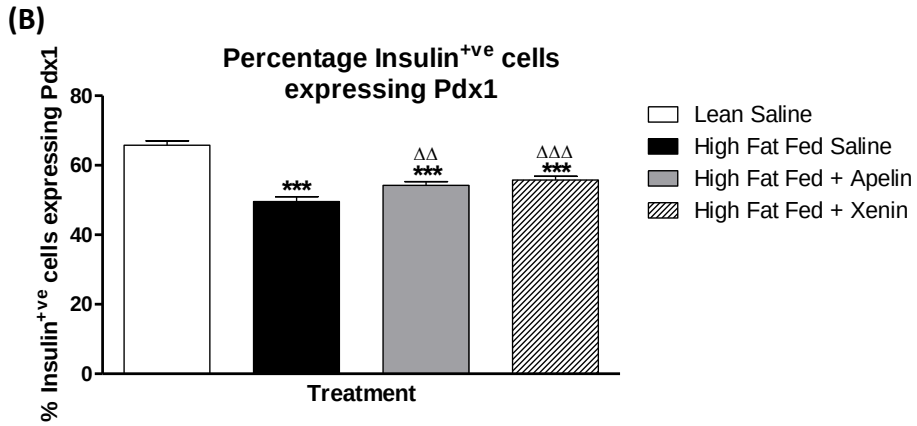

Pdx1 Expression Analysis

(A) Representative images of islets from mice treated with saline, streptozotocin, streptozotocin plus pGlu-apelin-(Glut-pal)-amide and streptozotocin plus xenin-25-GluPal on Pdx1 expression. (B) Determined by histological analysis of insulin/Pdx1 double immunofluorescence staining showing insulin (red), Pdx1 (green) and DAPI (blue).

Values are mean ± SEM (n=8 mice/group). Comparisons versus saline control (*) or versus streptozotocin (Δ), significant when */Δp<0.05, **/ΔΔp<0.01 and ***p<0.001.

Chapter 7

General Discussion

7.1 Diabetes and Obesity

Diabetes is strongly associated with obesity with both of these disorders rapidly becoming major global epidemics of our lifetime. With the incidence currently estimated to increase to 693 million people within the next 25 years and the burgeoning economic costs of managing diabetes this will remain an issue for generations to come (Cho et al, 2018; Hex et al, 2012). Fully understanding the pathogenesis of diabetes remains key in the ultimate goal to effectively treat, manage and potentially arrest diabetes to a point where the disorder can do no harm.

7.2 Islet cell transdifferentiation in the pathogenesis of diabetes

7.2.1 Islet plasticity in the pathogenesis of diabetes

Over the past decade, islet cell plasticity has been shown to be feasible by genetic manipulation of alpha/beta cell specific transcription factors to drive either beta-to-alpha cell or alpha-to-beta cell transdifferentiation. Evidence of this plasticity and transdifferentiation has been reported using animal models and with human clinical biopsies. Work by others has shown that type-2 diabetes in mice is associated with loss of beta cell identity and resultant transdifferentiation (Talchai et al, 2012; Thorel et al, 2010; Chera et al, 2014; Ye et al, 2015; Wang et al, 2014). Studies in non-human primates have shown that their beta cells are similarly plastic and that they are able to dedifferentiate during high fat diet induced diabetes (Fiori et al, 2013). Given this growing breadth of evidence, it is plausible that similar physiology occurs in humans. In fact, studies have shown that human islets, from donors of various age and sex, can rapidly convert into glucagon producing alpha cells without genetic manipulation of transcription factors (Spiker et al, 2013). Additionally, immunohistochemical

analysis of human organ donor material revealed that 31.9% of beta cells were dedifferentiated in type-2 diabetics compared with 8.7% in non-diabetics, with 84% of insulin positive cells showing reduced mature beta cell transcription factors (FOXO1, NKX6.1 and MAFA). These factors were also found in glucagon and somatostatin producing cells (Cinti et al, 2015). This strongly supports the view of beta cell dedifferentiation and potential beta-to-alpha transdifferentiation in type-2 diabetes. These authors go on to suggest this mechanism acts to protect beta cells from death, preserving them for redifferentiation when suitable metabolic conditions arrive (Cinti et al, 2015). As such, identifying pharmacologic agents that prevent this change or enable redifferentiation of transdifferentiated beta cells provides a novel approach for beta cell restoration therapy.

In addition to this endocrine plasticity, evidence of a neogenic niche within islets has recent been described (Huising et al, 2018). Located at the islet periphery where beta and alpha cells meet lies a population of immature beta cells which the authors speculate may be former beta cells that underwent beta-to-alpha cell transdifferentiation based on a stimulus arising from their specific microenvironment, ie signalling between alpha and beta cells within the islet periphery. Given the extensive paracrine signalling already known to occur within the islet this theory explaining what triggers beta cell transdifferentiation is plausible.

Work described in this thesis attempts to identify transdifferentiation *in vitro* and *in vivo* by showing beta cell transdifferentiation within multiple low dose streptozotocin, high fat fed diet induced and multiple hydrocortisone mouse models of diabetes. Once characterised the next step was to identify anti-diabetic agents that

would prevent or reverse this transdifferentiation for beta cell restoration therapy (Figure 7.1).

7.2.2 Cell lines to model beta cell transdifferentiation

The use of cell lines offers a cost effective and large supply of highly proliferative, homogenous biological material that bypasses ethical concerns associated with use of animals (Kaur and Dufour, 2012; MacDonald et al, 1990). A good cell line maintains functional features similar to the primary type that it is derived from, however this can be hard to judge if the primary cell's physiology is not fully understood. Generation of cell lines involve genetic manipulation may alter the native physiology of the cell, it's functions and responses to stimuli (Kaur and Dufour, 2012). Serial passage of cell lines can result in phenotypic variation over time to the point where they may not accurately represent primary cells. Because of these drawbacks, beta cell lines may not be best suited to study transdifferentiation. Despite this, the chance of finding an animal based alternative to studying beta cell dedifferentiation and transdifferentiation should still be sought after. For studying transdifferentiation, cell lines offer a unique advantage over animal models. *In vivo* models only allow assessment of transdifferentiation at limited time points, usually restricted to the start and end of treatments. *In vitro* cell based studies allow investigations at many more time points, under strictly controlled conditions, to examine the order of changes involved in beta cell transdifferentiation. Studies adopting this approach have demonstrated that loss of mature beta cell markers

precedes the ectopic expression of progenitor and alpha cell markers (Diedisheim et al, 2018).

The present research explored three widely used beta cell lines, exposing them to different stress conditions in an attempt to find an environment that promotes beta cell dedifferentiation or transdifferentiation. INS-1 and MIN6 cells proved most useful for modelling beta cell transdifferentiation. Both of these cell lines displayed consistent changes in insulin and glucagon expression when exposed to lipotoxic or cytokine mediated toxicity. These culture conditions in particular consistently resulted in an increase in cells co-expressing insulin and glucagon. Present findings are backed up by others that have utilised INS-1 and MIN6 cells to investigate beta cell dedifferentiation (Chen et al, 2018). Similarly these authors have cultured cells in glucotoxic conditions (22.2mM and 33.3mM glucose) or with angiotensin-2 and in both cell lines noted reduction in expression of mature beta cell genes (insulin and Pdx1) and increases in progenitor genes (Ngn3 and Oct4) (Chen et al, 2018).

To provide relevance to human disease, studies have been done utilising EndoC-βH1, a human beta cell line to study beta cell plasticity (Diedisheim et al, 2018). These authors found fibroblast growth factor 2 (FGF2) induced beta cell dedifferentiation in these cells determined by reduced expression of beta cell markers (*INS, MAFB* and *GCK*) and ectopic expression of progenitor markers (*MYC, HES1, SOX9* and *NGN3*). Interestingly, this dedifferentiation was reversed upon removal of FGF2 and Importantly primary human islets cultured in FGF2 supplemented media showed similar signs of beta cell dedifferentiation showcasing this process is plausible in humans and could potentially occur in diabetes (Diedisheim et al, 2018).

7.2.3 Multiple low dose streptozotocin as a model for transdifferentiation

Streptozotocin is a selective beta cell toxin that induces diabetes through beta cell demise. When given through a multiple low dose (50mg/kg body weight) protocol streptozotocin induces insulitis in addition to its direct toxicity on beta cells to ultimately reduce islet function and number (Gleichman, 1998; Bonnevie-Nielsen et al, 1981; Like and Rossini, 1976). The present lineage tracing experiments, utilising *Ins1*$^{cre/+}$;Rosa26-eYFP C57Bl/6 mice, showcase extensive beta-to-alpha transdifferentiation associated with loss of beta cell markers (Pdx1) in this model of diabetes. Furthermore this current work aids to characterise this animal model showcasing its worsening hyperglycaemia, reductions in plasma and pancreatic insulin levels and concomitant increases in circulating and pancreatic glucagon levels. Within the pancreas, islet area is severely compromised due to loss of beta cell mass despite expansion of alpha cell mass, with this finding matched by others (Vasu et al, 2015; O'Brien et al, 1996). Lineage tracing and analysis of apoptosis and proliferation has determined that this alpha cell expansion is a combination of beta-to-alpha cell transdifferentiation and alpha cell proliferation outweighing alpha cell apoptosis. This transdifferentiation in combination with increased beta cell apoptosis accounts for the dramatic loss of beta cell mass observed in these mice. This marked increase in beta-to-alpha cell transdifferentiation makes this a suitable model for investigating transdifferentiation, despite the initial diabetogenic insult differing from the pathogenesis of type-2 diabetes.

7.2.4 Diet induced high fat feeding as a model for transdifferentiation

High fat diet induced obesity is strongly associated with development of a diabetic phenotype, highly comparable to the characteristics seen in human type-2 diabetes, and as such is used commonly as model of type-2 diabetes (King et al, 2012). This model has been used in rodents (mice and rats) as well as non-human primates to recreate diabetes. Indeed, high fat fed non-human primates have been shown to have dedifferentiated beta cells (Fiori et al, 2013) implicating this process in humans and this model as a relevant way to study and explore beta cell transdifferentiation. This thesis investigated high fat-fed NIH Swiss mouse islets and noted significant expansions in beta and alpha cell masses (Vasu et al, 2017). This was associated with an increase in cells co-expressing insulin and glucagon, highly suggestive of beta-to-alpha cell transdifferentiation. High fat fed *Ins1*$^{cre/+}$;Rosa26-eYFP C57Bl/6 mice put on high fat diet for 8 weeks exhibited substantial weight gain although they did not exhibit overt hyperglycaemia or elevated pancreatic insulin content unlike other strains of mice such as NIH Swiss (Gault et al, 2007; Moffett et al, 2015; Vasu et al, 2017). These transgenic mice however did show elevations in circulating insulin and glucagon levels with reduced pancreatic glucagon content, the former likely a reflection of insulin resistance. This was confirmed during a glucose tolerance test when these high fat fed mice retained their hyperglycaemia after 60 minutes of receiving a glucose load. The islets of these mice were adapted to their insulin resistant environment as shown by an expanded beta cell and alpha cell mass collectively increasing islet area. Beta cell proliferation and hypertrophy was found to account for this increase. However prolonged insulin resistance causes beta cell stress resulting in beta cell apoptosis and loss of beta cell identity (Pdx1) leading to

beta-to-alpha cell transdifferentiation. This combined with increased alpha cell proliferation accounts for the expansion of alpha cell mass seen in these mice. These findings confirm validity for the use of these transgenic mice and high fat feeding as a model for examining beta cell transdifferentiation.

7.2.5 Multiple hydrocortisone as a model for transdifferentiation

To instil insulin resistance, hydrocortisone can be dosed to mice to model the pathology of type-2 diabetes (Bailey and Flatt, 1982; Swali et al, 2008). In line with previous studies using WT C57Bl/6 mice, *Ins1*$^{cre/+}$;Rosa26-eYFP C57Bl/6 mice dosed with hydrocortisone maintained non-fasting glucose levels. However they showed increased circulating and pancreatic insulin levels, likely reflective of their insulin resistance (Vasu et al, 2015). The present studies examined this model further showing plasma glucagon is also elevated in these mice. Beta cell proliferation has previously been shown to be the cause of the expanded beta cell mass observed in these mice, with the present studies supporting this view (Vasu et al, 2015). Unlike past studies these transgenic mice did not exhibit a noteworthy increase in alpha cell mass (Vasu et al, 2015; Khan et al, 2016). This is likely due to the increase in alpha cell apoptosis outweighing beta-to-alpha cell transdifferentiation. Given that these mice do not exhibit substantial expansions in alpha cell mass with most alpha cells succumbing to death, this model may not be as well suited for exploring transdifferentiation as compared to streptozotocin and high fat models.

7.2.6 Other animal models of transdifferentiation

Research conducted by Latreille at Imperial College London has focused on stress induced dysfunctional microRNAs (miRNA) as the underlying cause of diseases. These authors identified a specific mRNA, miR-7, in beta cells which when overexpressed in transgenic mice resulted in diabetes with impaired insulin secretion and beta cell dedifferentiation. The latter was defined by reductions in beta cell markers (Pdx1, Nkx6.1, Mafa and Neurod1) and activation of pre-endocrine marker Sox9 (Latreille et al, 2014). Interestingly alpha cell and somatostatin markers were upregulated offering the potential to study beta-to-alpha cell transdifferentiation (Mak and Latreille, 2018). Similarly in obesity induced diabetes, db/db mice and humans with type-2 diabetes, miR-7 was found to be dysregulated. These authors suggest that inhibition of miR-7 resulted in therapeutic benefit against diabetes restoring functional beta cell mass by reversal of beta cell dedifferentiation and improving beta cell function (Mak and Latreille, 2018).

Db/db mice are commonly used as an animal model of diabetes and obesity. Functional mutation in the leptin receptor impairs leptin signalling resulting in hyperphagia, obesity, beta cell dysfunction and diabetes. These mice have been shown to exhibit reductions in beta cell specific markers associated with increased progenitor markers and as such are used by many to examine beta cell dedifferentiation. Activation of RAS signalling, by angiotensin-2, has been shown to potentiate beta cell dedifferentiation in these mice and induces the transdifferentiation of beta cells into alpha cells (Chen et al, 2018). Treatment with an ACE inhibitor was shown to reverse this dedifferentiation and potentially prevent or reverse this beta-to-alpha cell transdifferentiation (Chen et al, 2018). The present

thesis examined islet morphology in db/db mice and similarly noted signs of beta-to-alpha cell transdifferentiation shown by an increase in alpha cell mass and bi-hormonal cells expressing both insulin and glucagon. The drawback however is that lineage tracing is not possible making it impossible to fully determine dedifferentiation and transdifferentiation. This could be potentially overcome though selective cross breeding with our transgenic *Ins1*$^{cre/+}$;Rosa26-eYFP mice to generate offspring with the recessive db/db gene with specific YFP tagging of their beta cells. Beta cell dedifferentiation and transdifferentiation could then more accurately be quantified in db/db diabetes.

7.3 Effect of anti-diabetic agents on beta cell transdifferentiation

7.3.1 Effect of incretins on transdifferentiation

Incretin peptides GLP-1 and GIP have already been shown beneficial against diabetes improve islet function in a plethora of ways. These include but are not limited to potentiating glucose-stimulated insulin secretion, suppression of glucagon secretion and promotion of satiety (Mest et al, 2005; Arthen and Schmidtz, 2004; Song et al, 2017; Nauck et al, 1997; Flint et al, 1998). Until recently studies examining the effect of incretins on beta cell transdifferentiation has been limited. This thesis has explored the possibility that using clinically prescribed GLP-1 receptor agonist, liraglutide, and a DPPIV inhibitor, sitagliptin, affect this process. Table 7.1 summarises the studies found in this thesis. In streptozotocin induced diabetic mice, both agents were able to reduce beta-to-alpha cell transdifferentiation. Given that these drugs only modestly reduced hyperglycaemia at the doses employed, it is likely that this benefit

in restoring beta cell identity is a direct effect of increasing incretins rather than secondary to alleviating glucotoxic stress. This is of particular importance as alleviation of hyperglycaemia shown elsewhere in this thesis using insulin and by others has been found to prevent beta-to-alpha cell transdifferentiation and reverse beta cell dedifferentiation respectively (Wang et al, 2014). Similarly, the improvement in beta cell transdifferentiation caused by these agents may be due to the reduction in energy intake, given that calorie restriction has been noted to reduce beta cell dedifferentiation (Sheng et al, 2015). Liraglutide and sitagliptin increase circulating and pancreatic insulin concomitant with reduction in glucagon levels. This supports the idea that these agents may be involved in the prevention or inhibition beta-to-alpha cell transdifferentiation. These effects on glycaemia, circulating and pancreatic hormones are consistent with previous research (Ansarullah et al, 2013; Takeda et al, 2012; Wang et al, 2015; Millar et al, 2017; O'Harte et al, 2018). In high fat fed diabetes, both liraglutide and sitagliptin were able to reduce beta-to-alpha cell transdifferentiation. This reduction, along with increased alpha cell apoptosis likely accounts for the reduced alpha cell mass seen in sitagliptin treated mice. Liraglutide treated high fat fed mice did not show a reduction in alpha cell mass likely due to increases in alpha cell proliferation countering apoptosis and transdifferentiation. Increasing circulating incretin levels failed to improve beta cell transdifferentiation in hydrocortisone treated mice. In db/db mice however, liraglutide reduced alpha cell mass possibly due to prevention of beta-to-alpha cell transdifferentiation, although without lineage tracing this cannot be confirmed. GIP antagonism had no notable impact on islet morphology in db/db mice (Pathak et al, 2015). Very recent studies have shown that GLP-1 therapy can increase beta cell mass

through stimulation of alpha-to-beta cell transdifferentiation which potentially contributes to the changes in beta cell mass seen within this thesis (Lee et al, 2018).

7.3.2 SGLT2 inhibition on transdifferentiation and alpha cell hyperplasia

The selective SGLT2 inhibitor dapagliflozin is used to reduce glycaemia by increasing renal excretion of glucose. This insulin independent approach to reducing glycaemia offers potential for combination therapy with traditional anti-diabetic agents that potentiate beta cell function. Table 7.2 summarises the effects of dapagliflozin in diabetic models tested within this thesis. Unexpectedly SGLT2 inhibitors were found to increase islet alpha cell mass as noted in these present studies and by others (Millar et al, 2017; Millar et al, 2016; Bonner et al, 2015; Merovci et al, 2014; Zambrowicz et al, 2013). The present study aimed to explore the causes of this alpha cell expansion theorising that beta-to-alpha cell transdifferentiation could be culpable. However when tested, dapagliflozin did not exacerbate beta-to-alpha cell transdifferentiation in streptozotocin diabetes, despite testing at high and low doses of dapagliflozin, or in hydrocortisone diabetes. In fact dapagliflozin produced a modest reduction in beta-to-alpha cell transdifferentiation in high fat fed diabetes. Literature has similarly shown SGLT inhibition not to reverse beta cell dedifferentiation, with these authors suggesting that alpha cell mass expands to compensate against lowering glycaemia (Ishida et al, 2017). This effectively rules out worsening of beta-to-alpha cell transdifferentiation as the cause of alpha cell mass expansion however these studies consistently showed SGLT2 inhibition to reduce alpha cell apoptosis.

7.3.3 Effect of apelin and xenin on transdifferentiation

Apelin is an adipokine that has recently been shown to be involved in glucose metabolism, potentiating glucose stimulated insulin release (O'Harte et al, 2017). Apelin knockout mice are hyperglycaemic with reduced glucose tolerance and insulin sensitivity, all of which were remedied by exogenous apelin dosing (Yu et al, 2010). Xenin is a gut derived peptide that has similarly been shown to augment glucose stimulated insulin release (Taylor et al, 2010). Chemical modifications of both of these peptides (pGlu-apelin-(Glut-pal)-amide and xenin-25-GluPal) improved their biological half-life making them suitable drug candidates for the treatment of diabetes. The present study helps characterise their function in three animal models of diabetes and to assess whether they can impact beta cell transdifferentiation, with results summarised in Table 7.3. In streptozotocin diabetes, apelin and xenin were as effective as incretin based therapies at preventing beta-to-alpha cell transdifferentiation, whilst also increasing beta cell proliferation. Similarly in high fat fed diabetes both novel peptides reduced beta cell transdifferentiation and increased beta cell resistance to apoptosis. These studies add to growing evidence highlighting the beneficial effects of apelin and xenin in the hope they will result in clinical trials to provide an efficacious, safe and economical approach to treat diabetes.

7.4 Scope for future work

Future work should aim to elucidate the mechanisms GLP-1 receptor agonists and DPPIV inhibitors prevent beta-to-alpha cell transdifferentiation. Fully understanding the mechanisms of this transdifferentiation process will provide opportunities to

develop targeted novel treatments for the restoration of beta cell mass. This could potentially be done through the use of *Ins1*$^{cre/+}$;Rosa26-eYFP C57Bl/6 mouse islets *ex vivo* where the surrounding metabolic environment can be strictly controlled. Other widely used anti-diabetic agents including sulfonylureas, meglitinides and thiazoldinediones may also be able to impact beta cell transdifferentiation. The latter in particular has been used in db/db mice to reduce beta cell secretory workload however this was insufficient to restore dedifferentiated beta cells (Ishida et al, 2017). Although not a pharmacologic agent the benefit of calorie restriction on improving beta cell responses in diabetes has been widely shown. Calorie restricted db/db mice exhibit reduced levels of beta cell dedifferentiation (Sheng et al, 2015). Thus, it would be interesting to explore the combination of dietary restriction with anti-diabetic drugs. Whether maintaining functional beta cell mass solely through prevention or reversal of beta cell transdifferentiation is sufficient to treat diabetes remains to be answered. Fully understanding the molecular triggers and pathways that lead to beta cell transdifferentiation will allow further investigation into this. The remit of this thesis has focused on beta-to-alpha cell transdifferentiation, however there is a possibility that stressed beta cells may transdifferentiate to somatostatin secreting delta cells. Further immunohistochemistry would reveal this, however preliminary staining with GFP and somatostatin shows no co-expression in streptozotocin treated mice, suggesting little to no beta-to-delta transdifferentiation in this model (Figure 7.2).

7.5 Concluding remarks

This thesis has highlighted the relevance of beta cell plasticity in the pathogenesis of diabetes with emphasis on beta-to-alpha cell transdifferentiation. This has been demonstrated by lineage tracing of beta cells in multiple low dose streptozotocin, high fat fed and multiple hydrocortisone models of diabetes. This transdifferentiation process likely accounts for the increase in alpha cell mass and hyperglucagonemia seen in type-2 diabetics. Reversion of these transdifferentiated cells back to functional beta cells offers a novel approach for beta cell restoration therapy. Incretin based therapies, apelin and xenin maintained beta cell identity by preventing beta-to-alpha cell transdifferentiation showing proof of concept. These promising findings will hopefully lead to further investigations into the mechanisms involved in transdifferentiation in the hope to develop specific agents capable of restoring beta cell mass and treating diabetes.

Table 7.1: Effects elicited by liraglutide or sitagliptin in streptozotocin, high fat fed and hydrocortisone diabetes

	STZ	STZ Lira	STZ Sita	HFF	HFF Lira	HFF Sita	HC	HC Lira	HC Sita
Body Weight	***	***	*** Δ		*** ΔΔΔ		***	***	***
Calorie Intake	*	*** ΔΔΔ	*** ΔΔΔ	***	***	***	*	ΔΔΔ	ΔΔΔ
Fluid Intake	** ***	*** ΔΔΔ	*** ΔΔΔ	***	ΔΔΔ ***	ΔΔΔ ***	***	***	*** ΔΔΔ
Blood Glucose	***	ΔΔΔ ***	Δ ***		ΔΔ	ΔΔ		** ΔΔΔ	** Δ
Plasma Insulin	**	ΔΔΔ	ΔΔ	*	***	**	**	**	*** Δ
Pancreatic Insulin	***	ΔΔΔ	Δ		*** ΔΔΔ	*** ΔΔΔ	**	ΔΔ *	*
Plasma Glucagon	***	ΔΔ **	*	***	ΔΔ *	ΔΔ	*		Δ
Pancreatic Glucagon	**	ΔΔΔ	ΔΔ *	*		*		Δ	
Islet Area	**	ΔΔΔ	Δ	***	***	Δ ***	***	***	***
Beta cell area	**	*	*	***	Δ ***	ΔΔ ***	***	***	***
Alpha cell area	***	***	***	***	***	Δ			Δ
Percentage beta cell	***	***	*** ΔΔΔ	***	ΔΔΔ	Δ *	***	ΔΔ ***	ΔΔΔ ***
Percentage alpha cells	***	***	*** ΔΔΔ			Δ			
Islet architecture	***	ΔΔΔ *	Δ ***	***	ΔΔ	**			
Insulin^{-ve}, GFP^{+ve} cells	***	ΔΔΔ ***	ΔΔ ***	***	ΔΔΔ ***	ΔΔ ***	***	***	***
Glucagon^{+ve}, GFP^{+ve} cells	***	Δ **	Δ **	***	ΔΔΔ **	***	***	Δ ***	***
Beta cell apoptosis	*	Δ **	Δ **	*	Δ	ΔΔΔ	***	ΔΔΔ	Δ *
Alpha cell apoptosis	***	Δ	**	***	***	***	***	ΔΔΔ **	***
Beta cell proliferation		*** ΔΔΔ		**	**	**	***	***	***
Alpha cell proliferation	***		Δ	*		Δ			
Pdx1 expression	***	ΔΔΔ	ΔΔΔ *	***	Δ ***	***	***	ΔΔΔ	***
Key	**No change**			**Increased**			**Decreased**		
	*** vs saline - *p<0.05, **p<0.01, ***p<0.001** **Δ vs STZ/HFF/HC – Δp<0.05, ΔΔp<0.01, ΔΔΔ p<0.001**								

Table 7.2: Effects elicited by dapagliflozin or insulin in streptozotocin, high fat fed and hydrocortisone diabetes

	STZ	STZ LD Dapa	STZ HD Dapa	STZ Insulin	HFF	HFF LD Dapa	HC	HC LD Dapa
Body Weight	***	*** ΔΔΔ	*** ΔΔΔ	ΔΔΔ		*** ΔΔΔ	***	***
Calorie Intake	*	*** ΔΔΔ			***	***	*	ΔΔΔ
Fluid Intake	**	*** Δ	*** Δ	ΔΔ	***	ΔΔΔ ***	***	Δ
Blood Glucose	***	***	ΔΔ ***	ΔΔΔ ***		Δ		
Plasma Insulin	***	Δ	***	ΔΔΔ	*	**	**	***
Pancreatic Insulin	***	**	*** ΔΔΔ	ΔΔ		Δ	**	Δ
Plasma Glucagon	***	ΔΔΔ	ΔΔ	ΔΔ **	***	Δ *	*	**
Pancreatic Glucagon	***	ΔΔΔ	Δ ΔΔΔ	Δ	*	** ΔΔ		
Islet Area	**	*	***	Δ	***	***	**	*** ΔΔΔ
Beta cell area	**	*** ΔΔΔ	*** ΔΔΔ	*	***	***	***	*** ΔΔΔ
Alpha cell area	***	***	***	*	***	*** Δ		* ΔΔΔ
Percentage beta cell	***	*** ΔΔΔ	*** ΔΔΔ	ΔΔ ***	***	ΔΔΔ	***	***
Percentage alpha cells	***	*** ΔΔΔ	*** ΔΔΔ	ΔΔ ***				***
Islet architecture	***	ΔΔ ***	ΔΔ ***	ΔΔΔ	**	*		
Insulin^{-ve}, GFP^{+ve} cells	***	***	Δ ***	ΔΔΔ **	***	Δ ***	***	***
Glucagon^{+ve}, GFP^{+ve} cells	***	***	***	ΔΔ *	***	***	***	***
Beta cell apoptosis	*	**	***	Δ **	***		***	ΔΔΔ
Alpha cell apoptosis	***	ΔΔΔ	*** ΔΔΔ	ΔΔ	**	***	***	ΔΔΔ
Beta cell proliferation		*	*** Δ		*	*** Δ	***	ΔΔΔ **
Alpha cell proliferation	*	Δ	**	ΔΔΔ	**			*
Pdx1 expression	***	***	ΔΔΔ	ΔΔΔ	***	Δ ***	***	***

Key	No change	Increased	Decreased
	* vs saline - *p<0.05, **p<0.01, ***p<0.001 Δ vs STZ/HFF/HC – Δp<0.05, ΔΔp<0.01, ΔΔΔ p<0.001 LD – low dose dapa 1mg/kg, HD – high dose dapa 5mg/kg		

Table 7.3: Effects elicited by pGlu-apelin-(Glut-pal)-amide or xenin-25-GluPal in streptozotocin, high fat fed and hydrocortisone diabetes

	STZ	STZ Apelin	STZ Xenin	HFF	HFF Apelin	HFF Xenin
Body Weight	***	ΔΔΔ	ΔΔΔ		* Δ	
Calorie Intake	*	*** ΔΔΔ	***	***	***	***
Fluid Intake	**	*** ΔΔΔ	*** ΔΔΔ	***	ΔΔΔ ***	ΔΔΔ ***
Blood Glucose	***	***	Δ ***			Δ
Plasma Insulin	**	ΔΔΔ	Δ	*		***
Pancreatic Insulin	***	***	*		* ΔΔΔ	*** ΔΔΔ
Plasma Glucagon	***	ΔΔ	ΔΔΔ	***	ΔΔΔ	ΔΔ
Pancreatic Glucagon	**	*	**	*		
Islet Area	**	**	Δ	***	Δ ***	Δ ***
Beta cell area	***	**	Δ *	***	Δ ***	Δ ***
Alpha cell area	***		ΔΔ	***	ΔΔ	ΔΔ
Percentage beta cell	**	***	Δ ***	***	***	***
Percentage alpha cells	***	***	ΔΔ ***	***	***	***
Islet architecture	***	ΔΔΔ ***	ΔΔΔ ***	**	Δ	***
Insulin^{-ve}, GFP^{+ve} cells	***	ΔΔΔ ***	ΔΔΔ ***	**	ΔΔΔ ***	ΔΔΔ ***
Glucagon^{+ve}, GFP^{+ve} cells	***	ΔΔΔ *	ΔΔ *	***	ΔΔΔ **	ΔΔΔ
Beta cell apoptosis	***	Δ **	ΔΔΔ	*	ΔΔ	ΔΔΔ
Alpha cell apoptosis	***	***	Δ	***	***	**
Beta cell proliferation		*** ΔΔ	*** ΔΔ	**	***	***
Alpha cell proliferation	***		**	***	ΔΔ	Δ
Pdx1 expression	***	ΔΔΔ	ΔΔ ***	***	ΔΔ ***	ΔΔΔ ***
Key	**No change**		**Increased**		**Decreased**	
	*** vs saline - *p<0.05, **p<0.01, ***p<0.001 Δ vs STZ/HFF/HC – Δp<0.05, ΔΔp<0.01, ΔΔΔ p<0.001**					

Figure 7.1: Characterisation and prevention of beta-to-alpha cell transdifferentiation in mouse models of diabetes

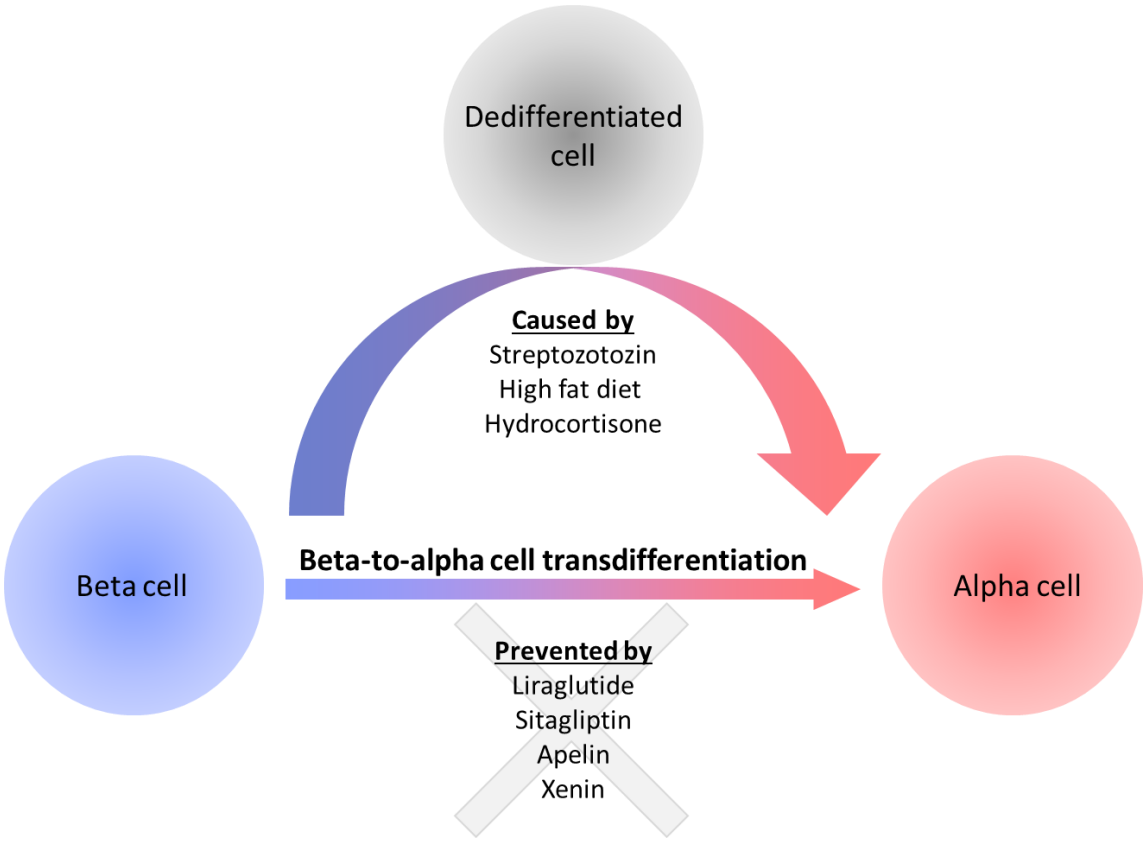

Beta-to-alpha cell transdifferentiation can occur directly (straight arrows) or indirectly (curved arrows) via an initial dedifferentiation of beta cell markers before upregulation of alpha cell markers. This transdifferentiation has been shown to occur in multiple low-dose streptozotocin, high fat fed and hydrocortisone mouse models of diabetes. Beta-to-alpha cell transdifferentiation can be prevented or reversed (grey cross) by incretin therapies, liraglutide and sitagliptin, and non-classical peptides, apelin and xenin.

Figure 7.2: No evidence of beta-to-delta transdifferentiation in STZ-treated *Ins1*$^{cre+/-}$;Rosa26-eYFP C57Bl/6 mice

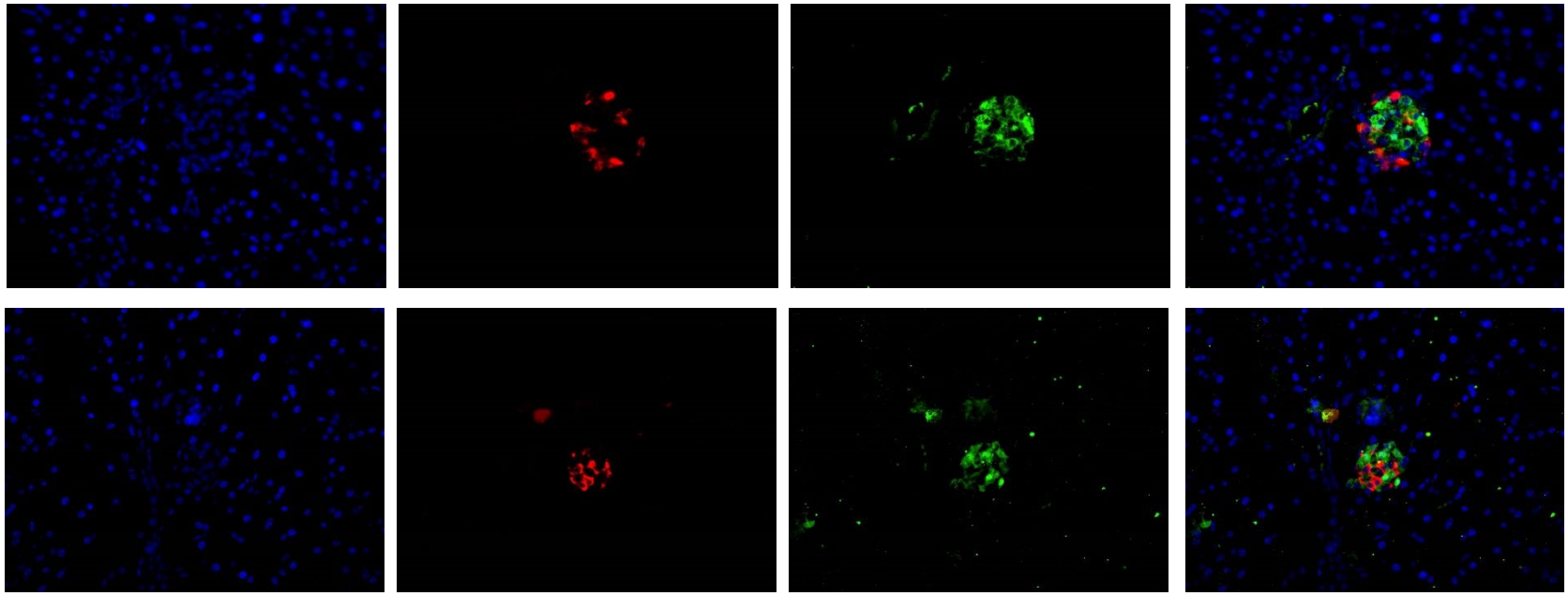

Somatostain / GFP / DAPI

Representative images of islets from streptozotocin treated mice stained for somatostatin (red), GFP (green) and nuclei (blue). Populations of somatostatin positive cells are distinct from GFP positive cells, a strong contraindication of beta-to-delta cell transdifferentiation.

Chapter 8

References

Abbott CA, Malik RA, Ernest RE, Kulkarni J and Boulton AJ 2011 Prevalence and characteristics of painful diabetic neuropathy in a large community-based diabetes population in the UK *Diabetes Care* **34** 2220-2224

Abdelgadir E, Rashid F, Bashier A and Ali R 2018 SGLT-2 inhibitors and cardiovascular protection: lessons and gaps in understanding the current outcome trials and possible benefits of combining SGLT-2 inhibitors With GLP-1 Agonists. *Journal of Clinical Medicine Research* **10(8**) 615

Accili D, Ahrén B, boitard C, Cerasi E, Henquin J-C and Seino S 2010 What ails the β-cell*? Diabetes, Obesity and Metabolism* **12** S1-3

Al-Awar A, Kupai K, Veszelka M, Szűcs G, Attieh Z, Murlasits Z, Török S, Pósa A and Varga C 2016 Experimental diabetes mellitus in different animal models *Journal of Diabetes Research* 9051426

Alexiou C, Zimmerman JP, Schick RR and Schusdziarra V 1998 Xenin – a novel suppressor of food intake in rat *Brain Research* **800** 294-299

Anlauf M, Weihe E, Hartschuh W, Hamscher G and Feurle GE 2000 Localization of xenin-immunoreactive cells in the duodenal mucosa of humans and various mammals. *Journal of Histochemistry & Cytochemistry* **48(12)** 1617-1626.

Ansarullah, Lu Y, Holstein M, DeRuyter B, Rabinovitch A, Guo Z 2013 Stimulating β-cell regeneration by combining a GPR119 agonist with a DPP-IV inhibitor *PLoS ONE* **8(1)** e53345

Arthen B and Schmidtz O 2004 GLP-1 receptor agonists and DPP-4 inhibitors in the treatment of type 2 diabetes *Hormone and Metabolic Research* **36** 867-876

Asfari M, Janjic D, Meda P, Li G, Halban PA and Wollheim CB 1992 Establishment of 2-mercaptoethanol-dependent differentiated insulin-secreting cell lines. *Endocrinology* **130(1)** 167-178

Ashcroft FM, Proks P, Smith PA, Ämmälä C, Bokvist K and Rorsman P 1994. Stimulus–secretion coupling in pancreatic β cells. *Journal of Cellular Biochemistry* **55**(S1994A) 54-65

Baetens D, Stefan Y, Ravazzola M, Malaisse-Lagae F, Coleman DL and Orci L 1978 Alteration of islet cell populations in spontaneously diabetic mice *Diabetes* **27(1)** 1-7

Baggio LL and Drucker DJ 2007 Biology of incretins: GLP-1 and GIP *Gastroenterology* **132(6)** 2131-2157

Bailey CJ and Day C 2018 Treatment of type 2 diabetes: future approaches. *British medical bulletin*

Bailey CJ and Flatt PR, 1982 Hormonal control of glucose homeostasis during development and ageing in mice *Metabolism-Clinical and Experimental* **31(3)** 238-246

Banting FG and Best CH 1922 The internal secretion of the pancreas *The Journal of Laboratory and Clinical Medicine* **7** 465-480

Bays H, Pi-Sunyer X, Hemmingsson JU, Claudius B, Jensen CB and Van Gaal L 2017 Liraglutide 3.0 mg for weight management: weight-loss dependent and independent effects *Current medical research and opinion* **33(2)** 225-229

Billington EO, Grey A and Bolland MJ 2015 The effect of thiazolidinediones on bone mineral density and bone turnover: systematic review and meta-analysis. *Diabetologia* **58** 2238-2246

Bloomgarden ZT 2000 American Diabetes Association Annual Meeting, 1999: diabetes and obesity, *Diabetes Care* **23 (1)** 118-124

Blum B, Roose AN, Barrandon O, Maehr R, Arvanites AC, Davidow LS, Davis JC, Peterson QP, Rubin LL and Melton DA 2014 Reversal of β cell de-differentiation by a small molecule inhibitor of the TGFβ pathway. eLife 3 e02809

Bonner C, Kerr-Conte J, Gmyr V, Queniat G, Moerman E, Thévenet J, Beaucamps C, Delalleau N, Popescu I, Malaisse WJ and Sener A 2015 Inhibition of the glucose transporter SGLT2 with dapagliflozin in pancreatic alpha cells triggers glucagon secretion *Nature Medicine* **21(5)** 512-517

Bonnevie-Nielsen V, Steffes MW and Lernmark Å 1981 A major loss in islet mass and β-cell function precedes hyperglycemia in mice given multiple low doses of streptozotocin *Diabetes* **30(5)** 424-429

Borg R, Kuenen JC, Carstensen B, Zheng H, Nathan DM, Heine RJ, Nerup J, Borch-Johnsen K Witte DR and ADAG Study Group 2010 Associations between features of glucose exposure and HbA1c the A1c-Derived average glucose (ADAG) study *Diabetes* **54** 69-72

Bosco D, Armanet M, Morel P, Niclauss N, Sgroi A, Muller YD, Giovannoni L, Parnaud G and Berney T 2010 Unique arrangement of alpha-and beta-cells in human islets of Langerhans *Diabetes* **59** 1202-1210

Bosco D, Orci L and Meda P 1989 Homologous but not heterologous contact increases the insulin secretion of individual pancreatic β-cells *Experimental Cell Research* **184(1)** 72-80

Boucher J, Masri B, Daviaud D, Gesta S, Guigné C, Mazzucotelli A, Castan-Laurell I, Tack I, Knibiehler B, Carpéné C and Audigier, Y 2005 Apelin, a newly identified adipokine up-regulated by insulin and obesity *Endocrinology* **146(4)** 1764-1771

Boudina S and Abel ED 2010 Diabetic cardiomyopathy, causes and effects. *Reviews in Endocrine and Metabolic Disorders* **11(1)** 31-39

Bouwens L 1998 Transdifferentiation versus stem cell hypothesis for the regeneration of islet beta-cells in the pancreas *Microscopy Research and Technique* **43(4)** 332-336

Bramswig NC and Kaestner KH 2011 Transcriptional regulation of α-cell differentiation *Diabetes, Obesity and Metabolism* **13** S13-20

Bresnick GH, Engerman R, Davis MD, de Venecia G, Myers FL 1976 Patterns of ischemia in diabetic retinopathy, *Transactions–American Academy of Ophthalmology and Otolaryngology* **81** OP694-709, 1976

Brissova M, Fowler MJ, Nicholson WE, Chu A, Hirshberg B, Harlan DM and Powers AC 2005 Assessment of human pancreatic islet architecture and composition by laser scanning confocal microscopy *Journal of Histochemistry & Cytochemistry* **53(9)** 1087-1097

Brubaker PL and Drucker DJ 2004 Minireview: glucagon-like peptides regulate cell proliferation and apoptosis in the pancreas, gut, and central nervous system. *Endocrinology* **145(6)** 2653-2659

Burke MA, Mutharasan RK and Ardehali H 2008 The sulfonylurea receptor, an atypical ATP-binding cassette protein, and its regulation of the KATP channel *Circulation Research* **102(2)** 164-176

Butler AE, Janson J, Bonner-Weir S, Ritzel R, Rizza RA and Butler PC. 2003 β-cell deficit and increased β-cell apoptosis in humans with type 2 diabetes *Diabetes* **52** 102-110

Butler PC, Meier JJ, Butler AE and Bhushan A 2007 The replication of beta cells in normal physiology, in disease and for therapy *Nature Clinical Practice Endocrinology & Metabolism* **11** 758-768

Cabrera O, Berman DM, Kenyon NS, Ricordi C, Berggren PO and Caicedo A 2006 The unique cytoarchitecture of human pancreatic islets has implications for islet cell function *Proceedings of the National Academy of Sciences* **103(7)** 2334-2339

Cederberg H, Saukkonen T, Laakso M, Jokelainen J, Härkönen P, Timonen M, Keinänen-Kiukaanniemi S and Rajala U 2010 Postchallenge glucose, A1C, and fasting glucose as predictors of type 2 diabetes and cardiovascular disease: a 10-year prospective cohort study *Diabetes Care* **33(9)** 2077-2083

Chalasani N, Younossi Z, Lavine JE, Diehl AM, Brunt EM, Cusi K, Charlton M and Sanyal AJ 2012 The diagnosis and management of non-alcoholic fatty liver disease: practice guideline by the American Association for the Study of Liver Diseases, American College of Gastroenterology, and the American Gastroenterological Association. *Hepatology* **55(6)** 2005-2023

Chasis H, Jolliffe N and Smith HW 1933 The action of phlorizin on the excretion of glucose, xylose, sucrose, creatinine and urea by man. *The Journal of Clinical Investigation* **12(6)** 1083-1090

Chen LH and Leung PS 2013 Inhibition of the sodium glucose co-transporter-2: its beneficial action and potential combination therapy for type 2 diabetes mellitus, *Diabetes, Obesity and Metabolism* **15(5)** 392-402

Chen H, Charlat O, Tartaglia LA, Woolf EA, Weng X, Ellis SJ, Lakey ND, Culpepper J, More KJ, Breitbart RE and Duyk GM 1996 Evidence that the diabetes gene encodes the leptin receptor: identification of a mutation in the leptin receptor gene in db/db mice *Cell* **84(3)** 491-495

Chen H, Zhou W, Ruan Y, Yang L, Xu N, Chen R, Yang R, Sun J and Zhang Z 2018 Reversal of angiotensin ll-induced β-cell dedifferentiation via inhibition of NF-κb signalling *Molecular Medicine* **24(1)** 43

Chen L, Klein T and Leung P 2012 Effects of combining linagliptin treatment with BI-38335, a novel SGLT2 inhibitor, on pancreatic islet function and inflammation in db/db mice *Current Molecular Medicine* **12(8)** 995-1004

Cho JM, Jang HW, Cheon H, Jeong YT, Kim DH, Lim YM, Choi SH, Yang EK, Shin CY, Son MH, Kim SH, Kim HJ & Lee MS 2011 A novel dipeptidyl peptidase IV inhibitor DA-1229 ameliorates streptozotocin-induced diabetes by increasing beta cell replication and neogenesis. *Diabetes Research and clinical Practice* **91** 72–79

Cho NH, Shaw JE, Karuranga S, Huang Y, da Rocha Fernandes JD, Ohlrogge AW and Malanda B 2018 IDF Diabetes Atlas: global estimates of diabetes prevalence for 2017 and projections for 2045 *Diabetes Research and Clinical Practice* **138** 271-281

Cinti F, Bouchi R, Kim-Muller JY, Ohmura Y, Sandoval PR, Masini M, Marselli L, Suleiman M, Ratner LE, Marchetti P and Accili D 2016 Evidence of β-cell dedifferentiation in human type 2 diabetes *The Journal of Clinical Endocrinology & Metabolism* **101(3)** 1044-1054

Collmbat P, Hecksher-Sorensen J, Broccoli V, Krull J, Ponte I, Mundiger T, Smith J, Gruss P, Serup P & Mansouri A 2005 The simultaneous loss of *Arx* and *Pax4* genes promotes a somatostatin-producing cell fate specification at the expense of the α- and β-cell lineages in the mouse endocrine pancreas *Development* **132** 2969-2980

Collombat P, Hecksher-Sørensen J, Krull J, Berger J, Riedel D, Herrera PL, Serup P and Mansouri A. 2007 Embryonic endocrine pancreas and mature beta cells acquire alpha and PP cell phenotypes upon arx misexpression *Journal of Clinical Investigation* **117** 961-970

Collombat P, Hecksher-Sorensen J, Serup P & Mansouri A 2006 Specifying pancreatic endocrine cell fates *Mechanisms of development* **123** 501–512

Collombat P, Xu X, Ravassard P, Sosa-Pineda B, Dussaud S, Billestrup N, Madsen OD, Serup P, Heimberg H & Mansuori A 2009 The ectopic expression of Pax4 in the mouse pancreas converts progenitor cells into alpha and subsequently beta-cells *Cell* **138** 449-62

Cooke JH, Patterson M, Patel SR, Smith KL, Ghatei MA, Bloom SR and Murphy KG 2009 Peripheral and central administration of xenin and neurotensin suppress food intake in rodents *Obesity* **17(6)** 1135-1143

Courtney M, Gjernes E, Druelle N, Ravaud C, Vieira A, Ben-Othman N, Pfeifer A, Avolio F, Leuckx G, Lacas-Gervais S, Burel-Vandenbos F, Ambrosetti D, Hecksher-Sorensen J, Ravassard P, Heimberg H, Mansouri A and Collombat P 2013 The inactivation of *Arx* in pancreatic α-cells triggers their neogenesis and conversion into functional β-like cells *PLOS Genetics* **9** e1003934

Cox AR, Lam CJ, Rankin MM, Rios JS, Chavez J, Bonnyman CW, King KB, Wells RA, Anthony D, Tu JX, Kim JJ, Li C and Kushner JA 2017 Incretin therapies do not expand β-Cell mass or alter pancreatic histology in young male mice *Endocrinology* **158 (6)** 1701-1714

D'Amicio M, Di Filippo C, Marfella R, Abbatecola AM, Ferraraccio F, Rossi F & Paolisso G 2010 Long-term inhibition of dipeptidyl peptidase-4 in Alzheimer's prone mice *Experimental Gerontology* **45(3)** 202-207

Da Silva Xavier G 2018 The cells of the islets of Langerhans *Journal of Clinical Medicine* **7(3)** 54

Davies JL, Kawaguchi Y, Bennett ST, Copeman JB, Cordell HJ, Pritchard LE, Reed PW, Cough SC, Jenkins SC, Palmer SM, Balfour KM, Rowe BR, Farrall M, Barnett AH, Bain SC and Todd JA 1994 A genome-wide search for human type 1 diabetes susceptibility genes *Nature* **371** 130-136

Deacon CF, Danielsen P, Klarskov , Olesen M & Holst JJ 2001 Dipeptidyl peptidase IV inhibition reduces the degradation and clearance of GIP and potentiates its insulinotropic and antihyperglycaemic effects in anesthetised pigs *Diabetes* **50(7)** 1588-1597

Deacon CF, Hughes TE & Holst JJ 1998 Dipeptidyl peptidase IV inhibition potentiates the insulinotropic effect of glucagon-like peptide 1 in the anesthetized pig *Diabetes* **47(5)** 764-769

Deacon CF, Nauck MA, Toft-Nielsen M, Pridal L, Willms B & Holst JJ 1995 Both subcutaneously and intravenously administered glucagon-like peptide I are rapidly degraded from the NH_2 terminus in type II diabetic patients and in healthy subjects *Diabetes* **44** 1126-1131

Dekel Y, Glucksam Y, Elron-Gross I and Margalit R 2009 Insights into modeling streptozotocin-induced diabetes in ICR mice *Lab Animal* **38(2)** 55-60

Derosa G and Maffioli P 2012 GLP-1 agonists exenatide and liraglutide: a review about their safety and efficacy *Current Clinical Pharmacology* **7** 214-228

Dhawan S, Georgia S, Tschen SI, Fan G, Bhushan A 2011 Pancreatic β-cell identity is maintained by DNA methylation-mediated repression of Arx. *Dev Cell* **20** 419-29

Diedisheim M, Oshima M, Albagli O, Huldt CW, Ahlstedt I, Clausen M, Menon S, Aivazidis A, Andreasson AC, Haynes WG and Marchetti P 2018 Modeling human pancreatic beta cell dedifferentiation *Molecular Metabolism* **10** 74-86

Dolenšek J, Rupnik MS and Stožer A 2015 Structural similarities and differences between the human and the mouse pancreas *Islets* **7(1)** e1024405.

Domanski M, Mitchell G, Pfeffer M, Neaton JD, Norman J, Svendsen K, Grimm R, Cohen J, Stamler J and MRFIT Research Group 2002 Pulse pressure and cardiovascular disease–related mortality: follow-up study of the Multiple Risk Factor Intervention Trial (MRFIT) *The Journal of the American Medical Association* **287(20)** 2677-2683

Domecq JP, Prutsky G, Leppin A, Sonbol MB, Altayar O, Undavalli C, Wang Z, Elraiyah T, Brito JP, Mauck KF and Lababidi MH 2015 Drugs commonly associated with weight change: a systematic review and meta-analysis *The Journal of Clinical Endocrinology & Metabolism* ***100*****(2)** 363-370

Dray C, Knauf C, Daviaud D, Waget A, Boucher J, Buléon M, Cani PD, Attané C, Guigné C, Carpéné C and Burcelin R 2008 Apelin stimulates glucose utilization in normal and obese insulin-resistant mice *Cell Metabolism* **8(5)** 437-445

Drucker DJ 2006 The biology of incretin hormones *Cell Metabolism* **3(3)** 153-165

Drucker DJ and Nauck MA 2006 The incretin system: glucagon-like peptide-1 receptor agonists and dipeptidyl peptidase-4 inhibitors in type 2 diabetes. *The Lancet* **368(9548)** 1696-1705

Federation ID 2013 IDF diabetes atlas. *Brussels: International Diabetes Federation*.

Feng L, Matsumoto C, Schwartz A, Schmidt AM, Stern DM and Pile-Spellman J 2005 Chronic vascular inflammation in patients with type 2 diabetes: endothelial biopsy and RT-PCR analysis *Diabetes Care* **28(2)** 379-384

Feurle GE, Hamscher G, Kusiek R, Meyer HE and Metzger JW 1992 Identification of xenin, a xenopsin-related peptide, in the human gastric mucosa and its effect on exocrine pancreatic secretion *Journal of Biological Chemistry* **267(31)** 22305-22309

Fineman MS, Cirincione BB, Maggs D and Diamant M 2012 GLP-1 based therapies: differential effects on fasting and postprandial glucose. *Diabetes, Obesity and Metabolism* **14(8)** 675-688

Fiori JL, Shin YK, Kim W, Krzysik-Walker SM, González-Mariscal I, Carlson OD, Sanghvi M, Moaddel R, Farhang K, Gadkaree SK and Doyle ME 2013 Resveratrol prevents β-cell dedifferentiation in non-human primates given a high fat/high sugar diet *Diabetes* **62** 3500-3513

Flatt PR, DeSilva MG, Swanston-Flatt SK, Powell CJ and Marks V 1988 Tumour formation and insulin secretion by clonal RINm5F cells following repeated subcutaneous transplantation in NEDH rats. *Journal of Endocrinology* **118(3)** 429

Flint A, Raben A, Astrup A and Holst JJ 1998 Glucagon-like peptide 1 promotes satiety and suppresses energy intake in humans *The Journal of Clinical Investigation* **101(3)** 515-520

Forbes JM and Cooper ME 2011 Mechanisms of diabetic complications *Physiological Reviews* **93(1)** 137-188

Fourlanos S, Narendran P, Byrnes GB, Colman PG, Harrison LC 2004 Insulin resistance is a risk factor for progression to type 1 diabetes *Diabetologia* **47** 1661-1667

Frank RN 2004 Diabetic retinopathy *New England Journal of Medicine* **350**: 48-58

Franz MJ, Van-Wormer JJ, Crain AL, Boucher JL, Histon T, Caplan W, Bowman JD and Pronk NP 2007 Weight-loss outcomes: a systematic review and meta-analysis of weight-loss clinical trials with a minimum 1-year follow-up. *Journal of the American Dietetic Association* **107(10)** 1755-1767

Freitas HS, Anhe GF, Melo KFS, Okamoto MM, Oliveira-Souza M, Bordin, S and Machado UF 2007 Na+-glucose transporter-2 messenger ribonucleic acid expression in kidney of diabetic rats correlates with glycemic levels: involvement of hepatocyte nuclear factor-1α expression and activity *Endocrinology* **149(2)** 717-724

Gallo LA, Wright EM and Vallon V 2015 Probing SGLT2 as a therapeutic target for diabetes: basic physiology and consequences *Diabetes and Vascular Disease Research* **12(2)** 78-89

Gallwitz B 2007 Sitagliptin: profile of a novel DPP-4 inhibitor for the treatment of type 2 diabetes *Drugs of Today* **43(1)** 13

Gao X, Cai X, Yang W, Chen Y, Han X and Ji L 2018 Meta-analysis and critical review on the efficacy and safety of alpha-glucosidase inhibitors in Asian and non-Asian populations *Journal of Diabetes Investigation* **9(2)** 321-331

Gault VA, Lennox R & Flatt PR 2015 Sitagliptin, a dipeptidyl peptidase-4 inhibitor, improves recognition memory, oxidative stress and hippocampal neurogenesis and upregulates key genes involved in cognitive decline *Diabetes Obesity and Metabolism* **17(4)** 403-413

Gault VA, Irwin N, Green BD, McCluskey JT, Greer B, Bailey CJ, Harriott P, O'Harte FP and Flatt PR 2005 Chemical ablation of gastric inhibitory polypeptide receptor action

by daily (Pro3) GIP administration improves glucose tolerance and ameliorates insulin resistance and abnormalities of islet structure in obesity-related diabetes *Diabetes* **54(8)** 2436-2446

Gault VA, Lennox R and Flatt PR 2015 Sitagliptin, a dipeptidyl peptidase-4 inhibitor, improves recognition memory, oxidative stress and hippocampal neurogenesis and upregulates key genes involved in cognitive decline. *Diabetes, Obesity and Metabolism* **17(4)** 403-413

Gazdar AF, Chick WL, Oie HK, SIMs HL, King DL, Weir GC and Lauris V 1980 Continuous, clonal, insulin-and somatostatin-secreting cell lines established from a transplantable rat islet cell tumor *Proceedings of the National Academy of Sciences* **77(6)** 3519-3523

Gershengorn MC, Hardikar AA, Wei C, Geras-Raaka E, Marcus-Samuels B & Raaka BM 2004 Epithelial-to-mesenchymal transition generates proliferative human islet precursor cells *Science* **306** 2261-2264

Gilbertson DT, Liu J, Xue JL, Louis TA, Solid CA, Ebben JP, Collins AJ 2005 Projecting the number of patients with end-stage renal disease in the United States to the year 2015 *Journal of the American Society of Nephrology* **16** 3736-3741

Green AD, Vasu S, McClenaghan NH and Flatt PR 2016 Implanting 1.1 B4 human β-cell pseudoislets improves glycaemic control in diabetic severe combined immune deficient mice *World journal of diabetes* ***7*****(19)** 523

Gromada J, Holst JJ and Rorsman, P 1998 Cellular regulation of islet hormone secretion by the incretin hormone glucagon-like peptide 1 *Pflügers Archive* **435(5)** 583-594

Grossman SL and Lessem J 1997 Mechanisms and clinical effects of thiazolidinediones *Expert Opinion on Investigational Drugs* **6(8)** 1025-1040

Guo S, Dai C, Guo M, Taylor B, Harmon JS, Sander M, Robertson RP, Powers AC and Stein R 2013 Inactivation of specific β cell transcription factors in type 2 diabetes. *The Journal of Clinical Investigation* **123(8)** 3305-3316

Habener JF & Stanojevic V 2012 α-cell role in β-cell generation and regeneration *Islets* **4(3)** 188-198

Haffner SM, Lehto S, Rönnemaa T, Pyörälä K and Laakso M 1998. Mortality from coronary heart disease in subjects with type 2 diabetes and in nondiabetic subjects with and without prior myocardial infarction *New England Journal of Medicine* **339(4)** 229-234

Halban PA, Praz GA and Wollheim CB 1983 Abnormal glucose metabolism accompanies failure of glucose to stimulate insulin release from a rat pancreatic cell line (RINm5F) *Biochemical Journal* **212(2)** 439-443

Han S, Hagan DL, Taylor JR, Xin L, Meng W, Biller SA, Wetterau JR, Washburn WN and Whaley JM 2008 Dapagliflozin, a selective SGLT2 inhibitor, improves glucose homeostasis in normal and diabetic rats *Diabetes* **57(6)** 1723-1729

Harper W, Clement M, Goldenberg R, Hanna A, Main A, Retnakaran R, Sherifali D, Woo V and Yale, J-F 2013 Clinical practice guidelines for the prevention and

management of diabetes in Canada: pharmacologic management of type 2 diabetes. *Canadian Journal of Diabetes* **37** S61-69

Hattersley AT and Thorens B 2015 Type 2 diabetes, SGLT2 inhibitors, and glucose secretion *New England Journal of Medicine* **373(10)** 974-976

Heller SR 2009 A Summary of the ADVANCE trial *Diabetes Care* **32** S357-S361

Heller SR, Stoffers DA, Liu A, Schedle A, Crenshaw BE, Madsen OD and Serup P 2004 The role of Brn4/*Pou3f4* and Pax5 in forming the pancreatic glucagon cell identity *Developmental Biology* **268** 123-134

Henquin JC and Rahier J 2011 Pancreatic alpha cell mass in European subjects with type 2 diabetes *Diabetologia* ***54*****(7)** 1720-1725

Herman GA, Bergman A, Stevens C, Kotey P, Yi B, Zhao P, Dietrich B, Golor G, Schrodter A, Keymeulen B and Lasseter KC 2006 Effect of single oral doses of sitagliptin, a dipeptidyl peptidase-4 inhibitor, on incretin and plasma glucose levels after an oral glucose tolerance test in patients with type 2 diabetes *The Journal of Clinical Endocrinology & Metabolism* **91(11)** 4612-4619

Hex N, Bartlett C, Wright D, Taylor M and Varley D 2012 Estimating the current and future costs of type 1 and type 2 diabetes in the UK, including direct health costs and indirect societal and productivity costs *Diabetic Medicine* **29** 855-862

Hirai FE, Tielsch JM, Klein BE, Klein R 2011 Ten-year change in vision-related quality of life in type 1 diabetes: Wisconsin epidemiologic study of diabetic retinopathy *Ophthalmology* **118** 353-358

Hu He KH, Lorenzo PI, Brun T, Jimenez Moreno CM, Aeberhard D, Vallejo Ortega J, Cornu M, Thorel F, Gjinovci A, Thorens B, Herrera PL, Meda P, Wollheim CB & Gauthier BR 2011 In vivo conditional Pax4 overexpression in mature islet beta-cells prevents stress-induced hyperglycaemia in mice *Diabetes* **60(6)** 1705-1715

Hummel, K.P., Dickie, M.M. and Coleman, D.L., 1966. Diabetes, a new mutafton in the mouse. *Science*, **153(3740):** 1127-1128.

IDF Diabetes Atlas Group 2013 Update of mortality attributable to diabetes for the IDF diabetes atlas: estimates for the year 2011 *Diabetes Research and Clinical Practice* **100** 277-279

Irwin N, O'Harte FP, Gault VA, Green BD, Greer B, Harriott P, Bailey CJ and Flatt PR 2006 GIP (Lys16PAL) and GIP (Lys37PAL): novel long-acting acylated analogues of glucose-dependent insulinotropic polypeptide with improved antidiabetic potential. *Journal of Medicinal Chemistry* **49(3)** 1047-1054

Ishida E, Kim-Muller JY and Accili D 2017 Pair-feeding, but not insulin, phloridzin, or rosiglitazone treatment curtails markers of beta-cell dedifferentiation in db/db mice *Diabetes* db161213.

Ishihara H, Asano T, Tsukuda K, Katagiri H, Inukai K, Anai M, Kikuchi M, Yazaki Y, Miyazaki JI and Oka Y 1993 Pancreatic beta cell line MIN6 exhibits characteristics of glucose metabolism and glucose-stimulated insulin secretion similar to those of normal islets *Diabetologia* **36** 1139-1145

Ito M, Kondo Y, Nakatani A, Hayashi K and Naruse A. 2001 Characterization of low dose streptozotocin-induced progressive diabetes in mice. *Environmental Toxicology and Pharmacology* **9** 71-78

Jabbour SA, Hardy E, Sugg J, Parikh S and Study 10 Group 2014 Dapagliflozin is effective as add-on therapy to sitagliptin with or without metformin: a 24-week, multicenter, randomized, double-blind, placebo-controlled study. *Diabetes Care* **37(3)** 740-750

Jiang YF, Chen XY, Ding T, Wang XF, Zhu ZN and Su SW 2015 Comparative efficacy and safety of OADs in management of GDM: network meta-analysis of randomized controlled trials. *The Journal of Clinical Endocrinology & Metabolism* ***100*****(5)** 2071-2080

Johansson K, Neovius M and Hemmingsson E 2013 Effects of anti-obesity drugs, diet, and exercise on weight-loss maintenance after a very-low-calorie diet or low-calorie diet: a systematic review and meta-analysis of randomized controlled trials *The American Journal of Clinical Nutrition* **99(1)** 14-23

Kanai Y, Lee WS, You G, Brown D and Hediger MA 1994 The human kidney low affinity Na+/glucose cotransporter SGLT2 delineation of the major renal reabsorptive mechanism for D-glucose *The Journal of Clinical Investigation* **93(1)** 397-404

Karaskov E, Scott C, Zhang L, Teodoro T, Ravazzola M and Volchuk A 2006 Chronic palmitate but not oleate exposure induces endoplasmic reticulum stress, which may contribute to INS-1 pancreatic β-cell apoptosis *Endocrinology* **147(7)** 3398-3407

Kaur G, and Dufour JM 2012. Cell lines: Valuable tools or useless artefacts *Spermatogenesis* **2(1)** 1-5

Kawasaki F, Matsuda M, Kanda Y, Inoue H and Kaku K 2005 Structural and functional analysis of pancreatic islets preserved by pioglitazone in db/db mice *American Journal of Physiology-Endocrinology and Metabolism* **288(3)** E510-E518

Khan D, Vasu S, Moffett RC, Irwin N and Flatt PR 2016 Islet distribution of Peptide YY and its regulatory role in primary mouse islets and immortalised rodent and human beta-cell function and survival *Molecular and Cellular Endocrinology* **436** 102-113

Khan D, Vasu S, Moffett RC, Irwin N and Flatt PR 2017 Differential expression of glucagon-like peptide-2 (GLP-2) is involved in pancreatic islet cell adaptations to stress and beta-cell survival *Peptides* **95** 68-75

Khan D, Vasu S, Moffett RC, Irwin N and Flatt PR, 2017 Influence of neuropeptide Y and pancreatic polypeptide on islet function and beta-cell survival *Biochimica et Biophysica Acta (BBA)-General Subjects* **1861(4)** 749-758

Kim A, Miller K, Jo J, Kilimnik G, Wojcik P and Hara M 2009 Islet architecture: A comparative study *Islets* **1(2)** 129-136

King AJ 2012 The use of animal models in diabetes research. *British Journal of Pharmacology* **166(3)** 877-894

Kitamura T 2013 The role of FOXO1 in β-cell failure and type 2 diabetes mellitus *Nature Reviews Endocrinology* **9** 615-623

Kjørholt C, Åkerfeldt MC, Biden TJ and Laybutt DR 2005 Chronic hyperglycemia, independent of plasma lipid levels, is sufficient for the loss of β-cell differentiation

and secretory function in the db/db mouse model of diabetes *Diabetes* **54(9)** 2755-2763

Knudsen LB, Nielsen PF, Huusfeldt PO, Johansen NL, Madsen K, Pedersen FZ, Thøgersen H, Wilken M & Agersø H 2000 Potent derivatives of glucagon-like peptide-1 with pharmacokinetic properties suitable for once daily administration *Journal of Medicinal Chemistry* **43(9)** 1664-1669

Laing SP, Swerdlow AJ, Slater SD, Burden AC, Morris A, Waugh NR, Gatling W, Bingley PJ and Patterson CC 2003 Mortality from heart disease in a cohort of 23,000 patients with insulin-treated diabetes *Diabetologia* **46(6)** 760-765

Latreille M, Hausser J, Stützer I, Zhang Q, Hastoy B, Gargani S, Kerr-Conte J, Pattou F, Zavolan M, Esguerra JL and Eliasson L 2014 MicroRNA-7a regulates pancreatic β cell function *The Journal of Clinical Investigation*, **124(6):** 2722-2735.

Leahy JL 2005 Pathogenesis of type 2 diabetes mellitus *Archives of Medical Research* **36** 197-209

Lebovitz HE and Feinglos MN 1978 Sulfonylurea drugs: mechanism of antidiabetic action and therapeutic usefulness *Diabetes Care* **1(3)** 189-198

Lebovitz HE 1997 Alpha-glucosidase inhibitors *Endocrinology and Metabolism Clinics of North America* **26(3)** 539-551

Lee YS, Lee C, Choung JS, Jung HS and Jun HS 2018 Glucagon-Like Peptide 1 increases β-Cell regeneration by promoting α-to β-cell transdifferentiation *Diabetes* **67(12)** 2601-2614

Lee GH, Proenca R, Montez JM, Carroll KM, Darvishzadeh JG, Lee JI and Friedman JM 1996 Abnormal splicing of the leptin receptor in diabetic mice *Nature* **379(6566)** 632-635

Lee SM, Choi SE, Lee JH, Lee JJ, Jung IR, Lee SJ, Lee KW and Kang Y 2011 Involvement of the TLR4 (Toll-like receptor4) signalling pathway in palmitate-induced INS-1 beta cell death *Molecular and Cellular Biochemistry* **354(1-2)** 207-217

Lehuen A, Diana J, Zaccoone P and Cooke A 2010 Immune cell crosstalk in type 1 diabetes *Nature Reviews Immunology* **10** 501-513

Lenzen S 2008 The mechanisms of alloxan- and streptozotocin-induced diabetes *Diabetologia* **51(2)** 216-226

Liao HW, Saver JL, Wu YL, Chen TH, Lee M and Ovbiagele B 2017 Pioglitazone and cardiovascular outcomes in patients with insulin resistance, pre-diabetes and type 2 diabetes: a systematic review and meta-analysis *British Medical Journal Open* ***7*(1)** p.e013927

Like AA and Rossini AA 1976 Streptozotocin-induced pancreatic insulitis: new model of diabetes mellitus *Science* **193(4251)** 415-417

Lin Y and Sun Z 2010 Current views on type 2 diabetes *Journal of Endocrinology* **1** 1-11

Liou AP, Paziuk M, Luevano JM, Machineni S, Turnbaugh PJ and Kaplan LM 2013 Conserved shifts in the gut microbiota due to gastric bypass reduce host weight and adiposity *Science Translational Medicine* **5(178)** 78ra41-178ra41

List JF, Woo V, Morales E, Tang W and Fiedorek FT 2009 Sodium-glucose cotransport inhibition with dapagliflozin in type 2 diabetes *Diabetes Care* **32(4)** 650-657

Lyu X, Zhu X, Zhao B, Du L, Chen D, Wang C, Liu G and Ran X 2017 Effects of dipeptidyl peptidase-4 inhibitors on beta-cell function and insulin resistance in type 2 diabetes: meta-analysis of randomized controlled trials *Scientific Reports* **7** 44865

Macdonald C, 1990 Development of new cell lines for animal cell biotechnology *Critical Reviews in Biotechnology* **10(2)** 155-178

Macdonald FR, Peel JE and Jones HB 2010 The novel SGLT2 inhibitor dapagliflozin sustains pancreatic function and preserves islet morphology in obese, diabetic rats *Diabetes Obesity and Metabolism* **12(11)** 1004-1012

Maiztegui B, Borelli MI, Madrid VG, Del Zotto H, Raschia MA, Francini F, Massa ML, Flores LE, Rebolledo OR & Gaglardino JJ 2011 Sitagliptin prevents the development of metabolic and hormonal disturbances, increased β-cell apoptosis and liver steatosis induced by a fructose-rich diet in normal rats *Clinical Science* **120** 73-80

Mak, TC and Latreille, M 2018 Generation of a novel mouse model to study pancreatic beta-cell dedifferentiation *American Diabetes Association* **67** supplement 1

Malaisse WJ 2003 Pharmacology of the meglitinide analogs *Treatments in Endocrinology* **2(6)** 401-414

Maleckas A, Venclauskas L, Wallenius V, Lönroth H and Fändriks L 2015 Surgery in the treatment of type 2 diabetes mellitus *Scandinavian Journal of Surgery* **104(1)** 40-47

Márquez-Aguirre AL, Canales-Aguirre AA, Padilla-Camberos E, Esquivel-Solis H and Díaz-Martínez NE 2015 Development of the endocrine pancreas and novel strategies for β-cell mass restoration and diabetes therapy *Brazilian Journal of Medical and Biological Research* **48** 765-776

Manigault KR and Thurston MM 2016 Liraglutide: a glucagon-like peptide-1 agonist for chronic weight management *The Consultant Pharmacist®* **31(12)** 685-697

Martin CM, Gault VA, McClean S, Flatt PR and Irwin N, 2012 Degradation, insulin secretion, glucose-lowering and GIP additive actions of a palmitate-derivatised analogue of xenin-*25 Biochemical pharmacology* **84(3)** 312-319

Mauer SM, Steffes MW, Ellis EN, Sutherland DE, Brown DM, Goetz FC 1984 Structural-functional relationships in diabetic nephropathy *Journal of Clinical Investigation* **74** 1143-1155

Meneghini LF, Orozco-Beltran D, Khunti K, Caputo S, Damci T, Liebl A and Ross SA 2011 Weight beneficial treatments for type 2 diabetes *The Journal of Clinical Endocrinology & Metabolism* **96(11)** 3337-3353

Merglen A, Theander S, Rubi B, Chaffard G, Wollheim CB and Maechler P 2004 Glucose sensitivity and metabolism-secretion coupling studied during two-year continuous culture in INS-1E insulinoma cells *Endocrinology* **145(2)** 667-678

Merovci A, Solis-Herrera C, Daniele G, Eldor R, Fiorentino TV, Tripathy D, Xiong J, Perez Z, Norton L, Abdul-Ghani MA and DeFronzo RA 2014 Dapagliflozin improves muscle insulin sensitivity but enhances endogenous glucose production *The Journal of clinical investigation* **124(2)** 509-514

Mest HJ and Mentlein R 2005 Dipeptidyl peptidase inhibitors as new drugs for the treatment of type 2 diabetes *Diabetologia* **48(4)** 616-620

Mietlicki-Baase EG 2016 Amylin-mediated control of glycemia, energy balance, and cognition *Physiology & Behavior* **162**: 130-140

Millar P, Pathak V, Moffett RC, Pathak NM, Bjourson AJ, O'Kane MJ, Flatt PR and Gault VA 2016. Beneficial metabolic actions of a stable GIP agonist following pre-treatment with a SGLT2 inhibitor in high fat fed diabetic mice *Molecular and cellular endocrinology* **420** 37-45

Millar P, Pathak N, Parthsarathy V, Bjourson AJ, O'Kane M, Pathak V, Moffett RC, Flatt PR and Gault VA 2017 Metabolic and neuroprotective effects of dapagliflozin and liraglutide in diabetic mice *The Journal of Endocrinology* **234 (3)** 255-267

Mithieux G 2009 A novel function of intestinal gluconeogenesis: central signalling in glucose and energy homeostasis *Nutrition* **25(9)** 881-884

Miyazaki JI, Araki K, Yamato E, Ikegami H, Asano T, Shibasaki Y, Oka Y and Yamamura KI 1990 Establishment of a pancreatic β cell line that retains glucose-inducible insulin secretion: special reference to expression of glucose transporter isoforms *Endocrinology* **127(1)** 126-132

Mogensen CE, Christensen CK, Vittinghus E 1983 The stages in diabetic renal disease with emphasis on the stage of incipient diabetic nephropathy *Diabetes* **32** 64-78

Monami M, Nreu B, Scatena A, Cresci B, Andreozzi F, Sesti G and Mannucci E 2017 Safety issues with glucagon-like peptide-1 receptor agonists (pancreatitis, pancreatic

cancer and cholelithiasis): data from randomized controlled trials *Diabetes, Obesity and Metabolism* **19(9)** 1233-1241

Naderpoor N, Shorakae S, de Courten B, Misso ML, Moran LJ and Teede HJ 2015 Metformin and lifestyle modification in polycystic ovary syndrome: systematic review and meta-analysis *Human Reproduction Update* **21(5)** 560-574

Nakashima K, Kanda Y, Hirokawa Y, Kawasaki F, Matsuki M and Kaku K 2009 MIN6 is not a pure beta cell line but a mixed cell line with other pancreatic endocrine hormones *Endocrine Journal* **56** 45-53

Nauck MA, Heimesaat MM, Orskov C, Holst JJ, Ebert R and Creutzfeldt W 1993 Preserved incretin activity of glucagon-like peptide 1 [7-36 amide] but not of synthetic human gastric inhibitory polypeptide in patients with type-2 diabetes mellitus *The Journal of Clinical Investigation* **91(1)** 301-307

Nauck MA, Meier JJ, Cavender MA, Abd El Aziz M and Drucker DJ, 2017 Cardiovascular actions and clinical outcomes with glucagon-like peptide-1 receptor agonists and dipeptidyl peptidase-4 inhibitors *Circulation* **136(9)** 849-870

Nauck MA, Niedereichholz U, Ettler R, Holst JJ, Ørskov C, Ritzel R and Schmiegel WH 1997 Glucagon-like peptide 1 inhibition of gastric emptying outweighs its insulinotropic effects in healthy humans *American Journal of Physiology-Endocrinology and Metabolism* **273(5)** E981-E988

NCD Risk Factor Collaboration 2016 Worldwide trends in diabetes since 1980: a pooled analysis of 751 population-based studies with 4.4 million participants *The Lancet* **387(10027)** 1513-1530

Nokins AL and Lernmark A 2001 Autoimmune type 1 diabetes: resolved and unresolved issues *Journal of Clinical Investigation* **108** 1247-1252

O'Harte FPM, Parthsarathy V, Hogg C, Flatt PR 2018 Long-term treatment with acylated analogues of apelin-13 amide ameliorates diabetes and improves lipid profile of high-fat fed mice *PLoS ONE* **13 (8)** e0202350

O'Brien, BA, Harmon BV, Cameron DP and Allan DJ 1996 Beta-cell apoptosis is responsible for the development of IDDM in the multiple low-dose streptozotocin model *The Journal of Pathology* **178(2)** 176-181

Obrosova IG 2009 Diabetic painful and insensate neuropathy: pathogenesis and potential treatments *Neurotherapeutics* **6(4)** 638-647

Okon EB, Chung AW, Rauniyar P, Padilla E, Tejerina T, McManus BM, Luo H and van Breemen C 2005 Compromised arterial function in human type 2 diabetic patients *Diabetes* **54(8)** 2415-2423

Papizan JB, Singer RA, Tschen SI, Dhawan S, Friel JM, Hipkens SB, Magnuson MA, Bhushan A and Sussel L, 2011 Nkx2. 2 repressor complex regulates islet β-cell specification and prevents β-to-α-cell reprogramming *Genes & development* **25(21)** 2291-2305

Pappachan JM Fernandez CJ and Chacko EC 2018 Diabesity and antidiabetic drugs *Molecular Aspects of Medicine* https:/doi.org/10.1016/.mam.2018.10.004

Pappachan, JM, Raveendran AV and Sriraman R 2015 Incretin manipulation in diabetes management *World Journal of Diabetes* **6(6)** 774

Parthsarathy V, Hogg C, Flatt PR and O'harte FP 2018 Beneficial long-term antidiabetic actions of N-and C-terminally modified analogues of apelin-13 in diet-induced obese diabetic mice *Diabetes, Obesity and Metabolism* **20(2)** 319-327

Parthsarathy V, Irwin N, Hasib A, Martin CM, McClean S, Bhat VK, Ng MT, Flatt PR and Gault VA 2016 A novel chemically modified analogue of xenin-25 exhibits improved glucose-lowering and insulin-releasing properties *Biochimica et Biophysica Acta (BBA)-General Subjects* **1860(4)** 757-764

Pathak V, Vasu S, Gault VA, Flatt PR and Irwin N 2015 Sequential induction of beta cell rest and stimulation using stable GIP inhibitor and GLP-1 mimetic peptides improves metabolic control in C57Bl/Ks *db/db* mice *Diabetologia* **(58)9** 2144-2153

Pintana H, Apaijai N, Chattipakorn N & Chattipakorn SC 2013 DPP-4 inhibitors improve cognition and brain mitochondrial function of insulin resistant rats *Journal of Endocrinology* **218** 1-11

Pi-Sunyer X, Astrup A, Fujioka K, Greenway F, Halpern A, Krempf M, Lau DC, Le Roux CW, Violante Ortiz R, Jensen CB and Wilding JP 2015 A randomized, controlled trial of 3.0 mg of liraglutide in weight management. *New England Journal of Medicine* **373(1)** 11-22

Porter WD, Flatt PR, Hölscher C and Gault VA 2013 Liraglutide improves hippocampal synaptic plasticity associated with increased expression of Mash1 in ob/ob mice. *International Journal of Obesity* **37(5)** 678

Porter WD, Kerr BD, Flatt PR, Holscher C and Gault VA 2010 Four weeks administration of Liraglutide improves memory and learning as well as glycaemic

control in mice with high fat dietary-induced obesity and insulin resistance *Diabetes, Obesity and Metabolism* **12(10)** 891-899

Pospisilik JA, Stafford SG, Demuth HU, Brownsey R, Parkhouse W, Finegood DT, McIntosh CHS and Pederson RA 2002 Long-term treatment with the dipeptidyl peptidase IV inhibitor P32/98 causes sustained improvements in glucose tolerance, insulin sensitivity, hyperinsulinemia, and β-cell glucose responsiveness in VDF (fa/fa) Zucker rats *Diabetes*, **51(4)** 943-950

Poucher SM, Cheetham S, Francis J, Zinker B, Kirby M & Vickers P 2012 Effects of saxagliiptin and sitagliptin on glycaemic control and pancreatic β-cell mass in streptozotocin-induced mouse model of type 2 diabetes *Diabetes, Obesity and Metabolism* **14** 918-926

Pournaras DJ, Glicksman C, Vincent RP, Kuganolipava S, Alaghband-Zadeh J, Mahon D, Bekker JH, Ghatei MA, Bloom SR, Walters JR and Welbourn R 2012 The role of bile after Roux-en-Y gastric bypass in promoting weight loss and improving glycaemic control *Endocrinology* **153(8)** 3613-3619

Pratley RE & Salsai A 2007 Inhibition of DPP-4: a new therapeutic approach for the treatment of type 2 diabetes *Current Medical Research and Opinions* **23(4)** 919-931

Qiao, Y.C., Ling, W., Pan, Y.H., Chen, Y.L., Zhou, D., Huang, Y.M., Zhang, X.X. and Zhao, H.L., 2017. Efficacy and safety of pramlintide injection adjunct to insulin therapy in patients with type 1 diabetes mellitus: a systematic review and meta-analysis. *Oncotarget*, *8*(39), p.66504-66515

Ribaric, G., Buchwald, J.N. and McGlennon, T.W., 2014. Diabetes and weight in comparative studies of bariatric surgery vs conventional medical therapy: a systematic review and meta-analysis. *Obesity Surgery*, **24(3):** 437-455.

Rorsman, P. and Braun, M., 2013. Regulation of insulin secretion in human pancreatic islets. *Annual review of physiology*, *75*, pp.155-179.

Rosenstock, J., Hansen, L., Zee, P., Li, Y., Cook, W., Hirshberg, B. and Iqbal, N., 2015. Dual add-on therapy in type 2 diabetes poorly controlled with metformin monotherapy: a randomized double-blind trial of saxagliptin plus dapagliflozin addition versus single addition of saxagliptin or dapagliflozin to metformin. *Diabetes care*, **38(3):** 376-383.

Rossetti, L., Smith, D., Shulman, G.I., Papachristou, D. and DeFronzo, R.A., 1987. Correction of hyperglycemia with phlorizin normalizes tissue sensitivity to insulin in diabetic rats. *The Journal of clinical investigation*, **79(5):** 1510-1515.

Sargsyan, E. and Bergsten, P., 2011. Lipotoxicity is glucose-dependent in INS-1E cells but not in human islets and MIN6 cells. *Lipids in health and disease*, **10(1):** 115.

Scheen, A.J., 2016. DPP-4 inhibitor plus SGLT-2 inhibitor as combination therapy for type 2 diabetes: from rationale to clinical aspects. *Expert opinion on drug metabolism & toxicology*, **12(12):** 1407-1417.

Seyer-Hansen K, Hansen J, Gundersen HJ 1980 Renal hypertrophy in experimental diabetes. A morphometric study. Diabetologia **18**: 501-505

Shapiro A.M, Lakey J.R, Ryan E.A, Korbutt G.S, Toth E, Warnock G.L, Kneteman N.M and Rajotte R.V. 2000 Islet Transplantation in Seven Patients with Type 1 Diabetes

Mellitus Using a Glucocorticoid-Free Immunosuppressive Regimen. *New England Journal of Medicine* **343**: 230-238

Sheng, C., Li, F., Lin, Z., Zhang, M., Yang, P., Bu, L., Sheng, H., Li, H. and Qu, S., 2016. Reversibility of β-cell-specific transcript factors expression by long-term caloric restriction in db/db mouse. *Journal of diabetes research*, 2016.

Shi XL, Ren YZ and Wu J 2011 Intermittent high glucose enhances apoptosis in INS-1 cells *Experimental diabetes research* 2011

Skelin M, Rupnik M and Cencič A 2010 Pancreatic beta cell lines and their applications in diabetes mellitus research A*LTEX-Alternatives to Animal Experimentation* **27(2)** 105-113

Song G, Yang D, Wang Y, de Graaf C, Zhou Q, Jiang S, Liu K, Cai X, Dai A, Lin G and Liu D 2017 Human GLP-1 receptor transmembrane domain structure in complex with allosteric modulators *Nature* **546(7657)** 312-315

Sosa-Pineda B, Chowdhury K, Torres M, Oliver G, Gruss P 1997 The Pax4 gene is essential for differentiation of insulin-producing beta-cells in the mammalian pancreas *Nature* **386** 399-402

Spijker HS, Ravelli RB, Mommaas-Kienhuis AM, van Apeldoorn AA, Engelse MA, Zaldumbide A, Bonner-Weir S, Rabelink TJ, Hoeben RC, Clevers H and Mummery CL 2013 Conversion of mature human β-cells into glucagon-producing α-cells *Diabetes* **62** 2471-2480

Spijker HS, Song H, Ellenbroek JH, Roefs MM, Engelse MA, Bos E, Koster AJ, Rabelink TJ, Hansen BC, Clark A and Carlotti F 2015 Loss of β-cell identity occurs in type 2 diabetes and is associated with islet amyloid deposits *Diabetes* db141752

Srinivas S, Watanabe T, Lin CS, William CM, Tanabe Y, Jessell TM and Costantini F 2001 Cre reporter strains produced by targeted insertion of EYFP and ECFP into the ROSA26 locus *BMC Developmental Biology* **1(1)** 4

Srinivasan K. and Ramarao P 2007 Animal model in type 2 diabetes research: An overview. *Indian Journal of Medical Research* **125(3)** 451-472

Stein SA, Lamos EM and Davis SN 2013 A review of the efficacy and safety of oral antidiabetic drugs *Expert Opinion on Drug Safety* ***12*****(2)** 153-175

Steiner DJ, Kim A, Miller K and Hara M 2010 Pancreatic islet plasticity: interspecies comparison of islet architecture and composition *Islets* **2(3)** 135-145

Steven S, Hollingsworth KG, Small PK, Woodcock SA, Pucci A, Aribisala B, Al-Mrabeh A, Daly AK, Batterham RL and Taylor R 2016 Weight loss decreases excess pancreatic triacylglycerol specifically in type 2 diabetes *Diabetes Care* **39(1)** 158-165

Strader AD, Vahl TP, Jandacek RJ, Woods SC, D'Alessio DA and Seeley RJ 2005 Weight loss through ileal transposition is accompanied by increased ileal hormone secretion and synthesis in rats *American Journal of Physiology-Endocrinology and Metabolism* **288(2)** E447-E453

Surwit RS, Kuhn CM, Cochrane C, McCubbin JA and Feinglos MN 1988 Diet-induced type II diabetes in C57BL/6J mice *Diabetes* **37(9)** 1163-1167

Swali A, Walker EA, Lavery GG, Tomlinson JW and Stewart PM 2008 11β-Hydroxysteroid dehydrogenase type 1 regulates insulin and glucagon secretion in pancreatic islets *Diabetologia* **51(11)** 2003-2011

Takeda Y, Fujita Y, Honjo J, Yanagimachi T, Sakagami H, Takiyama Y, Makino Y, Abiko A, Kieffer TJ and Haneda M 2012 Reduction of both beta cell death and alpha cell proliferation by dipeptidyl peptidase-4 inhibition in a streptozotocin-induced model of diabetes in mice *Diabetologia* **55** 404-412

Talchai C, Xuan S, Lin H.V, Sussel L & Accili D 2012 Pancreatic β-Cell Dedifferentiation as mechanism of diabetic β-cell failure *Cell* **150** 1223-1234

Tasyurek HM, Altunbas HA, Balci MK & Sanlioglu S 2014 Incretins: their physiology and application in the treatment of diabetes mellitus *Diabetes Metabolism Research and Reviews* **30(5)** 354-371

Tauschmann M and Hovorka R 2014 Insulin pump therapy in youth with type 1 diabetes: towards closed-loop systems *Expert Opinion on Drug Delivery* **11** 943-955

Taylor AI, Irwin N, McKillop AM, Patterson S, Flatt PR and Gault VA 2010 Evaluation of the degradation and metabolic effects of the gut peptide xenin on insulin secretion, glycaemic control and satiety *The Journal of Endocrinology* **(1)** 87-93

Thorel F, Nepote V, Avril I, Kohno K, Desgraz R, Chera S & Herrera PL 2010 Conversion of adult pancreatic alpha-cells to beta-cells after extreme beta-loss *Nature* **464:** 1149-1154

Thorens B, Tarussio D, Maestro M.A, Rovira M, Heikkila E & Ferrer J 2015 *Ins1*^{Cre} knock-in mice for beta cell-specific gene recombination *Diabetologia* **58** 558-565

Tuduri E, Lopez M, Dieguez C, Nadal A and Nogueiras R 2016 Glucagon-like peptide 1 analogs and their effects on pancreatic islets. *Trends in Endocrinology & Metabolism* **27(5)** 304-318

UK Prospective Diabetes Study Group 1998 Tight blood pressure control and risk of macrovascular and microvascular complications in type 2 diabetes *British Medical Journal* **317** 703-713

United Nations, Department of Economic and Social Affairs, Population Division, 2017 World Population Prospects: The 2017 Revision, Key Findings and Advance Tables ESA/P/WP/248.

Vallon V, Blantz RC, Thomson S 2003 Glomerular hyperfiltration and the salt paradox in early (corrected) type 1 diabetes mellitus: a tubulo-centric view *Journal of the American Society of Nephrology* **14**: 530-537

Van der Meuling T and Huising M.O 2015 The role of transcription factors in the transdifferentiation of pancreatic islet cells. *Journal of Molecular Endocrinology* **54** R103-R117

Vasilakou D, Karagiannis T, Athanasiadou E, Mainou M, Liakos A, Bekiari E, Sarigianni M, Matthews DR and Tsapas A 2013. Sodium–glucose cotransporter 2 inhibitors for type 2 diabetes: a systematic review and meta-analysis *Annals of internal medicine* **159(4)** 262-274

Vasu S, McClenaghan NH, Flatt PR, Molecular mechanisms of toxicity and cell damage by chemicals in a human pancreatic beta cell line, 1.1B4 *Pancreas* **45(9)** 1320-9

Vasu S, McClenaghan NH, McCluskey JT and Flatt PR 2013 Cellular responses of novel human pancreatic β-cell line, 1.1B4 to hyperglycaemia *Islets* **5(4)** 170-7

Vasu S, McClenaghan NH, McCluskey JT and Flatt PR 2013 Effects of lipotoxicity on a novel insulin-secreting human pancreatic β-cell line, 1.1B4, *Biological Chemistry* **394 (7)** 909-18

Vasu S, McClenaghan NH, McCluskey JT and Flatt PR 2014 Mechanisms of toxicity by proinflammatory cytokines in a novel human pancreatic beta cell line, 1.1B4, *Biochemical and Biophysical Acta* **1840(1)** 136-145

Vasu S, McClenaghan NH, McCluskey JT and Flatt PR 2015 Differential molecular and cellular responses of GLP-1 secreting L-cells and pancreatic alpha cells to glucotoxicity and lipotoxicity *Experimental Cell Research* **336(1)** 100-8

Vasu S, Opeolu OO, Moffett RC, Conlon JM, Flatt PR and Abdel-Wahab YHA 2017 Anti-diabetic actions of esculentin-2Cha(1-30) and its stable analogues in a diet-induced model of obesity-diabetes, *Amino Acids* **(49)10** 1705-1717

Vasu S, Moffett RC, Thorens B and Flatt PR 2014 Role of endogenous GLP-1 and GIP in beta cell compensatory responses to insulin resistance and cellular stress. *PLoS One*, **9(6)** e101005

Vaus S, Moffett RC, McCluskey JT, Hamid MH, Irwin N & Flatt PR 2013 Beneficial effects of parenteral GLP-1 delivery by cell therapy in insulin-deficient streptozotocin diabetic mice *Gene Therapy* **20** 1077-1084

Vestri S, Okamoto MM, De Freitas HS, Dos Santos RA, Nunes MT, Morimatsu M, Heimann JC and Machado UF 2001 Changes in sodium or glucose filtration rate

modulate expression of glucose transporters in renal proximal tubular cells of rat *The Journal of Membrane Biology* **182(2)** 105-112

Vilsbøll T 2009 The effects of glucagon-like peptide-1 on the beta cell *Diabetes*, *Obesity and Metabolism* **11** 11-18

Wang Z and Gleichmann H 1998. GLUT2 in pancreatic islets: crucial target molecule in diabetes induced with multiple low doses of streptozotocin in mice *Diabetes* **47(1)** 50-56

Wang Z, York NW, Nichols CG and Remedi MS 2014 Pancreatic β cell dedifferentiation in diabetes and redifferentiation following insulin therapy *Cell metabolism* **19(5)** 872-882

Wanner C, Inzucchi SE, Lachin JM, Fitchett D, von Eynatten M, Mattheus M, Johansen OE, Woerle HJ, Broedl UC and Zinman B 2016 Empagliflozin and progression of kidney disease in type 2 diabetes *New England Journal of Medicine* **375(4)** 323-334

Watanabe M, Houten SM, Mataki C, Christoffolete MA, Kim BW, Sato H, Messaddeq N, Harney JW, Ezaki O, Kodama T and Schoonjans K 2006 Bile acids induce energy expenditure by promoting intracellular thyroid hormone activation *Nature* **439(7075)** 484-489

Weinberg N, Ouziel-Yahalom L, Knoller S, Efrat S & Dor Y 2007 Lineage tracing evidence for the in vitro dedifferentiation but rare proliferation of mouse pancreatic β-cells *Diabetes* **56** 1299-1304

Weir GC, Aguayo-Mazzucato C and Bonner-Weir S 2013 β-cell dedifferentiation in diabetes is important, but what is it? *Islet* **5** 233-237

Wice BM, Wang S, Crimmins DL, Diggs-Andrews KA, Althage MC, Ford EL, Tran H, Ohlendorf M, Griest TA, Wang Q and Fisher SJ 2010 Xenin-25 potentiates GIP action via a novel cholinergic relay mechanism. *Journal of Biological Chemistry* pp.jbc-M110.

Wieczorek G, Pospischil A and Perentes E 1998 A comparative immunohistochemical study of pancreatic islets in laboratory animals (rats, dogs, minipigs, nonhuman primates) *Experimental and Toxicologic Pathology* **50(3)** 151-172

Winzell MS and Ahrén B 2004 The high-fat diet–fed mouse: a model for studying mechanisms and treatment of impaired glucose tolerance and type 2 diabetes *Diabetes* **53(suppl 3)** S215-S219

Wright EM 2001 Renal Na+-glucose cotransporters. *American Journal of Physiology-Renal Physiology* **280(1)** F10-F18

Yan H, Xie H, Ying, Y, Li J, Wang X, Xu X and Zheng X 2018 Pioglitazone use in patients with diabetes and risk of bladder cancer: a systematic review and meta-analysis *Cancer management and research* **10** 1627-1628

Yki-Järvinen H 2004 Thiazolidinediones *New England Journal of Medicine* ***351*****(11)** 1106-1118

Yoon KH, Ko SH, Cho JH, Lee JM, Ahn YB, Song KH, Yoo SJ, Kang MI, Cha BY, Lee KW and Son HY 2003 Selective β-cell loss and α-cell expansion in patients with type 2 diabetes mellitus in Korea *The Journal of Clinical Endocrinology & Metabolism* **88(5)** 2300-2308

Zambrowicz B, Ding ZM, Ogbaa I, Frazier K, Banks P, Turnage A, Freiman J, Smith M, Ruff D, Sands A and Powell D 2013 Effects of LX4211, a dual SGLT1/SGLT2 inhibitor,

plus sitagliptin on postprandial active GLP-1 and glycemic control in type 2 diabetes *Clinical therapeutics* **35(3)** 273-285

Zinman B, Wanner C, Lachin JM, Fitchett D, Bluhmki E, Hantel S, Mattheus M, Devins T, Johansen OE, Woerle HJ and Broedl UC 2015 Empagliflozin, cardiovascular outcomes, and mortality in type 2 diabetes *New England Journal of Medicine* **373(22)** 2117-2128